MICROMORPHOLOGY, SITE SPATIAL VARIATION AND PATTERNING, AND CLIMATE CHANGE AT THE MEAD SITE (XBD-071): A MULTI-COMPONENT ARCHAEOLOGICAL SITE IN INTERIOR ALASKA

A

THESIS

Presented to the Faculty

of the University of Alaska Fairbanks

in Partial Fulfillment of the Requirements for the Degree of

MASTER OF ARTS

By

Phoebe J Gilbert, B.A.

Fairbanks, Alaska

May 2011

MICROMORPHOLOGY, SITE SPATIAL VARIATION AND PATTERNING, AND CLIMATE CHANGE AT THE MEAD SITE (XBD-071): A MULTI-COMPONENT ARCHAEOLOGICAL SITE IN INTERIOR ALASKA

By

Phoebe J. Gilbert

RECOMMENDED:

Dr. Jim E. Beget

Dr. Nancy H. Bigelow

Dr. Joel D. Irish

Dr. Ben A. Potter, Advisory Committee Chair

Dr. Joel D. Irish, Chair, Department of Anthropology

APPROVED:

Dr. G. Burns Cooper, Dean, College of Liberal Arts

Dr. Lawrence K. Duffy, Dean of the Graduate School

Apr 4, 2011

Date

Abstract

The Mead Site, located in the Tanana River Valley in Interior Alaska, is a deeply buried archaeology site with multiple occupations and excellent preservation. The site provides a rare opportunity to study the human/climate relationship in prehistory.

Magnetic susceptibility, micromorphology, geochemical and spatial analysis were utilized to (1) determine the amount of post-depositional disturbance at the site, (2) see if there are detectable buried surfaces that indicate cultural occupation in the upper stratigraphic layers and, (3) investigate the paleosols at the site and determine if the occupations at the site correlate with ameliorating climate.

The results show that the upper three cultural zones are heavily disturbed by taphonomic processes to the point that assignment of the remains to cultural zones is suspect. The lower two components have also been affected by post-depositional disturbance, but the patterning of cultural remains in these zones is primarily a reflection of the original depositional context. No buried surfaces were detected in the upper stratigraphic layers, and the paleosols are natural in origin but are anthropogenically enhanced. The cultural zones at the site are more closely associated with cool episodes than with periods of ameliorating climate.

Table of Contents Page

Page

Page

Page

List of Figures

List of Tables Page

List of Appendices

Acknowledgments

This thesis would not have been possible without the help of a great number of people. First, I would like to thank my committee, Jim E. Beget, Nancy H. Bigelow, Joel D. Irish, and Ben A. Potter for their help and encouragement throughout the years, particularly Ben for his support and willingness to let me undertake this study. I have benefited greatly from his advice and his knowledge of subarctic archaeology; I would especially like to thank him for sharing his views of regional chronologies and methodology, and always encouraging me to think of the "bigger picture".

This project was supported by Denali LLC, who provided the funding that made the 2009 field school excavation at the Mead Site possible, and the University of Alaska Fairbanks (UAF) Department of Anthropology, which supported me throughout this study with Teaching and Research Assistantships. The Geist Fund, Harvey Shields Fellowship, Hopkins Fellowship, and the Alaska Quaternary Center provided funding and supplies.

In addition to my committee, I would like to thank the professors and mentors over the years who where always more than willing to help me study and understand subjects and concepts generally thought of as outside the realm of anthropology. I would like to thank Dr. David Stone of the Paleomagnetism Laboratory, UAF; for graciously donated lab space and the use of the Bartington Susceptibility meter for this analysis; Dr. Rainer Newberry for his assistance with both the petrographic microscope and the XRF spectrometer; and especially Dr. Ken Severin of the Advanced Instrumentation Laboratory, UAF (where portions of this work were performed), without whose help and advice this project would not have been possible.

I would also like to thank all of the participants of the 2009 field school, as well as Barbara Crass and Chuck Holmes for sharing their knowledge and their support. Thanks to Randy Tedor and Gilbert Qu Feng (my fellow RAs at the Mead Site) for the great discussions and friendship and to Josh Reuther who was always game for a discussion on anything geoarchaeological. I am indebted to Sam Coffman for his friendship and help during this project, and for not leaving me stranded at the site one late night in October.

I have been lucky enough to have a great group of friends who are also archaeologists and who have supported me throughout this project-- thanks to all of you. My deepest gratitude goes to my family: my mother and father have always supported me, and the morals and ethics they instilled in me as a child helped me complete this project. My sisters, Faye and Martha, have been both the best of friends and always there when I needed them (especially when editing). Finally, I want to express my deepest appreciation to my partner Chris Ciancibelli, for his patience and support during the last three years.

1 Introduction

One common investigation at any archaeological site is the examination of the spatial patterning of features and artifacts. From these patterns general activity areas of an occupation can be designated, and hypotheses about human behavior from these spatial patterns drawn (Schiffer 1972). Intra-site spatial patterns are used in archaeological studies to designate activity areas at sites and are the basis for higher level theory regarding human behavior and site function (Schiffer 1972). It is necessary when conducting this type of analysis to question if the spatial patterning observed by the archaeologist is actually the result of the people who once were at the site, or of post-depositional non-cultural factors. It is possible that the spatial patterning many archaeologists attribute to cultural processes are actually the result of taphonomic and non-cultural site formation processes. Taphonomic processes such as rodent burrowing and freeze-thaw cycles can shift the location of artifacts after burial as well as distort the stratigraphy and natural features at a site, it is important to separate the taphonomic post-depositional effects from the cultural processes that formed a site.

As Schiffer notes (1983:680), "even when multiple lines of evidence are brought into the analysis, the genesis of complex deposits formed by many processes may, in our current state of knowledge remain uncertain". The work presented here examines these 'multiple lines of evidence' through the use of micromorphology, in conjunction with environmental magnetism and geochemical analysis.

This project is a geoarchaeological analysis of the Mead archaeological site (XBD-071), located in Interior Alaska (Figure 1.1). The Mead Site is one of three multi-component sites with Late Pleistocene occupations in the Shaw Creek Flats area dating to around 14,000 cal yrs BP (Dilley 1998; Holmes 2001). The other two sites of importance in the Shaw Creek Flats area are Broken Mammoth and Swan Point (Figure 1.1) (Holmes 1996; Holmes 2001; Holmes, et al. 1996; Yesner, et al. 1992).

Swan Point has the earliest generally accepted component of any site in eastern Beringia (Bever 2001; Hamilton and Goebel 1999; Holmes 2008; Holmes, et al. 1996; Potter, et al. 2010; Yesner and Pearson 2002), and Broken Mammoth's faunal assemblage from the lower components has provided insight into the wide diversity of taxa used by humans at the end of the Pleistocene (Yesner 2001). The Mead Site, located between Swan Point and Broken Mammoth has long been noted as being an important site for Alaskan archaeology (see Holmes 2001; Holmes and Yesner 1992; Yesner, et al. 1992), but until recently little work has been conducted at the site.

Dilley (1998) presented a study of the geoarchaeology and a general climate history of the Tanana River Basin, but did not investigate the site formation processes at the Mead Site or the relation of the artifacts and faunal remains to their surrounding contexts. Further investigation of the site will contribute greatly to theories of timing and duration of the Peopling of the New World.

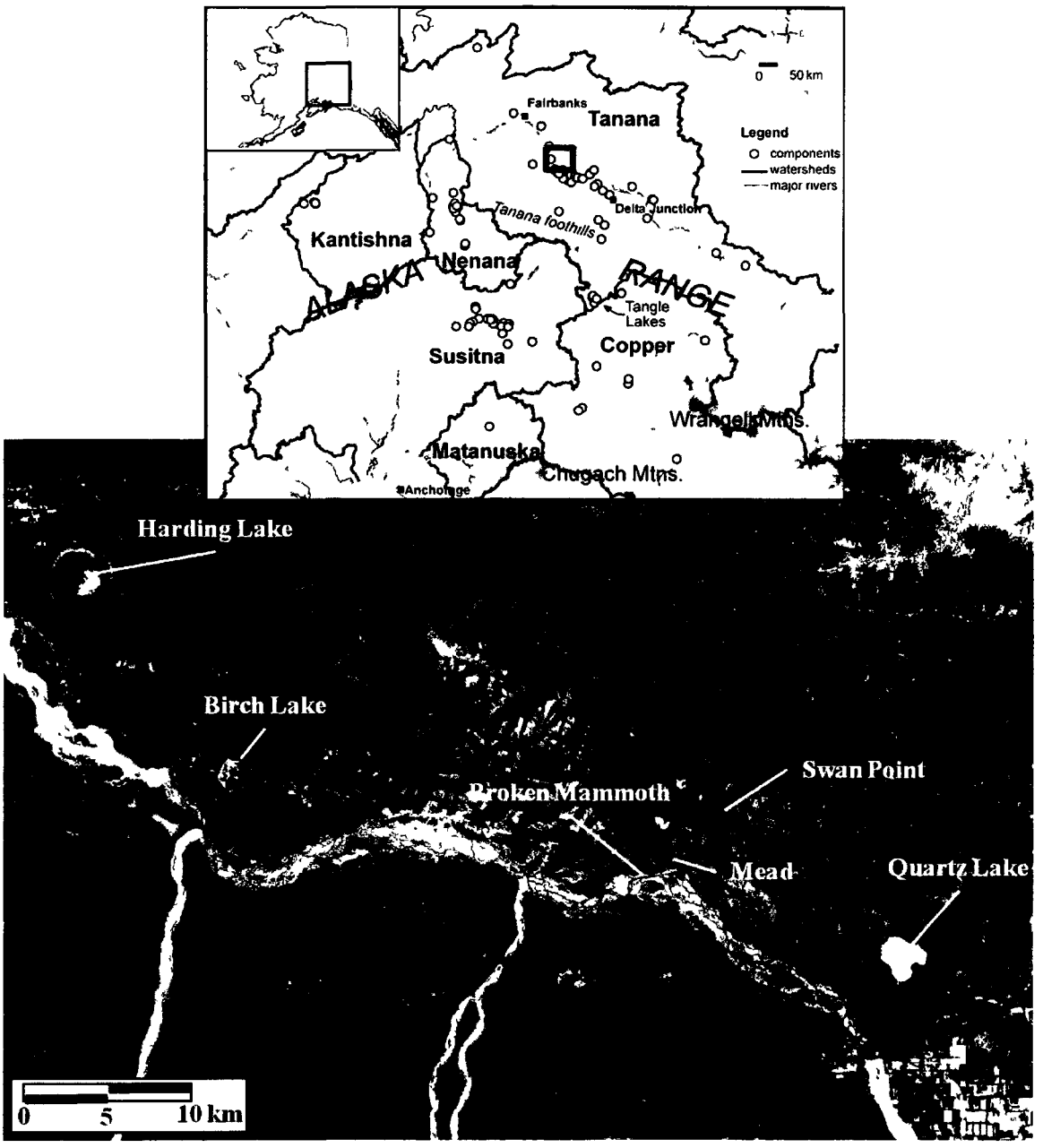

Figure 1.1 Study Area (top map from Potter 2008b, his Fig.1)

In addition to examining the spatial patterns at the Mead Site, this study also examines the relationship between climate and occupation Questions of paleo-climate/human interactions on the occupational landscape of Alaska have intrigued archaeologists for years. Many of the theories of the populating of the new world are directly based on an inferred link between climate, geography, and

migration. For example, Yesner (2001:317) hypothesized that the ameliorating climate at the end of the last glacial period was part of the reason that Eastern Beringia was colonized as the warming climate and change in vegetation created an attractive environment that "pulled" humans into the new world, Hoffecker et al. (1993) wrote that the colonization of Eastern Beringia most likely resulted from changes in environmental variables, specifically the spread of trees. They hypothesize that these trees provided a robust fuel source for the migrating populations which had not been available before. This concept of "climate determinalism" is a common theme in Alaskan archaeology and multiple reviews have been written regarding the broad scale correlations between complexes, regions, and climate (see Bever 2001; Bigelow and Powers 2001; Hoffecker and Elias 2007; Mason and Bigelow 2008; Mason, et al. 2001; Potter 2008c). Climate determinalism is examined here on the smaller, site specific scale, and this study applies a different data set that than commonly used by archaeologists to tackle this question. It contributes to growing body of information used to investigate landscape use, climate, and occupation.

1.1 Research Objectives:

The purpose of this study is twofold. First, it is an investigation of the intrasite patterning of artifacts in relation to their context at the Mead Site. Secondly, it is an investigation of possible correlations between occupations at the Mead Site with past climate change through analysis of the sediments and soils at the site. This approach provides detailed information about the depositional, contextual, and taphonomic relationships between the artifacts, faunal remains and sediments, which is used to understand the spatial patterning of the site.

The study of occupations and climate change at the Mead Site will ultimately provide greater understanding of paleo-climate/human interactions on the occupational landscape of interior Alaska. This study has been carried out through an investigation of the buried occupational surfaces at the Mead Site. These buried surfaces may indicate discrete intervals when the site would have been available for occupation, and which may correlate with times of environmental stability in the area. This relationship between environmental stability and occupation has been examined before on a coarse scale through regional syntheses and reviews (see Dilley 1998; Hoffecker and Elias 2007; Mason, et al. 2001); the data presented here is of a much finer scale than these regional reviews and provides new insight regarding this relationship.

Analysis of the sediments and soils for occupational surfaces were conducted through, micromorphology, magnetic susceptibility and geochemical data, in conjunction with the spatial analysis of cultural remains from all components. Based on the age, excellent faunal preservation, and regional location of this site, a continued geoarchaeological investigation of the site is warranted.

1.2 Research Questions:

(1) Do the cultural components at the Mead Site correspond to periods of ameliorating climate in Interior Alaska? For the purposes of this study, ameliorating climate is defined as warmer conditions. The null hypothesis is that the components at the site do not correspond to periods of ameliorating climate; the alternative hypothesis is that they do correspond to periods of ameliorating climate. If the null hypothesis cannot be rejected what does this correlation imply for site use and occupation as well as theories of human paleodynamics in the region?

(2) Are the paleosols at the Mead Site the result of natural or cultural processes? The null hypothesis is that the paleosols formed through natural processes; the alternative hypothesis is that the paleosols formed through, or were enhanced by, cultural processes. If the paleosols are indicative of human occupation what are the implications of this correlation?

(3) Are there detectible buried occupational surfaces in the Upper Loess stratigraphic section of the Mead Site? The null hypothesis is that there are no detectible buried occupational surfaces in the Upper Loess; the alternative hypothesis is that there are detectible buried occupational surfaces in the Upper Loess. If the null hypothesis can be rejected, do these surfaces correspond with times of environmental stability in the region and how can this research inform future studies at geologically similar sites?

(4) To what extent does the intrasite patterning of cultural remains at the Mead Site appear to be the result of post-depositional disturbances and taphonomic processes? Once the degree of taphonomy and post-depositional disturbance has been determined, are there activity areas evident at the site, and if so what are the implications for site use? The null hypothesis is that the cultural remains are still in their primary context and that taphonomic processes have not substantially altered the site assemblage, while the alternative hypothesis is that the cultural remains are in secondary context and taphonomic processes have significantly altered the site assemblages. How can this inform future studies of patterning at other sites?

2 Background

2.1 Study Area

The Mead Site is located on the west edge of the Shaw Creek Flats in the greater middle Tanana River Basin in Interior Alaska. This basin (Figure 2.1) encompasses three physiographic regions; the Tanana Lowlands, the Yukon-Tanana Uplands, and the eastern section of the Alaska Range (Wahrhaftig 1965).

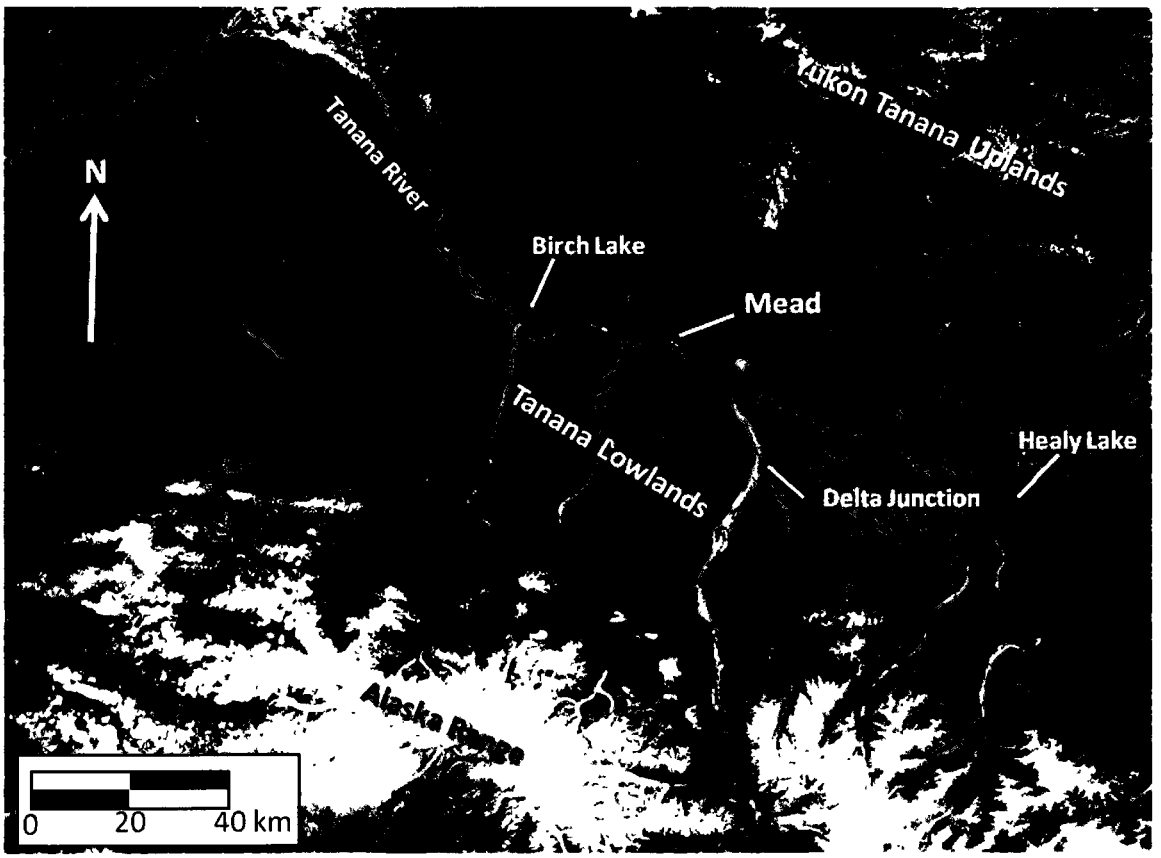

Figure 2.1 Tanana River Basin

The Tanana Lowlands are characterized by the presence of the Tanana River and its large floodplain which is covered in alluvium. This region is bounded to the south by the Alaska Range and to the north by the Yukon-Tanana Uplands. From Healy Lake in the east to Birch Lake in the west, the Tanana River drops 120 meters (m) in elevation from 365 m to 245 m (Dilley 1998: 32; Wahrhaftig 1965).

Tributaries to the Tanana River are the Gerstle River, the Delta River, Healy Lake, and Shaw Creek (Dilley 1998). The Tanana River Basin is a low lying area, and much of it is characterized by muskeg bog, black spruce, discontinuous permafrost, and accompanying thaw lakes (Ferrians 1965).

The Yukon-Tanana Uplands are characterized by Precambrian gneiss and schist rocks that are expressed as low, rounded ridgelines and mountains. These rise from 210m near the Tanana River to heights of 1250m north of the Shaw Creek Flats (Pewe 1965). Sedimentary deposits in the Uplands are characterized by thick accumulations of aeolian sediments in the valley regions (Pewe 1965).

The Alaska Range is one of the major ranges in Alaska and is characterized by mountains that contain the highest peaks in North America and valley glaciers that flow out of the mountains. The mountains are the source of many of the braided glacial streams that merge with the Tanana River.

The Tanana River headwaters are located near the Canadian border, and the river flows for 380 km before merging with the Yukon River (Pewe and Reger 1983). The River basin is filled with glaciofluvial sediments that are 250 m thick in places (Begét and Keskinen 2003; Pewe and Reger 1983). These overlay a somewhat craggy base, of which the exposed hilltops are seen today as small rounded knolls in the basin (Pewe and Reger 1983). The river is braided with channels that change yearly and which meanders back and forth across its wide floodplain.

Below the headwaters the river flows through Pleistocene age sand dunes and has a fine grain load and a low gradient (Fernald 1965). Continuing downstream to the middle Tanana valley area, the river load becomes coarser due to the addition of the glacial sediments from the outwash streams emerging from the Alaskan Range (Anderson 1970). The gradient also increases here and the river becomes more braided (Anderson 1970). At the confluence with the Delta River (upriver of the Mead Site) the load becomes coarser and the river more braided. Near Fairbanks, the river gradient decreases, as does the grain size of the load (Anderson 1970). This trend continues up to the confluence with the Yukon River. Close to its confluence with the Yukon River, the Tanana River meanders widely and is generally less braided (Fernald 1965). Many of the lakes (Healy, Quartz, Birch) in the Tanana River Basin formed in part during the Delta Glaciation (the penultimate glaciation) when the river aggraded and the streams flowing out of the Yukon-Tanana Uplands were dammed (Pewe 1965).

2.2 History of Research

The Mead Site (XBD-071) is a deeply buried multicomponent site located near the confluence of Shaw creek and the Tanana River (Figure 1.1). There are several such sites in the Tanana River Valley, the others being the Swan Point (XBD-156), Upward Sun River (XBD-298), and the Broken Mammoth (XBD-121) sites (Holmes 1996; Holmes, et al. 1996; Potter, et al. 2011). The Mead Site was most recently excavated during the summer 2009 field season when two large block excavations were opened on the east and West Lobes of the site by the University of Alaska Fairbanks field school (Figure 2.2 and Figure 2.3).

The site was first described geologically in guide books to interior Alaska (Pewe 1965; Pewe and Reger 1983).

The site was discovered archaeologically in the early 1970's and small block excavations were carried out by Holmes in 1990 and 1992 (Figure 2.2). Because of the limited extent of this excavation, as well as the differences in collection strategy and research questions addressed, no spatial analysis will be conducted on the cultural remains from this earlier excavation. The site has an excellent viewshed to the south of the Shaw Creek Flats. The site itself (Figure 2.4) is located on a south/southeast facing bluff edge of a rock quarry that was used during the 1950's and 1960's (Dilley 1998).

Testing for the site boundaries has not yet revealed the limits of the Mead Site. Positive test pits continue upslope (north) of the 2009 field school location for roughly 300 meters. Additional tests to both the east and west of the 2009 field school location (still located on the main land feature) were also continuously positive. This hints at a wide occupation area at the Mead Site and indicates the vast potential for future field work at the site.

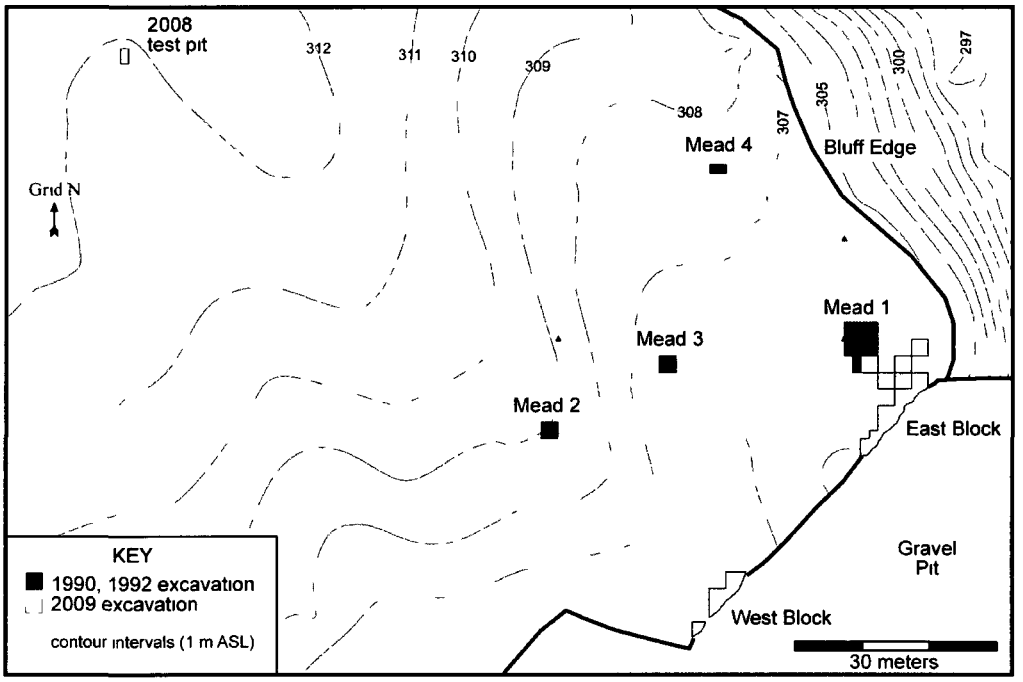

Figure 2.2 Overview of site and all excavations

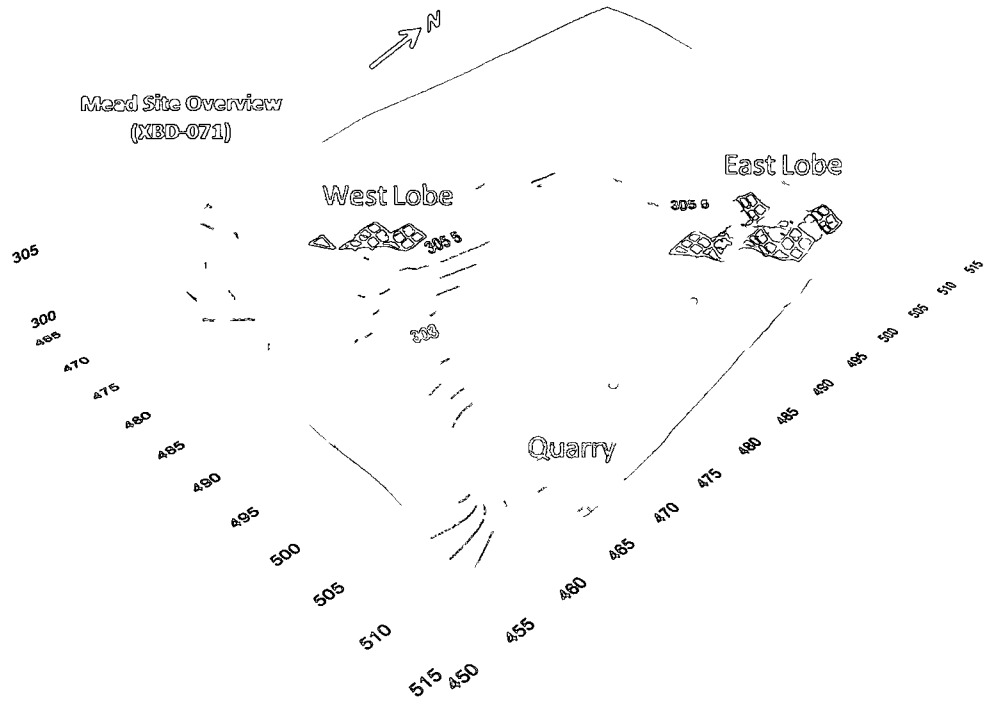

Figure 2 3 Overview of area excavated during the 2009 Field School

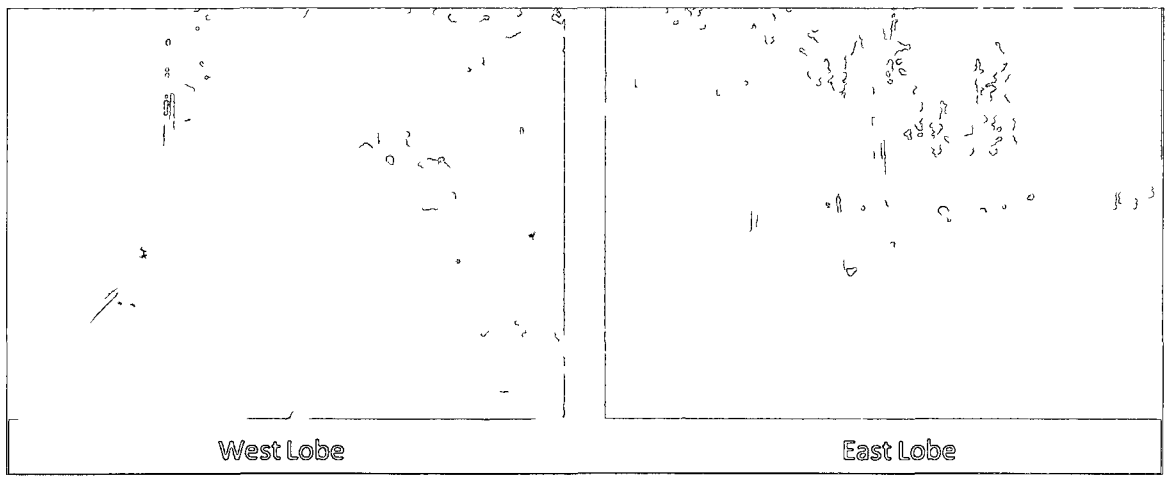

Figure 2 4 View of the Site looking north from the Excavated Quarry

The stratigraphy of the Mead Site was first recorded by Pewe in 1965. Pewe set out a sequence based on the different glacial events in the area. He interpreted that the loess at the site resulted from the Donnelly glaciation (25,000 to 9,500 cal yr BP), and the sand resulted from the Delta Glaciation (75,000 cal yr BP to 26,000 cal yr BP) (1965). Pewe also described a mammoth tusk eroding out of the bluff face. In subsequent archaeological investigation of the site, this tusk fragment was found to be in association with the lowest cultural zone (CZ 4).

The stratigraphy of the Mead Site begins on weathered gneissic bedrock with occasional quartz intrusions. Ventifacts have been found at the contact of this bedrock and the overlying layers. Above the bedrock in some places is a colluvial layer of angular pebbles and boulders. This is overlain by aeolian sediment, which can be 4 meters deep in areas. Dilley divides the stratigraphy into 4 units (Figure 2.5). He divides the aeolian deposits into a Lower Sand (Unit 2), which overlies the weathered bedrock (Unit 1). Unit 3 is composed of loess and three paleosol complexes, which were dated to 7620 ± 100 14C yrs BP, 10,400 ±170 14C yrs BP, and 11,500 ± 90 14C yrs BP (Dilley 1998). Above Unit 3 is Unit 4 loess, which is characterized by micaceous sandy silt with massive bedding and sporadic sand lenses (Dilley 1998). The upper region of Unit 4 is composed of a modern Sub-Arctic Brown forest soil. These designations are those used by Dilley and are elaborated upon in this project as the designations of Units 3 and 4 are too coarse grained for a closer spatial and geoarchaeological investigation. Detailed stratigraphic descriptions are found in Chapter 3.

Preliminary results of the most recent excavation indicate over 3,000 artifacts and close to 5,000 faunal remains (the majority of which are fragmentary) were recovered. From CZ1a 6 flakes and 33 bone fragments were collected. From CZ 1b two feature areas were identified and 1,985 flakes, 3 end scrapers, 1 biface fragment, 1 burin spall, 3 modified flakes, 2 end scrapers, and 19 microblades were recovered along with 4,418 bone fragments. From CZ 2 432 flakes, 2 microblades and 12 bone fragments were recovered, the majority of which may be from a possible feature. From CZ 3, 238 flakes, 2 modified flakes, 1 microblade, 343 bone fragments, and several fragments of ivory were collected and two hearths were identified. From the oldest component, CZ 4, 323 flakes, 1 modified flake, and 50 bone fragments were recovered and one possible activity area was identified. These findings will be elaborated on in Chapter 4.

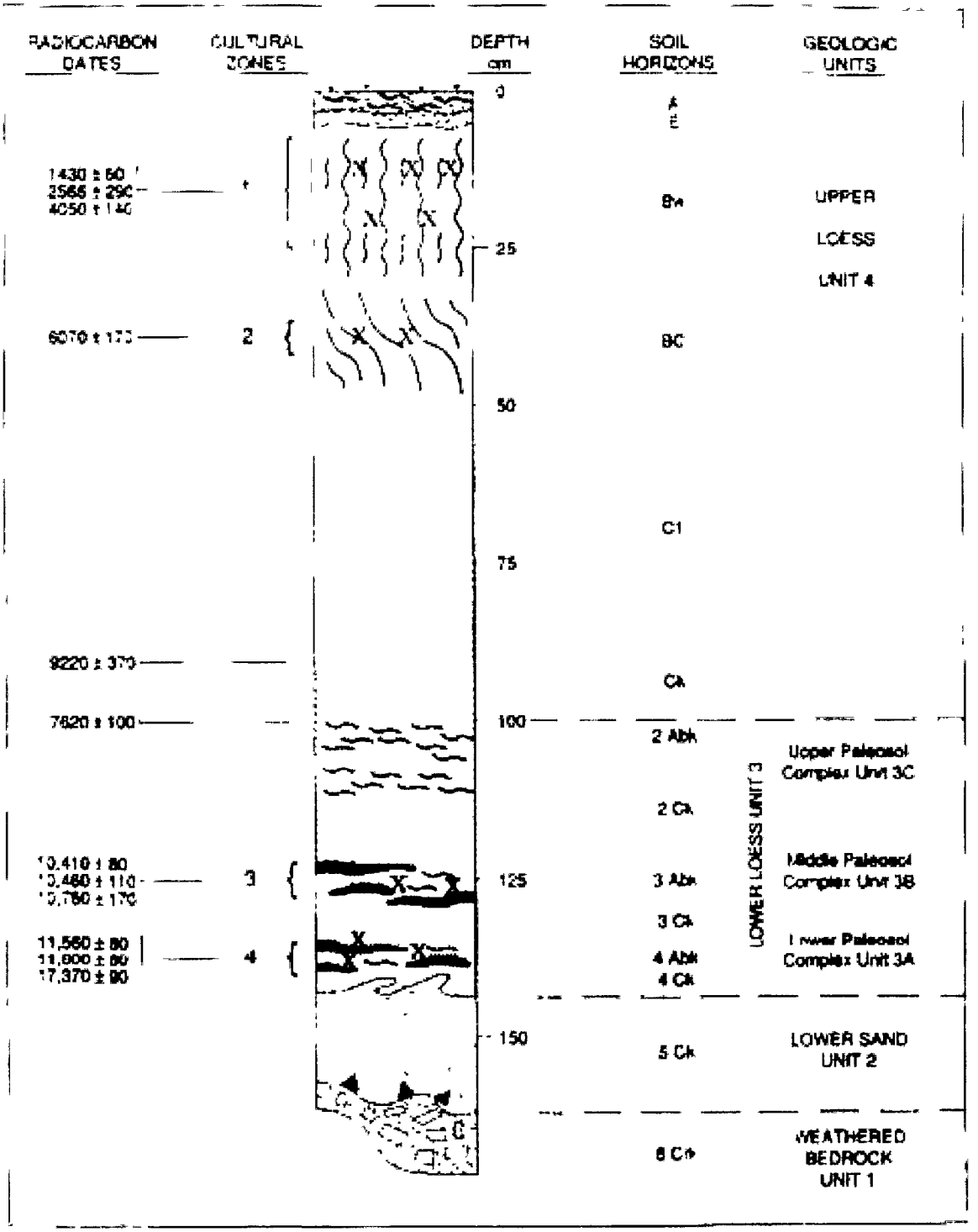

Figure 2.5 General Profile from Dilley (1998) (his figure 3.8)

2.3 Cultural Chronology

The cultural chronology of prehistory in the Tanana River Basin is based largely on the techno-complexes from a handful of sites in interior Alaska. Below are definitions of "tradition" and "complex", a brief summation of interior Alaska's chronology, and the synthesis by Holmes (2008) which is used her to tie the chronology together.

A tradition is "a (primarily) temporal continuity represented by persistent configurations in technologies or other systems of related forms" (Willey and Phillips 1958:37), whereas a "complex" is more similar to the shorter derived "phase" (Willey and Phillips 1958:22). The cultural continuity of traditions can exist through long time spans and over large geographic regions. Dixon (1985:48) distinguishes "traditions" from "complexes" by the differences in duration and geographic reach of complexes. In general, complexes have similar technological continuity, but have more constrained regional and chronological bounds (Dixon 1985).

To be able to see transition from one tradition to the next there must be some change in the cultural continuity that is observed. Dumond notes this by saying that the bounds of a tradition can be seen in "a pervasive, systematic change in material culture, and secondly by a change in economic indicators" (1982:39). It is hard to note changes in economic indicators at the majority of sites in the region, due to the poor faunal preservation; however, due to the recent efforts of a few investigators in the area (Potter 2000; Potter 2005; Potter 2008a; Potter 2008b; Potter 2008c; Potter, et al. 2007), an understanding of economic indicators is being developed. Most of this research is based on the Gerstle River site and hopefully as more sites with robust faunal assemblages are investigated similar sets of research questions will be applied to them, allowing for correlation of economic indicators in the study region. Until such a time, we must depend upon material culture to guide us from one tradition to the next.

2.3.1 Swan Point/ Dyuktai

The Swan Point Dyuktai Phase is characterized by the remains found at Swan Point, including burins, bifacial tools, scrapers, retouched flakes, ivory implements, and most importantly, blade and microblade technology (Holmes 2001). This phase encompasses the oldest dated sites in the Tanana River valley (Swan Point, Broken Mammoth and Mead), although only Swan Point contains microblades. The microblade technology at Swan Point is similar to that of the Dyuktai tradition of Siberia, which has been interpreted as evidence for an early continuum relationship (Holmes 2001).

2.3.2 Nenana Complex

As originally defined, the Chindadn/ Nenana Complex is the oldest complex in interior Alaska. Cook defined the Chindadn complex in 1969 based on his excavations at the Healy Village Site in interior Alaska (Cook 1969). The materials of the Chindadn complex are similar to both those of the Denali

Complex and the American Paleoarctic tradition, except for the occurrence of small triangular bifacial points, or Chindadn points, which are absent in the assemblages of the later Denali complex and American Paleoarctic tradition (Cook 1969).

The Nenana Complex was defined by Powers and Hoffecker in 1989, mainly based on Component 2 at the Dry Creek site. This complex is also defined as a blade and core complex with bifacial technology and an absence of microblade technology (Powers and Hoffecker 1989). Present at many Nenana Complex sites are the triangular "Chindadn" points that Cook used to define the Chindadn complex; but emphasis on defining the Nenana Complex is placed on the blade and core technology, and the lack of microblade technology (Powers and Hoffecker 1989:278). This complex dates to approximately 11,800-11,000 yrs BP and is also typified by lithic assemblages of the oldest components at Walker Road, Moose Creek, and Owl Ridge (Goebel, et al. 1991; Pearson 1999; Phippen 1988; Powers and Hoffecker 1989). Dates from Dry Creek Component 2 placed the Nenana Complex as older than the Denali Complex. Because of this, for the last several decades it was assumed that the earliest settlers of the area lacked microblade technology. The association of Chindadn points with microblade technology at the Healy Lake Site has been questioned by some (Hoffecker, et al. 1993), as this is in opposition to a microblade-free Nenana tradition.

2.3.3 Denali Complex

West proposed the Denali Complex in 1967 as an early core and blade complex that also contains bifaces and burins. The Denali Complex dates to approximately 10,600- 7,000 yrs B.P. (Hoffecker 2001) and has been described as a complex rather than a tradition (West 1967). This designation of a complex, rather than a tradition, is interesting in light of the definition above, as Denali (as originally defined) has continuity of material over a large region and time span.

The artifacts attributed to this complex are bifacial knives, microblade technology, endscrapers, lanceolate projectile points, and burins (Mobley 1996; West 1967). The complex was defined by West (1967; 1975) based on the assemblages found at Donnelly Ridge (the type site), The Campus Site, several Tangle Lakes sites, Dry Creek Component 2, several sites at Ft. Wainwright (Blair Lakes) and a few sites located in the Susitna River Canyon region. The Tangle Lakes sites are surface sites that were dated purely on their lithic assemblage.

2.3.4 Northern Archaic Tradition

When first formally proposed by Charles Scheweger and then Douglas Anderson in 1968 (Esdale 2008:10), the Northern Archaic tradition explained the existence of a number of sites that did not fit into the current cultural complexes of northwestern Alaska (Anderson 2008). The artifact assemblage typified by the Northern Archaic levels at Onion Portage were seen by the archaeologists of the time(Anderson 1988; Dumond, et al. 1976; MacNeish 1964) to be very different from those of the northwest Alaskan

coast, but similar to those of Interior Alaska, the Yukon, and even further south (Anderson 1988:87). Workman (1978) was a proponent of population replacement and proposed a route for the Northern Archaic groups that started in the south, wound its way north through the Yukon Territory, into the Brooks Range, then to the area of Onion Portage, and then south, into the Interior (Esdale 2008:11). Morrison (1987) explained the Northern Archaic Tradition as resulting from diffusion of notched projectile points from south to north (Esdale 2008:11).

The tradition was defined mainly by its techno-complex (Anderson 1988), composed of large choppers, notched pebbles, crescent-shaped bifaces, stemmed projectile points, and most importantly, notched projectile points (Esdale 2008). Anderson saw a closer similarity between these artifacts and the Eastern Woodland Archaic assemblages of the contiguous United States than those of the Paleoarctic assemblage found at Onion Portage (Esdale 2008).

When originally proposed, the Northern Archaic was linked to the spreading of the boreal forest, however, as early as 1988 Anderson was questioning the association (88). Today, depending upon the variables and proxies utilized, different answers to this question can be produced. Esdale's synthesis shows a strong preference for the mountain regions, while Mason and Bigelow describe a "push-pull" type relationship, as the emergence of the Northern Archaic correlates with a retreat of tree line, and the emergence of peat land and forest in the interior (2008).

2.3.5 Athapaskan Period

At around 1,500-1,000 yrs B.P. the Athapaskan period began in interior Alaska (Griffin and Chesmore 1988:64). It is also typified by the emergence of copper in the archaeological record and a decreased reliance on lithic tools (Dixon 1985; Franklin, et al. 1981). This tradition is defined in part by ethnographic evidence of cultural continuity for the last thousand years. Some archaeologists have argued that this tradition grew from cultures already inhabiting the region (i.e. Cook 1975) while others saw it as the result of a new population migrating to the area (i.e. Aigner, et al. 1986). Cook saw this tradition as reaching as far back as 11,000 B.P., based on the upper levels found at the Healy Lake Village and Garden sites (1969). This conclusion appears a bit spurious, especially in light of the taphonomic problems at these sites. Where the Athapaskan population came from, as well as when they came into the area is little understood, and there are multiple hypotheses regarding this research question (Aigner, et al. 1986; Cook 1975; Holmes 1986).

An element that might help with future determinations of this question is the White River Ash, which occurs sporadically in the area, and which has been dated to 1,400 BP (Workman 1974). Workman has hypothesized that the effect of this eruption had a catastrophic affect on the landscape, resulting in flooding, erosion, and a large reduction in the amount of vegetation (1974:240). Such a catastrophic event may have caused a mass migration of the population out of the fallout zone and into unaffected areas.

These areas were quite probably already inhabited, and this migration may have induced a, "widespread accelerated cultural change indicative of intensified contacts datable roughly into the First Millennium A.D." (Workman 1974:255).

2.3.6 Synthesis

The synthesis that is applied in this research is one that combines both cultural and environmental criteria and was first published in Holmes (1995). In this synthesis, Holmes sets out environmentally and ecologically defined Periods that are used to divide prehistory into neutral units of which serve as the backdrop for the cultural traditions.

In this synthesis Holmes places the Swan Point Dyuktai tradition as the first Phase of the East Beringian tradition (from 15,500-13,500 cal BP), which corresponds to the Beringian Period. The Beringian period is encompasses the time from before forests were established in Alaska, and the Bering Land Bridge was still in existence.

Phase II of the East Beringian tradition is composed of the Chindadn/ Nenana traditions from 13,500-11,500 cal BP, and corresponds with the Transitional Period. The transitional period begins with the start of the Younger Dryas cooling event and is defined by changes in climate and by megafauna' extinctions (Holmes 2008).

The remainder of the Holocene up till the Historic Period is categorized as the Taiga Period, which is further divided into the Early, Middle, and Late Taiga Period. The Taiga Period is defined by a landscape dominated by birch-spruce woodland. The Early Taiga period is from 9,500-6,000 cal yr BP, the Middle Taiga Period is from 6,000 to 3,000 cal yr BP, and the Late Taiga Period is from 3,000 to 500 cal yr BP (Holmes 2008). The Denali tradition from 11,500-8,500 cal BP spans from the Transitional Period into the Early Taiga Period. The Denali tradition is followed by what Holmes describes as a "Transitional Northern Archaic" period form 8,500-6000 cal BP (2008), which corresponds with the Early Taiga Period. This is followed by the Northern Archaic tradition, which Holmes brackets from 6,000 cal BP to just before 2,000 cal BP (corresponding to the Middle and Late Taiga Periods), and which is followed by the Athapaskan tradition (Late Taiga Period), which spans the remainder of the Holocene up to contact (Holmes 2008).

2.4 Glacial History

The Wisconsin glaciation was the final glaciation in this region. The terminal deglaciation took place from 14,000 to 9,500 cal yr BP (all radiocarbon dates were calibrated using the intercalc04 curve in CalPal Software) (Pewe and Reger 1983). In the Delta Junction area the Wisconsin Glaciation is divided into the Donnelly and the Delta Glaciations. The Delta Glaciation is the older of the two, beginning around 75,000 cal yr BP and ending around 26,000 cal yr BP (Begét and Keskinen 2003). The Donnelly glaciation is the most recent glaciation and took place from 25,000 to around 9,500 cal yr BP (Leehan 1981; Pewe and

Reger 1983). During the Donnelly Glaciation, the thickness of the ice in the Donnelly Dome area (approximately 40 miles south of the Mead Site) has been estimated to have been 975 m thick. Donnelly Dome would still have been partially exposed at this time (Leehan 1981; Pewe and Holmes 1964). Recent work has shown that the Donnelly moraine stabilized around 17000 cal yr BP, which is contemporaneous with the stabilization of other Alaska Range moraines and helps to synchronize the Donnelly Glaciation with other Alaska Range terminal glaciations (Matmon, et al. 2010).

The Riley Creek Glaciation, which took place between the Nenana Valley and the region north of the Alaska Range, has four well documented advances which may correspond with those of the Donnelly Glaciation. The first advancement, Riley Creek I, took place from 25,000 to 20,000 cal yr BP. The next advancement, Riley Creek II, was from 18,700 to 15,800 cal yr BP. The third advancement was Riley Creek III from 15,200 to 13,500 cal yr BP. The final advancement was the Riley Creek IV, from 12,700 to 10,500 cal yr BP. This final advance is believed to have been marked by cooler and wetter climate (TenBrink and Waythomas 1985). There was an additional small advance of the Riley Creek glacier from 7,000 to 6,500 cal yr BP (Calkins 1988). Similar small glacial advances in the eastern Alaska Range have been dated at 5,600, 4,600, 4000, 1400, 800, and 300 cal yr BP (Begét 1994; Reger and Pewe 1969; Reger, et al. 1993). The Shaw Creek Flats, as well as much of the Yukon-Tanana Uplands, was not glaciated during the Donnelly Glaciation and so may have served as refugia for certain biotas during this time (Guthrie 1990).

2.5 Climate and Paleoecology

The modern regional climate is subarctic continental, with long winters and short summers (Streten 1969). Weather patterns are influenced by the Aleutian Low of the Gulf of Alaska and the weather systems of the North Pacific Ocean (Streten 1969). The Alaska Range blocks a large percentage of the warm, moist oceanic air masses from reaching this region, and so it is generally dry with an average modern annual precipitation of 12.94 inches, the majority of which falls as rain during the warmer months (National Climate Data Center, 2011). Mean temperature in the winter is -17 °C (National Climate Data Center, 2011) and at the winter solstice the area only receives 4 hours of light (Streten 1969). Today the area is infamous for the strong winds that move through the low valley regions, especially during the winter months. These winds are responsible for transporting the aeolian sediments observed at the Mead Site, as well as the erosion seen in the area. It is common for temperature inversions to form over the river during the winter months, which in turn result in pocketed areas that will sometimes have over a 12°C temperature difference with only slight changes in topographical relief (Dilley 1998; Wendler, et al. 1980).

Vegetation of the region falls under the larger umbrella of the boreal forest/taiga. This region also contains patches of relic steppe tundra vegetation which is found on the well drained south facing bluffs near the Tanana River, (Young 1982; Zazula, et al. 2005) such as where the Broken Mammoth

archaeological site is located. Young (1982) believes that these present day patches can be used as an analog for a more widespread vibrant form of this vegetation that was most likely present during the late glacial Period throughout Beringia. This conclusion has been called into question by others, however, as pollen data from the area indicates a different, less diverse paleo plant biome than that seen in these "relic" plant communities (see Ritchie and Cwynar 1982).

Major paleoclimatic events that may correspond to human occupation at the Mead Site which will be discussed below are the Bolling/Allerod, the Younger Dryas, the Holocene Thermal Maximum and the 8.2k event (Beget 2001; Bigelow and Powers 2001: 189; Kaufman, et al. 2004).

2.5.1 Bolling/Allerod

The Bolling/Allerod warming event began around 16,000 cal years BP (Viau, et al. 2008) and is marked by a warmer and wetter than previous climate. This warming event has been correlated with a rise in lake levels and a shift in vegetation from tundra to dwarf birch and willow (Bigelow and Edwards 2001; Mann, et al. 2001). It is during this time of warming and changing vegetation that the extinctions of megafauna begins to take place (Halle, et al. 2009; Hopkins 1982) and that the presence of humans is first evidenced in interior Alaska at Swan Point (Holmes 2001). Hopkins (1982) termed this period the Birch Zone because of palynologist Livingstone's (1955) work which documented the increase in birch (*Betula*) pollen observed in cores.

There is general consensus among researchers that this time was definitely warmer and wetter than the preceding glacial period (Anderson and Brubaker 1993; Barber and Finney 2000; Bartlein, et al. 1991; Bartlein, et al. 1995; Edwards and Barker 1994; Edwards, et al. 2001; Hu, et al. 1996). Abbott et al. (2000), through the use of lake-level reconstruction at Birch Lake and radiocarbon dates obtained from pollen and macrofossils found that prior to 12,700 14C yrs BP (14990 +/-100 cal yr BP) the lake was either seasonally dry or dry year round, indicating aridity in the region. After this period Birch Lake was affected by increased effective moisture and rapid lake level rise that was interrupted by a period of increased aridity (from 11,600 to 10,600 14C years BP (13,460 to12,610 cal yr BP) which was most likely due to the Younger Dryas) (Abbott, et al. 2000).

Viau et al. (2008:1442), through the use of pollen diagrams and the modern analogue technique (MAT) reconstructed temperature and precipitation during this time period and found that precipitation increased during the Bolling/Allerod to a maximum at around 11,000 cal yrs BP, and then rapidly decreased until 8,000 cal yrs BP.

2.5.2 Younger Dryas

The Younger Dryas (YD) was a cold period that took place roughly 12,900 to 11,700 cal yr BP (Broecker, et al. 2010). As evidenced by the ^{18}O ratios from the Greenland ice cores, this event began with

gradual cooling and terminated with a century of dramatically colder temperatures (Steffensen, et al. 2008), although the regional expression of the YD varies (Kokorowski, et al. 2008). While multiple theories over the catalyst for this cold period have been put forward (ranging from bolide impacts to the draining of proglacial Lake Agassiz) the most well supported theory at this time is that the Younger Dryas is a Dansgaard-Oeschger (DO) cold event (Mangerud, et al. 2010; Stuiver and Grootes 2000).

DO events are believed to result from changes to the thermohaline circulation (THC) of the north Atlantic, which allows fresh water to stay on the surface of the ocean (Boyle and Keigwin 1987; Clark, et al. 2002). Under normal conditions of THC, warm water circulates to the north where it cools and sinks at high latitudes and then upwells back to the surface of the ocean at lower latitudes. When the THC is interrupted, fresh water (which is less dense than salt water) stays on the surface of the ocean and freezes into sea ice, creating a positive feedback loop; the sea ice increased albedo while inhibited heat being released from the oceans which caused major shifts in wind patterns which helped to cool the climate (Brauer, et al. 2008). The climate was one of extreme cold in the northern regions (especially around the North Atlantic) and a weakened Asian monsoon (Qiao, et al. 2009).

The Younger Dryas is indicated in the Tanana Valley through a change in vegetation and pollen from lake cores (Begét, et al. 1991; Bigelow 1997; Bigelow, et al. 1990a; Bigelow and Edwards 2001; Kokorowski, et al. 2008). During this time there was a reversal to sage and grasses in the pollen record, indicating a colder and drier climate (Bigelow 1997:151). Hoffecker and Elias (2007) note that one of the strongest signatures for the Younger Dryas is the increase in bison remains found at archaeological sites that date to this time period which they say indicates an increase in the amount of steppe habitat. At the end of this period woodlands begin to be established on the landscape with the expansion of *Populus*, and *Alnus* is seen for the first time in the region (around 9,000 14C yr BP (10,120 +/-110 cal yr BP)) (Anderson, et al. 2004). Lake levels at this time were low while seasonality was high, with summer temperatures being warmer and winter temperatures being colder than they are today (Barber and Finney 2000; Bartlein, et al. 1991). Winter precipitation may also have been greater during the winter as the Aleutian low was likely seasonally stronger in the winter (Kokorowski, et al. 2008). At Birch lake, drier and cooler conditions are inferred for the YD from an increase of *Artemisia* in the pollen record and a decrease in the lake's level. The pollen record from Harding Lake has increased levels of *Populus*, but the dating of this increase is suspect, as decay counting 14C analysis was used on 10cm core slugs (other lake cores which were dated by AMS show the *Populus* zone being 2000-1000 yrs younger than those dated on core slugs using decay counting) (Bigelow and Powers 2001). Because of this, the rise in *Populus* seen at Harding Lake is believed to occur after the YD.

Much of Interior Alaska is in the extended rain shadow of the Alaska Range and so the increase in aridity may have been exponential during this time (Bigelow 1997). This climatic period is expressed in a sand layer found at several archaeological sites in the region (Broken Mammoth, Dry Creek, and Upward

Sun River) and is believe to indicate windy conditions, a lack of surface vegetation to stabilize the landscape, a lack of soil formation, and continued aeolian deposition (Bigelow 1997; Bigelow, et al. 1990b; Potter, et al. 2008).

The effect of the Younger Dryas on paleo-populations has not been concretely determined and there is contention as to whether populations were little affected by this event (Bigelow and Powers 2001; Mason, et al. 2001), or if it punctuates a population decline in the region (Bever 2006; Potter 2008d). A general species distribution was constructed by Yesner (1996) from the faunal remains at the Broken Mammoth site for the period just after the Younger Dryas. The assemblage was mainly composed of bison, wapiti and caribou remains, where as the earlier occupation at the site (which correlated with the Birch zone) was mainly composed of small mammal and bird remains (and some bison bones). Mason et al. (2001:541) hypothesize that the loess dunes that formed during this period may have been utilized to disadvantage these larger mammal species. A caveat to this discussion is the unreliable nature of caribou (in terms of migration routes). Burch (1972) noted that a reliance on caribou might actually be an indication of decreased population.

The YD signal is not well expressed at many of the sites in interior Alaska, and this is most likely due to two factors. The first of these, which was mentioned above, is because the Alaska Range blocks weather systems from the ocean. Much of the ocean produced cooling that is evident in other areas would not reach the interior. Also, during the YD a high pressure system is believed to have been located to the north of Alaska and during the summer this high pressure system would have resulted in drier and warmer conditions (Edwards, et al. 2001).

2.5.3 Holocene Thermal Maximum

The Holocene Thermal Maximum (HTM) (11,500 to 9,100 cal yr BP) started due to a strong summer insolation anomaly which was most likely catalyzed by the Milankovitch cycle (Kaufman, et al. 2004). Insolation was higher in the summer and lower in the winter than at present (Kutzbach, et al. 1998). Temperatures in the arctic and subarctic during this event were estimated to have been 5-8°C warmer than present. The rapid rise in temperature may have taken place over a very short time period, with estimates ranging from 5 to 50 yrs (Hoek and Bos 2007; Prasad, et al. 2006). This short time frame of rapid temperature increase most likely resulted from the amplification of the Milankovitch Maximum by a number of variables, chief among them the reduced albedo of ice-free Beringia. Range expansions of beetles (Nelson and Carter 1987), beaver (MCCulloch and Hopkins 1966), aquatic plants, and *Populus balsamifera* (Brubaker, et al. 1983; Mann, et al. 2002) are evident during this time, indicating warming temperatures. In the Yukon-Tanana upland area well-developed soils formed around 11 cal yr BP (Porter 1988; Weber, et al. 1981).

At the end of the Holocene Thermal Maximum there is evidence of spruce moving into the Tanana River Valley (Bigelow 1997; Bigelow and Powers 2001) which is tentatively linked to a decrease in population (Potter 2008d; West 1981). Paludification has been linked to black spruce expansion which may have hindered human movement across the land. Mason et al. (2001) and Potter (2008d) also found an inverse correlation between Denali occupations and the HTM.

Reconstruction of Birch Lake water levels at the beginning of this period indicate the climate was dry and warm and that summer precipitation was 25-40% less than present while the end of the HTM saw a rise in lake levels and moisture (Abbott, et al. 2000; Barber and Finney 2000; Bigelow and Edwards 2001).

2.5.4 8.2k Event

The 8.2 ka event (the "younger" Younger Dryas) is a cooling event and is more ephemeral in the paleoclimate record than the Younger Dryas (Beget 2001). Unlike the gradual cooling seen for the Younger Dryas period, the 8.2 k event began very abruptly with rapid cooling taking place in possibly a matter of months (Alley 2007; Alley and Agustsdottir 2005). As with the Younger Dryas event, there are many hypothesis as to the catalyst (e.g. the final sudden draining of Lake Agassiz which would have caused an influx of fresh water into the oceans and shut down the thermalhaline circulation) and termination (e.g. increase in the greenhouse affect due to a massive influx of methane to the atmosphere resulting from the Storegga landslide off the coast of Norway) of this event (Barber, et al. 1999; Beget and Addison 2006).

There is a decline in spruce pollen which correlates with this event (Bigelow 1997; Shimer 2009), although if the decline is due to competition from other species or from changing climate is not concretely established (Anderson and Brubaker 1994). Peat sections near Fairbanks show signs of aridity during this time, which has been credited to resulting from colder conditions (Andreev and Peteet 1997). It appears that loess deposition may have overtaken pedogenic processes, which has been attributed to resulting from a more glacial climate (Bigelow and Beget 1991; Muhs, et al. 1997).

A population spike has been noted by some (Mason, et al. 2001) as a result in inferred increased numbers of caribou. Caribou do better in cold and arid conditions than in warm and wet conditions (due to the smaller amount of snow fall and increased growth of lichen) (Mason, et al. 2001). The supporting evidence for this population spike is somewhat tenuous (Potter 2008b; Potter 2008d). The number of sites that have been radiocarbon dated to this event is small, thus any correlations between site occupation and the 8.2k event are fragile and subject to change as more sites are investigated.

As evidenced by the Greenland ice cores (GRIP and GISP2) in addition to the 8.2ka event there are four other cooling events during the early Holocene which may have lasted for tens or hundreds of years. These are recorded at 11,100, 9,950, 8,800, and 8,500 cal yr BP (Alley 2004; O'Brien, et al. 1995; Rasmussen, et al. 2007). Evidence of all five of these cooling events is ephemeral in Alaska as their signal is partially obscured due to the melt water pulses from the ice sheets (Ehlers and Gibbard 2004).

2.5.5 Mid to Late Holocene

In comparison to the rest of the Holocene and Late Pleistocene record, there is a dearth of information on the climate and paleoecology for the Mid to Late Holocene, this is most likely the result of several factors. First, the preservation of proxies may be poor (i.e. lack of preservation in soil due to acidic conditions from the modern boreal forest or lack of resolution in lake cores). Second, the climate and paleoecology was similar to present day conditions and so little time is spent investigating this period. Finally, the tendency of researchers to focus on the late glacial/early Holocene in regards to climate determinalism as this was the period when colonizing populations were believed to enter the New World. Regardless, this period is the most visible in the archaeological record of Interior Alaska and there is no reason to assume that climate would have had any less of an effect on paleopopulations than in the preceding periods.

During the Mid to Late Holocene there are several periods of rapid climate cooling. These are dated to 6000-5000 cal yr BP (with a cold spike at 5,600 cal yr BP), 4,200-3,800 cal yr BP, and 3,500-2,500 cal yr BP (Mayewski, et al. 2004). A decrease in the amount of organic sediment in lake cores from the Northwest Canada after 2000 cal yr BP suggest a cooler than present climate and may represent Neoglaical cooling (Ruhland, et al. 2009). It is also during this time that the fire regime of the state changed to more frequent fires which has been linked to the increase in black spruce populations (Hu, et al. 2006; Mason and Bigelow 2008).

Prior to 4,000 cal yr BP, the Tanana River Valley was cooler and wetter than present day. From around 4000 yrs BP to 400 yrs BP the climate of the Tanana Valley is believed to have been drier and warmer than at present, as evidenced by fewer and less intense floods of the Tanana River (Mason and Beget 1991). Flood deposits indicate that after 400 yrs BP the climate again became cooler and wetter than the preceding period (Mason and Beget 1991). There is a perceived increase in population after 6,000 cal yr BP due to an increase in the abundance of sites dating to this period; however the increase in sites may be due to biased sampling methods and preservation in the record (Potter 2008d).

2.5.6 Pollen

Before 16,000 cal yrs BP the pollen record is dominated by forbs and graminoids. The Birch Zone (indicated by the presence of dwarf birch and willow) began just after 16,000 cal yrs BP and is marked by a significant increase in birch pollen in the record and a change from herbaceous tundra to shrub tundra (Anderson, et al. 2004; Ritchie and Cwynar 1982; Yesner 2001). The Birch Zone lasted for approximately 6,000 years. The catalyst for this change in vegetation is believed to be the wetter and warmer conditions during this time (Finney, et al. 2004). At 14,000 ± 250 cal yr BP the pollen record from Birch lake shows *Betula* as being the dominant constituent with Cyperaceae and *Salix* also making contributions (Bigelow and Powers 2001).

At 13,000 ± 250 cal yrs BP *Betula* is still the dominant constituent at Birch Lake with *Salix* showing up in the record in small percentages indicating a birch shrub tundra with willow (Bigelow and Powers 2001). Also during this time period Birch Lake shows a moderate amount of *Artemisia* pollen, which grows in alpine or arid conditions. *Salix* appears in the record in high percentages around 12,000 ± 250 cal yr BP (although *Betula* is still the dominant pollen represented). *Populus* was the dominant vegetation in Interior Alaska forests from 13 ka to 10 ka and resulted in a *Populus* dominated woodland (Anderson, et al. 2004; Edwards, et al. 2005).

After the Birch rise, white spruce appears in the macrofossil and pollen record at around 10,000 cal yr BP, although it is not well represented in many records until the main Spruce Rise (black and white spruce) (beginning after 9,000 cal yr BP) (Brubaker, et al. 2005). *Alnus* also appears in the pollen record in the Central Alaska around 10 cal yr BP, although it is absent from the Birch Lake pollen record until after 9,000 cal yr BP. This dearth of *Alnus* pollen has been attributed to continuing aridity in the Tanana River Valley (Bigelow and Powers 2001). By 6,800 cal yr BP the present day vegetation of boreal forest was established in the area (Anderson, et al. 2004; Bartlein, et al. 1991).

Both macrofossil and pollen distributions are also important to paleoclimate reconstruction, but there are limitations to their application in paleoclimate reconstruction. Pollen can more easily travel via wind, and certain plant species produce more pollen than others. The pollen records found in lakes could be misrepresentative of the actual paleo-vegetation of an area. Not all plants produce pollen, and macrofossil and pollen survivorship is contingent on multiple factors such as the morphology of the macrofossil and the environmental conditions to which it is subjected. Due to the coarse nature of loess, it is a poor environment for macrofossil and pollen preservation.

2.6 Loess

Studies of the Tanana River loess have been extensive (see Beget 1996; Beget 2001; Beget, et al. 1990; Dilley 1998; Lagroix and Banerjee 2006a; Lagroix and Banerjee 2006b; Muhs, et al. 2001; Muhs, et al. 2003; Muhs, et al. 2008; Muhs and Bettis 2003; Muhs and Budahn 2006) and there is ongoing discussion over the mineralogy and geochemistry of loess in the Tanana River Valley. Rate of deposition, distance to source, and other variables inform contextual understanding of archaeological sites as well as understanding of preservation of faunal material, and must be taken into consideration when attempting to elucidate site formation processes.

Previous studies (Muhs, et al. 2003; Muhs and Budahn 2006) of Alaskan loess have determined that it is mainly composed of quartz and mica. Its clay mineralogy is composed of Mg-rich chlorite, smectite, kaolinite, mica, clay-sized quartz, plagioclase, and feldspars, with plagioclase being the most abundant clay mineral (Muhs, et al. 2003).

While not as high in carbonates as other North American loess, Interior Alaskan loess is moderately to highly calcareous (Muhs and Budahn 2006). By comparing the sediment carbonate content of Tanana, Yukon and Nenana River silt (the sources of loess) to that of visually unaltered loess, Muhs and Budahn (2006) found that the loess had significantly lower carbonate content than the river silts, indicating that this "unaltered" loess has actually experienced leaching. This is an important principle for vegetation reconstruction, as the boreal forest is more acidic than herb tundra vegetation, and so leaching under herb tundra vegetation would require a slower sedimentation rate than under the boreal forest (Muhs and Budahn 2006).

Loess forms in glacial and periglacial environments through two main processes, frost shattering and glacial grinding (Muhs and Bettis 2003). The silt-sized particles that result from these two processes are deposited in glacial till, and then reworked and transported by glacial outwash and other fluvial processes. At any point in this continuum these small particles can be entrained and then deposited by wind.

The relationship between aeolian deposition and glacial episodes is important for paleoclimate reconstructions. Loess deposition occurs through almost continuous "background dust flux" and through discreet aeolian depositional events (Beget 2001). Through geochemical studies of loess weathering, source area and wind directionality can all be examined.

Studies of loess and aeolian sands have yielded excellent records of glacial and interglacial cycles. The sedimentary structure of loess deposits is influenced by a number of different variables such as, wind intensity, distance to source, storminess, and soil formation. Loess sedimentology along with environmental magnetism and tephrachronology has been strongly positively correlated with ice and marine core records to indicate climate change (Beget 1996; Beget 2001; Beget, et al. 1990; Muhs, et al. 2008; Muhs and Bettis 2003).

There are two schools of thought on the relationship between loess deposition and glaciation. In the first it is believed that an increase in loess deposition indicates glaciation, while paleosol development indicates periods of decreased deposition and interglacial environments (Pewe 1965; Pewe 1975).

In the first view, magnetic susceptibility has been utilized as a proxy for glacial periods, as higher magnetic susceptibility values may indicate glacial periods, while lower values can indicate warmer periods (Beget 1996; Beget 2001; Bettis, et al. 2003; Bigelow, et al. 1990b; Lagroix and Banerjee 2002; Lagroix and Banerjee 2006a; Lagroix and Banerjee 2006b; Muhs, et al. 2008; Muhs and Budahn 2006; Muhs, et al. 2004). At the end of the late Pleistocene and the beginning of the early Holocene there were large loess depositional events in Alaska that may have been seasonally produced (Thorson and Hamilton 1977). It is believed that these events resulted from large areas of exposed bare ground in the floodplains in interior Alaska (Pewe 1965), and estimates of the wind direction and intensity of these loess storms can be found in the orientation and extend of dunes (Hopkins 1982). It has been proposed that the rise of forests and alder

around 9,000 cal BP decreased the source area for loess, thus decreasing the depositional events seen in the record (Mason, et al. 2001).

The second view holds that glaciation is important for the formation of loess, but that its deposition and accumulation takes place during non-glacial periods. Muhs et al. (2003) found that only moderate deposition took place during glaciation, and that vegetation is a key factor in loess accretion. In their study they found that while glacial periods produced the loess particles the conditions during these times (cold and increased wind) were not conducive for loess buildup. Instead it was during periods when thick vegetation could form on the landscape (such as the boreal forest in Alaska) that loess accumulation was highest; as this vegetation served as an effective trap for the loess. In the model these investigators put forward loess accumulation in central Alaska occurs because of the presence of the tall vegetation rather than an intensification of glacial conditions.

2.7 Site Formation Processes

Site formation processes are a critical element of archaeological investigations because archaeologists utilize the patterning of artifacts to infer past behavior. Site formation processes identify patterns of past human activity and separate them from natural and more recent human processes.

2.7.1 History

Studies of site formation developed out of New Archaeology, which promoted the theoretical approach involving the identification of behaviors that are common to all cultures across time (Binford and Binford 1968; Clarke 1968; Watson 1985; Willey and Sabloff 1993). Regardless of what else New Archaeology did, the attention to scientific and systematic methods used by the new archaeologists was later applied to multiple sub-disciplines, such as archaeometry, geoarchaeology, and taphonomy (Stein 2001).

Studies into site formation processes began in earnest in the 1960s and 1970s when archaeologists began to notice that the location of artifacts could shift after deposition (Stein 2001). During the 1970s a number of archaeologists began investigating and publishing on site formation processes. Foremost among them was Schiffer, whose works on site formation processes brought their importance to the attention of the larger archaeological community. Schiffer is mainly known for his work on the behavioral theoretical approach, which included investigations into formation processes, and his attempts to create laws and theories to explain the archaeological record (1972). He also expounded the idea that archaeologists had to distinguish between the natural and cultural processes that influenced artifacts after they had been deposited in order to infer behavioral information (Schiffer 1972).

2.7.2 Systemic Context

In his 1972 article, Schiffer set out a flow model to show the different stages that an artifact could potentially go through. The first such stage is the systemic context which, "labels the condition of an element which is participating in a behavioral system" (1972:157). Systemic context is further broken down into five processes; procurement, manufacture, use, maintenance, and discard (1972:160). Each of these five processes can then be further broken down into different stages, and these stages can be broken down into one or multiple activities (1972:160). Systemic context relies on the theory that certain processes took place at certain locations and that at these locations the odds of finding a particular artifact are greater than at other unrelated locations.

With the final process, discard, the use-life of an artifact comes to an end. According to Schiffer this is when the artifact first becomes classified as refuse. Schiffer sets out three different types of refuse. Primary refuse results from discard of an artifact at the location of its use. Secondary refuse results from the discard of artifacts at locations that are different from the locations at which they were used (i.e. a midden). The final type of refuse is termed "de facto refuse" and it refers to artifacts that were never actually discarded but are still found in archaeological context, which is the next stage in Schiffer's flow model (1972:160). Schiffer describes archaeological context as, "materials which have passed through a cultural system, and which are now the objects of investigation of archaeologists" (1972:157).

Schiffer was not alone in the quest to distinguish primary and secondary site formation processes from each other and determine their impact on the archaeological record. Multiple other publications from the late 1970s and early 1980s also put forward hypotheses regarding whether the patterning of artifacts found at archaeological sites resulted from processes different from the primary cultural process (e.g. Bocek 1986; Erlandson 1984; Gifford-Gonzalez, et al. 1985; Rick 1976; Stein 1983; Villa 1982). It was during this time that experimental research began to discern the effects of natural processes by controlling for certain variables. Formation processes were also of interest to archaeologists who were not behavioral archaeological theorists, but rather utilized formation processes concepts in their methodological approaches (e.g. Bar-Yosef 1993; Nash and Petraglia 1987). From concerns regarding formation processes and the patterning of deposits grew the sub-field of geoarchaeology, first termed by Renfrew in 1973 (Renfrew 1976).

During the 1980s the basic unit of site formation analysis changed from the artifact to the deposit. This change increased the importance of geoarchaeology to all investigations as it showed that site formation analysis was important at all types of sites, not just those of great antiquity (Goldberg, et al. 2001; Stein 2001).

While much of the theory behind behavioral archaeology has come under criticism, the concept of the transformative secondary site formation processes gained importance for the understanding of archaeological sites. There are three types of processes that need to be considered in investigations of

formation processes. The first of these are the primary cultural processes that form the archaeological record, including such activities as procurement, use, maintenance, and discard of materials and artifacts. Cultural processes are responsible for the behavioral patterning of artifacts at different locations at a site (activity areas). The second type of process is also cultural in nature and encompasses those processes that disturb, remove, or distort the primary cultural processes. The third type of natural processes are those that alter, remove, or preserve the original material record. The second and third types account for the transformative nature of the archaeological record and are generally termed secondary site formation processes.

2.7.3 Soil Formation Processes

Natural site formation processes are incredibly important to understand spatial patterning of artifacts and deposits. One of the most important and basic of these processes is that of pedogenesis, or soil formation. To understand pedogenesis and its importance in archaeology, it is necessary to first have an understanding of the basics of pedology and soil geomorphology.

Soil geomorphologists and pedologists have outlined a series of models for the processes of soil formation, the variables that drive the processes, and how soils change as landscapes evolve (Birkeland 1999; Schaetzl and Anderson 2005). The most basic of these models is the "multiple-process model" (Schaetzl and Anderson 2005) wherein soils are thought to form as the result of biogeochemical processes that are determined by the ecosystem. This relationship can also be expressed as the "internal soil-forming processes" which are driven by the "external soil-forming factors" (Buol, et al. 1997). In the "multiple-process model" Simonson (1959; 1978) groups the internal pedogenic processes into four categories: addition (such as organic material), losses (leaching of different materials), transfers (illuviation of clay or iron), and transformations (decomposition of organic material). The external soil-forming factors are outlined in the State Factors model.

First put forward by Jenny (1941; 1980) the five external factors in the State Factors model are climate, organisms (both plant and animal), relief (topography and landscape setting), parent material, and time. Their relationship is expressed in the equation $S=f(cl, o, r, p, t)$ and is known as the CLORPT model (Birkeland 1999). In this equation soil is a function of the interaction of the five factors, and while the equation can never actually be "solved", the effects of each factor can be modeled by holding all of the other factors constant and examining the variation of that particular factor (Jenny 1980). These qualitative statements are described as sequences (the climosequence, biosequence, toposequence, lithosequence, or chronosequence) while the resulting quantitative statements are described as functions (climofunction, biofunction, topofunction, lithofunction, or chronofunction) (Birkeland 1999; Jenny 1980; Schaetzl and Anderson 2005). There are problems with this type of modeling, as each of the five factors is not truly independent (with the exception of time), and as the factors do not really explain either landscapes or the

actual pedogenic process (they describe the external factors that affect the soil). None the less these factors need to be considered when trying to discern site formation processes.

Bidwell and Hole (1965) augmented the State Factors model to include the effects of human activity, which can modify the traditional five factors. For example, the R factor (relief) can be modified when cultures construct terraces or dig canals. Amundson and Jenny (1991) account for the influence of human activity by creating a sixth factor, the anthropogenic state factor.

Another key concept in soil geomorphology that is important to this discussion is the relationship between the stability of a landscape and its soils. Soils generally form on stable landscapes (landscapes that are undergoing no major erosion or aggradation). The K-cycle model by Butler (1959; 1982) depicts landscapes and soils as "periodic phenomena" in which there are unstable phases of erosion and deposition (Ku) and stable phases (Mercader, et al. 2002) during which pedogenesis takes place.

The final model that merits discussion here is the soil evolution model (Johnson and Watson-Stegner 1990) which combines aspects of the three models described above for a more dynamic representation of pedogenic processes. It explicitly employs the concept of soil formation as a non-linear process that has two types of pedogenesis: progressive and regressive. Progressive pedogenesis includes the factors and processes that increase soil development and horizonation, while regressive pedogenesis includes the factors and processes that create haploidization (Johnson and Watson-Stegner 1990). The processes of site formation which result from pedogenic processes are usually divided into the categories of horizonation and haploidization. Horizonation processes are those that produce soil horizons, while haploidization processes are those that mix soils (Schaetzl and Anderson 2005).

Soil horizons result from the alteration of soil parent material and are grouped into a series of categories. Variables that produce soil horizons are: accumulation and humification of organics at the soil surface, the removal of clay, the mixing and humification of organics into the parent material, leaching, weathering, development of the soil structure, and illuviation (Duchaufour 1998). The easiest way to examine these processes is from the top down, beginning with the organic horizon.

The O horizon is composed mainly of soil organic matter and is divided into three categories: leaf litter, peat bogs (wet peats), and blanket bogs (dry peats) (Buol, et al. 1997). Each of these types of O horizons influences the archaeological record to different extents. For example, organic preservation is generally better in wet peat settings than dry peat settings due to the anaerobic nature of these bogs (Holliday 2004).

The A horizon (a mineral soil) is characterized by the addition of humified (decomposed) organic material, and is the most dynamic region of the soil column (Buol, et al. 1997; Schaetzl and Anderson 2005). Because of this, archaeological deposits that are located in A horizons are more likely to be affected by diagenic processes. The A horizon is also characterized by decalcification and desalinization (loss of calcium carbonate and slats) and elluviation (loss of clay-size particles).These losses, when combined with

the addition of the humic organic material, lead to acidification of the A horizon, which is a very important factor for archaeological preservation (more acidic conditions lead to less organic preservation of archaeological remains). The modern boreal forest of Interior Alaska is acidic in nature and results in poor preservation of organic remains. A horizons are also the zones where most floral (such as root growth) and faunal (such as ground squirrel) activity is found in the soil column, and as a result are the most disturbed by these processes (Johnson and Watson-Stegner 1990).

The E horizon is the horizon of elluviation (leaching via water) of clay, sesquioxides and humus (Schaetzl and Anderson 2005). Elluviation results in the destruction of the primary bedding of the soil column and most organic material. Sites that exhibit E horizons have poor preservation.

The B horizon is characterized by leaching, illuviation (addition), weathering, and soil formation (Schaetzl and Anderson 2005). In B horizons it is common for the primary bedding to be destroyed due to mixing of the sediments from flora and fauna and the translocation and illuviation of different minerals. These processes can also affect archaeological sites. Illuviation of bases (such as calcium carbonate) into B horizons will enhance preservation of organics, while illuviation of sesquioxides (such as iron) will inhibit preservation of organics. Fluctuations in the water table can also inhibit the preservation of organics and is evidenced from gleyed horizons.

There is little recorded data on the effects of horizonation processes on archaeological sites, with the exception of micromorphological studies (see Courty, et al. 1989; Goldberg 2000; Goldberg and Berna 2010; MacPhail and Goldberg 1990). Haploidization processes, on the other hand, are well evidenced in archaeological research and account for the majority of disturbances to primary site context.

The most common haploidization processes at archaeological sites are those of bioturbation (including floralturbation and faunalturbation). Floralturbation is the mixing and disturbance of soils through plant growth and fuanalturbation results from animal activities. Freeze-thaw processes (cryoturbation), gravity (graviturbation), shrink-swell processes (argilliturbation), and wind movement (aeroturbation) also result in haploidization (Grave and Kealhofer 1999; Holliday 2004; Johnson and Watson-Stegner 1990; Schiffer 1987).

Bioturbation is indicated at a site by; tilt and orientation of cultural remains (non-horizontal orientation), a lack of intact features, diffusion (both vertically and horizontally) of clustered remains, mixing or movement of remains resulting from a single activity, and by the visual correlation of bioturbation and artifact location (Holliday 2004: 283; after Michie 1990).

Faunalturbation can result from a variety of burrowing activities by a diverse range of creatures (e.g. earthworms, ants, termites, ground squirrels and other small animals) and can result in the mixing of soils, changes in the stratigraphic relationships between archaeological deposits and soil horizons, the preferential destruction of delicate artifacts, the downward movement of coarser grained sediments, and the upward movement of finer grained sediments (Butler 1995; Hole 1981; Leigh 2001; Mitchell 1988; Pierce

1992; Waters 1992; Wood and Johnson 1978). Faunalturbation can also cause stones and artifacts that were originally at the surface of a site to move downward and form subsurface "stone lines" and artifact horizons (Balek 2002; Erlandson 1984; Johnson 1990; Johnson and Watson-Stegner 1990; McBrearty 1990). Burrowing by larger animals can cause large stones to move both up and down, so stone lines are not necessarily produced by this type of bioturbation (Mello Araujo and Marcelino 2003). In addition to mixing the soil, termites and ants also increase the pore space in soil, which can in turn increase the dissolution of bone and other organics at archaeological sites (Cahen and Moeyersons 1977; McBrearty 1990).

Floralturbation is the mixing of soils by plants, mainly due to the process of root growth (Johnson 1990; Wood and Johnson 1978). Roots can break artifacts, disturb features, add organic material to soil horizons, and create pathways for other materials to travel through the soil column (e.g. Anderton 1999; Johnson and Watson-Stegner 1990). The most destructive type of floralturbation results from tree uprooting, or tree throw (Limbrey 1975; Wood and Johnson 1978). Tree throws can mix the A and B horizons, disturb archaeological features, and produce stone lines (Callum 1995).

Argilliturbation results from the mixing of soils due to the swelling and shrinking of clay minerals due to wetting and drying respectively (Schaetzl and Anderson 2005). Seasonal wetting and drying cycles of soils rich in clay material (Vertisols) can result in the formation of large cracks in the soils which can destroy the soil stratigraphy as well as displace artifacts (Duffield 1970; Hofman 1986; Morris, et al. 1997; Wood and Johnson 1978).

Disturbance due to freeze-thaw cycles is termed cryoturbation and can have similar effects to argilliturbation on archaeological assemblages (Wood and Johnson 1978). Cryoturbation effects on archaeological assemblages are frost heave and thrust, involutions, gelifluction, and frost cracking; in Alaska these effects have been investigated mainly through experimental studies (Bowers, et al. 1983; Hilton 2002; Hilton 2003; Hopkins and Giddings 1953; Mackay, et al. 1961; McKennan and Cook 1968; Reid 1984; Schweger 1985; Thorson and Hamilton 1977; Thorson 1990; Wilson 1990; Wood and Johnson 1978). All of these processes work to obscure, and distort the natural stratigraphy at sites, as well as re-orient artifacts and move them through the soil profile.

Aeroturbation (wind effects) can also alter sites. Wind can help preserve the primary context of artifacts through burial, but it can also erode the landforms on which assemblages were first deposited, thus destroying their primary contexts (such as lag surfaces through the process of deflation) (Rapp and Hill 2006). Graviturbation or mass wasting is the movement down-slope of deposits. This movement can be slow (soil creep, solifluction) or fairly fast (landslides, slope failure) (Rapp and Hill 2006). Many times these processes are the result of cryoturbation or other bioturbational processes, such as at Iyatayet or at the Engigstack site (Hopkins and Giddings 1953; Mackay, et al. 1961).

Formation processes of sites are also dictated by the landform and environment of an area (caves, basins, alluvial settings, deserts, etc.) (the CL and R factors of the State Factor Model) as well as by the depositional system for sediments (alluvial vs. aeolian vs. lacustrian) (Rapp and Hill 2006). Another factor in site formation is welded soils. These are soils that are shallowly buried or incorporated into the pedon of the overlying soil due to their thickness and length of stability; these two soils overlap and meld together (Retallack 1990). Welded soils can have obscured A horizons which can create problems for interpretation of archaeological site contexts.

Equifmality is also very important in discussions of site formation processes. An artifact found below the surface soil, for example, may have arrived at its location through bioturbational processes or simply through depositional processes (see Leigh 1998; Leigh 2001; Van Nest 2002). Grain size analysis, micromorphology, geochemical analysis, landscape evaluation, and dating are used to separate these different processes from one another.

Pedogenic processes, including diagenic alterations (which are all alterations that a sediment undergoes after it has been deposited), are those processes that produce or change soils, and these processes can also alter archaeological deposits. Pedogenic processes include translocation and gains and losses of materials in the soil profile (Buol, et al. 1997). Pedoturbation, the mixing processes related to soil formation, can also disturb artifacts and the context of sites (Schiffer 1987).

Secondary cultural processes can involve any number of different activities. Site reuse, excavation, plowing, etc. all have the possibility of disturbing the original cultural deposits at a site (Herz and Garrison 1998; Waters 1992). Human activities can also influence the five factors of soil formation. Location is important in trying to determine these secondary cultural processes, as many times landscape location is a factor in the reuse of sites and the duration of occupation. Exposed ridgelines or knolls (such as at the Mead Site) with good viewsheds are commonly believed to be lookout sites. It is probable that these sites were utilized by multiple different groups of people over time, and that the more recent occupations disturbed the cultural remains left at these sites by earlier groups of people. Many times these secondary cultural processes are readily evident at sites (obvious cross-cutting of earlier features and stratigraphy), while other times there might be little or no real evidence of these secondary cultural processes (such as at surface lithic scatters or other surface sites). Chemical alteration due to human activities is also a prevalent disturbance at archaeological sites (Eidt 1985; Holliday 2004).

2.8 Micromorphology

Micromorphology analysis studies the *in situ* structure of sediments and soils and supplies information regarding site formation processes and spatial variation not available at the macroscopic level of analysis (Goldberg and MacPhail 2006). Methodology ensures that the undisturbed samples are used in thin section so the composition, texture, and fabric observed through the microscope are the same as that of

the intact soils in the field. The utility of micromorphological analysis has been shown at a number of recent excavations from around the world (for example see Homsey and Capo 2006; Kelly, et al. 2006; Matthews, et al. 1997; Schiegl, et al. 2003). Past landscape surfaces can be reflected in the pedofeatures found in thin sections (French 2003). By studying the pedofeatures, microstructure, and microfacies of the sediments at the Mead Site through thin section analysis, it is possible to distinguish pedogenic and diagenic features and to interpret the site formation processes. The fabric of a soil's microstructure is determined by what it formed in (the parent material) and the alterations during pedogenesis (McCarthy 2002).

For example, subangular blocky peds are usually described as Bt horizons and are formed by the shrinking and swelling of clays (Retallack 1988). Also, the birefringent fabrics of soils can give clues to the site formation processes (Fitzpatrick 1993). Weakly birefringent clay accumulations are an indication of age in the soil (the more orientated, the older the soil) and they result from wetting and drying cycles and bioturbation (Fitzpatrick 1993). A mixture of well-orientated and weakly orientated birefringent clay accumulations may indicate soils disturbance and secondary deposition (Fitzpatrick 1993).

By looking at the orientation of laminated clays, illuviation may be discerned. Illuviation of clay necessitates periods of wetness (when the clay becomes mobile) followed by periods of dryness (when the clay is deposited) (Schaetzl and Anderson 2005). This too can indicate disturbance of the soil that would cause variation in spatial patterning. Micromorphology will be used here to investigate the soil fabric and composition.

2.9 Environmental Magnetism

Magnetic susceptibility (χ) measures the grain size and concentration of the magnetic constituent of loess. Changes in magnetic susceptibility at a site can result from both cultural and natural processes and can be utilized to designate activity areas, track sediment sources, and as a proxy for climate change (Ellwood, et al. 1996; J. and Bozarth 2008; Peters and Thompson 1999; Tite 1972).

Studies of the magnetic susceptibility of loess in Alaska and China have shown that the magnetic susceptibility signal correlates to variations of ocean oxygen-isotope ratios (Kukla, et al. 1988) In the loess sequences of China; χ variation is the result of pedogenic and diagenic processes (Crumley 1992; Kukla, et al. 1988). Paleosols have higher signals while loess has lower signals in China.

The enhanced signal of the paleosols in the Chinese loess series is the result of several processes. The first of these is differing rates of loess deposition between cold and warm periods (Kukla, et al. 1988; Xiaomin, et al. 1994; Yang, et al. 2004). Due to the small particle size of fine-grained magnetite, it is consistently deposited via the background dust fall. During periods of ameliorating climate, loess deposition decreases and as a result there is a higher ratio of fine-grained magnetite to the coarser magnetic

mineral constituent. Studies have shown that during soil forming processes in Alaska there is also a constant background dust fall punctuated by large dust fall events (Beget 1996; Muhs and Bettis 2003).

The enhanced signal may also be due to pedogenic and diagenic processes. Heller, et al. (1993), found that the processes of compaction and decalcification in loess profiles result in higher ratios of magnetic materials. Fine-grained magnetite can also be produced by bacteria and through oxidation of non-magnetic iron, and so may be the result of both authigenic and detrital sources (Crumley 1992). Burning can also cause an increase in magnetic enhancement (Weston 2002).

Verosub et al. (1993) have shown that authigenic minerals form even during periods of loess deposition, indicating that soil forming processes were taking place during the periods of time visually marked by the loess deposits as well as the paleosols. They note that, "most of the magnetic susceptibility signal in both the paleosols and the loess in China is due to pedogenesis" (Verosub, et al 1993:1011).

In Alaska, the main control of χ is variation in the grain size of magnetic materials resulting from changes in wind intensity. Increasing χ values indicate greater wind intensity (Beget 1996; Beget 2001; Bettis, et al. 2003; Bigelow, et al. 1990b; Lagroix and Banerjee 2002; Lagroix and Banerjee 2006a; Lagroix and Banerjee 2006b; Muhs, et al. 2008; Muhs and Budahn 2006; Muhs, et al. 2004; Pye 1987). Pedogenesis also contributes to the magnetic signal in Interior Alaska. At the archaeological site of Dry Creek (HEA-005), Crumley (1992) found that the robust paleosols at the site had enhanced susceptibility due to pedogenic processes.

Sharpe (1996) found that variation in magnetic profiles in the Shaw Creek area resulted from changes in grain size as well as cultural activity and pedogenesis, and that the degree of alteration could be used as a proxy for both changes in environmental conditions and human activity. Using a variety of magnetic parameters Sharpe found that the lower loess horizons resulted from reduced wind intensities (as compared with the underlying sand), while the upper loess resulted from increased wind intensity and/ or increased aridity.

Environmental magnetism studies can also indicate if a sediment or soil was once at the surface of a landform (Davidson and Shackley 1976). Surface or past surface sediments may have a higher magnetic susceptibility than subsurface soils due to weathering (Davidson and Shackley 1976). By tracking the weathering of buried sediments at the Mead Site, clues to the taphonomic processes affecting the site can be examined.

2.10 Bulk Density

Bulk density is a physical measurement of the ratio of mass to volume of a sample and can be utilized to understand the porosity of a sample (Courty, et al. 1989). Bulk density measurements help to determine the shrink-swell abilities as well as other physical properties of a soil. Bulk density measurements are necessary for the geochemical analysis in this study, and while they provide a basic

measurement of porosity, they do not provide any information regarding the cause of the porosity. Fluctuations in bulk density in a profile can be due to; presence of roots, particle size changes, density of particles, presence or absence of organic materials, or burrowing by animals (Courty, et al. 1989).

2.11 Geochemical Analysis

Geochemical analysis can be utilized to distinguish cultural features from natural features and to understand weathering of soils and sediments, which can be utilized as a proxy for climate and surface exposure (McCarthy and Plint 2003).

By calculating the gains or losses of elements in comparison to immobile constituents present in a soil (Zr or Ti) weathering and translocation of elements can be seen (McCarthy and Plint 2003). Loss of K may result from alteration of mica or K-feldspar while loss of Na indicates alteration of plagioclase. Mica, K-feldspar, and plagioclase are silicates, and when they are altered by hydrolysis silicic acid is produced which in turn results in a loss of SiO_2 (Muhs, et al. 2008). If low ratios of K and Na over the immobile constituents correspond with low ratios of Si over the immobile constituents then these ratios may reflect weathering of mica, K-feldspar, and plagioclase. Likewise, if weathering of aluminosilicate clay minerals has taken place (smectite, chlorite) this should also be reflected in a lower ratio of Si over the immobile constituents' ratio (Muhs, et al. 2008). Loss of Ca and Mg through a soil profile indicates weathering of carbonates, while losses of Fe and Mn reflect movement of these elements and of weathering and gains reflect increases in oxidation and soil hydration (Retallack 2001).

Fluctuations in strain can result from alternating wet and dry conditions, which could be a proxy for seasonality or larger scale climate changes (Retallack 2001). Additionally, changes in the immobile constituents of a soil (Ti/Zr ratios) can be indicative of changes is deposition (McCarthy 2002).

The amount of chemical weathering by hydrolysis increases along with temperature and moisture. The warmer and wetter the conditions, the greater the loss of Ca, Mg, Na, and K in a profile (Sheldon, et al. 2002). The chemical index of alteration (CIA) is a measurement of the amount of weathering in a soil and is used in this study. It is calculated by taking the amount of Al_2O_3 and dividing it by the amount of Al_2O_3 (alumina), CaO (lime), Na_2O (soda), and K_2O (potash), and then multiplying by 100. Alumina, lime, soda, and potash are all alkalides that are found mainly in micas and feldspars, and so the CIA is a measurement of the weathering of micas and feldspars (Sheldon, et al. 2002). As the clay content of a soil increases, Ca, K and Na decrease, and Al should increase, resulting in a higher CIA (Sheldon and Tabor 2009).

Temperature is very important when trying to understand the weathering of soils, as liquid water facilitates many chemical processes. If the temperature is below freezing (such as the modern mean annual temperature for Fairbanks is) then less weathering of soils is possible as the amount of liquid water available is less than in warmer times (Muhs, et al. 2008).

Phosphorous (P) can also be utilized to recognize buried soils. In most regions around the world, modern soils have high concentrations of P at their surface (resulting from biocycling), below which they are depleted in P (due to elluviation and plant uptake), below which they again have higher levels (as they are now out of the elluviation zone and below the plant root level) (Runge, et al. 1974). Alaskan loess has a similar enrichment at the very surface of the modern soil, but lacks the lower enrichment (Muhs, et al. 2000). Because of this, soils that show the "enrichment, depletion, enrichment" series can be interpreted as either weakly developed boreal forest soils or buried tundra soils (Muhs, et al. 2003).

Movement of elements through the soil column has repercussions for both patterning and preservation of cultural remains, especially of faunal material. A localized area void of faunal materials but with a high pH or an increase in sesqiuoxides may have once held faunal materials that were not preserved through time. All of these processes have the potential to obscure the original cultural depositional setting of the site, and so must be examined and taken into account when attempting to interpret intra-site patterning.

Geochemical analysis of sediments and soils can also elucidate evidence of human occupation (Cook and Heizer 1965; Eidt 1985; Manzanilla and Barba 1990; Schuldenrein 1995). Soils can become enriched in phosphorous (P), carbon (C), potassium (K), calcium (Ca) and nitrogen (N) due to cultural activity, and so changes in the concentrations of the elements through the soil profile can be used as an indicator of the intensity of human occupation (Holliday and Gartner 2007; Homsey and Capo 2006).

There are three commonly utilized applications for geochemical analysis in archaeology. The first of these, which is utilized in this study, is supporting activity area and feature designations by enhancement of certain elements. The second is utilizing the chemical analysis to locate and determine extent of sites, and the third is to identify activity areas for excavation (Cook and Heizer 1965; Eidt 1985; Lippi 1988; Manzanilla and Barba 1990; Parnell, et al. 2001; Sanchez and Canabata 1999; Schuldenrein 1995; Wells, et al. 2000).

Previous research at cave and settlement sites has found strong correlations between different activity areas and different elements. Hearths and other burned features exhibit increases in P (Holliday and Gartner 2007; Homsey and Capo 2006; Middleton and Price 1996). P is a good indicator of cultural activity because it has a low susceptibility to leaching, reduction, oxidation, or other diagenic processes (Eidt 1977; Holliday and Gartner 2007). Butchering areas show increases in Ca due to inputs of calcium from the faunal remains (Schuldenrein 1995).

In almost all of the studies cited above, the cultural occupations examined for geochemical analysis had very well developed robust cultural features. Due to the ephemeral nature of the occupations at the Mead Site and a dearth of robust midden and other cultural deposits visible on the macroscopic scale, attributing changes in the soils geochemistry to human activities must be done in conjunction with a detailed knowledge of the natural processes that are likely to have affected the site, the natural movement

of elements through the soil profile, and the spatial location of cultural remains. Also, the geochemical data used in this study is from a few profiles at the site and so while interpreted as being representative of the general geochemical profile at the site, this analysis does not include data from many areas where the geochemical profile may have been altered from anthropogenic activities (such as Features 1, 2, and 3).

2.12 Scale

Scale, both temporal and spatial, is always an important issue in archaeology. In studies such as this one, where variables with vastly different scales are utilized to test hypotheses, assumptions have to be made regarding the relationships of the different variables. This study utilizes variables on the geologic scale (soils formation, loess deposition, climate change) in conjunction with variables on the human scale (occupation, feature areas). Attempting to correlate multi-millennial climate events and geological events with single archaeological occupations is not easily done, and as correlation does not equal causation, caution should be applied to not over interpret the temporal or spatial similarities that appear in the archaeological and paleoclimate/geological record. Additionally, many of the variables (i.e. orbital forcing, solar insulation, cloud cover, methane release, etc) that affect climate change are not well understood and there are large empirical gaps in our understanding of how these different variables affect each other and what exactly their influence on climate is or how they influence prehistoric humans (see Alley and Agustsdottir 2005; Anderson, et al. 2005; Beget and Addison 2006; Bigelow and Edwards 2001; Edwards, et al. 2001; Guthrie 2001; Kaufman, et al. 2004; Mason, et al. 2001; Mayewski, et al. 2004)

Geographic scale is also an issue; the spatial data from the Mead Site comes from 48 1x1m units, while the magnetic susceptibility data comes from profiles from nine units, and the geochemical data comes from only one unit (with single samples from 2 other units). While it would have been ideal to have obtained geochemical and magnetic susceptibility data from every profile from all 48 units, this was not feasible under the scope of this project. It is assumed that the magnetic susceptibility and geochemical data used in this study to make interpretations and conclusions are representative of the magnetic susceptibility and geochemistry of the entire site.

The climate and paleoecological data used in this study comes from sites less than 30 miles away to ones halfway around the world. The resolution of these data is temporally low when compared to the high resolution of the archaeological record at the Mead Site, but it is assumed that they are representative and can be utilized for interpretation at the Mead Site.

3 Methods and Procedures

3.1 Field Work

Fieldwork for this project took place from May 18th 2009 to June 20th2009, when the site was excavated during the University of Alaska Fairbanks (UAF) Archaeological Field School under the direction of Dr. B. A. Potter and Dr. C. E. Holmes. All units were excavated down to the lower bedded sands or bedrock levels. Additional fieldwork was conducted in September when the author returned to the site to collect more samples and draw unit profiles. Soil analysis was conducted at the University of Alaska Fairbanks Department of Geology and Geophysics Labs, under the supervision of Dr. Ken Severin (Director- Advanced Instrumentation Laboratory (AIL)), and at the Department of Anthropology's Archaeological lab, under the supervision of Dr. Ben Potter during 2009 and 2010.

The spatial location of all samples collected was recorded and all *in situ* soil samples were photographed in place for later spatial correlation and control. All test unit faces sampled were photographed pre and post sampling. In addition to daily notes, detailed site wide data and observations were collected and analyzed.

A 1x1 meter arbitrary grid pattern was applied at the site and 2 datum's were established, one on the East Lobe, and one on the West Lobe. A methodological excavation change was implemented 5 days into the field season when the excavators switched from digging horizontal arbitrary 5 cm levels to digging contoured arbitrary 5 cm levels. This change was well documented in the field notes, and was confined to only the uppermost 10 cmbs. All artifacts recovered *in situ* were three-point-provenienced and documented. All artifacts recovered *in situ* were given a field specimen (FS) number and bagged individually. All sediments were sifted through 8" mesh screen, and all artifacts and ecofacts recovered from the screens were recorded and bagged according to provenience and material type.

A total of 52 units were excavated during the field school from the east and West Lobes. Number designations were applied to sampled profiles by the author (Fig.3.1). Over 3,000 artifacts were recovered and four features were excavated. Features 1 and 2 are flake scatters, while Features 3 and 4 are hearths. Feature 3 contains flakes, small bone fragments, and scattered charcoal while Feature 4 contains flakes, small bone fragments, and a large amount of charcoal. Both features 1 and 4 are located at the West section of the site. Features 2 and 3 were all located at the East section of the site. Geochemical data was obtained from the hearth matrix from Feature 4, but no geochemical analysis was conducted on soils associated with Features 1, 2, or 3.

3.2 Stratigraphy

Master horizon designations are described following Schaetzl and Anderson (2005). Subdivisions of master horizons are denoted with number and arbitrary letter designations; these should not be confused with defined suffixes for master soil horizons (i.e. Oa or Bh). All corresponding unit designations (noted in

parenthesis) are from Dilley (1998). Two different parent material types are evident at the site (Figure 3.2). The lower stratigraphic levels formed in Pleistocene age sands, and are characterized by low angle bedded laminations and numerous krotovinas. The other parent material which composes the majority of the sediments at the site is loess.

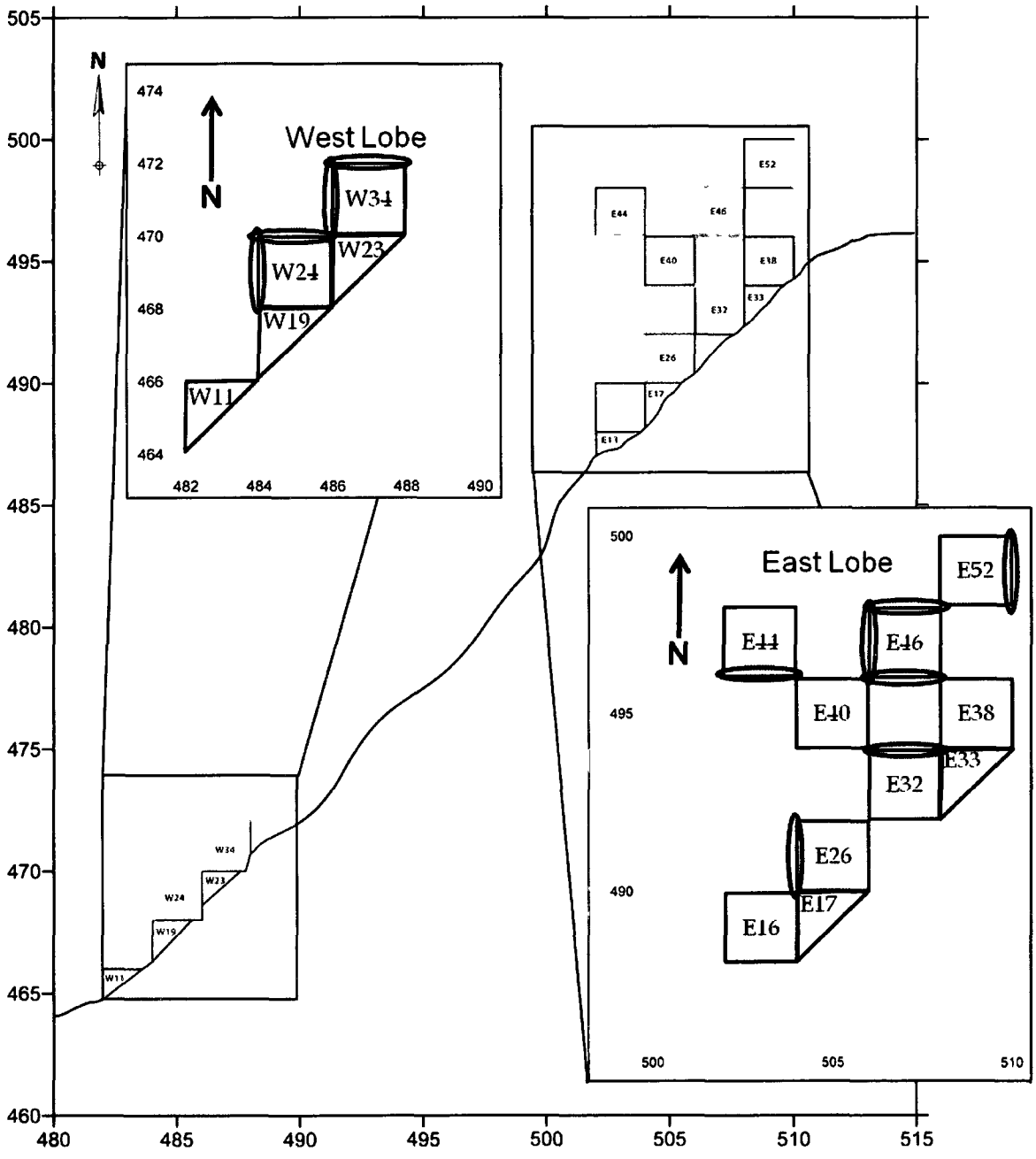

Figure 3.1 Profiles of Excavation Blocks and Profiles Sampled

The loess can be further divided into the lower and upper loess. The lower loess is characterized by a slightly finer grain size than the Upper loess and paleosols development, while the Upper loess exhibits massive bedding and no paleosols development. In some of the units excavated a thin sand layer was evident at the contact between the upper and the lower loess. The acidity of the soils at the Mead Site decrease with depth; the modern forest soil exhibits acidic pH, while the lower loess is neutral to alkaline in nature (Dilley 1998).

Site stratigraphy begins on the R horizon (Unit 1) Birch Creek Schist, felsic gneiss of Yukon-Tanana Crystalline technostratigraphic terrane (Dilley 1998). Few units were excavated to this stratigraphic level. It is composed of frost-shattered angular bedrock that grades from small pebbles intermixed with sand, to large boulders, to solid bedrock. At the upper contact of this layer are pedogenic carbonate laminae and coatings that are generally less than 1mm in thickness.

The C5 horizon (Unit 2) is composed of light gray coarse sand with interbedded and laminated fine sand to fine silty sand. The laminations range from several centimeters to 10cm thick, and have a low bedding angle. Calcium carbonate root casts are found throughout, as are coarse sand krotovinas, and quartz ventifacts. These ventifacts are found at the abrupt, irregular contact with the R horizon. No cultural material was recovered from this layer. Most units were excavated down to the top of the C5 horizon.

The C4 horizon (Unit 3A and 3B) is composed of laminated silt and sand that range in color and hue from dark yellow brown (7.5YR 3/2) to light gray (5YR 5/2). Thought to have been a sterile layer as at Broken Mammoth and Swan Point, the discovery of a large mammal long bone fragment exhibiting cut marks that was excavated from the East Lobe may be associated with this layer.

The C3 horizon (Unit 4) is composed of 10YR 4/6 (dark yellowish brown) sand, and is believed to be an expression of the Younger Dryas cooling event. The C3 horizon is discontinuous across the site and is not well expressed in many of the excavated units; it is found within the lower loess.

The lower loess, C2 (Unit 3/4 and 4), ranges in color from a yellowish brown to a brown silt and contains the paleosols complexes. The C2 horizon was further divided into the C2b and C2a horizons in some units at the site due to diagenic alterations. However, as C2a and C2b have very similar texture and very similar color, in some excavated units no distinction was made between these two horizons.

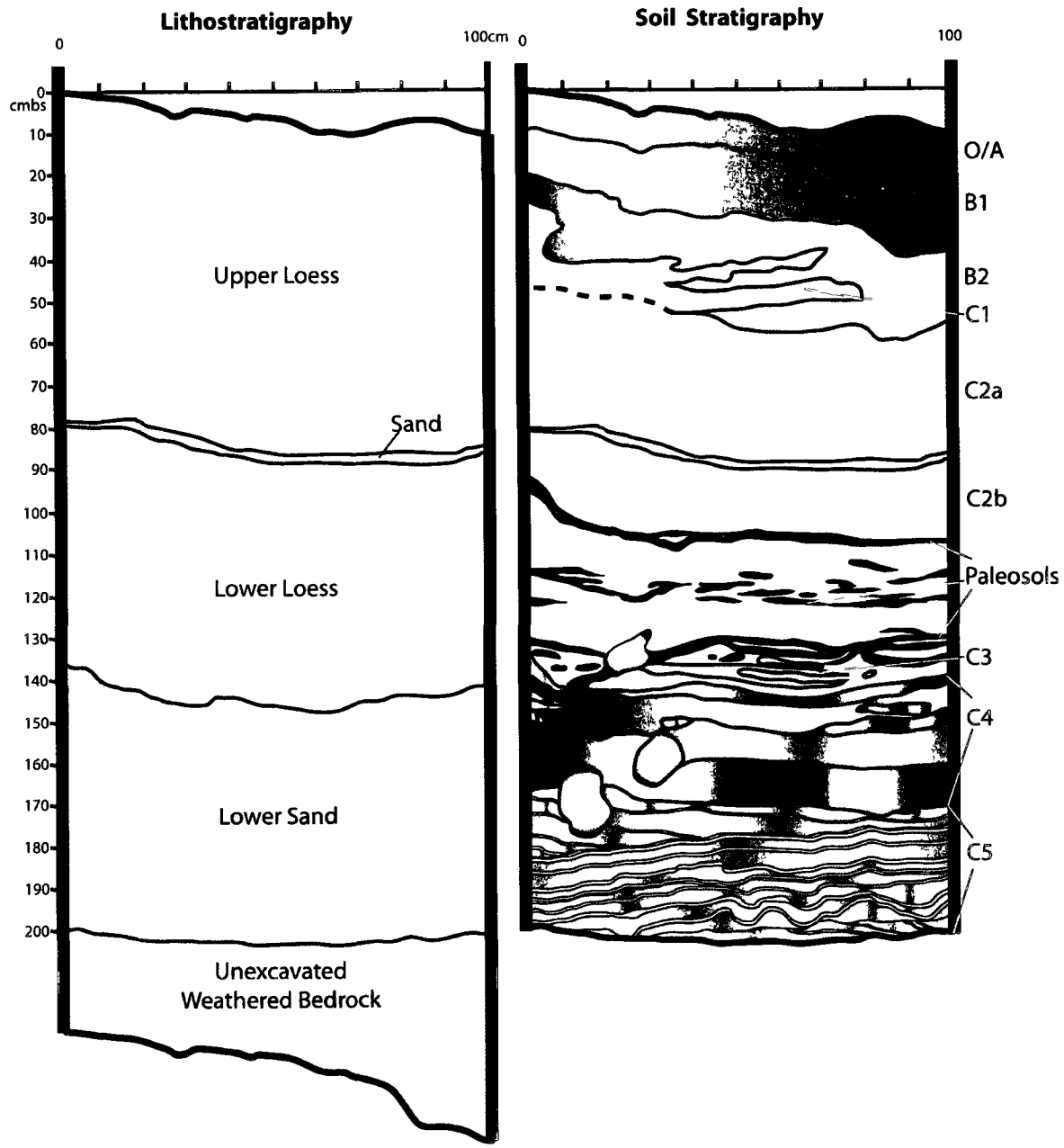

Figure 3.2 Generalized Profile with Lithostratigraphy and Soil Stratigraphy

The C2b horizon (Unit 3/ 4) is a 10YR 5/4-5/3 (yellowish brown to brown) silt containing the lower paleosol complexes and common iron oxide mottles. Calcium carbonate nodules and laminations were observed throughout. The paleosols found here range from discontinuous undulating bands 1 cm in diameter to thicker lens-like occurrences several centimeters in thickness. Small charcoal pieces, as well as charcoal flecking, were observed in all of the paleosol complexes. Depending upon the degree of expression, two (an Upper and a Lower) or three (Upper, Middle and Lower) complexes were noted as being present by excavators. When only two complexes are noted, the Middle Complex has been grouped with the Upper complex and is its lower bound. The C2b grades into the C2a in a faint ephemeral transition that was not evident in all units excavated.

The C2a Horizon (Unit 4) is a 10YR 5/4 (yellowish brown) fine silt with rare iron oxide mottles and calcium carbonate nodules/ laminations throughout. In some profiles at the site a thin sand lens was observed within the C2a horizon. This sand lens is composed of a 10YR 5/1 very fine sand and is generally 2 to15 cm thick.

C1 (Unit 4) is composed of a 10YR 4/6 (dark yellowish brown) fine silty sand. It is found in sub-position to the B horizons; although in some units it was observed as "pockets" between layers of B. Roots are rare to common, charcoal is rare. Rare to no small rocks and pebbles were observed. Cultural Material was recovered from this layer.

The B3 horizon (Unit 4) is composed of a 7.5YR 3/4 (dark brown) thin, compact clay band (lamella) that is discontinuous across the site. The general orientation of the lamella is parallel to the modern surface, and to most stratigraphic horizons, although in some units it was observed following disturbed sediment interfaces as well. The lamella is undulating and will sometimes fork into multiple bands that will pinch off or merge together again. Average thickness when well expressed is 1-2 mm. Expression across the site is poor, with the East Lobe exhibiting thicker bands. The lamella both crosscut and follows the stratigraphic horizons at the site.

The B2 horizon (Unit 4) is a 7.5YR 4/4 (brown) fine silt with common frequent roots and charcoal. Rare to no small rocks and pebbles were observed in this stratigraphic layer. Disturbances to the B2 horizon are due to cryoturbation and bioturbation from root and rodent runs, as well as swallow nests. Cultural material was recovered from this layer.

The B1 horizon is similar to the B2 horizon in texture and is composed of a 10YR 4/4 (dark yellowish brown) fine silt. This is a mineral horizon with rare to no small rocks and pebbles. Roots and charcoal are very common, disturbances include bioturbation and cryoturbation. Cultural material was recovered from this layer. In many of the excavated units no distinction was made between the B1 and B2 horizons; for clarity they are grouped together in most instances simply as the B horizon.

A thin E horizon was noted in some excavated units, although this horizon is poorly expressed across the site and not well developed. This E horizon is light gray brown silty loam. Above the E horizon

(when present) is the A horizon. The A horizon is a 10YR3/3-3/4 (dark brown) fine loamy silt mineral soil. Rare to no rocks and pebbles were observed in this stratigraphic layer. Roots are common throughout. Disturbances include bioturbation from root-runs and cryoturbation.

The O horizon is a 10YR 4/2 to 2/2 (light gray brown to dark brown) fine loam with a thin layer of spruce needle litter and organic material in various stages of decomposition. Historic and prehistoric artifacts were found in this horizon. In many of the units the O and A horizons were grouped together and excavated as a single stratigraphic unit; the O/A horizon. Because of this, for the majority of the analysis conducted in this study the O/A horizon is the designation used (unless otherwise noted).

The bluff face on which many of the excavated units are located is riddled with swallow nests and tunnels. Because of this, the provenience of rodent and bird bones located from units abutting the bluff is questionable unless recovered with artifacts. Microfaulting is also evident in both the bluff face and the excavated profile walls.

3.3 Micromorphology

3.3.1 Procedure

In situ soil samples were collected from 3 profiles (Table 3.1). These samples varied in size from 7 x 4 x 5 cm to 10 x 15 x 8 cm. The outline of each block was scored in the loess, and then carefully carved out (Figure 3.3). The loess was sufficiently cohesive so that each sample could then be removed with only the aid of a trowel. Each sample was wrapped in tissue and secured with plastic and tape. Orientation and location were recorded, and samples were carefully packaged for transport to Fairbanks. The basal sand layers were not collected for micromorphological analysis due to the difficulty in collecting intact samples.

Upon arrival to Fairbanks, micromorphological samples were placed in the archaeology lab where they were then allowed to air dry for a period of 4 months to remove all water prior to impregnation with resin. Acetone replacement, which allows for the expedient removal of water from micromorphological samples, was not utilized as it can produce unwanted artifacts in the final thin sections (Courty, et al. 1989; Murphy 1986). Samples were partially unwrapped and placed in aluminum trays.

Table 3.1-Micromorphological Sample Information

Micromorphological Sample Location Information									
Sample #	**Block**	**Profile**	**North**	**East**	**Thickness**	**Depth (cmbd)**	**Notes**	**Sample Number**	**Lab Number**
1	W-34	North	472	486.6-486.7	11	154-128.5	YD sand, several well developed PS	N/A	N/A
2	W-34	North	472	486.77-486.83	5	130-119	PS in upper east corner, C2b	2.1	YTD-001
								2.2	YTD-002
3	W-34	North	472	486.88-486.95	6	122-110	C2b, PS in middle of sample	3.1	YTD-003
								3.2	YTD-004
4	W-34	North	472	486.75-486.82	8-4	112-96	Contains PS stringers	4.1	YTD-005
								4.1	YTD-006
5	W-34	North	472	486.32-486.39	7-5	98-83	C2b and C2a	5.1	YTD-007
								5.2	YTD-008
6	W-34	North	472	486.17-486.25	5-8	25-68	C2a and sand lens in top	N/A	N/A
7	W-34	North	472	487.09-487.17	5-7	73-55	C2a, sand, contact with C1, red mottles	7.1	YTD-009
								7.2	YTD-010
								7.3	YTD-011
8	W-34	North	472	486.72-486.8	4-9	54-38	C1/B	N/A	N/A
9	W-34	North	472	487.72-487.8	8-10	32-26	B with C1 in middle	N/A	N/A
10	E-46	West	496.5- 496.6	506	6-8	134-115	Contains PS stringers	N/A	N/A
12	E-52	North	500	509.42-509.44	4-5	54-47	Depth is from overburden, contains B3 lamellae	12.1	YTD-012

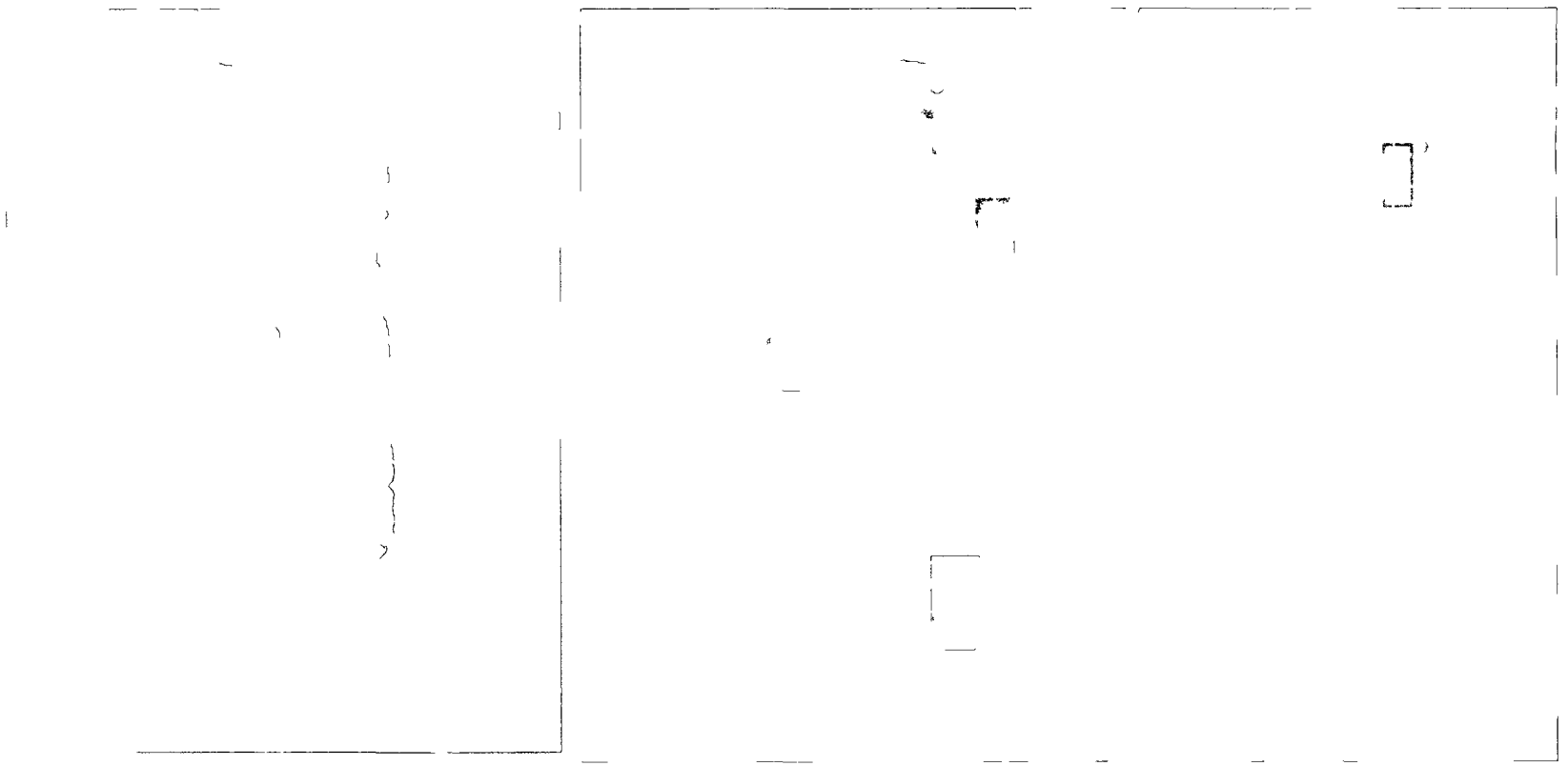

Figure 3 3 Thin Section Locations- Red outlined blocks were analyzed

Impregnation procedures and recipe followed Courty, et al. (1989) and Murphy (1986). The impregnating mixture used was composed of unsaturated vinylester resin that was thinned with styrene (vinyl benzene) and catalyzed with methyl ethyl ketone peroxide (MEKP). A very small amount of MEKP was used which resulted in both a long curing time and minimal shrinkage of the samples. Two parts unsaturated vinyl polyester resin were combined with 1 part Styrene and 0.007 parts MEKP and then manually mixed by hand for 10 minutes before being carefully poured into the aluminum trays. Samples were then placed in a vacuum chamber for 4-8 hours to ensure complete impregnation. After evacuation, samples were "topped off" with the remaining impregnation mixture before being placed in a fume hood to air dry for two months. At the end of this period, samples were partially cured by placing each sample in a vacuum oven at 40-50°C for 3 to 7 days. Samples were then placed under ultra-violet light to complete the curing process.

Due to the swelling of clays and subsequent distortion of the microfabric that can occur when exposed to water, samples were sent to Spectrum Petrography, a professional petrography lab in Oregon, for sectioning as all methods for sectioning at UAF involve exposure to water. Proper sectioning of soil samples such as these requires a kerosene or paraffin lubricated system. Of the 11 blocks collected, 6 were cut into thin sections and utilized for micromorphological analysis. Samples were prepared so that analysis under plain, polarized, and reflective light was possible. No coloring or other additives were placed on the slides. No cover slips were placed on the samples so that analysis such as x-ray microanalysis or scanning electron microscopy can be conducted in the future. Samples were bonded to glass slides measuring 51 x 75 mm and ground to a thickness of 30 μm (0.03 mm).

A high resolution scan of each slide was made prior to microscopic descriptions Samples were examined at the UAF geology department. Each sample was examined under plain polarized (PPL), cross polarized (XPL), and reflected light (RL). Continuous photomicrographs under both PPL and XPL were taken for each slide. Additional photomicrographs were taken of pedofeatures. A λ retardation plate (gypsum compensator) was utilized to help determine the orientation of clay particles on each slide. Thin sections were examined and microstructure, pedofeatures, organic remains, soil size, distributions, and mineral components were recorded.

Reflected light was utilized to distinguish iron-oxide mineral grains from organics, as both appear opaque under transmitted light. Reflected light also allows for qualitative measurements of the amount and degree of weathering of mineral grains. Reflected light analysis also allowed for a more accurate representation of the surface area of the iron-oxide mineral grains than transmitted light (due to the Holmes effect).

Images of features observed in transmitted light have a projected size that is dependent upon the thickness of the thin section, as the light passes through the slide to reach the observers eye. Images of features observed in reflected light on the other hand have a projected size that is dependent on one plane

(the surface of the slide) as the light does not pass through the slide but bounces off of it to reach the observers eye. Because of this, fine pores always appear larger in reflected light than in transmitted light, and opaque features always appear larger in transmitted light than in reflected light; this is the Holmes effect (Holmes 1927).

3.3.2 Description

Slides were examined and the microstructure, basic mineral components, basic organic components, groundmass, and pedofeatures were described. The description of the slides follows Stoops (2003), Bullock et al. (1985), Stoops et al (2010) and Courty et al. (1989).

3.3.2.1 Microstructure

Soil microstructure is the relationship of the solid constituents of the soil in relationship to pore space. Microstructure was determined through the analysis of the size, frequency, shape, sorting, and abundance of voids and primary particles of nonaggregated and aggregated (ped) material (Stoops 2003).

Peds were described in terms of type (granule, block, plate or prism), size, accommodation (the measure of the degree that the faces of a ped exhibit similar shapes and are described as, accommodated, partially accommodated, unaccommodated), degree of ped separation (weak, moderate, high), roughness, and pattern (clustered, banded, and random). Voids were described based on their morphology and classed as plane (flat voids), vugh (irregular, equidimensional voids that do not connect to other voids of a similar size), chamber (smooth-walled voids connected by channels), channel (tube shaped smooth walled voids with an arched cross section) or packing voids (forms the textural porosity of the soil).

3.3.2.2 Groundmass

Groundmass describes the base material of each thin section and encompasses the packing voids and fine and coarse material of the soil including, the mineral constituents, organic constituents, plant residues, and organic matter alternation; it does not include pedofeatures. Groundmass was described in terms of the coarse material composition and its fabric, and the fine material (or micromass) and its fabric. The coarse material was described in terms of its composition, size, and shape. Groundmass is expressed in terms of, the coarse/fine (c/f) related distribution (which is the relationship of smaller fabric units and pore space to the individual fabric units).

The particles that compose the micromass are too small to be individually examined under the microscope, and so the micromass was described in terms of its color, limpidity (transparency), and type of birefringence fabric (b-fabric). B-fabric is the description of the orientation and pattern of interference colors from clay aggregates when viewed under cross polarized light (Stoops 2003).

The organic constituents of each thin section were described according to their morphology, relief, color, and alteration. Plant residues were described as either organ residues (5 or more interconnected cells

of a single tissue type which may display the original structure of the organ), tissue residues (5 or more interconnected cells that do not display the original organ structure), or organic fine material (cell and cell residues, punctuations, organic pigment and amorphous organic fine material).

Root decomposition was classed following Blazejewski et al., (2005). Class 0 roots show no decomposition and the inner portion and sheath of the root are complete. Class 1 roots display sheathes and inner portions that are not complete, Class 2 roots are characterized by the presence of tissue fragments that are still identifiable and where the organics from the root have moved into the surrounding soil. Class 3 roots have no discernable tissue but the shape of the root is still visible, while Class 4 roots have no discernable tissue remains and the original shape of the root is ephemeral.

3.3.2.3 Pedofeatures

Pedofeatures are fabric units that are distinct from the surrounding material and which can be distinguished through their organic matter content, chemistry, grain size or some other change in internal concentration (Stoops 2003). Pedofeatures were classified based both on their morphology and origin of formation. Based on their origin of formation, pedofeatures were subdivided into two groups, matrix pedofeatures (which form from changes in the groundmass) and intrusive pedofeatures (which form external to the groundmass). Matrix pedofeatures were then further subdivided into impregnative (exhibit increases in certain constituents), depletion (exhibit decreases in certain constituents), or fabric pedofeatures (exhibit fabric which is different from that of the groundmass).

Matrix and intrusive pedofeatures were also classified by their morphology (including their related distribution pattern and crystallinity) based on their relationship to; voids, the surface of voids, the surface of aggregates, the surface of grains, or their lack of relationship to void or surfaces. Pedofeatures were grouped according to their composition (clay features, calcite features, etc) rather than their morphological type.

3.4 Environmental Magnetism

Environmental Magnetism samples were collected in $8cm^3$ plastic cubes that are designed for magnetic sample collection and measurement. The sampling strategy employed accounts for the variation in stratigraphy found across the site as well as the distribution of field observed artifact concentrations and features. Samples were collected continuously from nine profiles across the site (Figure 3.4). To obtain a complete profile, samples were collected from the basal sands as well as the overlying loess. Each profile face was prepared for sampling by cleaning with a plastic spatula to insure no metal fragments from excavation equipment would contaminate the samples. Cubes were labeled and then inserted into the profile face with a soft-blow hammer, where they were mapped and photographed before removal (Figure 3.5). After extraction the boxes were capped and allowed to air dry for 5 months. No treatment of these samples was conducted other than the removal of macroscopic organic material.

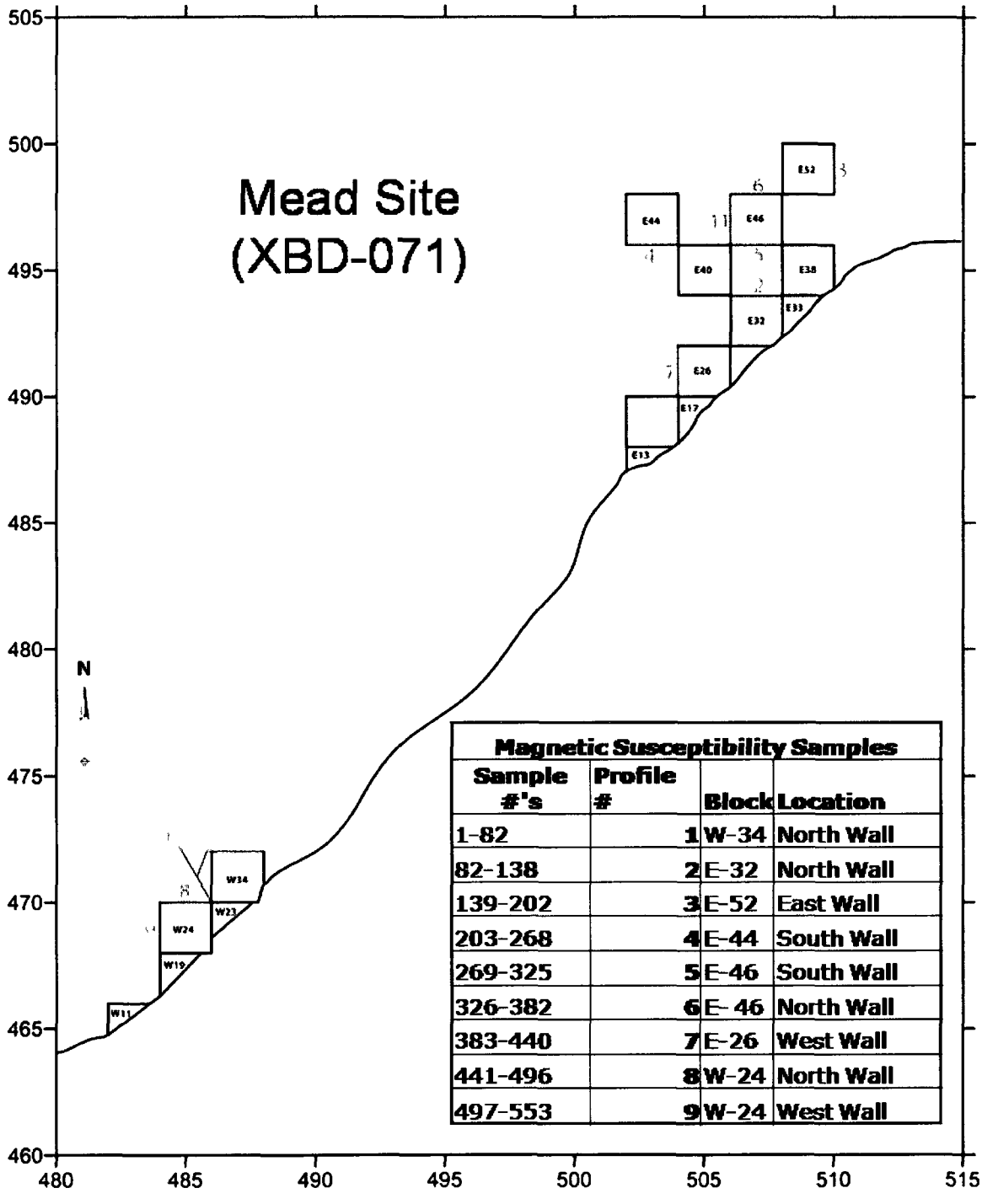

Magnetic Susceptibility Samples			
Sample #'s	Profile #	Block	Location
1-82	1	W-34	North Wall
82-138	2	E-32	North Wall
139-202	3	E-52	East Wall
203-268	4	E-44	South Wall
269-325	5	E-46	South Wall
326-382	6	E- 46	North Wall
383-440	7	E-26	West Wall
441-496	8	W-24	North Wall
497-553	9	W-24	West Wall

Figure 3.4 Location of magnetic susceptibility samples and numbered profiles

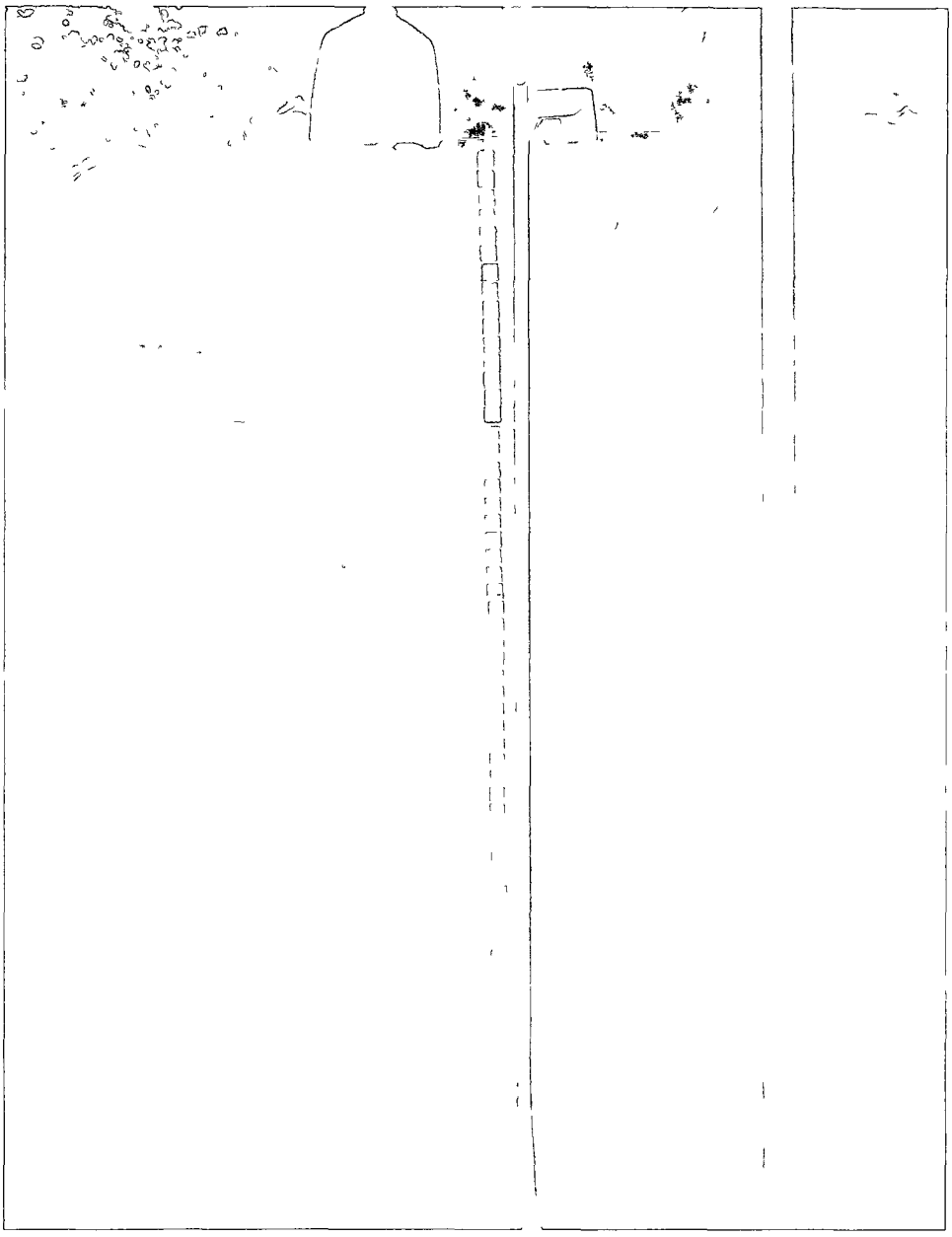

Figure 3.5 Magnetic susceptibility samples prior to removal from Profile #9

Samples were measured for room temperature volume magnetic susceptibility (κ). Mass magnetic susceptibility (χ) and frequency dependence (χ_{fd}) were calculated from these measurements. Low (κ_{lf}) (0.47 kHz) and High (κ_{hifi}) (4.7 kHz) frequency magnetic susceptibility were measured using a Bartington MS2 susceptibility system at the Paleomagnetism Laboratory, UAF. κ is a measurement of how easily each

sample was magnetized when it was exposed to a magnetic field, and its susceptibility is the ratio of induced magnetization *(M)* to the applied field strength *(H)*,

$$k = \frac{M}{H} \quad (1)$$

Both *M* and *H* are measured in A/m (SI units) and because of this, κ is dimensionless. Because κ is influenced by both volume and mass, mass specific susceptibility was also calculated which takes into account the bulk density of each sample. To obtain the mass susceptibility κ is divided by the sample's density (ρ),

$$\chi = \frac{\kappa}{\rho} \quad (2)$$

κ_{lf} measurements were recorded first for all samples, and then all κ_{hifi} measurements were recorded. All measurements collected were recorded in g/cc and converted to m^3/kg (SI units). Before and after each sample was measured a measurement was taken (the "air" readings) of the empty sample chamber to account for instrumental drift. When drift exceeded 1.2 on the second air reading, the meter was zeroed. Value corrections were made following Dearing (1999) using the formula:

$$\kappa_{corrected} = \kappa_{sample} - \left[\frac{(\kappa_{first\ air} + \kappa_{second\ air})}{2}\right] \quad (3)$$

The bulk ferromagnetic mineral composition as well as the ferromagnetic mineral grain size was discerned from the low-frequency susceptibility. As susceptibility is dependent on grain size and concentration, higher values can be indicative of larger grain size, higher concentrations of magnetic materials, or both.

Frequency-dependent susceptibility was calculated in percentage using the formula:

$$\chi_{fd}\% = \left(\frac{(\kappa_{lf} - \kappa_{hf})}{\kappa_{lf}}\right) \times 100 \quad (4)$$

The frequency-dependence percentage ($\chi_{fd}\%$) indicates the presence and level of superparamagnetic (SP) minerals grains in samples, and is an indication of pedogenesis with higher values indication translocation and transformations due to pedogenesis (Evans and Heller 2003). SP grains are very small (<40μm) and occur within the very-fine clay fraction. The frequency-dependence measurements can be used in a semi-quantitative manner to infer SP concentration through the soil profile. A $\chi_{fd}\%$ of less than 2.0 indicates that there are less than 10% SP grains in the sample, $\chi_{fd}\%$ between 2 and 10 indicates that there is a mixture of both SP and non-SP grains, $\chi_{fd}\%$ between 10 and14 indicates 75% of the sample are SP grains. Percentages greater than 14% are rare and are the result of investigator error, contamination, a poor sample, or anisotropy (Dearing 1999). Generally B and Bt horizons have increased frequency dependence, although this parameter is known to exhibit a large degree of variability (Evans and Heller 2003).

3.5 Bulk Density

Bulk density samples were collected from four profiles across the site (Figure 3.6). A sample was taken from each stratigraphic layer that was sufficiently thick enough to allow for complete insertion of the container without sampling of the other bounding layers. Samples were transferred to plastic bags, weighed, and left to air dry for 4 months after which they were reweighed. Additional bulk density calculations were computed for all magnetic susceptibility samples acquired. Bulk density values were determined following Blake and Hartge (1986).

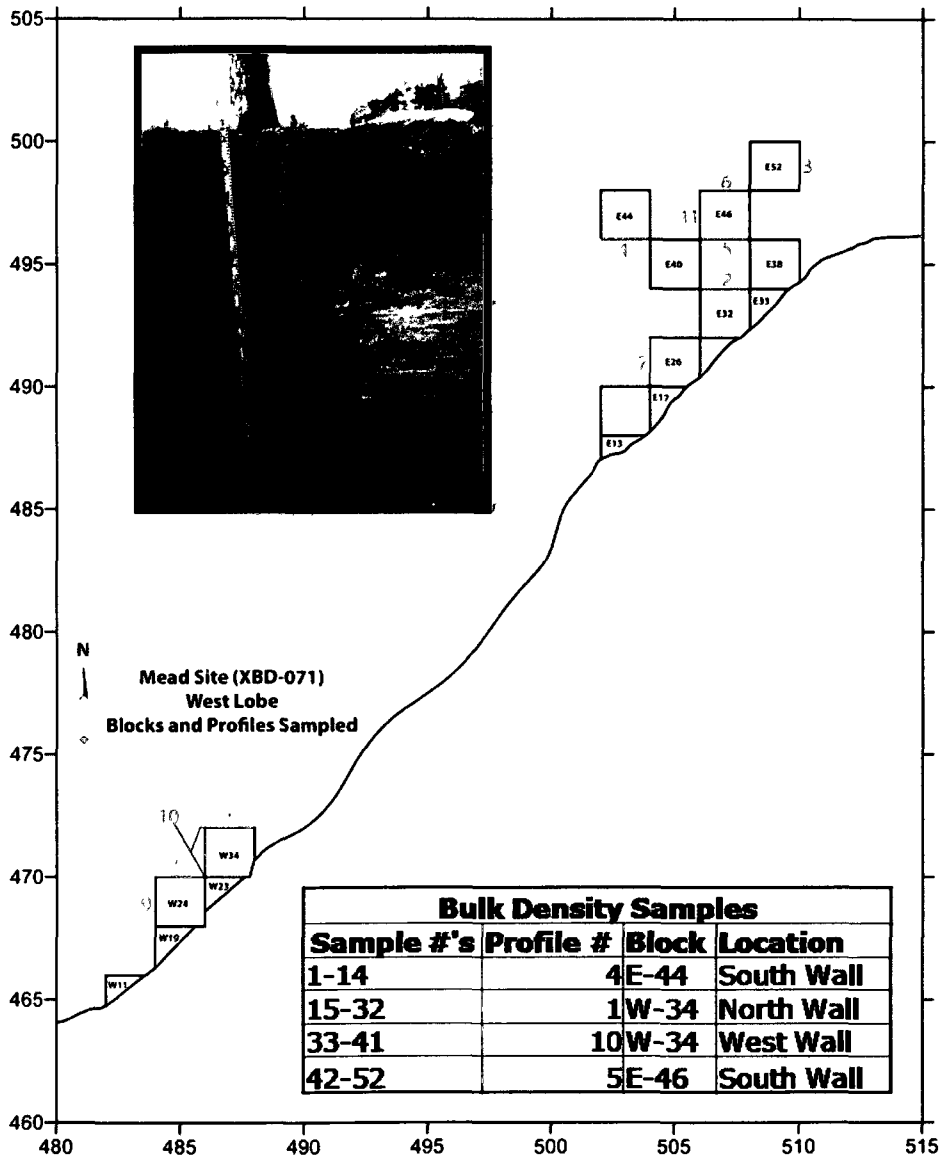

Figure 3.6 Bulk density sample location and numbered profiles

3.6 Geochemical Analysis:

Bulk density samples from profiles 1 and 4 and from Feature 4 were utilized for Geochemical analysis (Table 3.2). X-ray fluorescence (XRF) geochemical quantitative analysis was conducted on untreated samples. Macroscopic organic material was removed from each sample before processing. Samples were ground in a Mill Mixer for 5 minutes in aluminum vials. Vials were cleaned between each sample milling to minimize cross sample contamination. Approximately 10g of each powdered sample was mixed with polyvinyl alcohol before molding into 37mm diameter pressed powdered pellets. XRF analysis was conducted on the PanAnalytical Axios XRF housed at the Advanced Instrumentation Laboratory (AIL), UAF. An established routine was utilized for this analysis (see Appendix 4 for all geochemical data and calculations).

Calculations of concentration and relative error were calculated after applying compton and interfering peak corrections. Major analytes examined were, SiO_2, Al_2O_3, Fe_2O_3, CaO, MgO, Na_2O, K_2O, TiO_2, MnO, P_2O_5, and minors were; Cr, Ba, Sr, F, S, Cl, V, Co, Ni, Cu, Zn, As, Rb, Pb, W, Sn, and Sb. As the atomic number of oxygen is too small to be analyzed with XRF, all O values are theoretical.

Table 3.2 Thin section sample location and association

Sample	Strat	Block	North	East	cmbd	Notes
BD-15	A	W34	472	486.6	16	
BD-16	B1	W34	472	486.61	26	
BD-17	B2	W34	472	486.62	36	
B3	B2 &B3	W19	467.55	484.45	30	
BD-18	C1	W34	472	486.64	49	
BD-2	C1	E44	496	503.56	44	Between B, CZ1b scatter
BD-19	C2a	W34	472	486.26	58	
BD-20	C2a	W34	472	486.43	67	
BD-21	C2a	W34	472	486.62	82	
BD-22	C2b	W34	472	486.67	100	
Feat.4	hearth	W24	469.4	484.8	105	
BD-23	C2b & PS	W34	472	486.4	113	
BD-24	C2b & PS	W34	472	486.35	118	
BD-25	C2b & PS	W34	472	486.41	125	
PS E44	Ps	E44	496.75	503.25	127	
BD-26	C2b	W34	472	486.32	131	
BD-27	PS	W34	472	486.41	138	well developed
BD-28	Sand	W34	472	486.31	143	YD?
BD-29	Fine Sand	W34	472	486.37	148	
BD-30	Fine Sand	W34	472	486.39	157	Krotovinia
BD-31	Coarse San	W34	472	486.37	166	
BD-32	Fine Sand	W34	472	486.39	176	

Multiple calculations were used in this study to assess the chemical variation of the soil at the Mead Site. First the variation in the molecular ratios of oxides between the different soil horizons was examined. Second, the net gains or losses of elements between the soil horizons were examined. Finally, gains and losses of analytes were calculated using concentration ratios of each oxide relative to the immobile constituent Zircon (Zr). Both molecular and concentration ratios were calculated following Feakes and Retallack (1988). These calculations are standard computations in paleosols research (see Driese and Foreman 1992; Fitzpatrick 1993; Kahmann and Driese 2008; McCarthy 2002; McCarthy, et al. 1999; McCarthy and Plint 2003).

3.6.1 Molecular Ratios

Molecular ratios are calculated by dividing the weight percent of an oxide by its molecular weight, and then dividing that number to another oxides value using the same formula:

$$\frac{wt\%_i}{MW_i} / \frac{wt\%_j}{MW_j} \tag{5}$$

The molecular ratios of; Ba/Sr, Al/Si, Si/ Fe+Al, K+Na/Al, Na/K and Na/Al were calculated. Each of these ratios can be interpreted as resulting for a distinct chemical process, and can be used as indices of weathering.

Al/Si is used to determine clayeyeness by hydrolysis, as Al accumulates when clay minerals form and can be used to strengthen designations of Bt horizons (Hamer, et al. 2007; Ruxton 1968; Sheldon 2005). K+Na/Al is used to determine salinization and can be used as an indicator of aridity (Retallack 1991; Sheldon, et al. 2002). Because Na and K behave differently during pedogenesis, determinations of salinization and aridity should be accompanied by other indications of aridity such as evaporative minerals and pedogenic carbonate nodules. Na/Al is used to determine pedogenesis, as base elements are depleted relative to Al during pedogenic processes (Sheldon and Tabor 2009).

The trace element ratio of Ba/Sr is used to help determine leaching due to weathering, with lower ratios indicating less leaching, and higher ratios indicating more leaching (Retallack 1991; Sheldon 2006). Sr is more soluble in water than Ba, and so is more easily leached, and so illuvial horizons should have higher ratios of Ba/Sr than elluvial horizons (Sheldon and Tabor 2009; Vinogradov 1959).

The Chemical Index of Alteration (CIA) was calculated following Nesbitt and Young (1982) using the formula:

$$CIA = \left[\frac{Al_2O_3}{(Al_2O_3+CaO+Na_2O+K_2O)}\right] \times 100 \tag{6}$$

In addition to calculating the CIA, an additional weathering index was calculated that accounts for Mg-bearing minerals not examined in the CIA. The calculation the Mg (CIA) follows, Colman (1982), Retallack (2001), and Sheldon and Tabor (2009); the formula used was:

$$\frac{\sum Bases}{Al} = \frac{(Ca+K+Mg+Na)}{Al} \tag{7}$$

3.6.2 Concentration Ratios

Concentration ratios (CR) were calculated using the formula:

$$CR = \left(\frac{M_w}{M_p}\right)\left(\frac{Zr_w}{Zr_p}\right) \quad (8)$$

In this equation, M is the concentration of the oxide being examined in the parent material (p), and the soil horizon (w) and Zr is the immobile inert constituent. Sample BD26 was used as the parent material for all samples as it was stratigraphically lowest pure loess sample in the profile. Concentration ratios of <1 indicate relative losses in oxides while ratios of >1 indicate gains (Feakes and Retallack 1988).

3.6.3 Strain

The third approach to understanding the chemical variation of the soil at the Mead Site is a mass balance approach that looks at the volumetric changes (or "strain"). This approach measures the losses and gains of soil constituents due to pedogenesis. Strain (ε) was calculated following Sheldon and Tabor (2009) and Chadwick et al. (1990) using the formula:

$$\varepsilon_{i,w} = \frac{P_p C_{i,p}}{P_w C_{i,w}} - 1 \quad (9)$$

Where P is the bulk density of the parent material and C_i is the concentration of the element (expressed in wt %). Strain is referred to in terms of dilation (increase in volume of a soil) or collapse (decrease in volume of a soil) (Schaetzl and Anderson 2005). Collapse is indicative of elluviation while dilation is an indicator of illuviation (Schaetzl and Anderson 2005).

3.7 Spatial Analysis

The spatial analysis conducted for this study is in no way exhaustive. Analysis was conducted to determine the location of cultural zones and feature/activity areas from the 2009 excavation. Vertical back plots of artifacts and ecofacts recovered *in situ* were created for spatial analysis. Designated Cultural Zones (CZ) at the Mead Site have been established through the published literature (see Dilley 1998; Holmes 2001; Holmes 2008), and are used here. These zones are used to distinguish changes in cultural remains and are not necessarily indicative of individual occupations or cultures. They are used loosely as a means of tracking possible feature and activity areas.

Additional spatial analysis was conducted using Surfer ™ software. *In situ* artifacts were classed by 5 cm arbitrary excavation levels, and successive maps were produced to show the distribution and change in artifact and faunal remains location with depth. Visual qualitative analysis was then used to create a table showing the general trends of the *in situ* data for each excavation block and area. SPSS statistical software was used to find the number of each artifact type and bone for each 5 cm level in each excavated unit. Screened remains were classed by 5cm arbitrary excavation level and grid isopleth maps

were created with the Kriging method to illustrate changes in distribution and frequency of remains with depth.

All lithic material was weighed and classed by size. Each size class was measured by 5 mm class intervals; where SC2=5-10 mm, SC3= 10-15 mm, etc. SC1 was used to class lithics smaller than 5 mm, and SC17 was used to class lithics larger than 70 mm. SPSS analysis was then used to find the mean size class and weight of lithic material for each 5 cm arbitrary level to see if there are patterns of distribution that may indicate post-depositional disturbance.

Orientation of lithic and faunal materials was not systematically recorded during the 2009 excavation and so no in depth analysis of orientation is conducted here. This information should be recorded in the future as it will help determine post-depositional disturbance. All artifact concentrations were photographed *in situ* and the majority of the material found in the lower CZ's were found in horizontal or near horizontal positions, while much of the upper CZ material was found in vertical position. Additional spatial analysis that could be conducted in the future which would add in the interpretation of the Mead Site includes detailed faunal and lithic analysis, refitting, and raw material type frequency and distribution.

3.8 Loess Accumulation Rates

Accumulation rates were calculated following Stein et al. (2003) using the formula:

$$Total\ Accumulation\ Rate = \frac{(d_2 - d_1)}{(a_2 - a_1)} \times 100 \qquad (10)$$

where d_2 is the depth of the stratigraphically upper sample, d_1 is the depth of the stratigraphically lower sample, a_2 is the age of the upper sample, and a_1 is the age of the lower sample. It is assumed that the deposition rate between samples is constant.

4 Results

4.1 Micromorphology

This section outlines the general micromorphological characteristics seen throughout the soil profile and details important features as they relate to disturbance, weathering, and climate. Detailed micromorphological descriptions of each slide are reported in Appendix 1, and the scan of each slide is shown in Figure 4.1 (refer to Table 3.1 for sample descriptions and location information). While micromorphology can be used to distinguish anthropogenic features from natural ones, the limited number of samples used in this study does not allow for this analysis as no thin sections were created of feature areas.

With the exception of Sample 12, all of the thin sections display a compact grain microstructure with weak separation which in areas has a platy overprint (Figure 4.2 and Figure 4.4); occasionally a platy microstructure was observed (see Table 4.1 for generalized descriptions of each slide). The overall coarse/fine related distribution pattern (c/f RDP) is of single spaced to close porphyric and is poorly sorted with a random (occasionally banded) distribution pattern. When a banded distribution pattern was observed it was in isolated areas which exhibited higher ratios of fine organic matter and clay content than the surrounding microstructure. Voids are common and consist of complex packing as well as planar, regular vughes, and channel voids (Figure 4.3)

The microstructure of the loess is unoriented subangular to angular mica and quartz. Few feldspar minerals were observed overall with the most abundant feldspar mineral being plagioclase. The micromass of the loess has a stipple-speckled birefringence fabric (b-fabric) which is the result of the randomly oriented clay and silt particles. Calcium carbonate loose infillings are evident in the lower loess sections (Figure 4.2), while the upper loess displays fewer calcium carbonate loose infillings. Slides 4.2 and 5.2 exhibited needle fiber calcite as well. No clay laminations were observed in any thin section. Oblique arrangement of coarse grains was observed in some slides.

The platy microstructure observed results from repeated cycles of freeze/thaw and is the result of ice lensing. These ice lenses can be either micro or macroscopic occur when a series of ice fronts separate the fine particles from the coarser ones which results in banding (Dement 1962). Sample 12.1 (Figure 4.1) displays a lenticular platy to subangular blocky microstructure which is the result of advanced ice lensing.

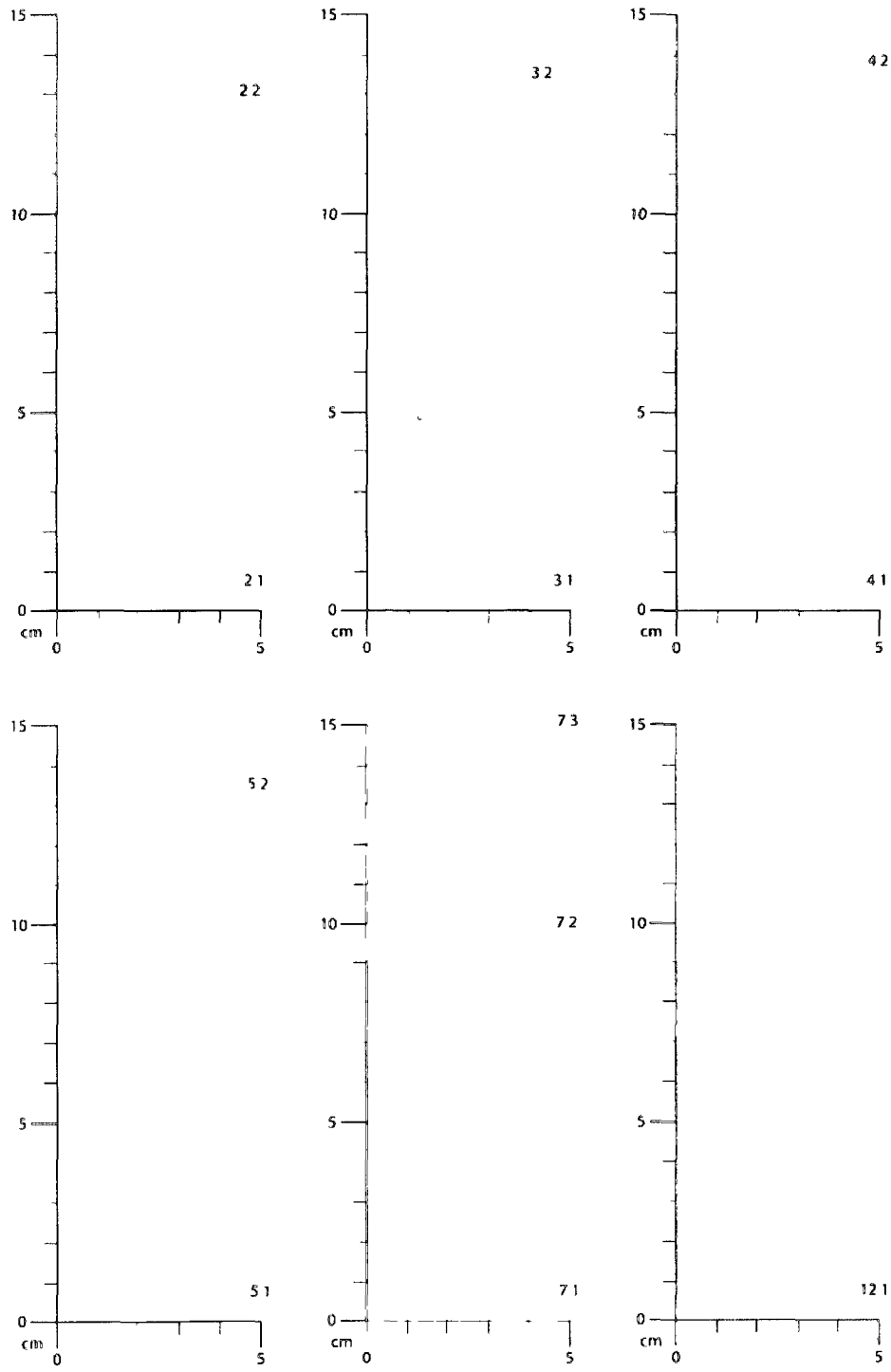

Figure 4.1 Scans of thin sections, slides are oriented so notch is "up" indicating the original surface orientation

Table 4.1 Micromorphological descriptions of thin sections

Sample Number	Stratigraphy	Microstructure	B-Fabric	Clay Concentrations	c/f Related Distribution Pattern	Voids	Pedofeatures	Organic Material	Mineral
2.1	PS in upper cist context C2b	compact grain	random undifferentiated to stipple speckled	void and grain coatings rare fine to concentrations or papulas	close porphyric to single spaced	vughs common unaccommodated planes	*infillings nodules*	plant residue bone fragments charcoal	unweathered magnetic carbonate infillings
2.2		compact grain with plasmic overprint	random stipple speckled	void and grain coatings rare fine to concentrations or papulas	close porphyric to single spaced	vughs rare unaccommodated planes	infillings nodules coatings	plant residue roots (class 0.2)	moderately weathered magnetic calcium carbonate infillings
3.1	C2b PS in middle of sample	compact grain with plasmic overprint that flows with to compact grain	random stipple speckled	void and grain coatings rare fine to concentrations or papulas	close porphyric to single spaced	vughs unaccommodated planes	infillings nodules coatings	charcoal organic residue roots (class 0.2)	moderately weathered magnetic calcium carbonate infillings
3.2		compact grain with plasmic overprint	random stipple speckled	void and grain coatings rare fine to concentrations or papulas	close porphyric to single spaced coarse grains exhibit oblique alignment	vughs unaccommodated planes	infillings nodules coatings passive features	plant residue roots (class 0.1)	moderately weathered magnetic calcium carbonate infillings
4.1	Contains PS stringers	compact grain with plasmic overprint	random stipple speckled	void and grain coatings rare fine to concentrations or papulas	close porphyric to single spaced	vughs unaccommodated planes	infillings nodules coatings	plant residue roots (class 0.4)	unweathered magnetic Fe oxide hypocoatings calcium carbonate infillings
4.2		compact grain with plasmic overprint	random stipple speckled	void and grain coatings rare fine to concentrations or papulas	close porphyric to single spaced coarse grains exhibit oblique alignment	vughs unaccommodated planes rare to few channel	infillings nodules coatings passive features	plant residue	weathered magnetic Fe oxide hypocoatings calcium carbonate infillings needle fiber calcite
5.1	C2b and C2a	compact grain to compact granular with plasmic overprint	random stipple speckled	void and grain coatings rare fine to concentrations or papulas	close porphyric to single spaced	vughs unaccommodated planes channels	infillings nodules coatings	plant residue tissue charcoal	weathered magnetic Fe oxide hypocoatings calcium carbonate infillings
5.2		compact grain with plasmic overprint	random stipple speckled	void and grain coatings rare fine to concentrations or papulas	close porphyric to single spaced coarse grains exhibit oblique alignment	vughs unaccommodated planes	*infillings nodules* coatings passive features	plant residue tissue roots (class 1.4)	weathered magnetic Fe oxide hypocoatings calcium carbonate infillings needle fiber calcite
7.1	C2a and contact with C1 redeposited blocks	compact grain with plasmic overprint	random stipple speckled	void and grain coatings rare fine to concentrations or papulas	close porphyric to single spaced coarse grains exhibit oblique alignment	vughs unaccommodated planes channels	infillings nodules coatings passive features	very frequent large organics (class 6.1)	weathered magnetic Fe oxide hypocoatings calcium carbonate infillings
7.2		compact granular to plasmic to compact granular	random stipple speckled	void and grain coatings rare fine to concentrations or papulas	open porphyric to single spaced coarse grains exhibit oblique alignment	vughs unaccommodated planes channels	loose continuous infillings nodules coatings pendent external hypocoatings frost shattered aggregates	plant residue (class 1.3) bone fragments charcoal	weathered magnetic Fe oxide hypocoatings calcium carbonate infillings
7.3		compact grain with plasmic overprint	random undulating stipple speckled	void and grain coatings rare fine to concentrations or papulas	close porphyric to single spaced coarse grains exhibit oblique alignment	vughs unaccommodated planes	loose continuous infillings nodules coatings pendent external hypocoatings frost shattered aggregates	very frequent organics tissue (charred) bone	weathered magnetic Fe oxide hypocoatings calcium carbonate infillings
12.1	B3 matrix	karstified plasmic to subangular blocky	random undulating stipple speckled	void and grain coatings and fine to concentrations rare papulas	close porphyric to single spaced coarse grains exhibit oblique alignment	vughs unaccommodated planes channel	loose discontinuous infillings nodules coatings passive features frost shattered aggregates	roots (class 0.4) plant residue charcoal	highly weathered magnetic Fe oxide hypocoatings calcium carbonate infillings

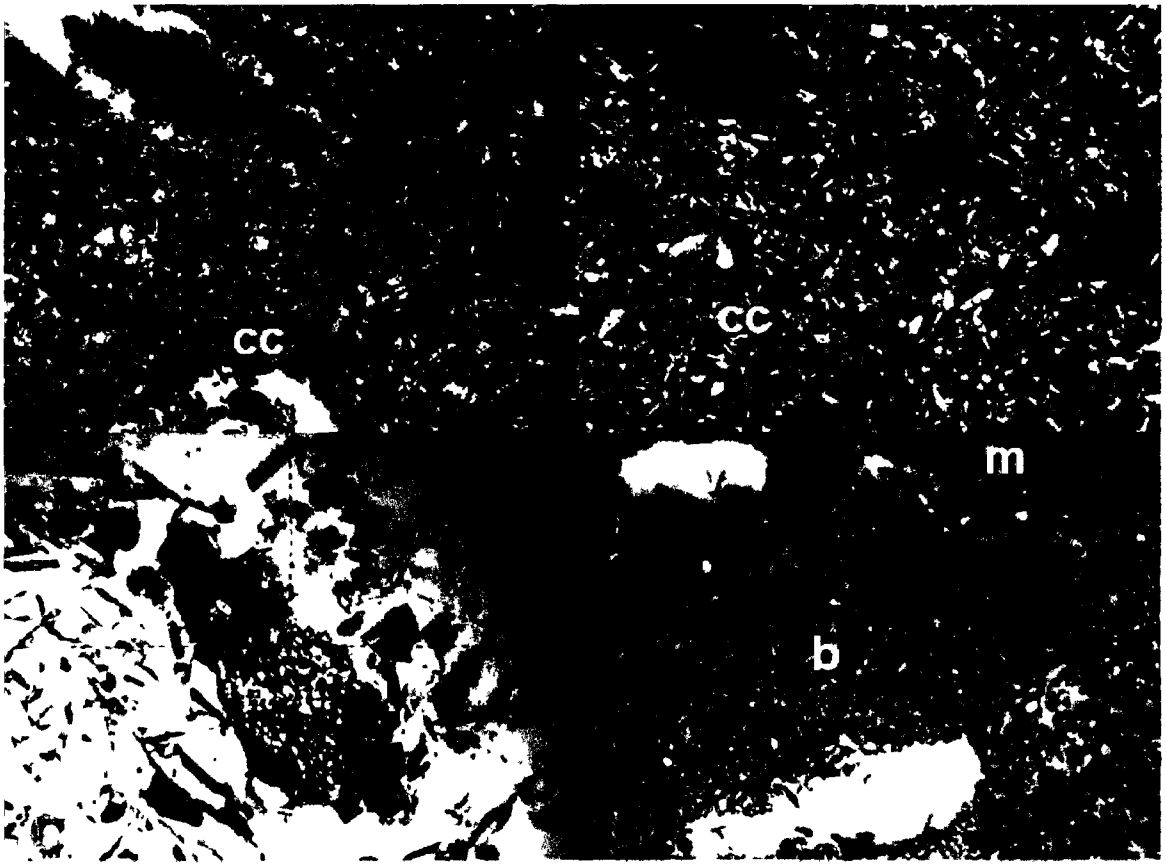

Figure 4.2 Thin Section Micrographs

a. Slide 2.1 (6.3x,plane polarized light (ppl), 1.8x 1.4mm)-Calcium carbonate infillings (cc) and root decomposition (class 2) b. Same as "a" in cross polarized light (xpl), c. Slide 5.1 (16x, ppl, 720x520μ) tissue fragment, and d. Slide 2.1 (5x, reflected light (rl), 2.3x1.8mm) bone (b), magnetite (m) and vughes (v).

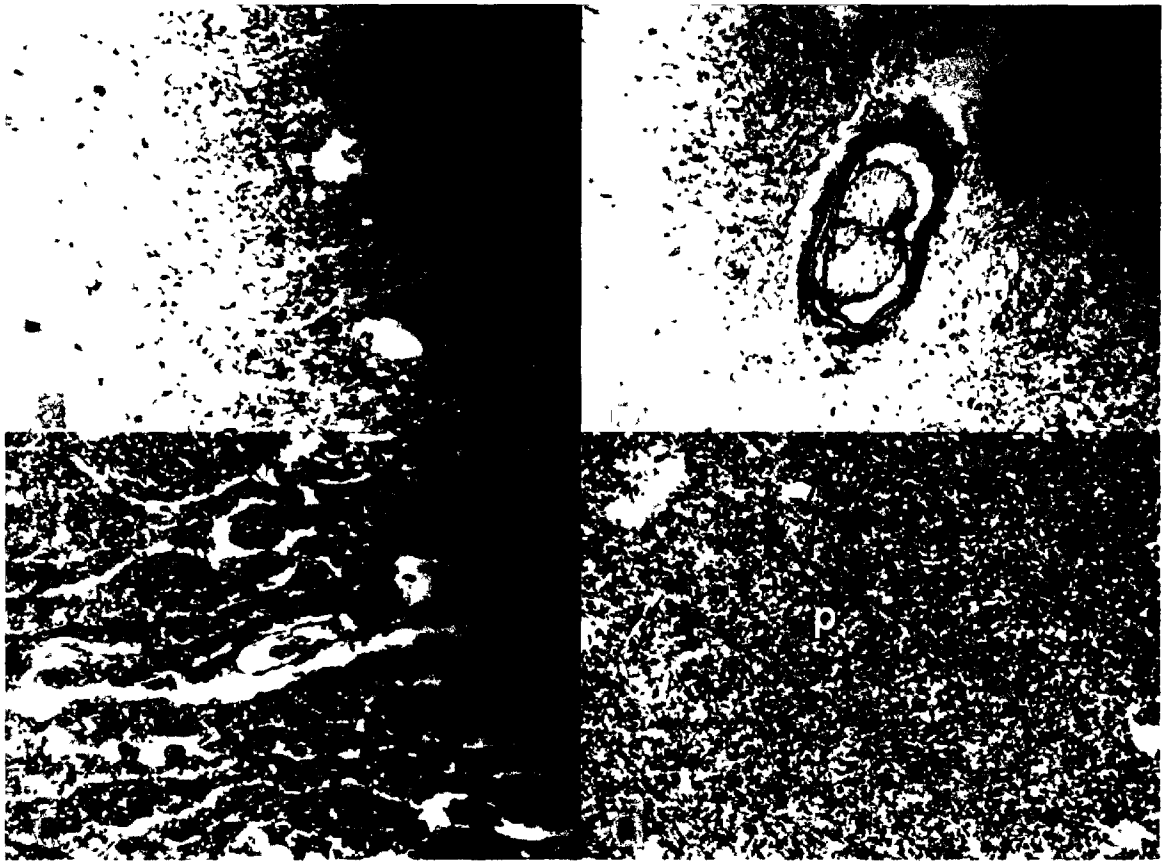

Figure 4.3 Thin Section Micrographs

a. Slide2.1 (2.5x, ppl, 4.5x3.5mm) Granular microstructure with platy overprint, b. Slide 5.1 (2.5x, ppl, 4.5x3.5mm) Root (class 0), c Slide 12.1 (2.5x, ppl, 4.5x3.5mm) Subangular Blocky to Lenticular microstructure of clay lamella, and d. Slide 4.2 (2 5x, ppl, 4.5x3.5mm) Passage feature (p).

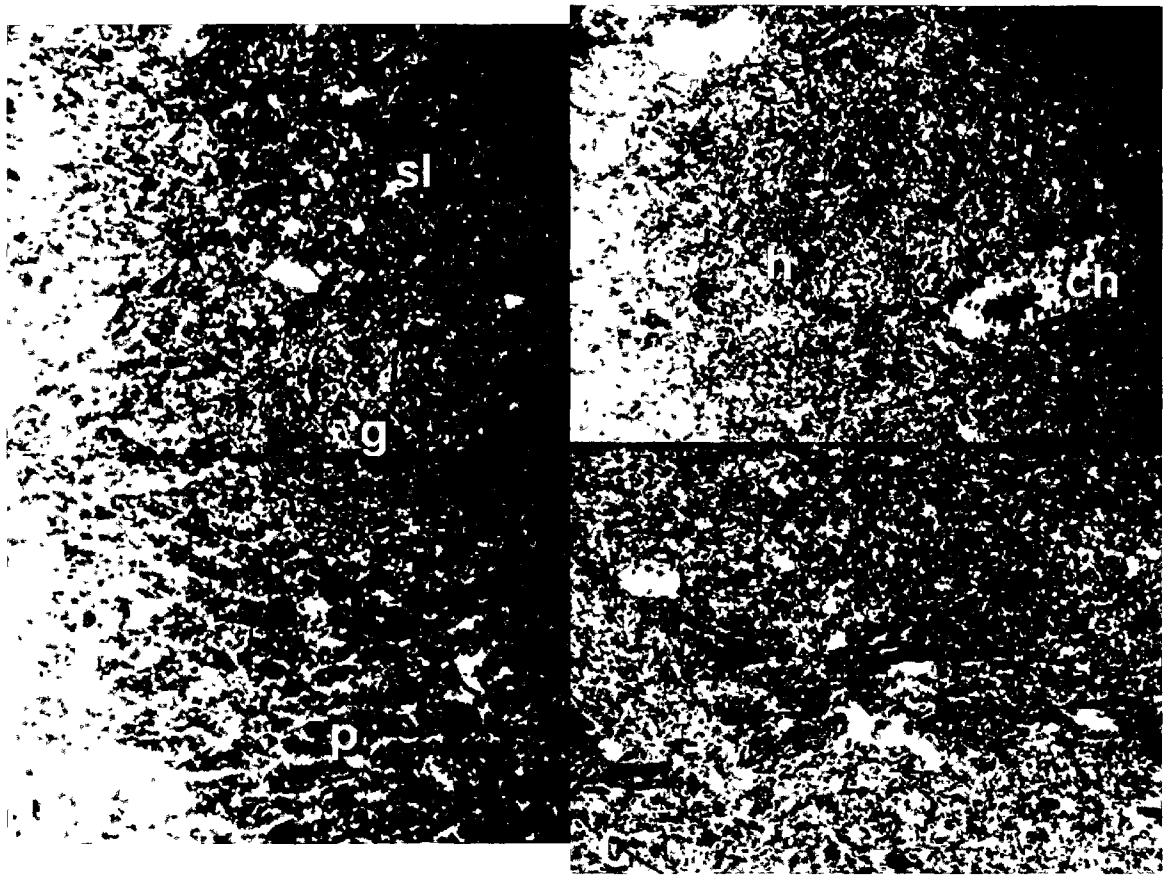

Figure 4.4 Thin Section Micrographs

a. Slide 7.2 (2.5x, ppl, 8x3mm) Transition from platy(p) to granular (g) microstructure, shows sand lens (sl), b. Slide 7.2 (2.5x, ppl, 4.5x3.5mm), Iron oxide hypocoating (h), and loose continuous infilling of channel void (ch), c Slide 4 2 (2 5x, ppl, 4.5x3 5mm) paleosol

All thin sections contained organic matter in varying amounts and degrees of decomposition. Organic concentrations, plant residues, excrements, organans (pedogenically derived organic coatings) and charcoal fragments were all observed. The majority of organic matter was well preserved and is representative of boreal forest vegetation (all samples examined are from above the lower paleosol complex).

Plant decomposition is a pedogenic processes that is the organic equivalent of mineral weathering (Buol, et al. 1997) and which results from both microbial activity and wetting/drying and/or freeze/thaw activities. Decomposition results in the formation of fine organic matter which appears in thin sections as dark staining which was observed in all thin sections. Most of the slides showed roots in various states of decomposition, with most exhibiting class 0 (no decomposition) to class 4 (no discernable tissue remains). Iron-oxide grains were observed in all thin sections. Reflected light was used to distinguish mineral from organic grains (which both appear opaque under transmitted light). Magnetite (Figure 4.2) was the most commonly observed mineral grain and evidence of weathering ranged from fresh to highly weathered, with most slides showing some evidence of weathering.

The micromorphological analysis shows that all samples examined have undergone some degree of pedogenesis and weathering. As is expected, the soils closest to the modern soil surface have undergone the greatest amount of pedogenic alteration (especially in the B horizons).The micromorphology of the B horizons shows pedofeatures typical of soils affected by cryoturbation and bioturbation as do the underlying C horizons to lesser extents. Passage features are found throughout the soil profile, with the exception of slides 4.1, 4.2, 5.1 and 5.2. Voids were expressed mainly as vughs, planes, and channels. Passage features (Figure 4.2) are infillings that have the same composition as the surrounding groundmass, but exhibit crescentric internal fabric the boundaries which are indistinct. The loose infillings observed generally consists of soil biota excrement (Figure 4.4).

The micromorphology indicates that the C2 loess has undergone weak pedogenic alteration and soil formation through time, but that these changes never outpaced loess deposition. The picture that emerges from the thin section analysis in the lower loess is of inceptisol type soils that were never buried quickly enough to remove them from the soil formation processes, and which were never established enough to develop any soil horizonation resulting in a weakly welded soil.

The paleosol stringers are thin Awb horizons which do not exhibit any other horizonation; no accompanying Bb horizons were observed in thin section or in the field in relation to these Awb horizons. The paleosols also appear to have been affected by diagenic alteration resulting in their platy microstructure; in all slides examined, areas that had more fine organic matter exhibited stronger platy microstructure than the surrounding groundmass (Figure 4.4). This indicates that these soils underwent freeze/thaw processes after deposition, as well as compaction. The plane voids are also an indication of

these processes. The oblique arrangement of the coarse fraction observed in several of the slides results from frost jacking, and also indicates freeze/thaw processes.

The micromorphological analysis indicates that there are no detectable buried occupational surfaces within the upper loess in the thin sections examined, which are assumed to be representative of the soil micromorphology for the entire site. It is highly likely that if there were such surfaces at one time they have been obscured by taphonomic disturbance and so are no longer detectable. A sand lens is evident in slide 7.2 (Figure 4.4), but this lens is not indicative of an occupational surface and does not correlate with the location of cultural remains found at the site.

The micromorphological analysis also indicates that weathering and soil formation has taken place throughout the profile to varying degrees. This weathering and post-depositional alteration indicates the upper loess horizons have undergone major diagenic transformations and that the cultural remains found in them are in secondary contexts. The lower horizons have also undergone diagenic transformations but not to the same extent as the upper horizons indicating that the cultural remains found in the lower horizons have not been disturbed to the same extent as the upper horizons.

4.2 Environmental Magnetism

Volume magnetic susceptibility (κ_{lf}), mass magnetic susceptibility (χ_{lf}) and frequency dependency ($\chi_{fd\,\%}$) values were examined at both a site wide and profile specific scale. For the site wide comparison, volume magnetic susceptibility, mass magnetic susceptibility and frequency dependency values were grouped according to general soil stratigraphy; sand, lower loess (C2), paleosols (PS and PS/C2), upper loess (C1), B and O/A/E horizons. All environmental magnetism data can be found in Appendix B. Samples from overburden or disturbed contexts were excluded from analysis. SPSS was used to generate descriptive statistics and a one-way analysis of variance (ANOVA) test was applied to determine if there are statistically significant differences in the mean values between each soil (Table 4.2). The data used is assumed to be an independent random sample from each population, from populations that are normally distributed, and from populations whose variances are all equal.

The null hypothesis is that the population means for each soil class are the same (that there is no difference in the averaged magnetic susceptibility or frequency dependency values for the soil classes). The alternative hypothesis is that there is a difference. The resulting ANOVA test showed statistically significant differences between the population means between soils groups for κ_{lf}, χ_{lf}, and $\chi_{fd\%\,at}$ the 0.05 level.

Table 4.2 ANOVA

ANOVA					
κlf					
	Sum of Squares	**df**	**Mean Square**	**F**	**Sig.**
Between Groups	1137163.654	5	227432.731	85.351	0.000
Withing Groups	1422936.869	534	2664.676		
Total	2560100.523	539			
χlf					
	Sum of Squares	**df**	**Mean Square**	**F**	**Sig.**
Between Groups	0.852	5	0.17	74.428	0.000
Withing Groups	1.223	534	0.002		

However, the Levene Statistic (Table 4.3) for each ANOVA shows that the assumption of homogeneity of variance is not true, and so Brown-Forsythe and Welch options were run, along with the Games-Howell post-hoc test (which does not rely on homogeneity of variance). The Welch and Brown-Forsythe significance values are both <0.05, so the null hypothesis can be rejected.

Table 4.3 Levene Statistic

Test of Homogeneity of Variances			
k_lf			
Levene Statistic	**df1**	**df2**	**Sig.**
29.221	5	534	0
X_fd			
Levene Statistic	**df1**	**df2**	**Sig.**
21.224	5	534	0
X_lf			
Levene Statistic	**df1**	**df2**	**Sig.**
57.703	5	534	0

The Games-Howell post-hoc test shows that there are statistically significant differences in the mean values of all three data sets between soil classes. (see Appendix 2 for all magnetic susceptibility data). The resulting plots of the means of each soil class for both κ_{lf} and χ_{lf} show a similar pattern for most soil classes (Figure 4.5). The sand has the highest κ_{lf} and χ_{lf}, which is most likely a product of the much larger particle size of this horizon; this is supported by low $\chi_{fd\%}$ for the sand class. C2 and C1 have similar

κ_{lf} and χ_{lf} values, which are much lower than the values from the sand layer. This is due to a change in parent material and grain size. The paleosols (PS and PS/C2) have mean values higher than the C1 and C2 soil classes and which are closer to the modern forest soil (B and O/A/E). This most likely indicates an increase in weathering or pedogenesis associated with these buried A horizons. The means of κ_{lf} and χ_{lf} depart from each other in the B and O/A/E horizons. While this could indicate changes in the primary sedimentary density of these upper horizons, the higher organic content (equaling lower density) in the O/A/E soil class is most likely the cause of this discrepancy.

Mean κ_{lf} and χ_{lf} were plotted against mean $\chi_{fd\%}$ (Figure 4.6). Frequency dependence is low in the lower loess and sands and increases substantially at the modern surface soil, with the highest percent being in the modern B horizon. Both the sand and C2 horizons have $\chi_{fd\%}$ of less than 2.0, indicating there are less than 10% superparamagnetic (SP) grains in these horizons. On a site wide scale, the paleosols do not exhibit any marked increase in mean frequency dependency; however individual profiles at the site do see spikes of frequency dependency at some of the paleosol levels, these spikes correspond to cultural remains and will be examined in detail below.

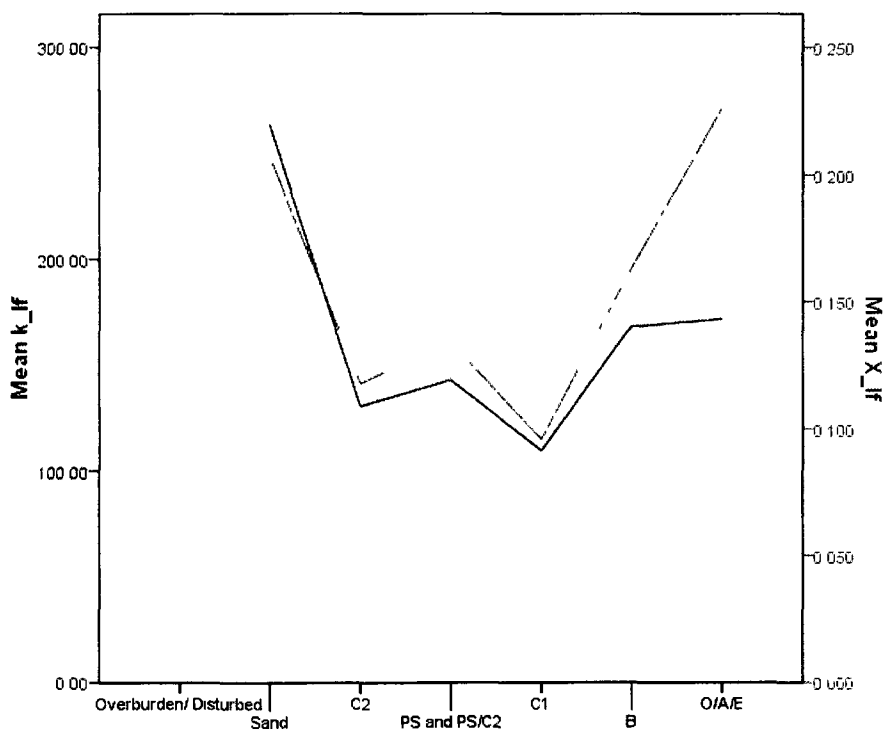

Figure 4.5 Mean κ_{lf} and χ_{lf}

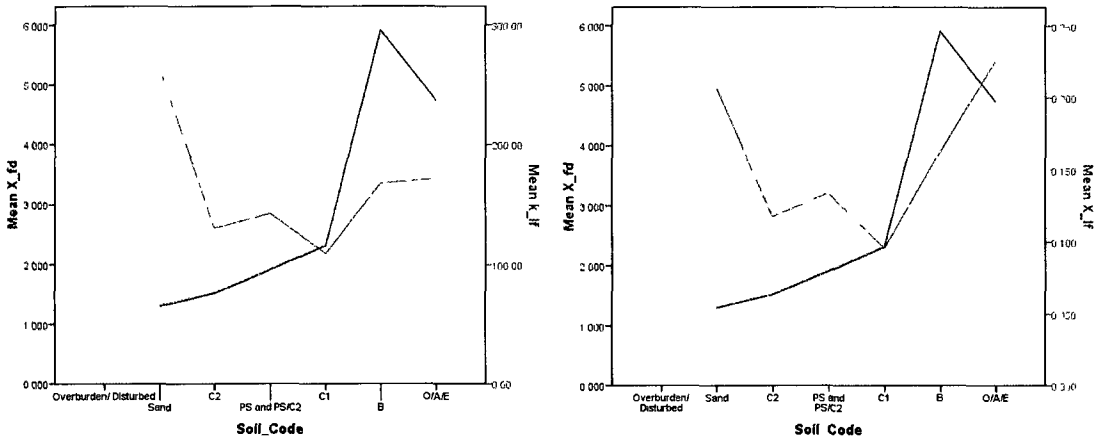

Figure 4.6 Mean χ_{lf} and $\chi_{fd\%}$ (left) and mean κ_{lf} and $\chi_{fd\%}$ (right)

At the profile specific scale, each soil horizon in each profile was grouped to fit the six soil classes outlined above, and volume magnetic susceptibility, mass magnetic susceptibility and frequency dependency values were plotted over these classes (Figure 4.7 and Figure 4.8). Spatial distributions of *in situ* bone and artifacts (grouped by 5cm arbitrary level) were then applied to each profile to see if the variations in of the environmental magnetism values correlated with the occurrence of cultural remains.

The picture that emerges from this analysis is one of variability across the site; many times the magnetic data has shifts that do not correlate with the generalized stratigraphy. In particular, most of the profiles in the C2 horizon exhibit a sudden decrease in κ_{lf} and χ_{lf} which is bracketed by spikes in $\chi_{fd\%}$. As both κ_{lf} and χ_{lf} correlate with grain size, and $\chi_{fd\%}$ indicates the presence and amount of SP mineral grains, it appears that there was a shift in grain size to smaller particles at these anomalies. However in some of the profiles there are drops in $\chi_{fd\%}$ which correspond to drops in κ_{lf} and χ_{lf} A drop in both of these parameters indicates that the concentration of magnetic material decreased, rather than grain size. This trend may be the transition zone between the C2a and the C2b loess (which is evidenced by an increase in iron oxide mottling), or it may be indicative of a change in climate. No cultural remains were recovered for the relative levels of these shifts; however it is interesting to note that in the one unit where cultural material was recovered from this level (E46, profile 5) there is a decrease in κ_{lf} and χ_{lf} and $\chi_{fd\%}$. The environmental magnetism of each profile is examined in detail below.

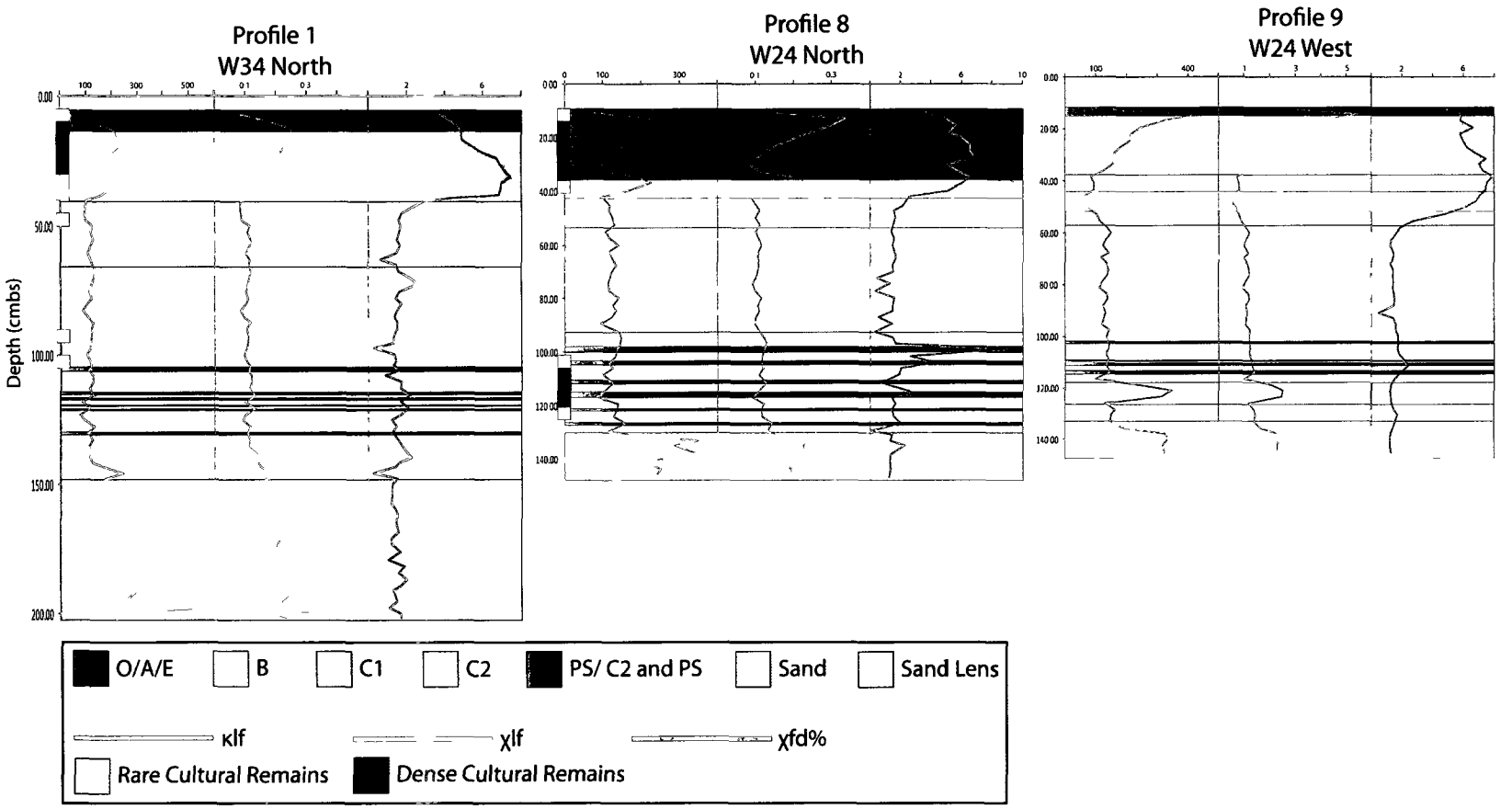

Figure 4.7 Magnetism Data, Soil Class, and Cultural Remains from West Lobe

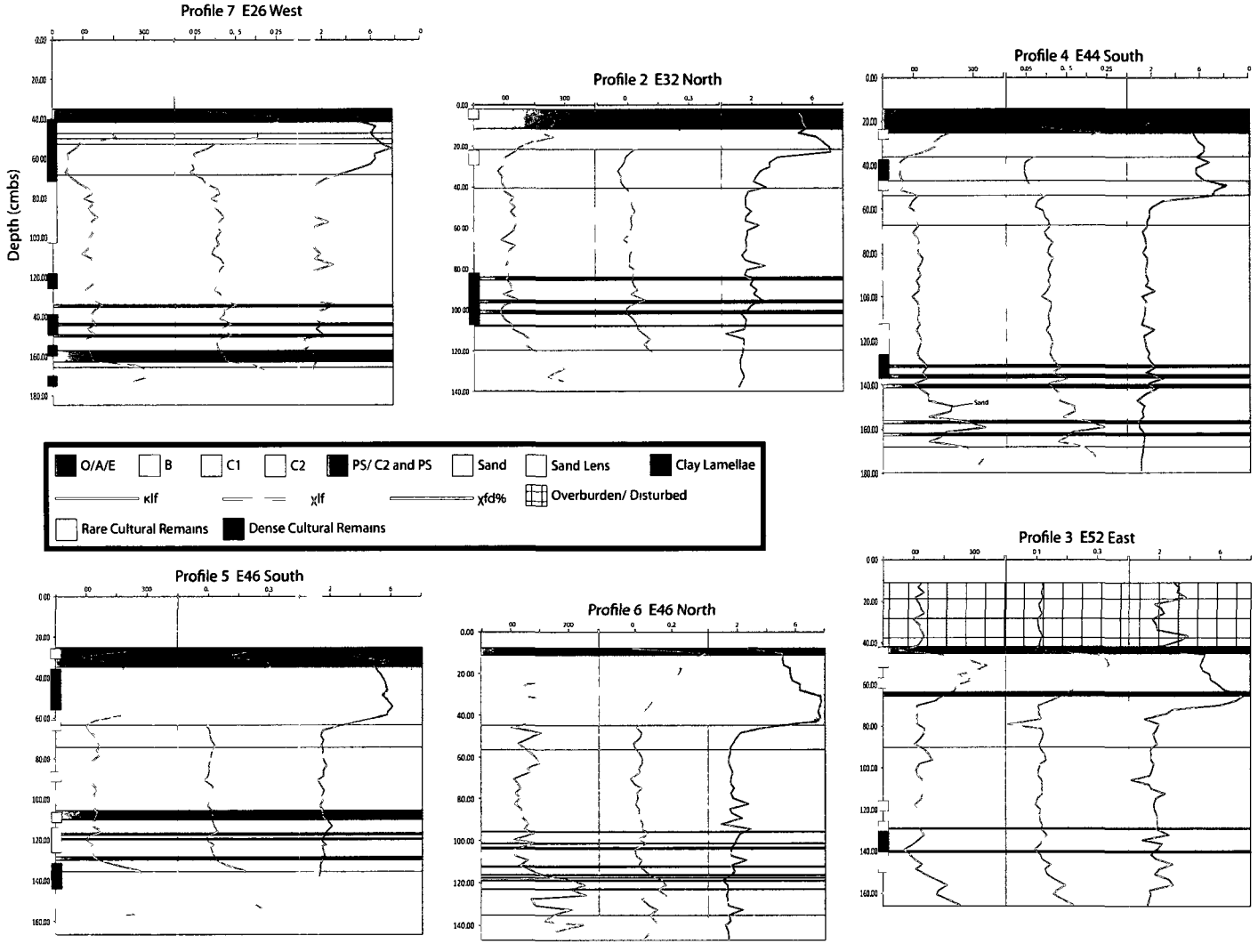

Figure 4.8 Magnetism Data, Soil Class, and Cultural Remains from East Lobe

Due to the variation noted in the field of the lower bedded sand, little time will be devoted in these profile analyses to their description. Also, some of the profiles schematics do not accurately show the different horizons from where the samples were collected (for example the drawing of profile 4 does not show the lowest paleosols which were recorded when the magnetic susceptibility samples were collected). When this is the case, the detailed information has been applied to the soil classification behind the magnetic data and not to the original profile drawing (as this information was only recorded for the specific area where the sample was taken and not the entire profile).

4.2.1 Profile 1 – W34 North

Profile 1 (Figure 4.9) exhibits an enhancement in both κ_{lf} and χ_{lf} and a decrease in $\chi_{fd\%}$ at 146 cmbs (Sample 23). Field descriptions of this sample note that it is a coarse sand, and may be an expression of the Younger Dryas. At 120.5 cmbs (Sample 31) there is an enhancement in κ_{lf}, χ_{lf} and $\chi_{fd\%}$, this is a sample of C2 with high iron oxide mottling. Above the area of iron oxide mottling the paleosols seem to correlate weakly with increases in κ_{lf}, χ_{lf}, and $\chi_{fd\%}$. Above the paleosols κ_{lf}, χ_{lf} (weakly) and $\chi_{fd\%}$ (strongly) all decrease at 90.5cmbs (Sample 44), but there is no stratigraphic change noted at this location. At 75.5 and 65.5 cmbs (Samples 51 and 55) there are enhancements of $\chi_{fd\%}$ but not of κlf or χ_{lf} in C2a that was noted as being sandier than the surrounding C2a. Finally, enhancement of κ_{lf}, χ_{lf} and $\chi_{fd\%}$ all increase substantially at the base of the B horizon and the decrease at the base of the O/A horizon but these enhancements in the modern forest soil do not correlate with the location of the cultural remains.

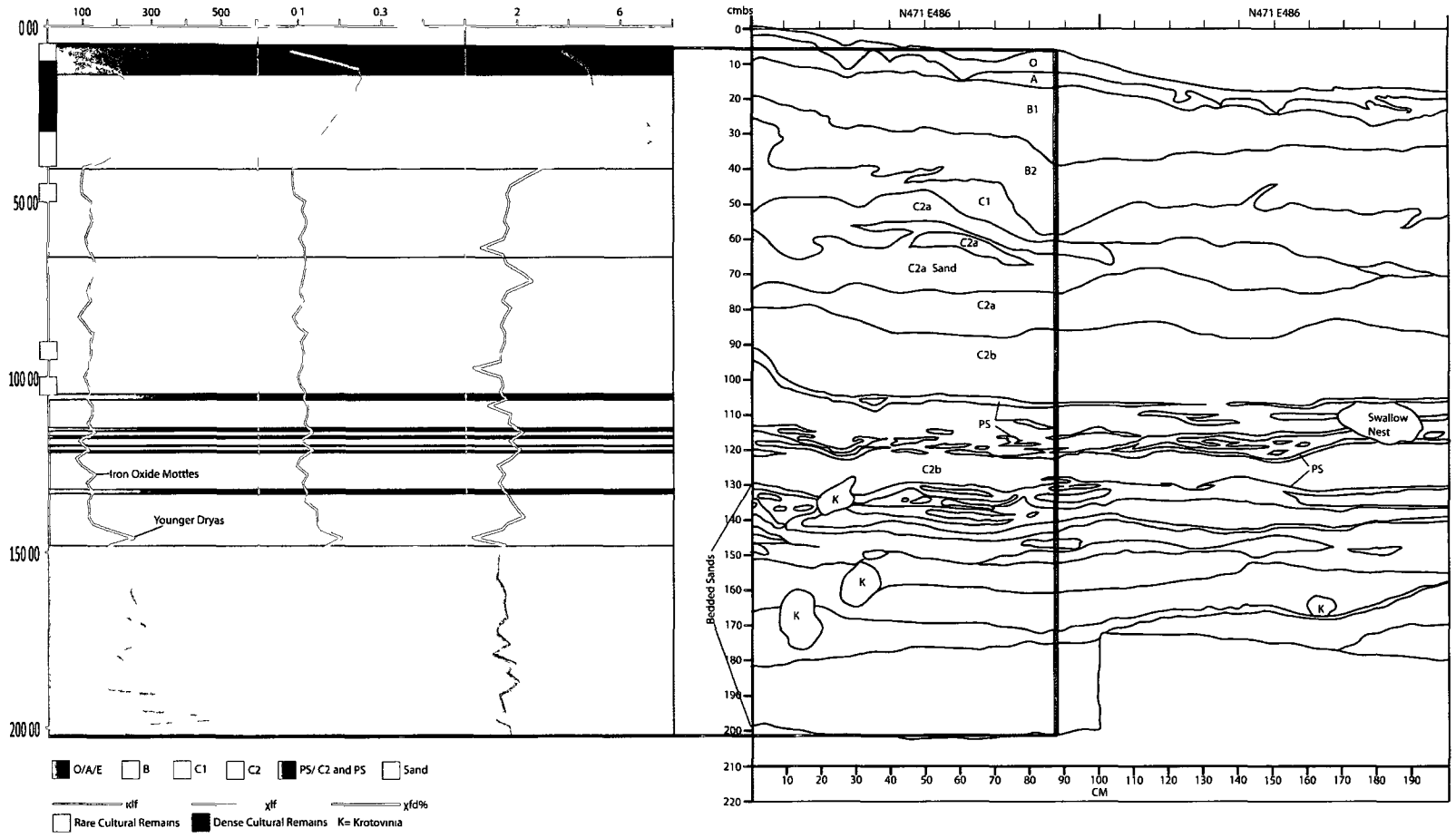

Figure 4.9 Profile 1 (Block W34 North Wall) Magnetic Susceptibility

4.2.2 Profile 2- E32 North

Profile 2 (Figure 4.10) exhibits an enhancement in both κ_{lf} and χ_{lf} and a decrease in $\chi_{fd\%}$ at 114.5 cmbs (Sample 92). The patterning and stratigraphic location of this signal is similar to the Younger Dryas signal noted in other profiles; however no sand lens was noted as being present in Profile 2. This may indicate that the Younger Dryas signal is detectable with magnetic susceptibility when it is not detectable macroscopically.

The magnetic susceptibility profile shows enhancement of κ_{lf}, $\chi_{lf,}$ and $\chi_{fd\%}$ at 95 cmbs (sample 100). This sample was taken at the stratigraphic location of Feature 3 (Figure 4.11) and the signal is much greater at the Feature 3 paleosol than at the other paleosols in this profile indicating anthropogenic enhancement of the soil.

There is a sharp increase in $\chi_{fd\%}$ above the uppermost paleosol that does not appear to correspond to any stratigraphic change or cultural remains. Above this, but between the C1/C2 contact there is a decrease in κ_{lf} and χ_{lf} while $\chi_{fd\%}$ remains the same; $\chi fd_{\%}$ does spike above this change. At 52 cmbs there is a decrease in κ_{lf}, and an increase in χ_{lf} and $\chi_{fd\%}$. This takes place in the C1 horizon where field notes describe a change from a sandy silt to a silt (as κ_{lf}, does not take into account sample density a change in particle size would be reflected in the κ_{lf} but not necessarily the χ_{lf} measurement). In profile 2 enhancement of κ_{lf}, χ_{lf} and $\chi_{fd\%}$ all increase substantially at the base of the B horizon and then decrease at the base of the O/A horizon.

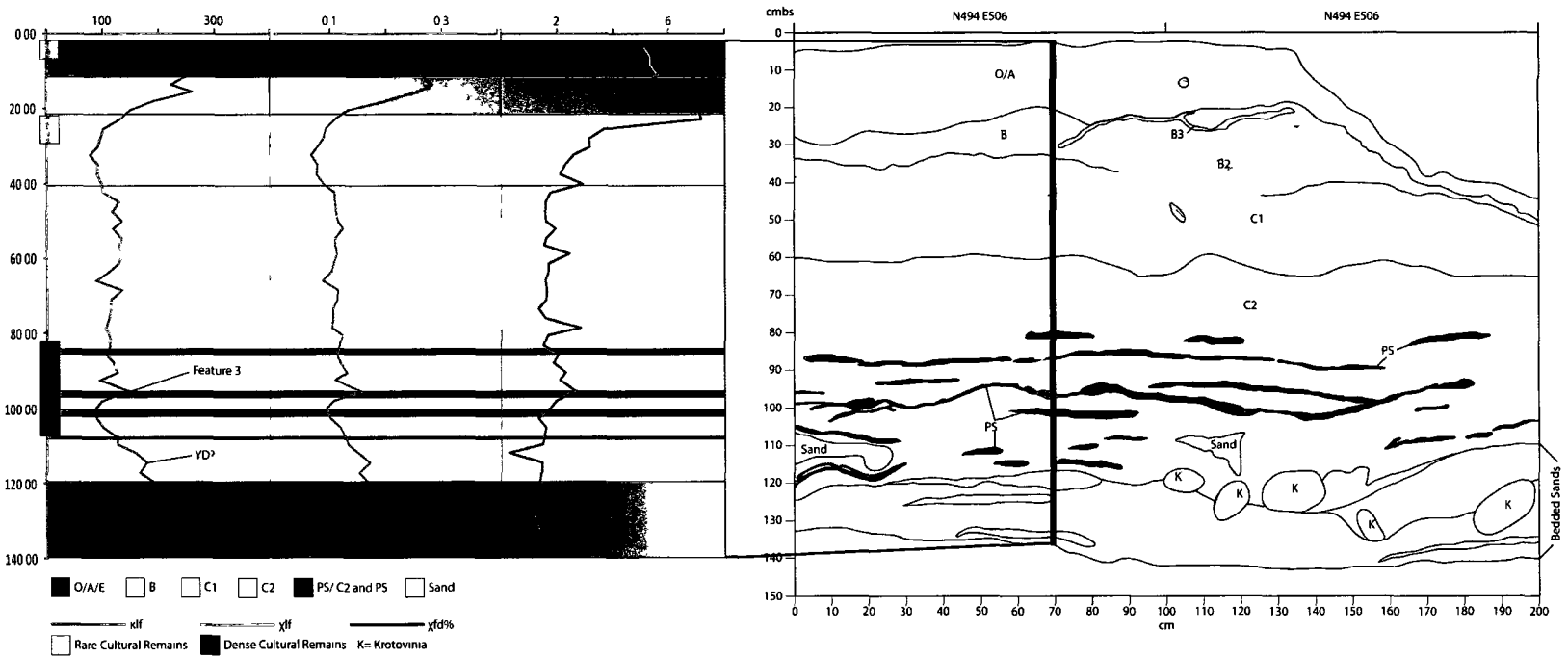

Figure 4.10 Profile 2 (Block E32 North Wall) Magnetic Susceptibility

Figure 4.11 Feature 3

4.2.3 Profile 3- E52 West

Enhancements of κ_{lf}, χ_{lf}, and $\chi_{fd\%}$ in the lower loess section of Profile 3 (Figure 4.12) correspond well with paleosol location with one noted exception. At 124 cmbs (Sample 151) the sample is composed of C2 and paleosol soil, and it exhibits no enhancement or depletion of κ_{lf} or χ_{lf} but does show depletion in $\chi_{fd\%}$ Above the stratigraphic location of the paleosols there are several variations in the signal of κ_{lf}, χ_{lf}, and $\chi_{fd\%}$, none of which correlate to any field observed changes in stratigraphy. Sample 158 (107 cmbs) exhibits decreases in κ_{lf} and χ_{lf} while $\chi_{fd\%}$ remains fairly constant. The location of this sample corresponds to the location of two flakes that were found *in situ*. At 96.5 cmbs (sample 167) there is a spike in κ_{lf} and χ_{lf} and a slight decrease in $\chi_{fd\%}$; this is a sample of C2 from just below the contact with the C1 horizon (this is the reverse pattern as was seen in profiles 1 and 2).

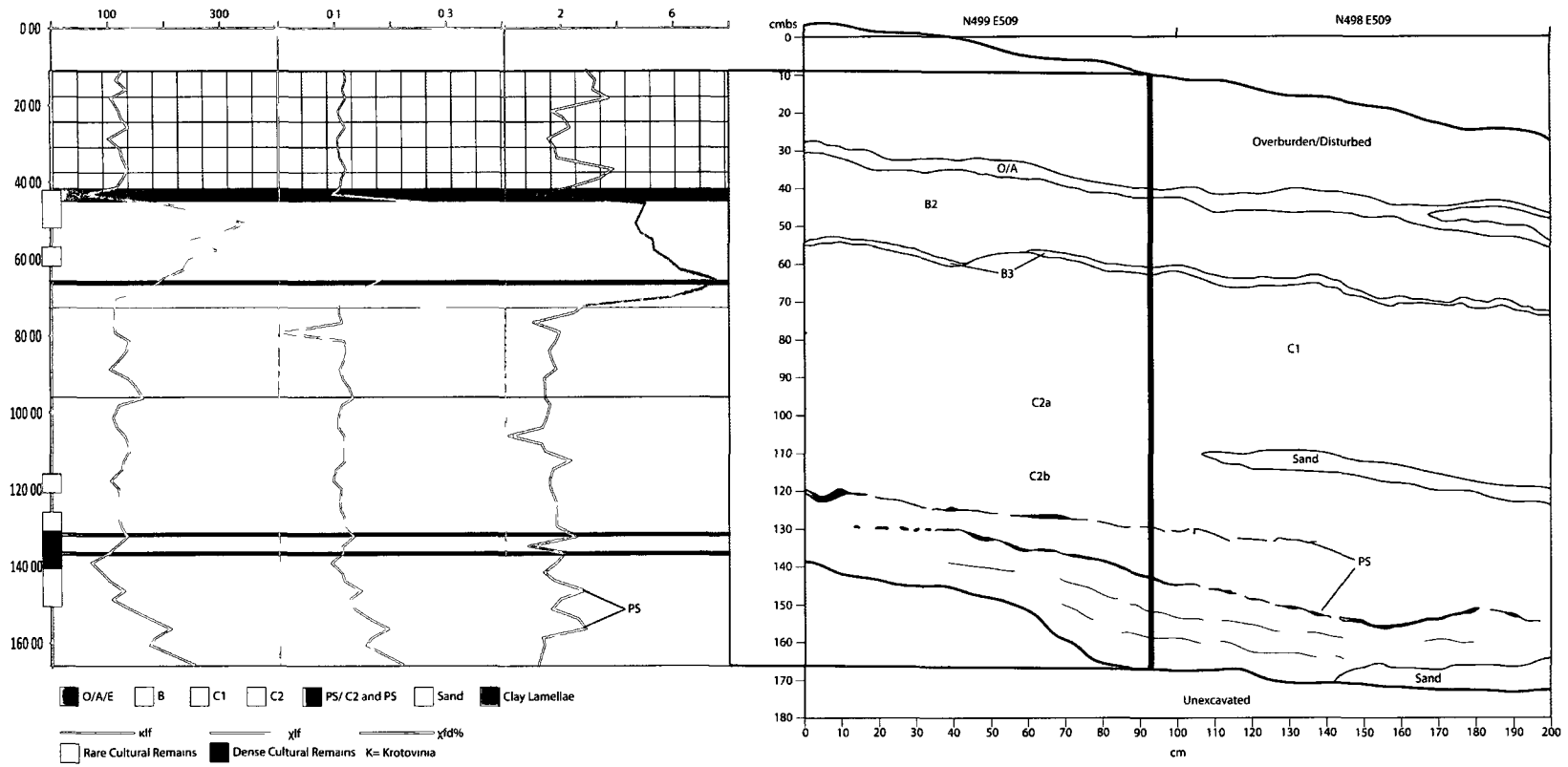

Figure 4.12 Profile 3 (E52 East Wall) Magnetic Susceptibility

4.2.4 Profile 4- E44 South

Profile 4 (Figure 4.13) exhibits enhancements in κ_{lf}, χ_{lf} with no change in $\chi_{fd\%}$ at 139.5 cmbs. This is the location of C2/sand that is pocketed between two paleosol stringers and may be an expression of the Younger Dryas cooling event, or may be associated with the lower bedded sands. Above these lower paleosols is another ephemeral layer of sand that shows enhancement of κ_{lf}, and χ_{lf}, but no change in $\chi_{fd\%}$, this might also be a signal of the YD.

Above the sand is another series of three paleosol stringers, the top two of which exhibit magnetic enhancement while the lowest does not. These are all located within 10 cm of each other and the top two correspond to the location of the CZ 4.5 bone scatter found in this unit (at 105 to 115 cmbs). It appears that here too the paleosols are enhanced by anthropogenic activity.

The next variation in signal is in the C2 horizon at 95 cmbs (Sample 229) that does not correspond with any stratigraphic changes (exhibits decrease in κ_{lf} and χ_{lf}, and an increase in $\chi_{fd\%}$). The next variation in κ_{lf} and χ_{lf} (decrease) is at 80 cmbs and does not correspond with any stratigraphic change; however the sample directly above it (at 77.5 cmbs, sample 236) does exhibit an enhancement of $\chi_{fd\%}$ and corresponds to a zone of increased iron oxide mottling.

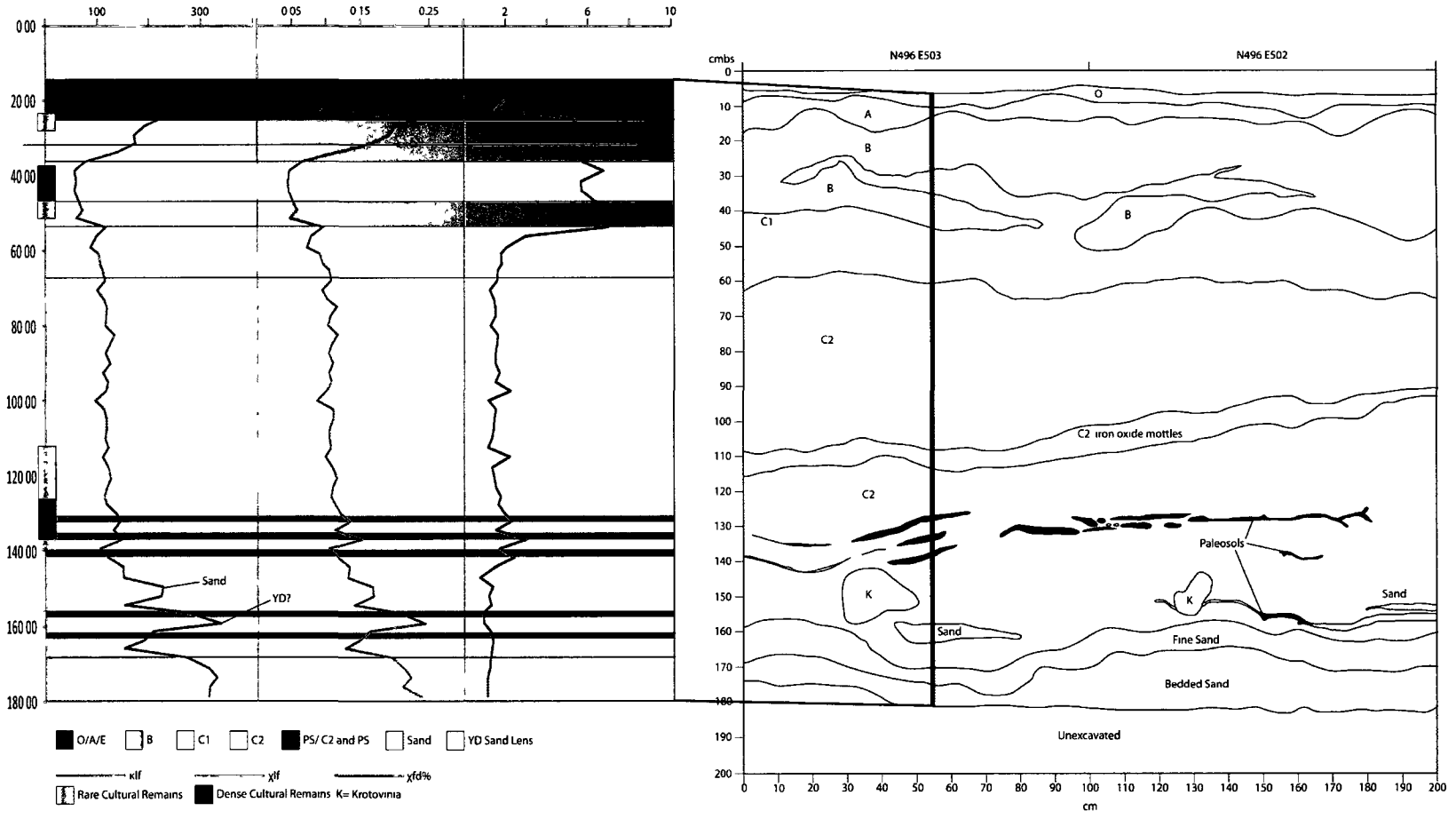

Figure 4.13 Profile 4 (E44 South Wall) Magnetic Susceptibility

A spike is evident at sample 254 at 34 cmbs which is the contact of the C1 and a pocket of Bw. This is followed by a span of fluctuation in the ms readings which corresponds with the B/C1 pocketed soil. $\chi_{fd\%}$ shows an overall enhancement that is typical of other B horizons in the profiles samples, but κ_{lf}, and χ_{lf}, show a decrease in signal, which appears to correspond to a decrease in the concentration of magnetic materials (as the $\chi_{fd\%}$ single indicates an increase in the SP grains). Above the B/C1 mixed zone the κ_{lf}, and χlf, are greatly enhanced along with $\chi_{fd\%}$. At the contact with the O/A horizon there is a decrease in κ_{lf}, χ_{lf}, and χ_{fd}.

4.2.5 Profile 5- E46 South

Profile 5 (Figure 4.14) exhibits variability in its magnetism that does not correspond with the cultural remains in the unit from CZ 4; however profile 6 (E 46 north) has variability that does correlate with the CZ 4 occupation (the CZ 4 remains in E46 were in the NE section). Profile 5 exhibits enhancements in κ_{lf}, χ_{lf}, and $\chi_{fd\%}$ at the base of the B horizon and then decreases at the base of the O/A horizon.

4.2.6 Profile 6- E46 North

For the most part the paleosols and enhancements in κ_{lf}, χ_{lf} and $\chi_{fd\%}$ do not correlate in Profile 6 (Figure 4.15), nor do changes in stratigraphy correlate with changes in magnetic susceptibility. It appears that the magnetic signal from both the south and north profiles of E46 exhibits variability that cannot be explained by the observed horizons of soil development or stratigraphic changes. These variations do not correspond with the location of cultural remains that were recovered from E46 either. This indicates other variables may be affecting the magnetic signal that have not been considered thus far.

4.2.7 Profile 7- E26 West

Enhancements of magnetic susceptibility correlate well with paleosols in profile 7 (Figure 4.16); however the variations in the C2 and C1 horizons do not appear to correlate with either stratigraphic changes or cultural remains.

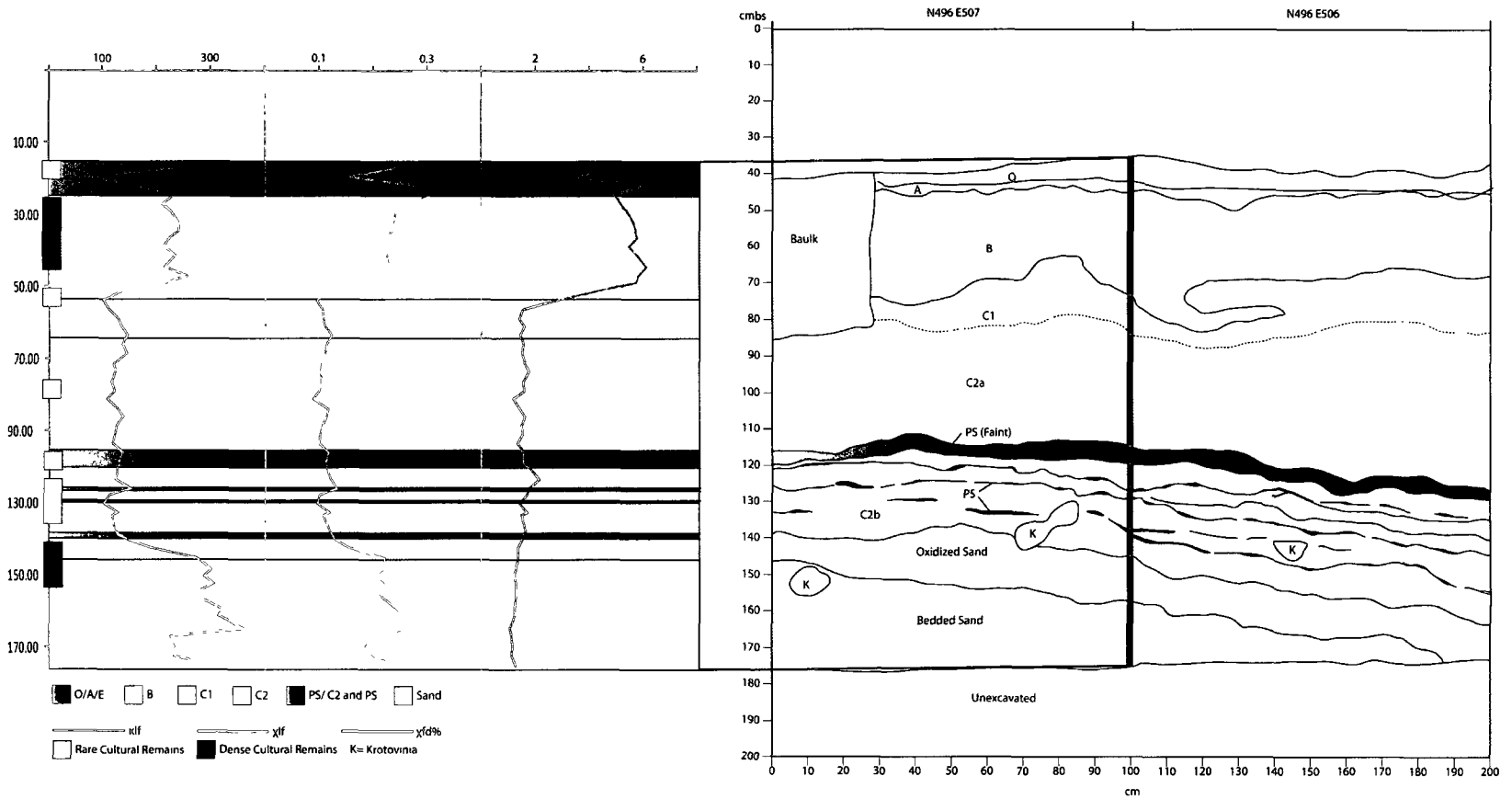

Figure 4.14 Profile 5 (E46 South Wall) Magnetic Susceptibility

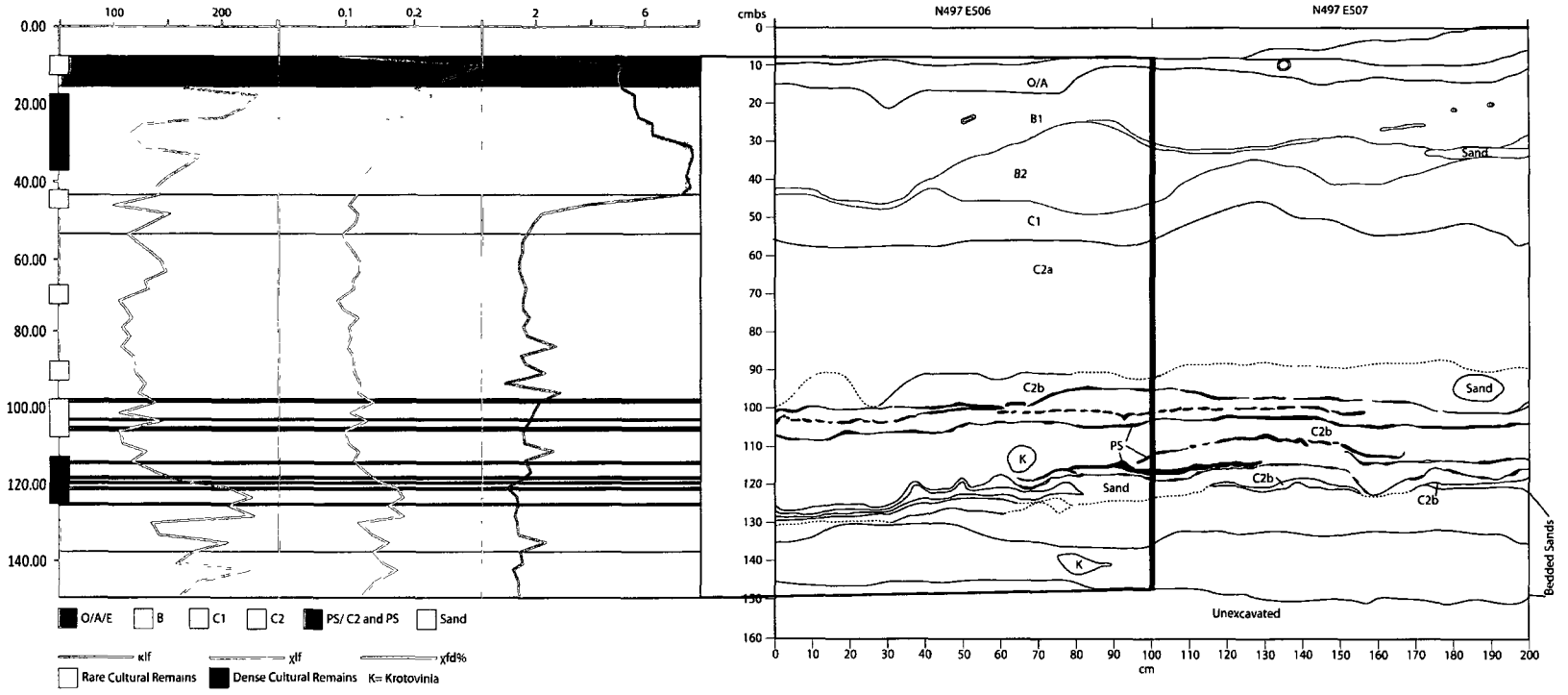

Figure 4.15 Profile 6 (E46 North Wall) Magnetic Susceptibility

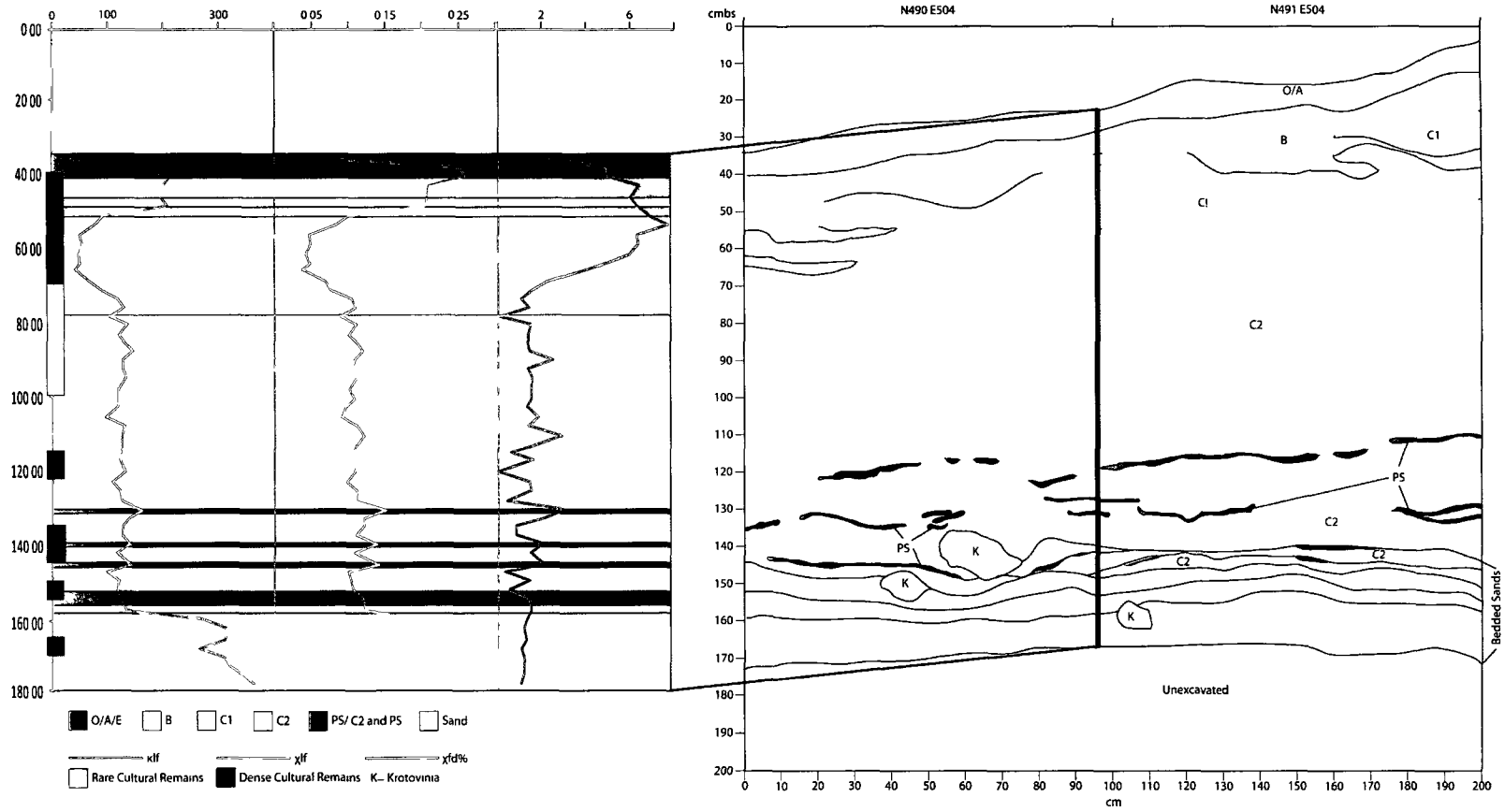

Figure 4.16 Profile 7 (E26 West Wall) Magnetic Susceptibility

4.2.8 Profile 8- W24 North

The largest spike in $\chi_{fd\%}$ other than those in the modern forest soil is observed in profile 8 (Figure 4.17) at 100 cmbs. $\chi_{fd\%}$ spikes to 8.97 in the upper well expressed paleosol in this unit; the location of which correlates with that of hearth Feature 4. The spike in $\chi_{fd\%}$ in Profile 8 is most likely the result of anthropogenic enhancement. As in other profiles examined, there is variation in the magnetic signal of the C2 and C1 horizons that does not correspond with either cultural remains or changes in stratigraphy.

4.2.9 Profile 9- W24 West

Profile 9 (Figure 4.18) shows differences in magnetic susceptibility from profile 8, which is interesting as they were taken from the same block. Profile 9 does show an increase in $\chi_{fd\%}$ of the lower paleosol at the level of hearth Feature 4 (this makes sense as the feature was located centrally east/west in the unit and towards the northern side of the block). Profile 9 has a lower sand horizon that was field identified as being related to the Younger Dryas and at this horizon there is a substantial increase in both κ_{lf} and χ_{lf} while $\chi fd_{\%}$ remains the same.

Profile 9 exhibits variation in the magnetic signal in the sterile zone between the upper and lower components that do not correspond with any field observed changed in stratigraphy. The upper soil horizons (B, E, A, O) follow the established pattern of enhancement in the B horizon and decrease in the O/A/E.

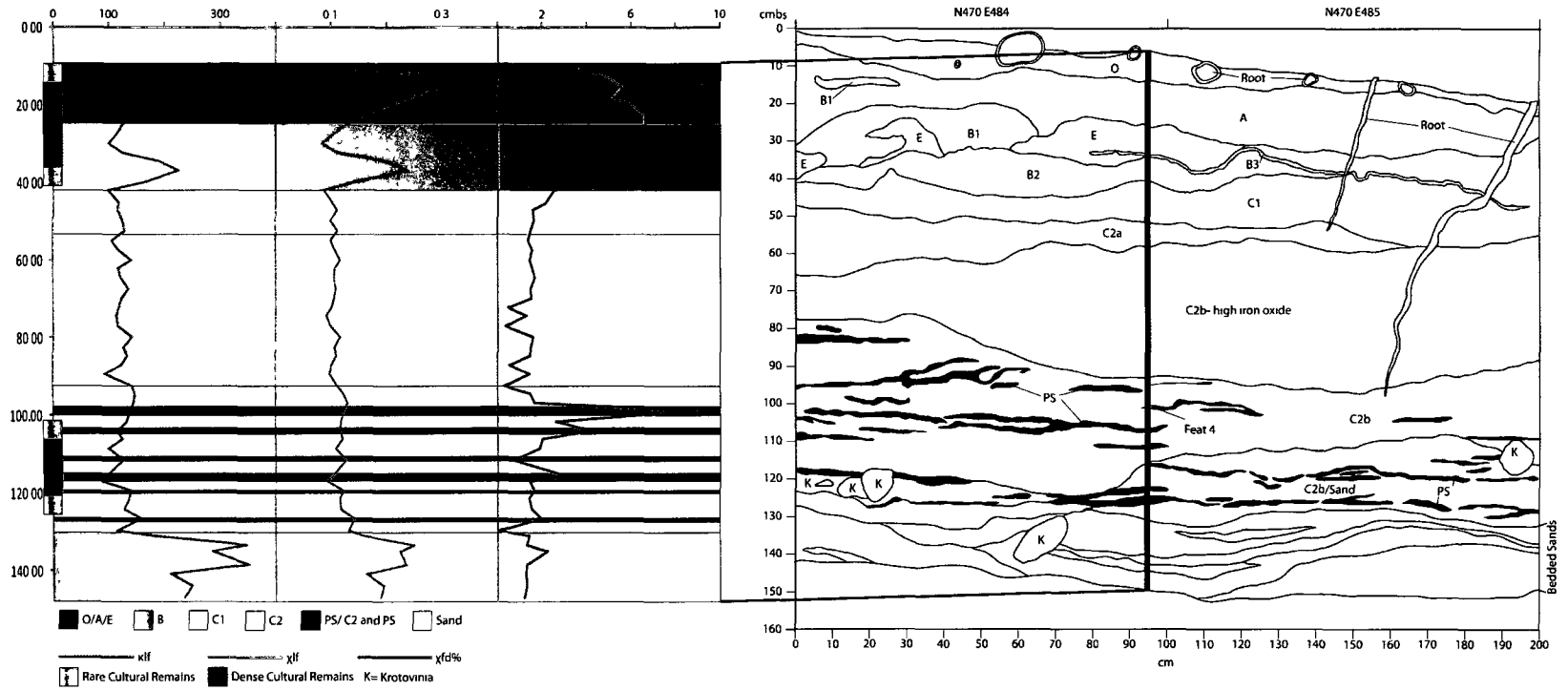

Figure 4.17 Profile 8 (W24 North Wall) Magnetic Susceptibility

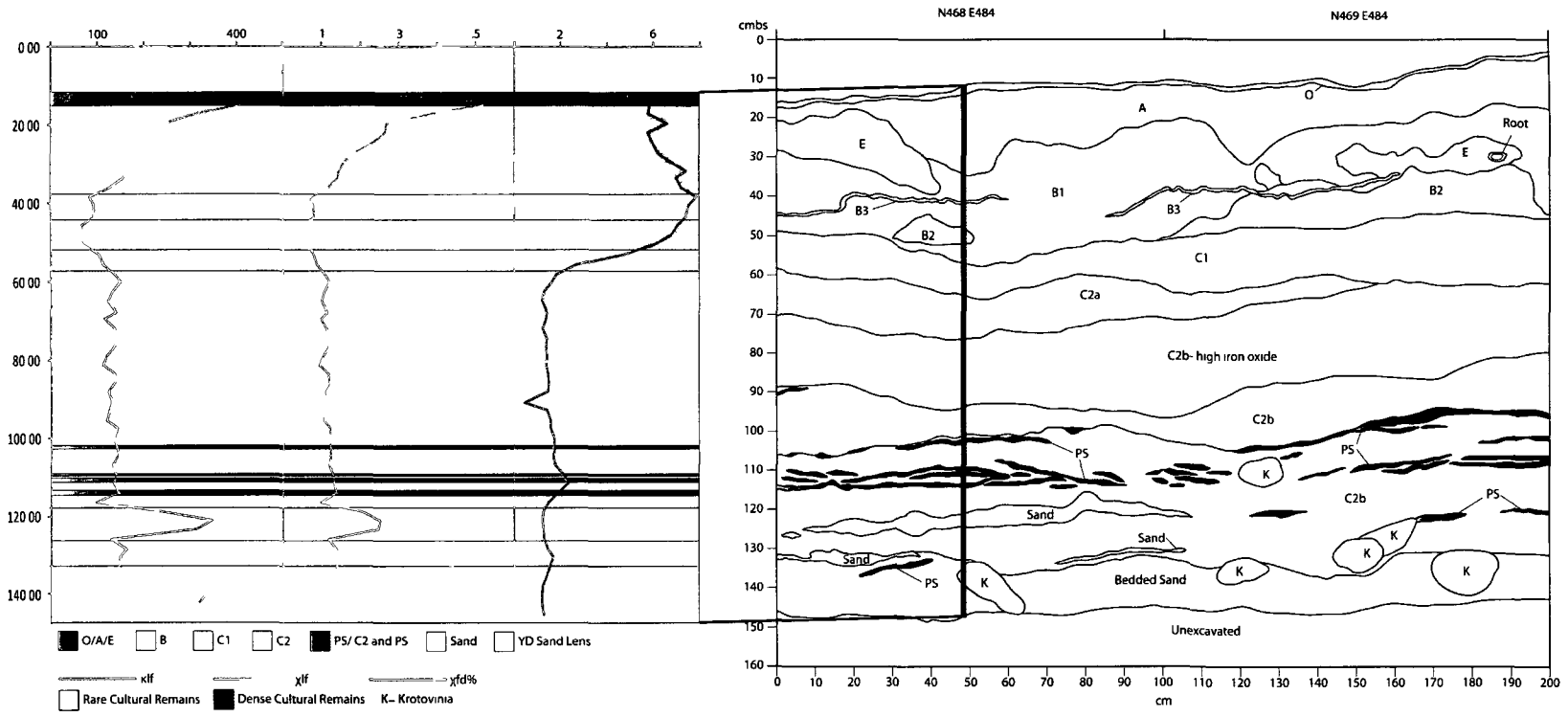

Figure 4.18 Profile 9 (W24 West Wall) Magnetic Susceptibility

4.2.10 Summary

Profile 1, 2, 4 and 6 all have sand horizons that were field identified as being possibly related to the Younger Dryas (YD) cooling event. Other sites in central Alaska (Dry Creek and other sites located in the Nenana Valley ~100km southwest of the Mead Site) also have sand horizons that are believed to correlate with the YD (Begét, et al. 1991; Bigelow, et al. 1990a) The sand horizons at the Mead Site show a consistent substantial increase in both κ_{lf} and $\chi_{lf,}$ while $\chi_{fd\%}$ values show little or no variation. This pattern is also seen in Profile 6, which does not exhibit the same well defined sand layer where the magnetic samples were collected. Both east and west of the sampling location however the stratigraphic profile depicts a sand layer that is separated from the lower sands by a thin layer of loess; this is interpreted as possibly being a YD signal. That this magnetic pattern is not evident at all profiles sampled at the site may be the result of variation in site specific deposition parameters such as paleotopography and of wind direction. The signal is evident in both the east and west areas of the site indicating that the cause of the signal was site wide.

The magnetic susceptibility profiles produced during this analysis indicate that the paleosols are the result of natural rather than cultural processes; however, there is strong evidence that the magnetic enhancement of these paleosols is fairly weak unless enhanced by anthropogenic activities. Many times the weakly expressed paleosols or those not associated with cultural remains have little to no enhancement, while all large spikes in susceptibility and frequency dependence occur where cultural remains are found.

4.3 Bulk Density

The bulk density of all magnetic susceptibility samples (n=553) was classed by general soil type and SPSS was used to generate descriptive statistics and a one-way analysis of variance (ANOVA) test to determine if there are statistically significant differences in the mean bulk density values between each soil (see appendix 2 for bulk density values and SPSS calculations). The data utilized is assumed to be: an independent random sample from each population, from populations that are normally distributed, and from populations whose variances are all equal.

As with the magnetic susceptibility data, the Levene Statistic (Table 4.4) shows that the assumption of homogeneity of variance is not true, and so again the Brown-Forsythe and Welch options were run, along with the Games-Howell post-hoc test. The Brown-Forsythe and Welch tests (Table 4.5) shows that there are statistically significant differences between the mean bulk density values of the soil classes, and the Games-Howell post-hoc test (Table 4.6) shows that these statistically significant differences are present between all of the soils classes analyzed.

Table 4.4 Levene Statistic for Mean bulk density by soil class

Density

Levene Statistic	df1	df2	Sig.
11.284	5	534	.000

Table 4.5 Welch and Brown-Forsythe statistics for mean bulk density

Density

	Statistic[a]	df1	df2	Sig.
Welch	46.630	5	142.431	.000
Brown-Forsythe	71.195	5	183.556	.000

a. Asymptotically F distributed.

Table 4.6 Games-Howell post-hoc test for mean bulk density

Multiple Comparisons

Dependent Variable:Density

	(I) Soil Code	(J) Soil Code	Mean Difference (I-J)	Std. Error	Sig.	95% Confidence Interval	
						Lower Bound	Upper Bound
Games-Howell	Sand	C2	.16557*	01820	.000	.1126	.2185
		PS and PS/C2	.21703*	.02462	.000	.1456	.2885
		C1	.13391*	02262	.000	.0685	.1993
		B	.19438*	.02153	.000	.1322	.2566
		O/A/E	.54268*	03776	.000	.4308	.6545
	C2	Sand	-.16557*	01820	.000	-.2185	-.1126

*. The mean difference is significant at the 0.05 leve .

Analysis of the bulk density data shows a general trend of high density at the base of the soil profile to lower density in the modern forest soil, with the exception of the C1 horizon (Figure 4.19). Lithiostratigraphically, the C2 is composed of the lower loess, which has a finer grain size than the upper loess (C1). The C1 has a higher bulk density than the C2, which is most likely due to its coarser gain size and the downward movement of fine constituents from the overlying horizons. The paleosols exhibit

slightly lower bulk density than their parent material (the lower loess) and this too is most likely due to the higher concentration of the less dense organics in the paleosols.

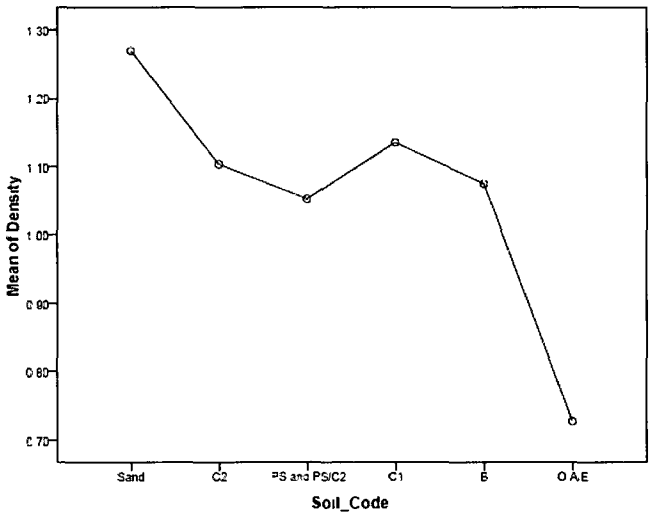

Figure 4.19 Mean Bulk Density (g/cc) by soil class

4.4 Geochemical Analysis

Ti and Zr were used to determine if the soil formed in a uniform parent material, as they are resistant to weathering. Zr/Ti and Ti/Zr ratios were calculated (Figure 4.20) and the resulting graphs depict two major shifts in the profile, one at BD-26 and a second at BD-20 which indicate sedentary succession shifts and which correspond to macroscopic changes in the lithography. Changes in the Zr/Ti ratio indicate changes in deposition, and the abrupt shift in Ti/Zr and Zr/Ti at BD-20 depicts the pedogenic boundary between the lower loess and the upper loess. The shift at BD-26 marks the transition from the sands to the lower loess. Zr was utilized as the immobile constituent in calculations for Strain (ε) and Concentration Ratios (CR) following Stiles et al. (2003) due to the coarse grained nature of the Mead Sites soils and sediments. (Stiles et al. (2003) found that Ti is located preferentially in the finer grained materials and Zr in the coarser grained materials and so they recommend using Ti as the immobile constituent for clay dominated soils and Zr for coarser grained soils).

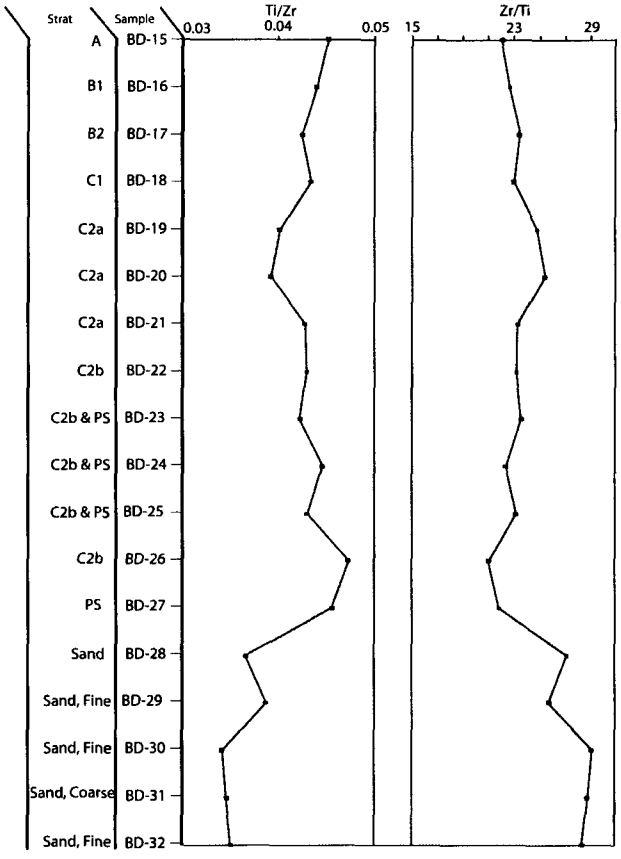

Figure 4.20 Ratios of immobile constituents

4.4.1 Molecular Ratios

The ratio of K+Na/Al shows a decrease from Bd-19 upward, while from BD-19 downwards a gradual increase in K+Na/Al was seen, with spikes at BD-28 and Bd-31 (Figure 4.21). Theses spikes may indicate an increase in salinity, which corresponds to the presence of carbonate formations in the profile, and is an expression of aridity. Bd-28 is a sand layer that may correspond to the Younger Dryas cooling event and which is separated from the lower bedded sands by a thin layer of very fine sand/loess. BD-31 is a coarse sand layer of the lower bedded sands.

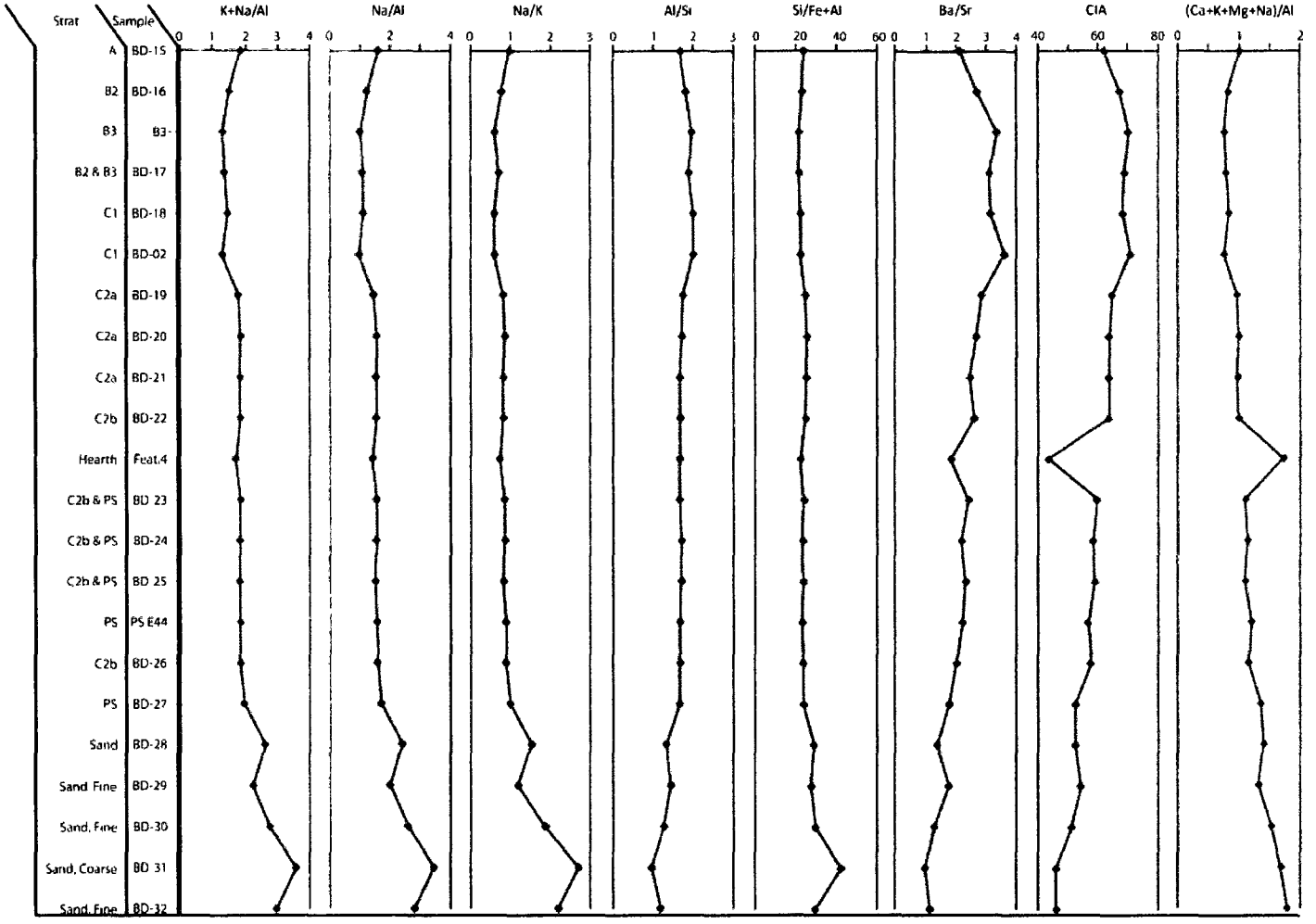

Figure 4.21 Molecular Ratios

The trace element ratio of Ba/Sr is used to help determine leaching due to weathering, with lower ratios indicating less leaching, and higher ratios indicating more leaching (Retallack 1991; Sheldon 2006). The ratio of Ba/Sr in the modern soil shows leaching from the A to the B horizons, with increased levels evident in the B3 horizons, indicating illuviation. Ba/Sr values greater than two indicate leaching conditions (Sheldon 2006). Below the modern B horizons there is a trend of steady lowering ratios down through the C1 horizon, indicating continued leaching downward through the profile. There is a spike in Ba/Sr at BD-02 (C1 soil that was pocketed between B) indicating that this sample is actually a weak B horizon that does not exhibit a strong color change. Below the C1 horizon there is a steady decrease in Ba/Sr which corresponds to the increase in pH. The C2 horizon exhibits a decrease in leaching. Both Feature 4 and the lower paleosol complexes exhibit Ba/Sr ratios which are less than two, indicating a lack of leaching or acidic conditions. The paleosols do not exhibit any differing trends in Ba/Sr values. Feature 4 has a very low ratio, as does Bd-28 (YD sand), indicating that little leaching took place.

The Chemical Index of Alteration (CIA) and Mg (CIA) both show weathering through the modern A and B horizons, a decrease in weathering at the C1 horizons, with the exception of BD-02 (the C1 between B), which shows a spike in CIA, indicating increased weathering and again indicating this C1 is a weak B. CIA values decrease steadily through the C2a and C2b soils, with significant decreases in value at Feature 4. The lower paleosols complex also indicates less weathering, as does the YD sand (BD-27). The lowest sands show a significant decrease in CIA, indicating a lack of weathering in the profile. Mg (CIA) results are inversely proportionate to those of the CIA, indicating that Mg-bearing minerals weathered similarly to feldspars.

The ratio of Al/Si, a weathering index, increases at BD-02, which is the lower boundary of the C1 (the upper loess). It also exhibits a slight jump at the B3 level (clay lamella) before decreasing in the upper 2 samples (indicating elluviation of Al into the lower modern soil stratums). The lower loess, which is encompassed from samples BD-27 to BD-19, exhibits fairly uniform rates of Al/Si, indicating little movement of Al through that section of the profile. Bd-28, just below the lower loess (YD layer) shows a marked decrease in Al/Si. The lower bedded sands exhibit a highly decreased ratio, with BD-29 showing a slight increase from the general trend of the lower sands (maybe because visually it is somewhere between the C2b and the sand).

4.4.2 Concentration Ratios

There is an increase in the CR of CaO at several points in the profile (Figure 4.22). By far the largest of these is the Feature 4 hearth, which contained small fragments and flecks of bone. There is also a spike at BD-27 which is from a well developed paleosol. Upon macroscopic investigation, this horizon was found to contain very common flecks and small fragments of bone. There is a slight decrease in CaO at

both BD-28 and at BD-31. There is a small spike in CaO at BD-17. BD-17 corresponds with cultural remains in CZ 1b which consist of small bone fragments and lithics. There is also a spike at BD-27, which is a well developed paleosol. By far the largest increase in CaO is at Feature 4, which is interpreted as resulting from enhancement from bone fragments found in the hearth.

P_2O_5 remains fairly constant throughout the profile, with 5 exceptions where it spikes to varying degrees (Figure 4.22). There are four small spikes and one large one (because of the magnitude of the largest spike, the smaller ones are difficult to see in Figure 4.22). The first of these is at BD-2, the second is associated with BD-18. The third is from BD-24, and the forth is at BD-30. Both BD-2 and BD-18 are samples of the C1 soil. BD-2 was taken from a "pocket" of C1 in E44 that occurs between the B horizons; a dense artifact scatter was recovered from this area. BD-24 was taken from a C2b/paleosol horizon, and BD-30 was obtained from the lower sand area, and is actually a sample of a krotovinia. This last sample is interesting, as it indicated that enhanced P may also be the result of non-cultural animal behavior at the site.

By far the largest spike in P is from the Feature 4 soil sample. Feature 4 exhibits over twice as much P as any other sample analyzed. The enhanced P values from both Feature 4 and from BD-2 indicate that anthropogenic input of P is detectable at the site. There is no noted increase in P at the location of Area 4 and Feature 1 (see Chapter 4.6). As soil P accumulates where it is deposited, the lack of an increase in P at this location indicates that the occupation which resulted in the creation of Feature 1 was short in duration.

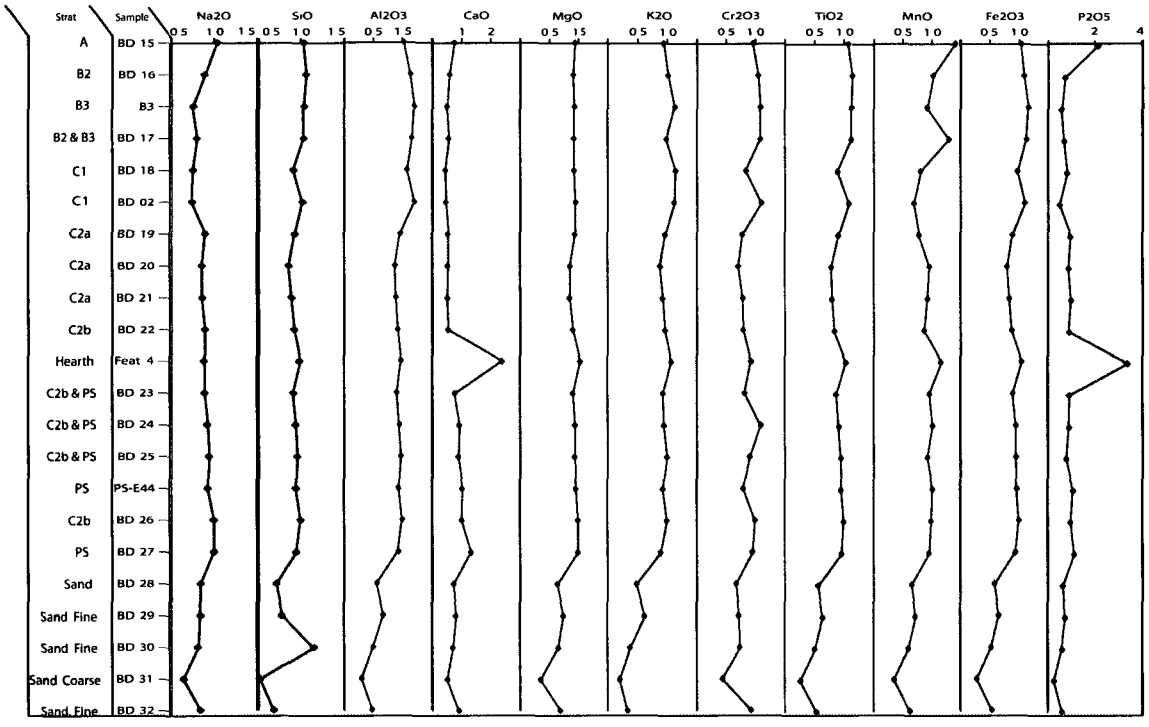

Figure 4.22 Concentration Ratios

4.4.3 Strain

Strain (ε) is the mass balance approach that looks at the volumetric changes through a soil. In the profile, K and Al have dilation, reflecting clay illuviation, while collapses of Sr, Mg, Ca and P in the profile reflects weathering (

Figure 4.23). Dilation is evident at BD-02 and B3; BD-02 is the C1 horizon that is sandwiched between B horizons, and B3 is the clay lamella. If these are both illuvial horizons then it would be expected that P would increase at these horizons as it moved down through the profile. However the increase in P in BD-02 may also be dependent upon anthropogenic processes. ε of P continues to decrease through the upper loess, indicating continued weathering ε of P gradually increases through the lower loess, which may be indicative of a decrease in weathering and/or illuviation of P from the above horizons. Interestingly, there is dilation of P at Feature 4 and at PS E44; this is due to the decreased density of these horizons. Feature 4 has a much greater dilation than the lower paleosols, indicating that these paleosols were not enhanced by cultural activities.

The fluctuating strain of Fe and Mn throughout the profile may be the result of alternating wet and dry conditions. Mn spikes at B3, BD-2, and BD-31; without these spikes there is a gain in Mn throughout the profile. The general trend for Fe is also gain through the profile. Strain calculations indicate that the C1 horizon that is pocketed in the B horizon is a zone of illuviation as is the clay lamella (B3).

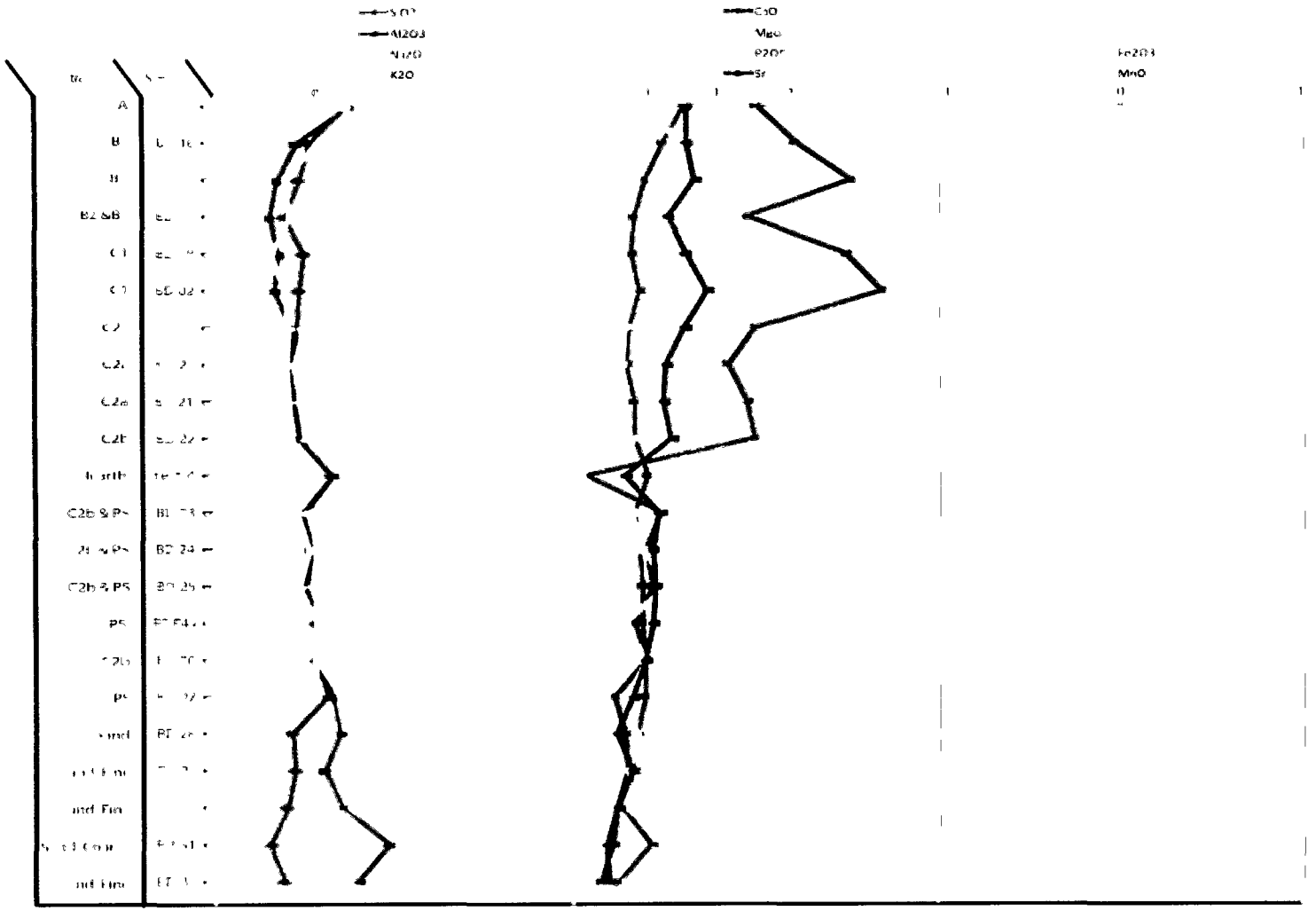

Figure 4.23 Calculations of Strain

4.5 Wood Identification

Three charcoal samples were selected for wood identification from Feature 4. Dr. Peter Wigand of Great Basin and Mojave Paleoenvironmental analyzed these samples. Identification of wood species can provide a temporal control that can be analyzed in regard to site disturbance and to the spatial distribution of certain species. All three samples returned identification as *Salix*. This falls within the expected range of species that are believed to have been in the area at the time the hearth was used, and its significance will be elaborated on in Chapter 5.

4.6 Dating and Spatial Analysis

Eleven new 14C dates were obtained as a result of this the 2009 excavation (Table 4.7). These new dates, along with 9 previous dates obtained from excavations in the 1990's gives a total of 19 dates for the site (Figure 4.24, excluded from this table are several dates with problematic provenience, see section 4.6.7 for more information). Material dated includes paleosols, charcoal associated with cultural material, and bone found in the lower bedded sands corresponding to Cultural Zone 4 (CZ 4). A total of 48 1x1 meter units were excavated down to the lower bedded sands. Faunal remains recovered include, bird, both large and small mammal, and several fragments of ivory.

Few formal tools were recovered from this most recent excavation, with a small number of microblades, biface fragments, and unifaces/scrapers recovered during the field season. The majority of lithic artifacts recovered were debitage. Raw materials found include chert, obsidian, rhyolite, basalt, quartzite, and the local bedrock. No diagnostic bifacial technology was obtained. Because of the lack of diagnostic lithic remains found at the site, no assignments to cultural traditions of the occupations at the site are made other than through correlations with radiocarbon dates.

The dates obtained for the upper horizons at the site exhibit age reversals; this is not an unexpected outcome as the stratigraphy shows disturbance due to cryoturbation. The dates on the lower horizons do not exhibit age reversals, although some interesting trends are evidenced by them which will be discussed further in this chapter.

Table 4.7 Radiocarbon dates and association from the 2009 excavation

ID	Mass (g)	Material	Depth (cmbs)	Association	Lab #	Date (c14 yrs BP)
W34-276	2.92	bone	33	B, with scraper	Beta-264523	770 +/- 40
SPC-4	0.2	charcoal	33	bottom of lowest B horizon	Beta-264529	4940 +/- 40
W24-240	0.8	charcoal	37 to 40	B, with mb	Beta-264531	5530 +/- 40
E13-51	0.4	charcoal	44	C1, middle (within B)	Beta-264524	6050+/-40
E13-52	0.1	bone	47	C1, middle (within B)	Beta-264525	4580 +/- 40
SPC-2	0.1	charcoal	80	Upper PS, top stringer	Beta-264528	7790 +/- 50
SPC-1	0.2	charcoal	92	Upper PS, bottom stringer	Beta-264527	10160 +/- 50
E32-SPC7	0.4	charcoal	96	Upper PS, bottom stringer	Beta-264526	10140 +/- 50
W24-360	0.4	charcoal	108	Feature 4 (hearth)	Beta-264532	10360 +/- 50
SPC-6	0.2	charcoal	113	Lower PS, bottom stringer	Beta-264530	11210 +/- 60
E17-199	13.83	charcoal	120	lower sands (C5)	Beta-264522	11460 +/- 50

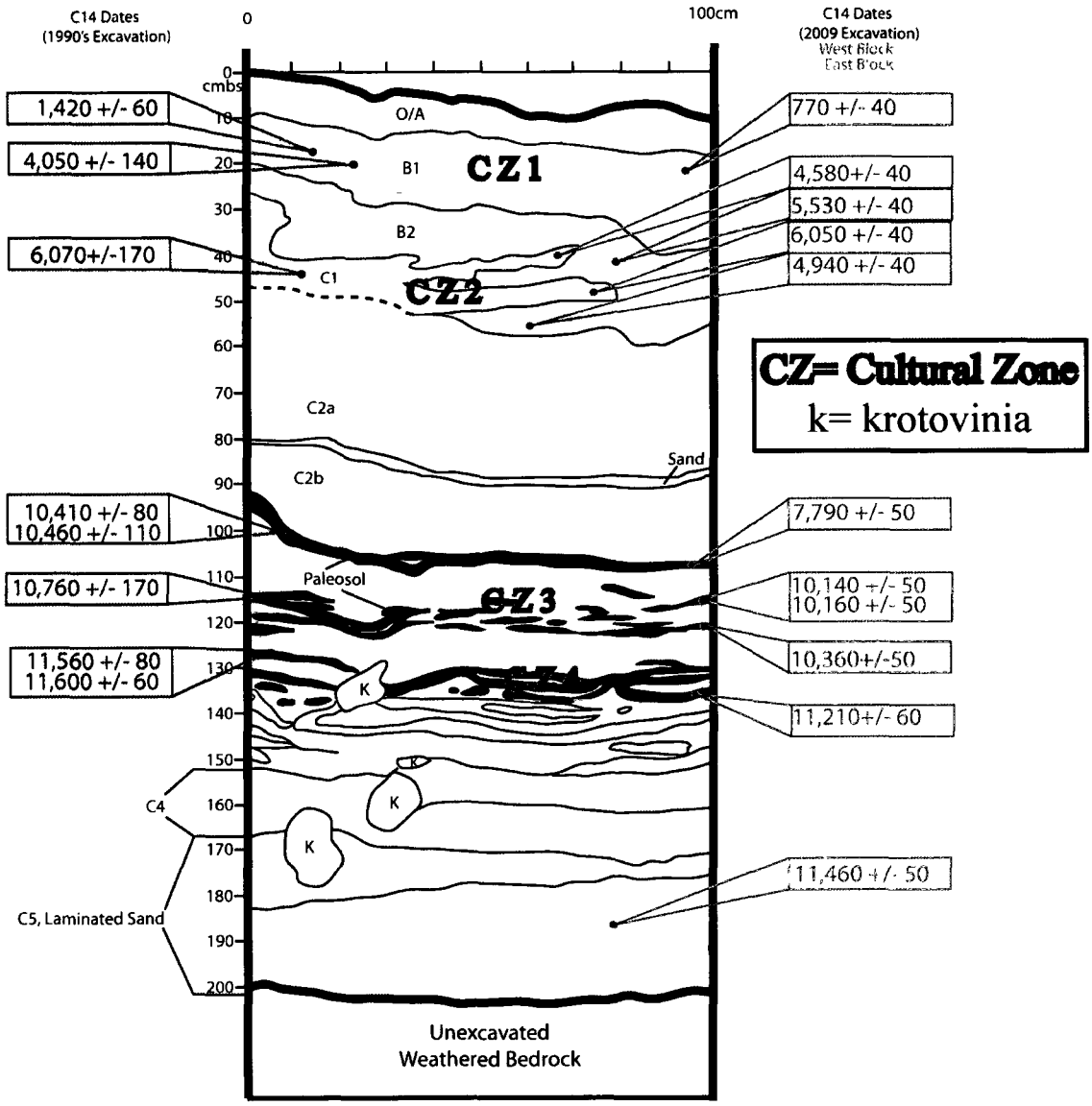

Figure 4.24 Radiocarbon dates with the generalized soil stratigraphic profile

The tables' generated show the trends of the *in situ* artifacts recovered from the excavation illustrates well the variation in location of remains across the site (Table 4.8 to Table 4.12). These trends are examined in detail below for each of the cultural zones (CZ's). During this spatial analysis it is assumed that the cultural remains are in their primary context in order to designate scatter, features, and areas. Once these labels have been assigned, the validity of these designations will be assessed.

Table 4.8 Generalized frequencies of *in situ* cultural remains by 5 cm arbitrary level

West Lobe Generalized		
Level (cmbs)	Bone	Lithics
0-5	Rare	Rare
5-10	High	High
10-15		
15-20	Decreasing	
20-25		
25-30	Rare	
30-35		Decreasing
35-40		
40-45		Small Cluster
45-50		
50-55		
55-60		
60-65		
65-70		
70-75		
75-80		
80-85		
85-90		
90-95	Rare	Scattered Remains
95-100		
100-105		Lithics W24
105-110	High Bone W24	Hearth lithic
110-115	Rare (n 2)	W24 Decreasing
115-120		
120-125	Rare	
125-130		
130-135		
135-140		
140-145		
145-150		

East Lobe Generalized	
Level (cmbs)	Bone and Lithics
0-5	Scattered Remains
5-10	
10-15	
15-20	
20-25	Bone and flakes
25-30	
30-35	Decreasing
35-40	
40-45	
45-50	
50-55	Scattered Remains
55-60	
60-65	
65-70	
70-75	
75-80	
80-85	Bone, flakes and rock
85-90	
90-95	
95-100	Scattered Remains
100-105	
105-110	
110-115	
115-120	Bone and flakes, E26
120-125	Bone, E44 (goes to 135 but tapers off)
125-130	
130-135	Rare bone and 1 flake in E44 and E40,rest of area is sterile
135-140	
140-145	
145-150	Bone in lower Sand

Key
Common cultural remains
Scarce cultural material
Rare cultural remains
No cultural remains

Table 4.9 West Lobe frequencies of *in situ* cultural remains by 5 cm arbitrary level

West Lobe				
Level (cmbs)	**W34**		**W24**	
	Bone	**Lithics**	**Bone**	**Lithics**
0-5	Rare	Sterile	Rare	Very Rare (n=1)
5-10	**High (goes into W-23, possible feature)**	**High**	Very Rare	**High (concentrated in NW1/4)**
10-15				
15-20				**High (concentrated in S 1/2)**
20-25				
25-30		Decreasing		Decreasing
30-35				
35-40		Rare		
40-45		**Feat 1**		
45-50				
50-55				
55-60				
60-65				
65-70				
70-75				
75-80				
80-85				
85-90	Rare (n=1)			
90-95				
95-100	Rare (n=2)		Rare (n=2)	
100-105				**Hearth Area (Feature 4)**
105-110			**High**	
110-115			Rare	
115-120				Decreasing
120-125			Rare (outside of W24)	
125-130				
130-135				
135-140				
140-145				
145-150				

Key
Common cultural remains
Scarce cultural material
Rare cultural remains
No cultural remains

Table 4.10 East Lobe frequencies of in situ cultural remains by 5 cm arbitrary level (Part 1)

East Lobe						
Level (cmbs)	Area 1 (E13, E16, E17 and E26)		E32		E38	
	Bone	Lithics	Bone	Lithics	Bone	Lithics
0-5		Sterile		Rare (n 2)		
5-10		Lithics				
10-15						
15-20				Rare (n 2)		
20-25						
25-30						
30-35						
35-40						
40-45		Decreasing to Rare				
45-50						
50-55						
55-60		Very Rare (n 2)				
60-65						
65-70						
70-75						
75-80						
80-85	Very Rare (n 1)					
85-90			Bone	Lithics	Bone, scattered	
90-95						Lithics
95-100						
100-105	Bone, scattered, Ivory in E16	Rare		Lithics		
105-110					Rare (n 1)	
110-115						
115-120	*Concentrated in E26*	Rare (n 3)				
120-125	Very Rare (n 1)					
125-130						
130-135						
135-140						
140-145						
145-150	Very Rare (n=1)					

Key
Common cultural remains
Scarce cultural material
Rare cultural remains
No cultural remains

Table 4.11 East Lobe frequencies of in situ cultural remains by 5 cm arbitrary level (Part 2)

East Lobe						
Level (cmbs)	E40		E44		E46	
	Bone	Lithics	Bone	Lithics	Bone	Lithics
0-5						Rare (n=1)
5-10						
10-15				Rare (n 1)	Rare (n 1)	
15-20		Rare				**Lithics, Scattered (not dense), microblades**
20-25						
25-30		**Lithics, Dense**		**Lithics, Dense Concentration**		
30-35		Rare (n=1)		Decreasing		Rare (n=1)
35-40						
40-45						
45-50						
50-55						
55-60						
60-65						Rare (n=1)
65-70						
70-75						
75-80						
80-85					Rare (n=1)	
85-90						
90-95					Rare (n 4)	
95-100		Rare (n 1)				Rare (n 1)
100-105	Rare (n=1)					
105-110		Rare (n=1 core)		Rare (n=1 rock)	**Bone (n=5)**	**Lithics**
110-115			Increasing, Scattered			
115-120	Rare (n=1)					
120-125						
125-130		Rare	**Bone**	Rare (n=1)		
130-135						
135-140			Decreasing			
140-145	Rare (n=1)					
145-150						

Key
Common cultural remains
Scarce cultural material
Rare cultural remains
No cultural remains

Table 4.12 East Lobe frequencies of in situ cultural remains by 5 cm arbitrary level (Part 3)

East Lobe		
Level (cmbs)	E52	
	Bone	Lithics
0-5		
5-10		
10-15		
15-20		Rare (n=2)
20-25		
25-30		Rare (n=2)
30-35		
35-40		
40-45		
45-50		
50-55		
55-60		
60-65		
65-70		
70-75		
75-80		
80-85		
85-90		Rare (n=2)
90-95		
95-100	Rare (n=2)	Increasing
100-105		**Lithics, Feature**
105-110	Rare (n=1)	
110-115		Decreasing
115-120	Rare (n=1)	
120-125		
125-130		
130-135		
135-140		
140-145		
145-150		

Key
Common cultural remains
Scarce cultural material
Rare cultural remains
No cultural remains

Two profile back plots (north and east) were created for each 2 m block (Figure 4.25 to Figure 4.40). These back plots show the vertical distribution off all *in situ* remains. In the majority of the blocks, the lower components are easily distinguished from the upper components, and artifact clusters can be discerned. Attempting to separate the CZ 1a, 1b, and 2 materials from each other is difficult on the back plots. There are not clear breaks in artifact distribution between these CZ's, and the distribution is scattered. Separation of CZ 3 and 4 is also difficult in some units. Part of the lack of clarity of the back plots is due to the slope over each 2 m block which distorts the distribution of the artifacts on the back plots. The spatial location of several of the feature and activity areas is evident in the back plots. Feature 3 (Figure 4.39) is well defined in W24, as is Scatter 5 in E52 (Figure 4.35). Activity Area 3 in the West Lobe (Figure 4.40) is a large but dense scatter of cultural remains that does not exhibit well defined vertical boundaries. A more detailed examination of the back plot data is given in the following sections in regards to the spatial distribution of each cultural zone.

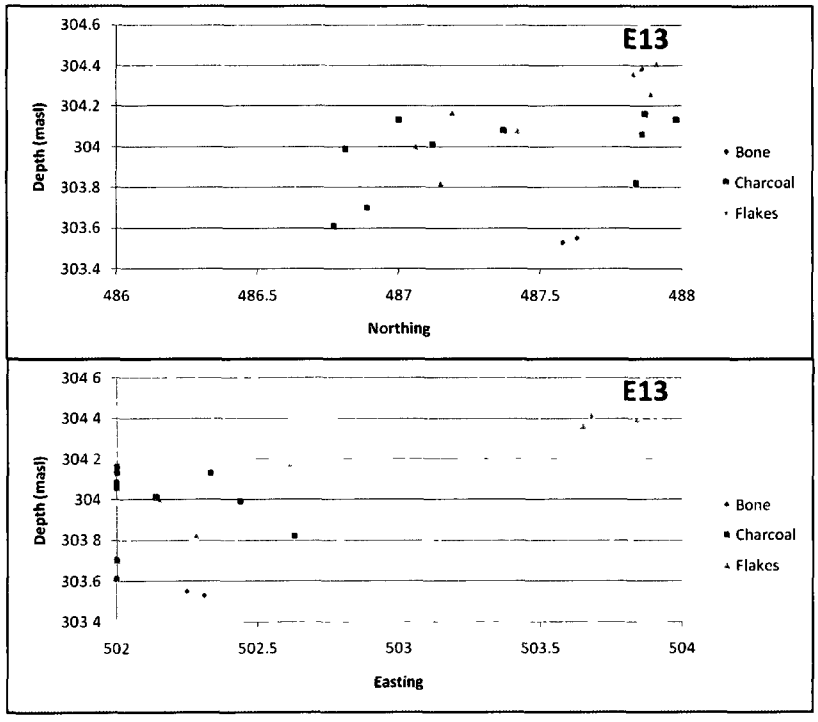

Figure 4.25 Block E13 back plots

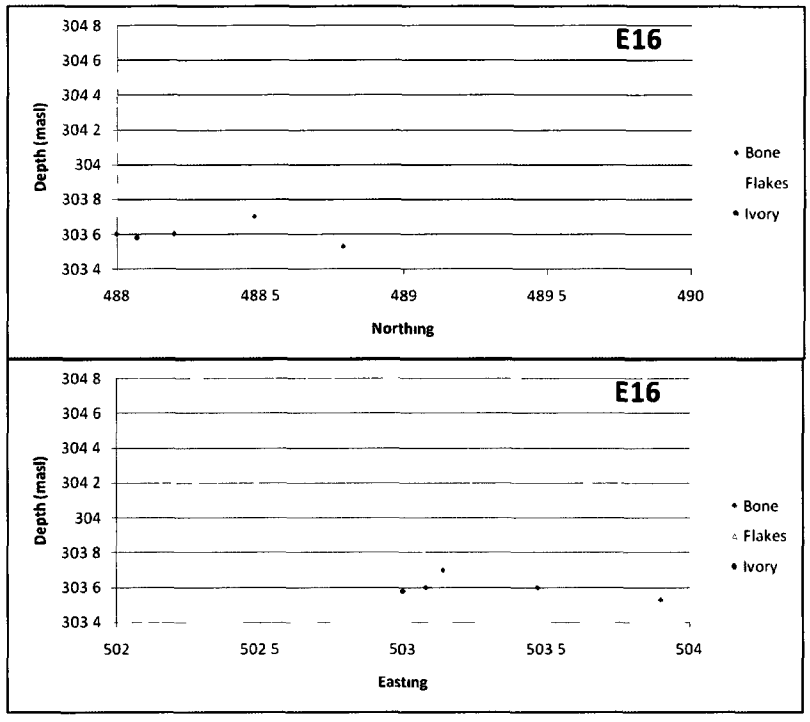

Figure 4.26 Block E16 back plots

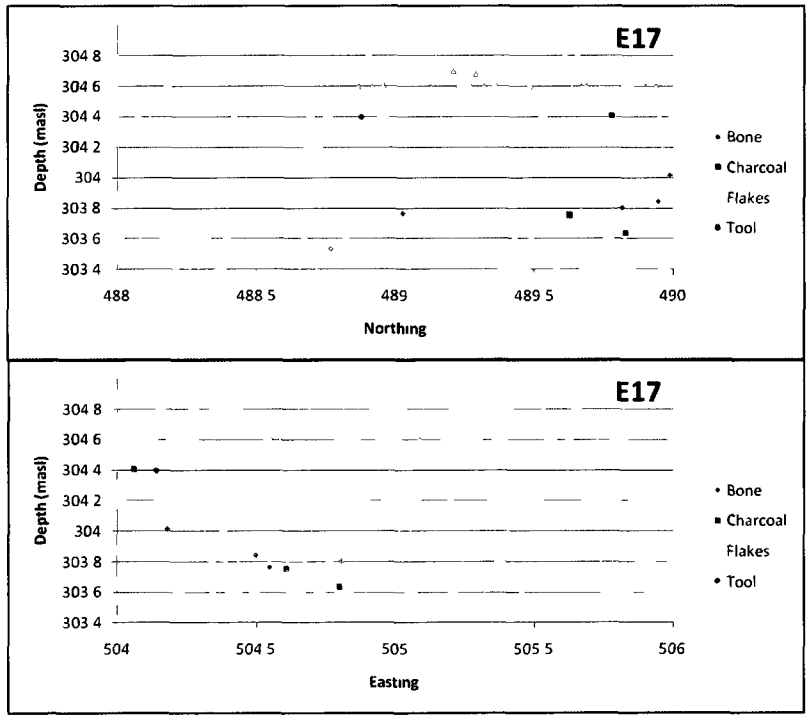

Figure 4.27 Block E17 back plots

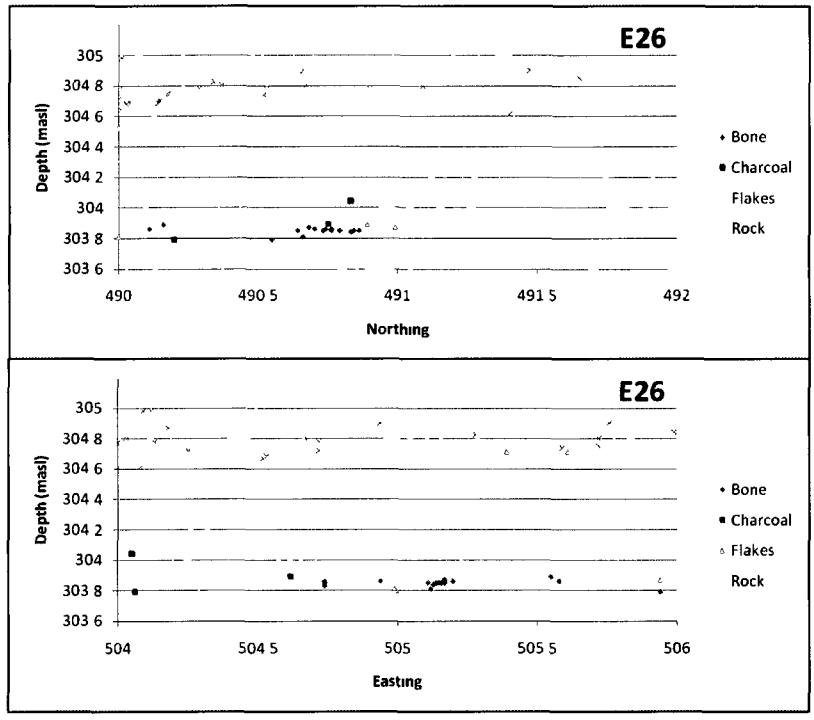

Figure 4.28 Block E26 back plots

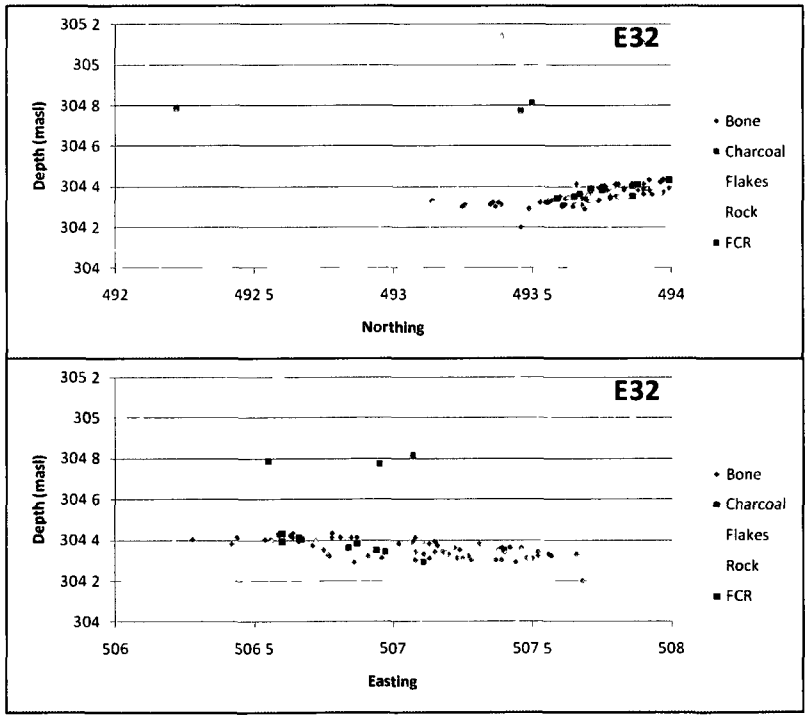

Figure 4.29 Block E32 back plots

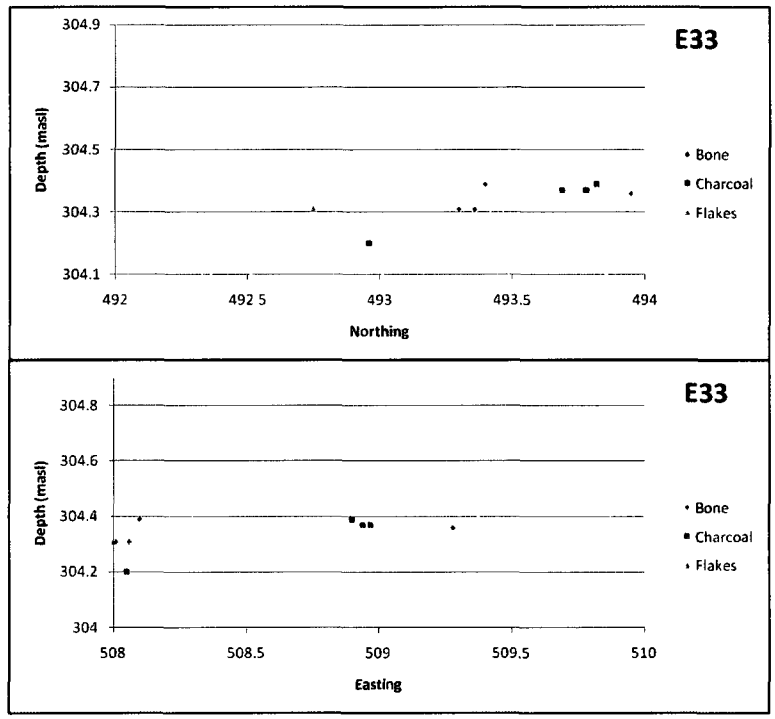

Figure 4.30 Block E33 back plots

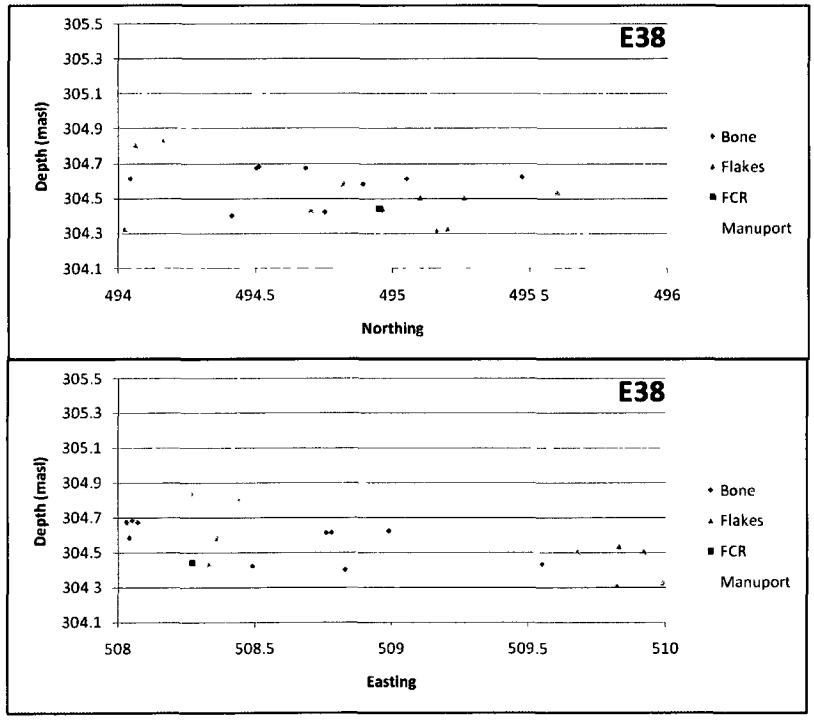

Figure 4.31 Block E38 back plots

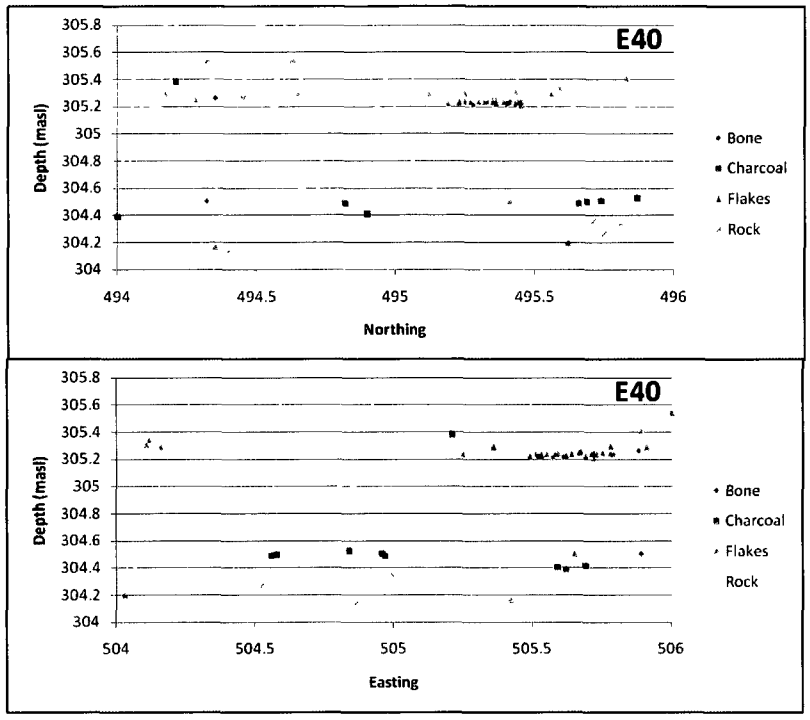

Figure 4.32 Block E49 back plots

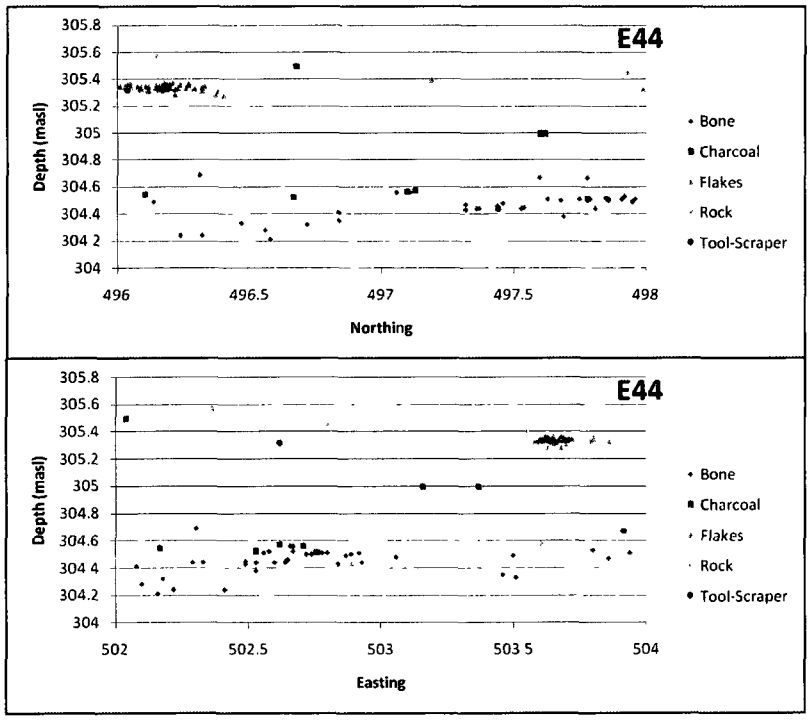

Figure 4.33 Block E44 back plots

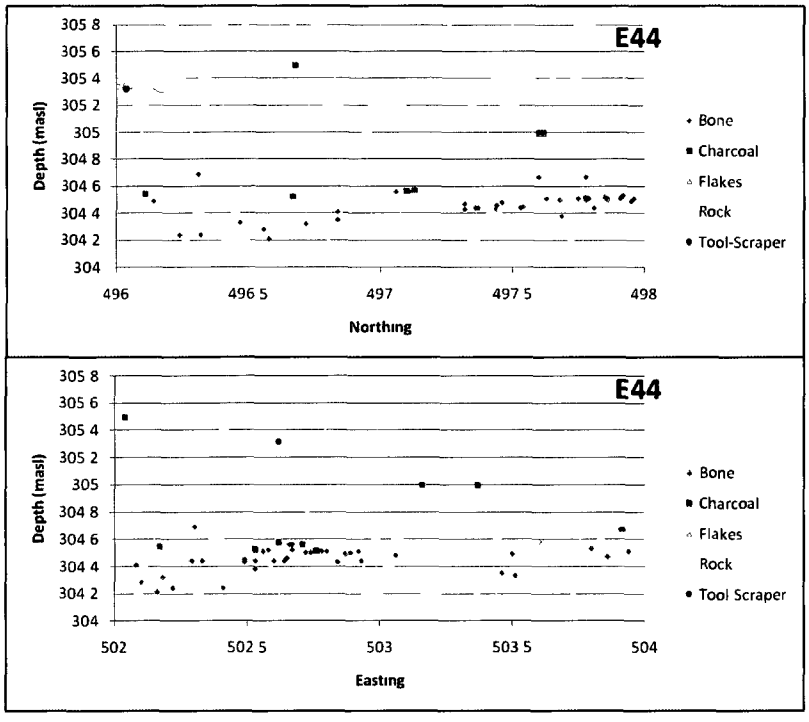

Figure 4.34 Block E46 back plots

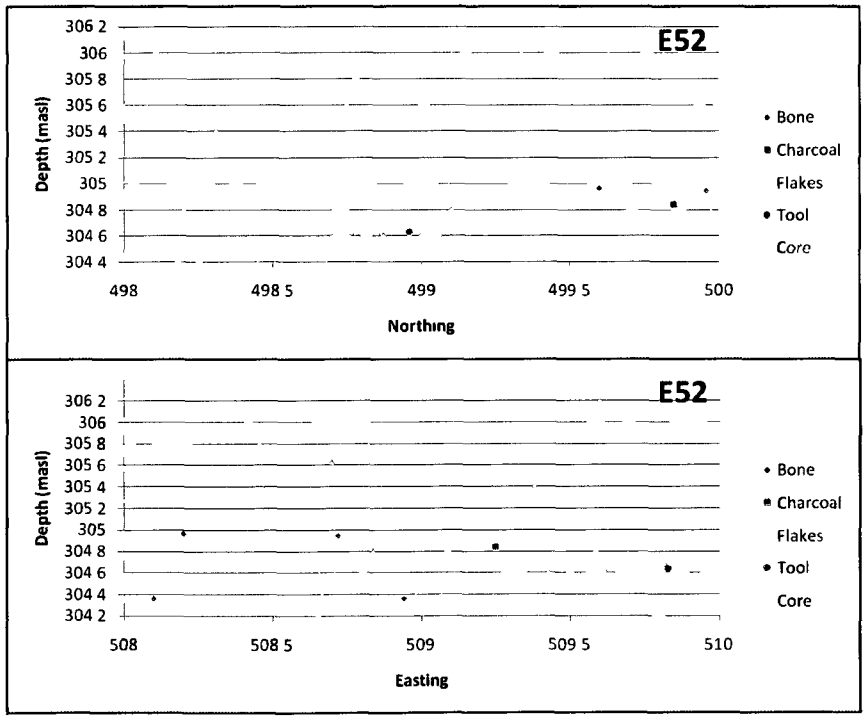

Figure 4.35 Block E52 back plots

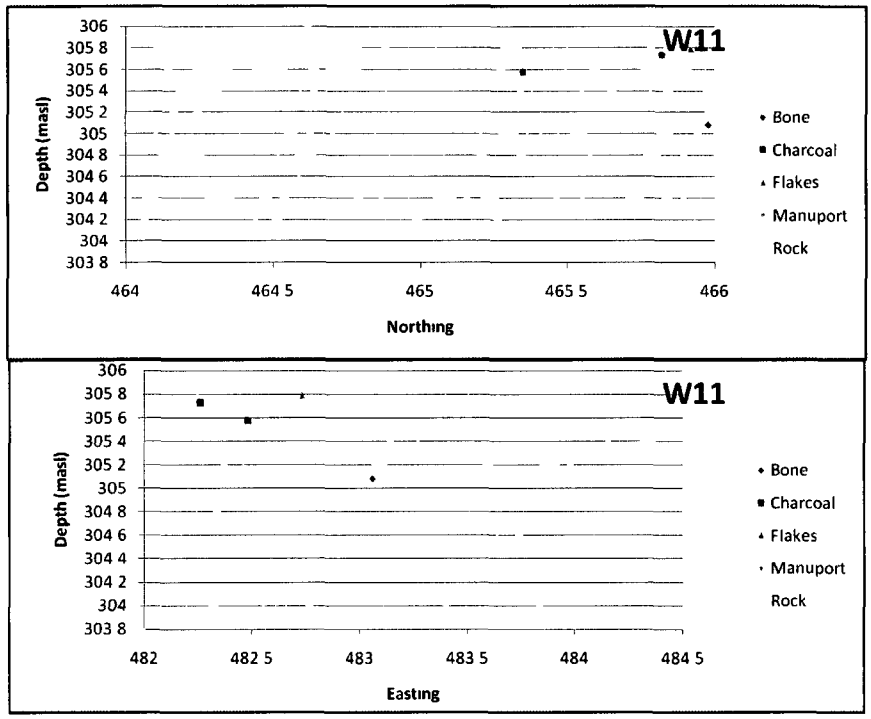

Figure 4.36 Block W11 back plots

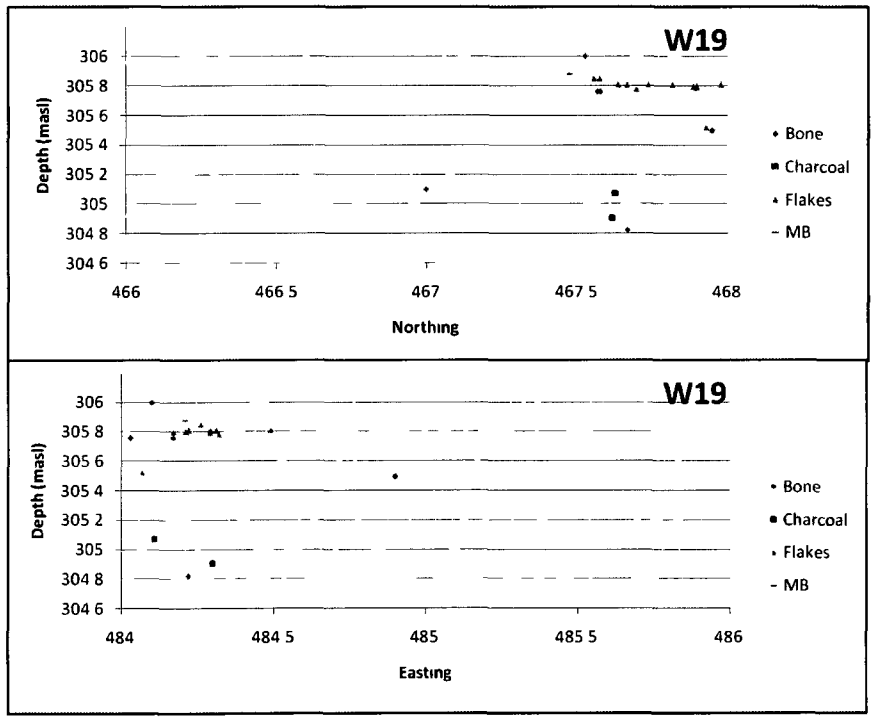

Figure 4.37 Block W19 back plots

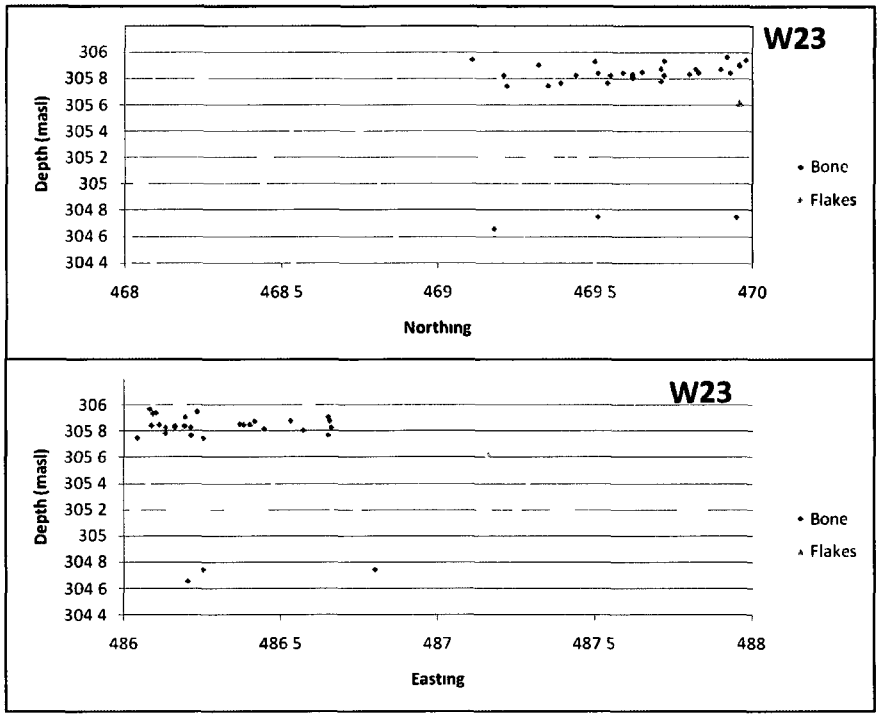

Figure 4.38 Block W23 back plots

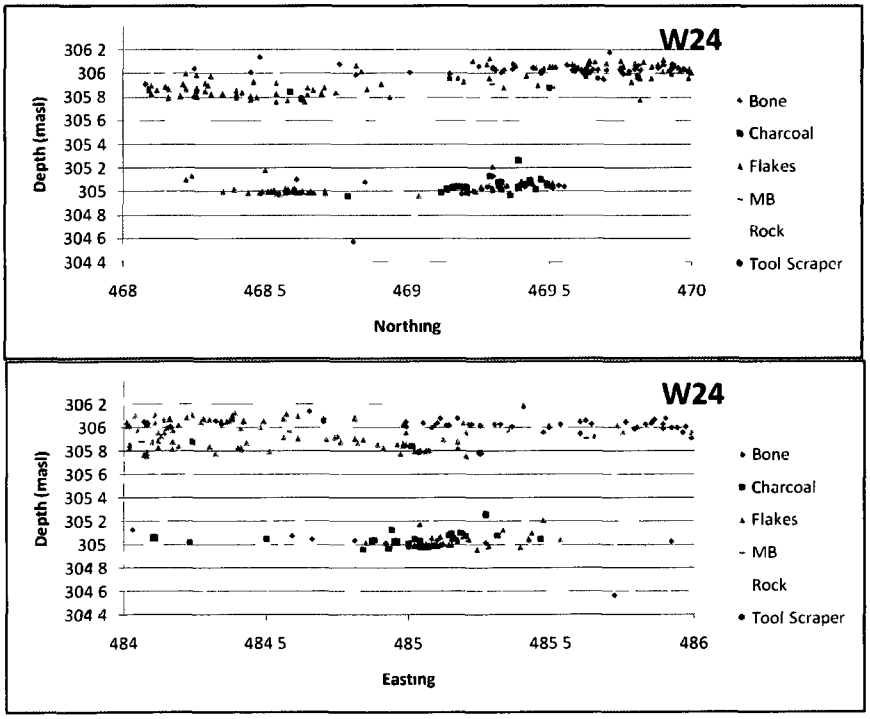

Figure 4.39 Block W24 back plots

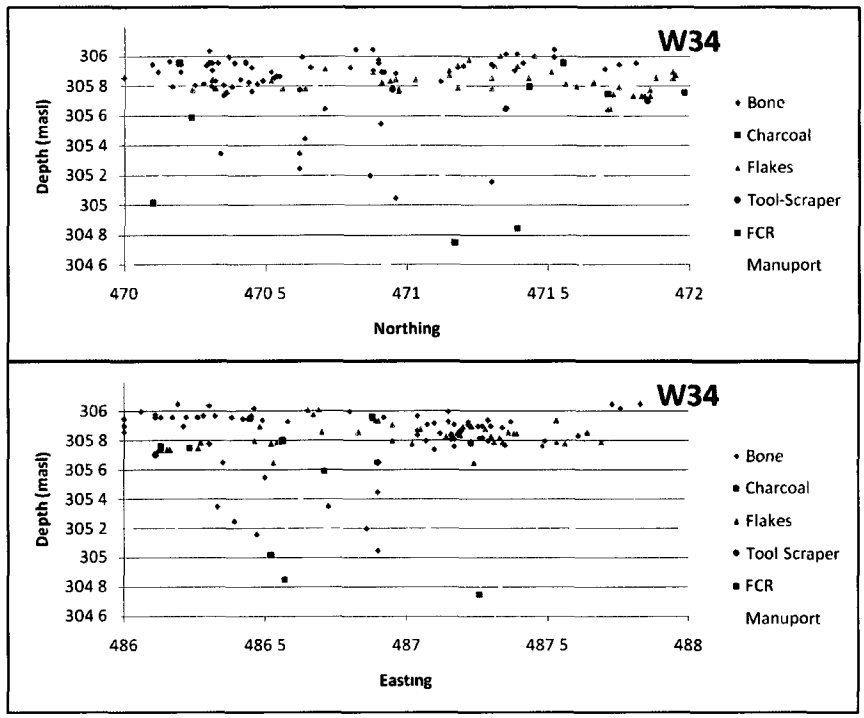

Figure 4.40 Block W34 back plots

4.6.1 CZ 4

Radiocarbon dates place the oldest occupation at the site between 11,210 ± 60 and 11,460 ±50 yr BP (13,109-13,500 cal yrs BP), which is right at the transition between Phase I and Phase II of the East Beringian Period and during the Beringian Period and the Chindadn/Nenana Tradition. This occupation corresponds with the Lower Paleosols at the site. CZ 4 remains were found in the lower paleosols and in the upper region of the underlying bedded sand (a single bone with cut marks was recovered from these sands in E16).

In the East Lobe (Figure 4.41) (in all spatial distribution figures the shaded areas are unexcavated blocks), CZ 4 is expressed in E52 as a dense quartzite lithic scatter (Scatter 5). Two cores, a scraper, and a large quantity of flakes were recovered *in situ*, and a large quantity of flakes were also recovered from the screen. No faunal material was recovered from the screen associated with this area, although several bone fragments were found *in situ* to the north and west of this lithic scatter. An additional smaller cluster of lithics and bone was found *in situ* just over two meters to the southwest of Scatter 5. The isopleth maps indicate a moderate number of lithics were recovered associated with this smaller scatter (Scatter 6); no bone was recovered from the screen. A single piece of fire cracked rock (fcr) was located to the northeast of Scatter 6.

Along the southwest edge of the East Lobe CZ 4 is a diffuse faunal and lithic scatter (Scatter 7). Bone, ivory, and lithics were recovered *in situ* from a 6m x 2m wide area running northeast/ southwest. It is likely that this scatter originally continued south of the excavated area into the quarried zone. Additional diffuse faunal remains and lithics were found *in situ* in all other blocks of the East Lobe, although screened faunal remains were recovered from only Scatter 7. With the exclusion of the screened remains from Scatter 5, two flakes were found in the screen from Scatter 7, and only one from the other blocks in the East lobe.

During spatial analysis an interesting pattern emerged in the NW area of the East Lobe; a diffuse bone scatter is noted in E44. These remains were found *in situ* below the level of the other scatters associated with CZ 4. For this reason these remains have been classed as CZ 4 (lower) (Figure 4.42). There are bone fragments that were recovered *in situ* from CZ 4 which corresponds with the location of this bone scatter. The designations of CZ 4 and CZ 4 (lower) are simply used to show the change in distribution with depth and are not meant to be indicative of separate occupations or cultural zones. They simply illustrate different spatial patterning in CZ 4.

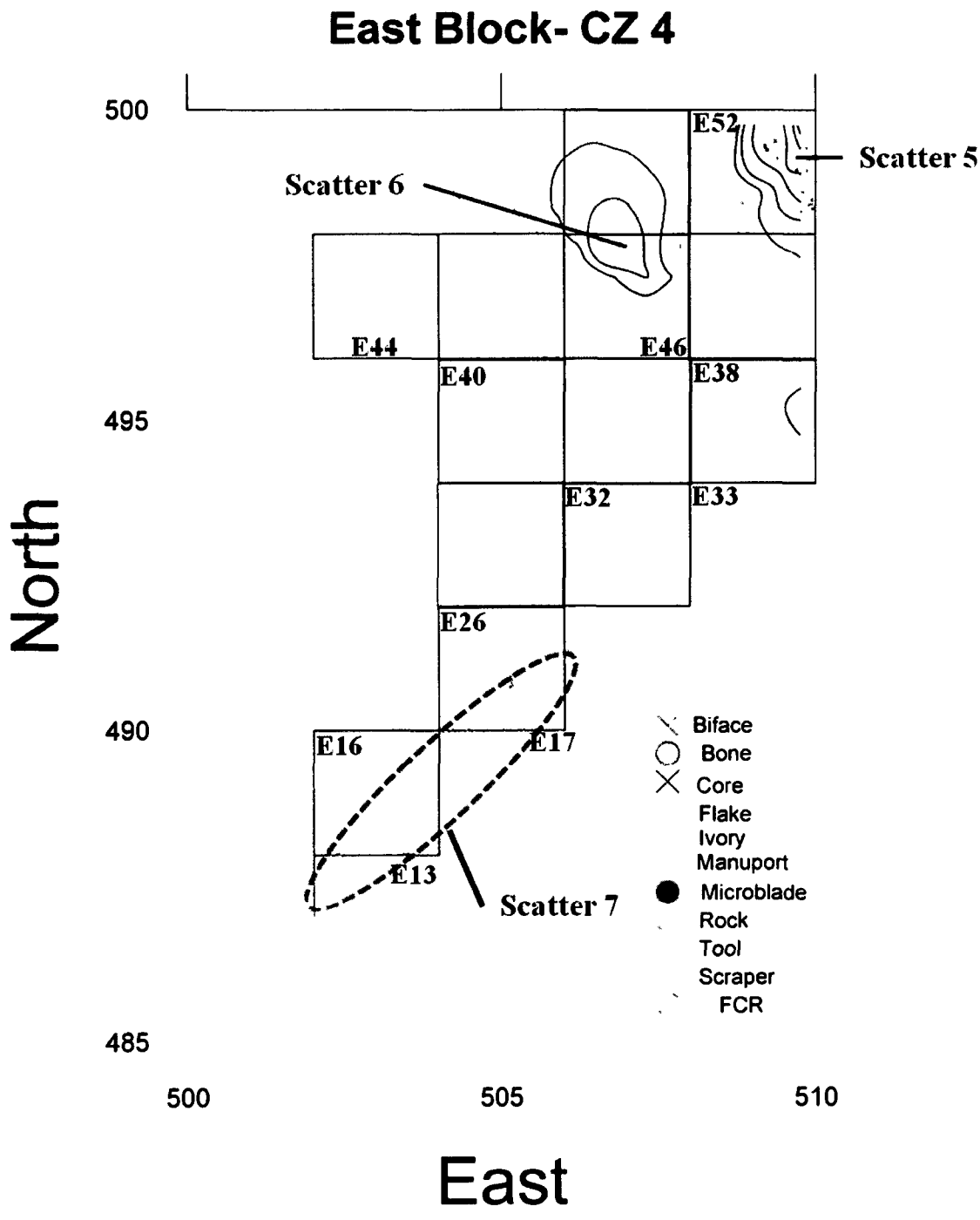

Figure 4.41 East Block CZ 4 with isopleth map of screened remains

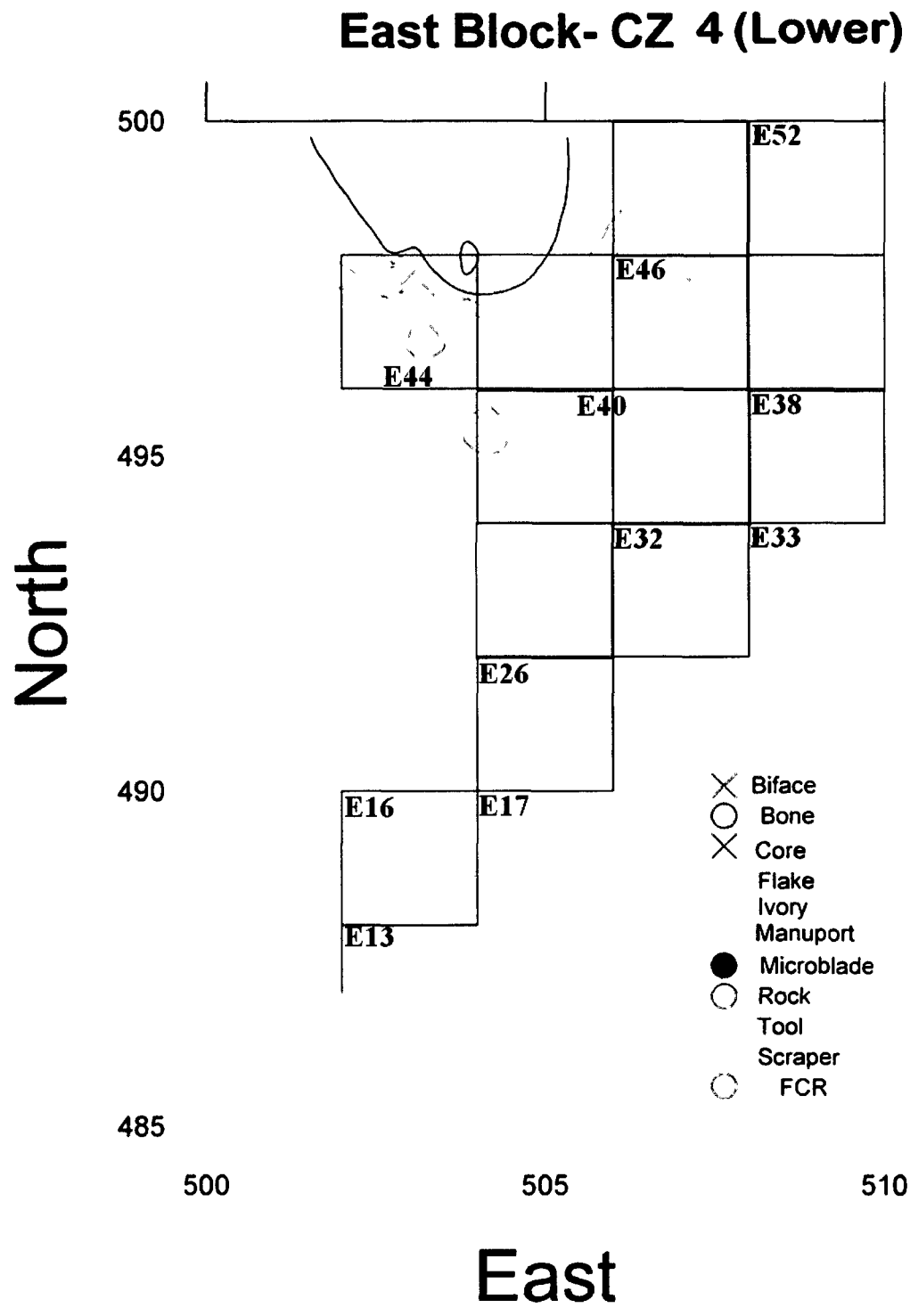

Figure 4.42 East Block CZ 4 (lower) with isopleth map of screened remain

In CZ 4 (lower) three flakes were found *in situ* for the entire East lobe, and no flakes were recovered from the screen. The majority of the bone fragments recovered from CZ 4 (lower) are well preserved and many are diagnostic. Screened faunal remains were recovered from E44 and E40, and *in situ* faunal remains were recovered from E44, E40, E26, and E16. This bone scatter is designated as belonging to CZ 4 (lower) based on its stratigraphic position, occurring in the lower paleosol complex. For the most part, the paleosols associated with the scatter in E44 are thin but well expressed continuous stringers that undulate slightly but show good stratigraphic relationships (Figure 4.43).

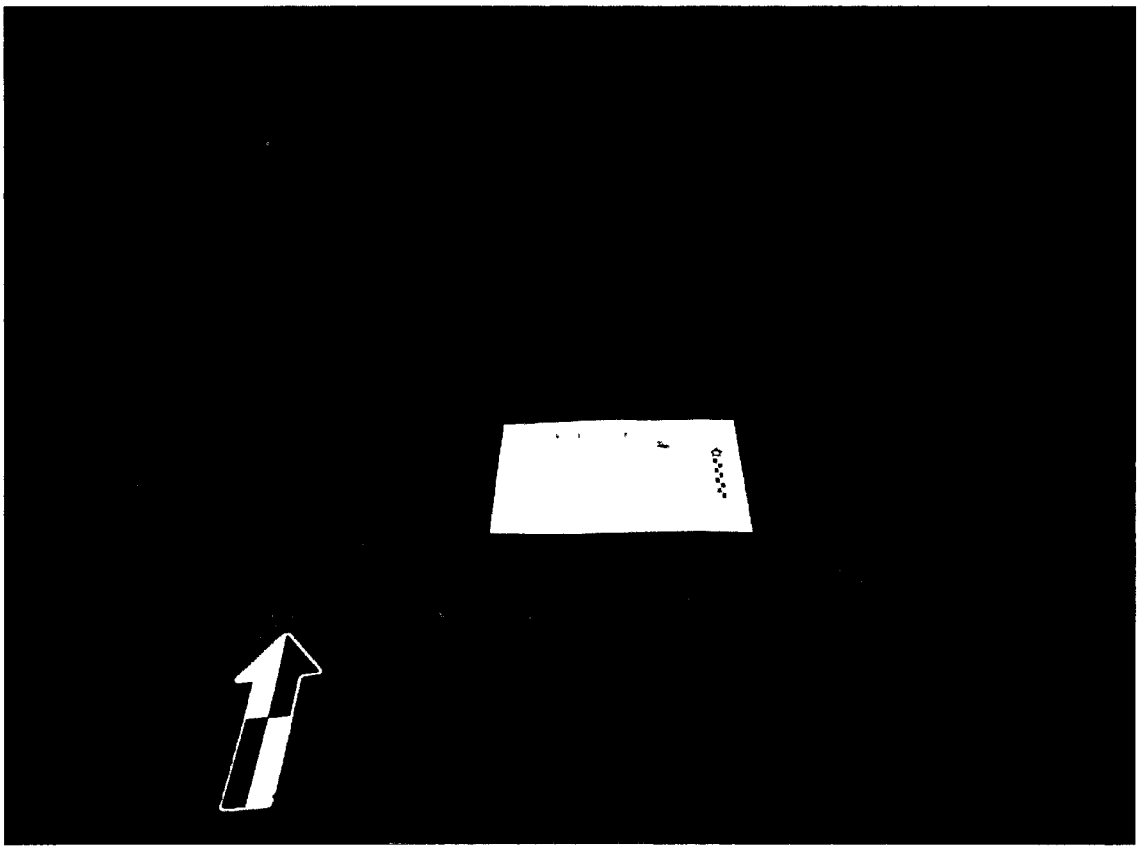

Figure 4.43 E44 CZ 4 (lower) bone scatter

CZ 4 (Figure 4.44) is poorly expressed at the West Lobe of the site, with only a few bone fragments and one flake recovered from the screen and no cultural remains found *in situ.* The bones recovered from the West lobe may be natural in origin and not the result of cultural processes.

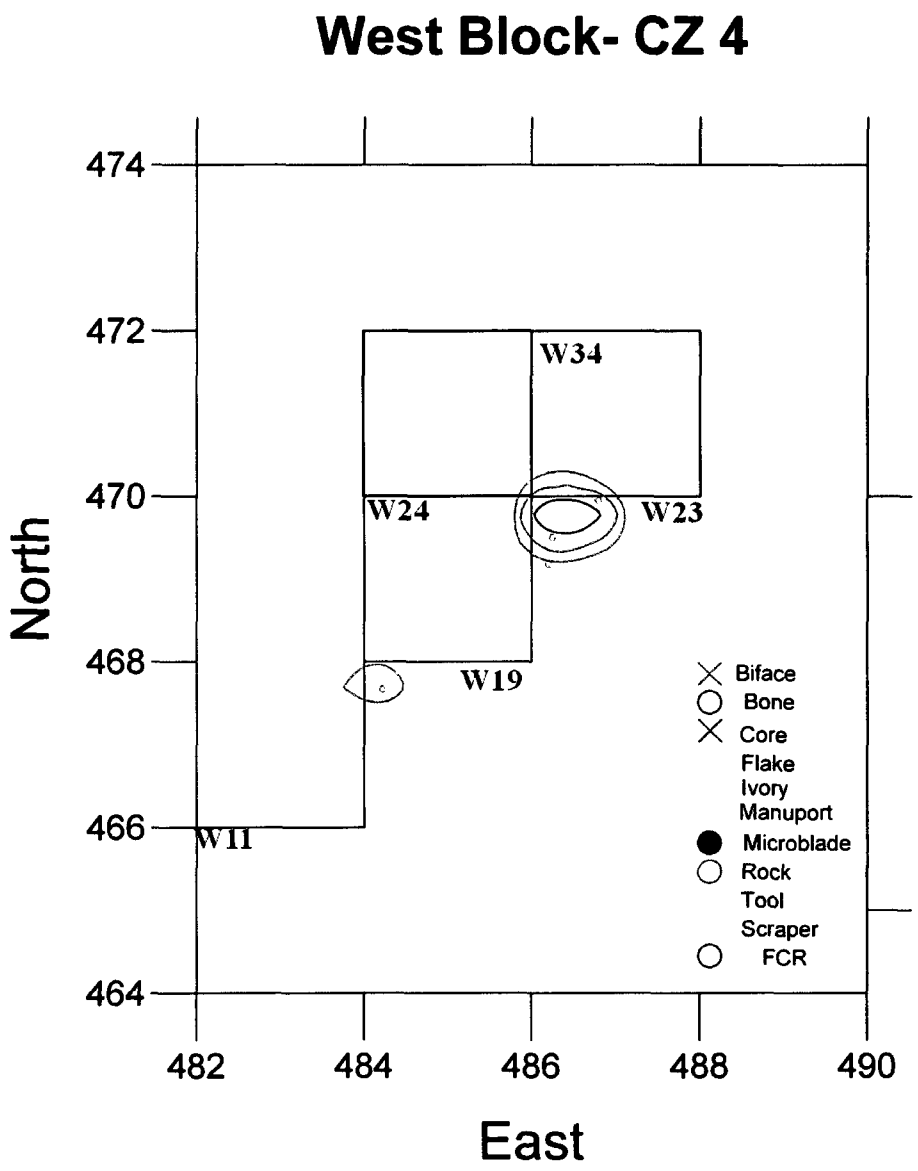

Figure 4.44 West Block CZ 4 with isopleth map of screened remains

4.6.2 CZ 3

Cultural Zone 3 (CZ 3) (Figure 4.45 and Figure 4.46) has been dated from 10,140 ± 50 to 10, 760 ± 60 14C yr BP (11,600 to 12,300 cal yr BP). This corresponds with Phase II of the East Beringian tradition and the Chindadn/Nenana Tradition. CZ 3 corresponds with the middle and upper paleosol complexes, and the calibrated age corresponds with the Younger Dryas cooling event. Two 14C dates that correspond to CZ 3 fall outside of the above range; one obtained in the first excavation of the site, and the second during

2009. Both of these dates come from material in the Upper paleosols. The 1992 date of 7,620 ± 100 14C years (8436 ±91yrs cal BP) was obtained from multiple charcoal fragments from the upper paleosols and is noted as being an unreliable date. The 2009 date of 7,790 ±50 14C yrs (8505 ± 55 yrs cal BP) was obtained from charcoal (SPC #2) from the upper paleosol and was one piece of charcoal. There is no reason to believe this date is unreliable. The charcoal used for this date was located in the north wall of E16 approximately 10 cm above and 25 cm east of the location of another piece of charcoal (SPC #1) that was dated to 10160 ± 50 14C yrs BP (11,812 ± 160 cal yrs BP).

CZ 3 remains found *in situ* in the East Lobe consist of a fairly dense concentration of fragmented bone, lithics, and fire-cracked rock (FCR) located in the northern half of E32, which has been labeled Feature 3 (Figure 4.47). Scattered faunal remains and lithics were also found *in situ* in E38, E46, and E52. As the isopleths maps show, very few lithics (n=3) were recovered from the screen, while a large number of bone fragments were. These screened bone fragments correspond with the dense cluster of remains in E32, as well as the remains in E38. This may indicate that these areas join and be one activity area, (the block north of E32 and West of E38 (E39) has not been excavated at this time).

In the West Lobe, a hearth (Feature 4) (Figure 4.48) has been dated to 10,360 ± 50 14C yrs (12,035 to 12,413 cal yrs BP) and its location correlates with CZ 3 (Figure 4.46). The hearth is located in the northern section of the block and a corresponding lithic scatter approximately 1m south of the hearth location is included in the feature area. Debitage found in association with Feature 4 have been described as either blue/gray chert or a dark gray silicified siltstone; however one flake found directly in the hearth is composed of this siltstone with bands of blue/gray chert and so it is assumed that these two material types came from the same core. A single microblade was found *in situ* in the lithic scatter south of the main hearth area. Almost all of the lithic remains associated with Feature 4 were found *in situ*; only one flake was recovered from the screen. Many of the flakes found south of the hearth are very small in size (1-2mm in length and width) while the flakes found in the hearth fill are larger. It appears that this distribution pattern is not the result of post-depositional disturbance, even though Feature 4 is truncated by a krotovinia.

Isopleth maps show two main concentrations of screened bone on the West Lobe in CZ 3; one in W24 and associated with the hearth, and the other in W34. As is the situation in the East Lobe, the block north of W24 and west of W34 (W33) has not been excavated yet. It is possible that the bone scatter associated with Feature 4 continues into W33.

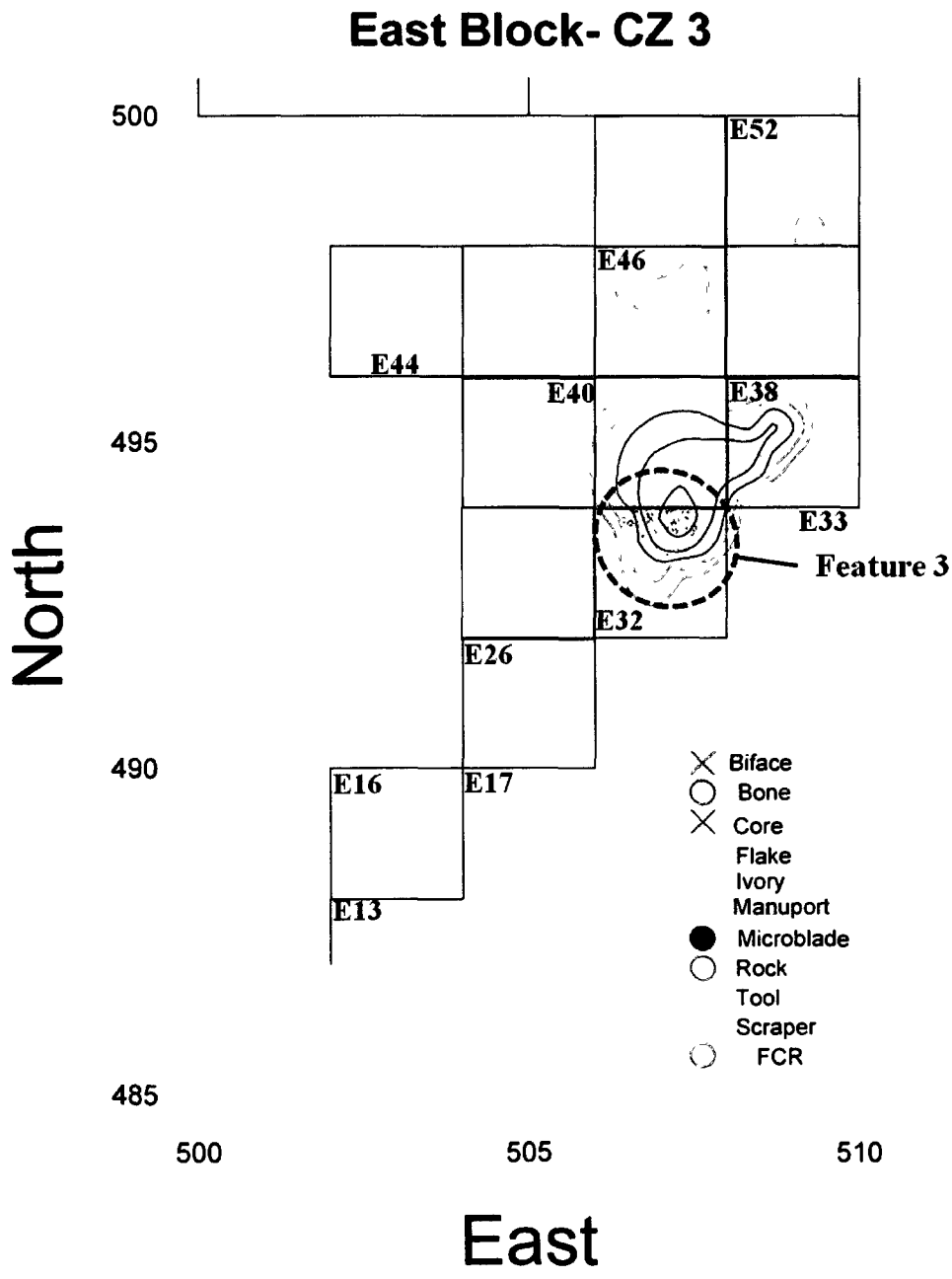

Figure 4.45 East Block CZ 3 with isopleth map of screened remains

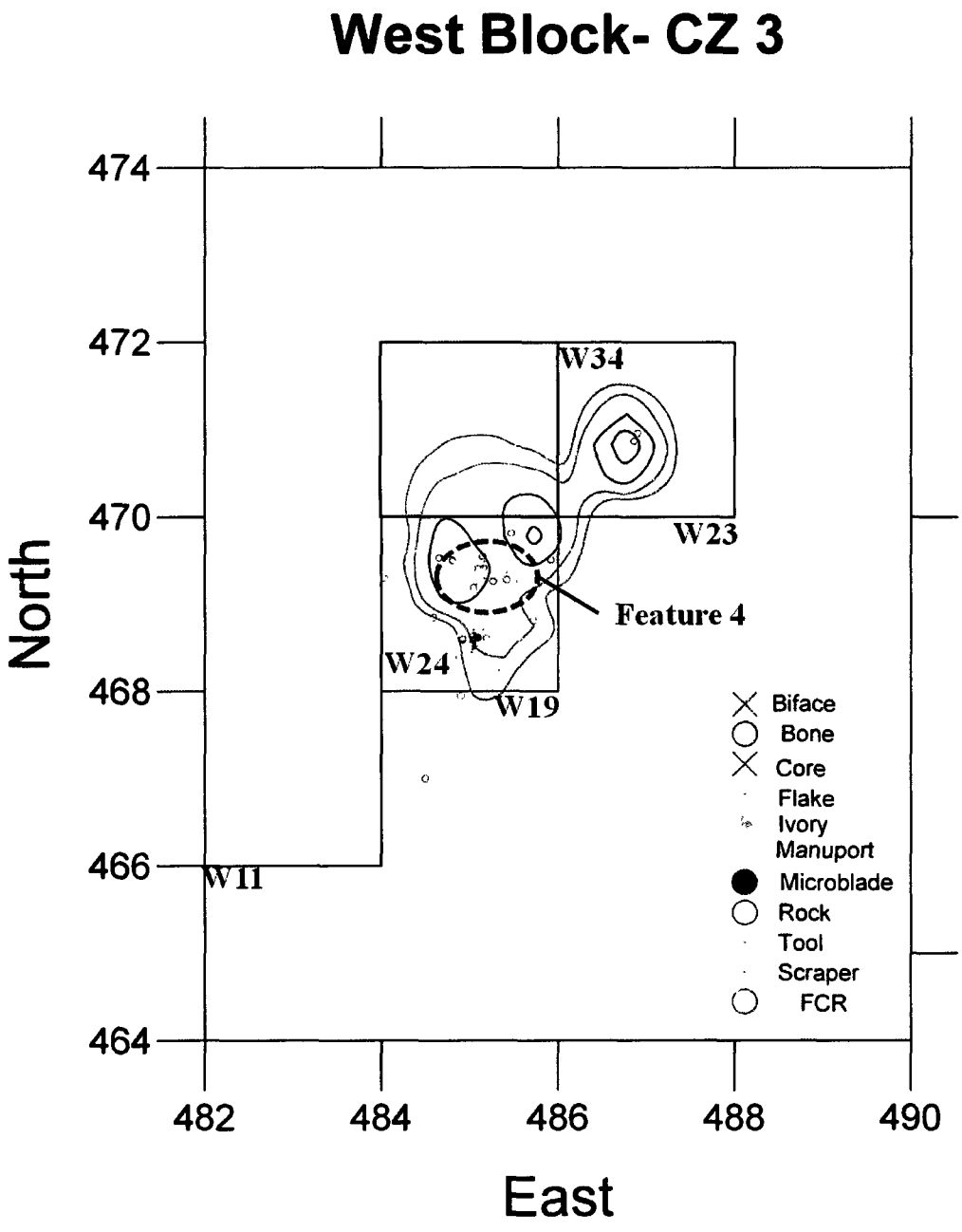

Figure 4.46 West Block CZ 3 with isopleth map of screened remains

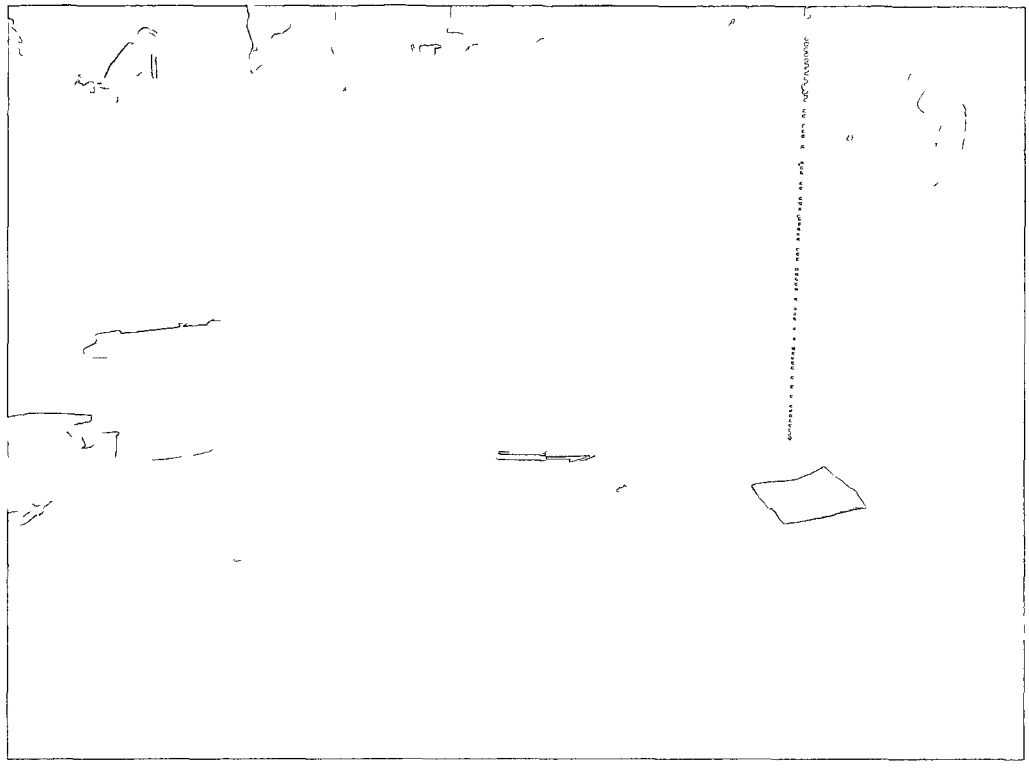

Figure 4.47 Feature 3

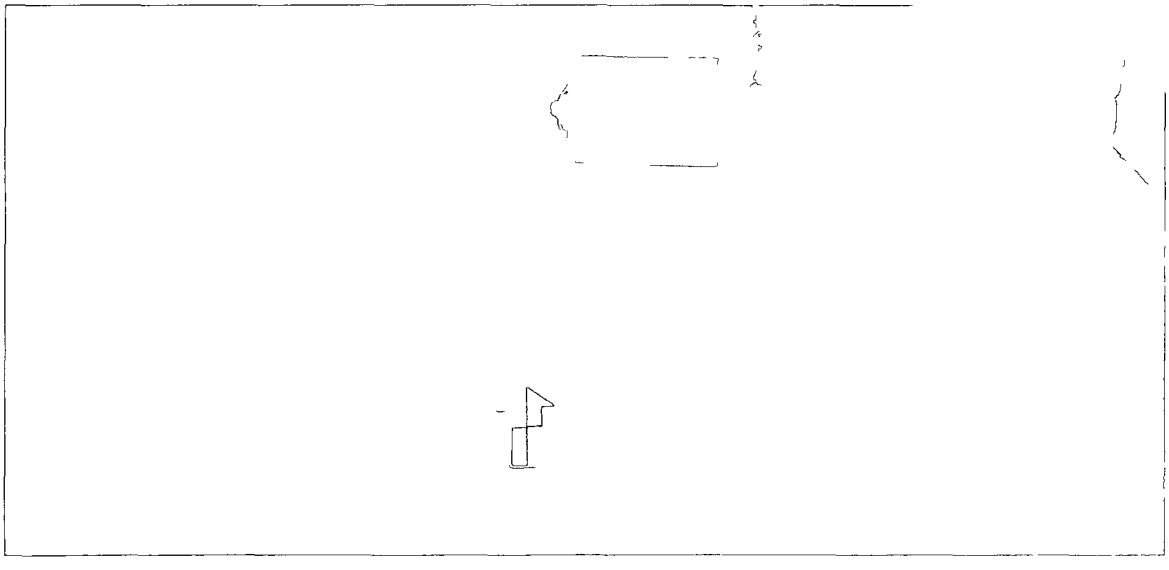

Figure 4.48 Feature 4

4.6.3 CZ 2

CZ 2 (Figure 4.49) is concentrated in a 2 m^2 area in the East Lobe and is located in the B/C1 horizon. It is composed of flakes, several bone fragments, and two microblades. Dates for CZ 2 are not concretely established, due to the age reversals in the modern forest soil. No charcoal or bone directly related to the artifacts found in CZ 2 was dated. However, if the oldest radiocarbon date from the modern forest soil is utilized (6050± 40 14C yrs BP) the calibrated age range for CZ 2 is 7,020 to 6780 cal yrs BP. These calibrated dates correspond to the Early Taiga Periods and the Northern Archaic Transitional Tradition. It is very possible that the CZ 2 remains could be classified with CZ 1b; this will be discussed in the summary section of this chapter.

In the West Lobe CZ 2 is expressed in a small isolated lithic scatter which was identified in the field as Feature 1 (Figure 4.50). A scraper and 10 flakes (some of which are pot lids and refit the scraper) were found in a small area in the NW corner of W34. At the time this feature was recorded it was noted that its designation as a feature was tenuous and that the artifacts recovered from it may have been part of the bone and lithic scatter found in the overlying levels and which has since been classified as belonging to CZ 1b. Many of these overlying bone fragments are burned and the lithics display pot lid scars. The scraper, as well as several of the artifacts, were noted as having oblique orientation. Due to heat-altered nature of the overlying cultural remains and those in Feature 1, and the taphonomic disturbance evident in the upper horizons at the site, it appears that the expression of CZ 2 in the West Lobe is simply an artifact of taphonomic mixing.

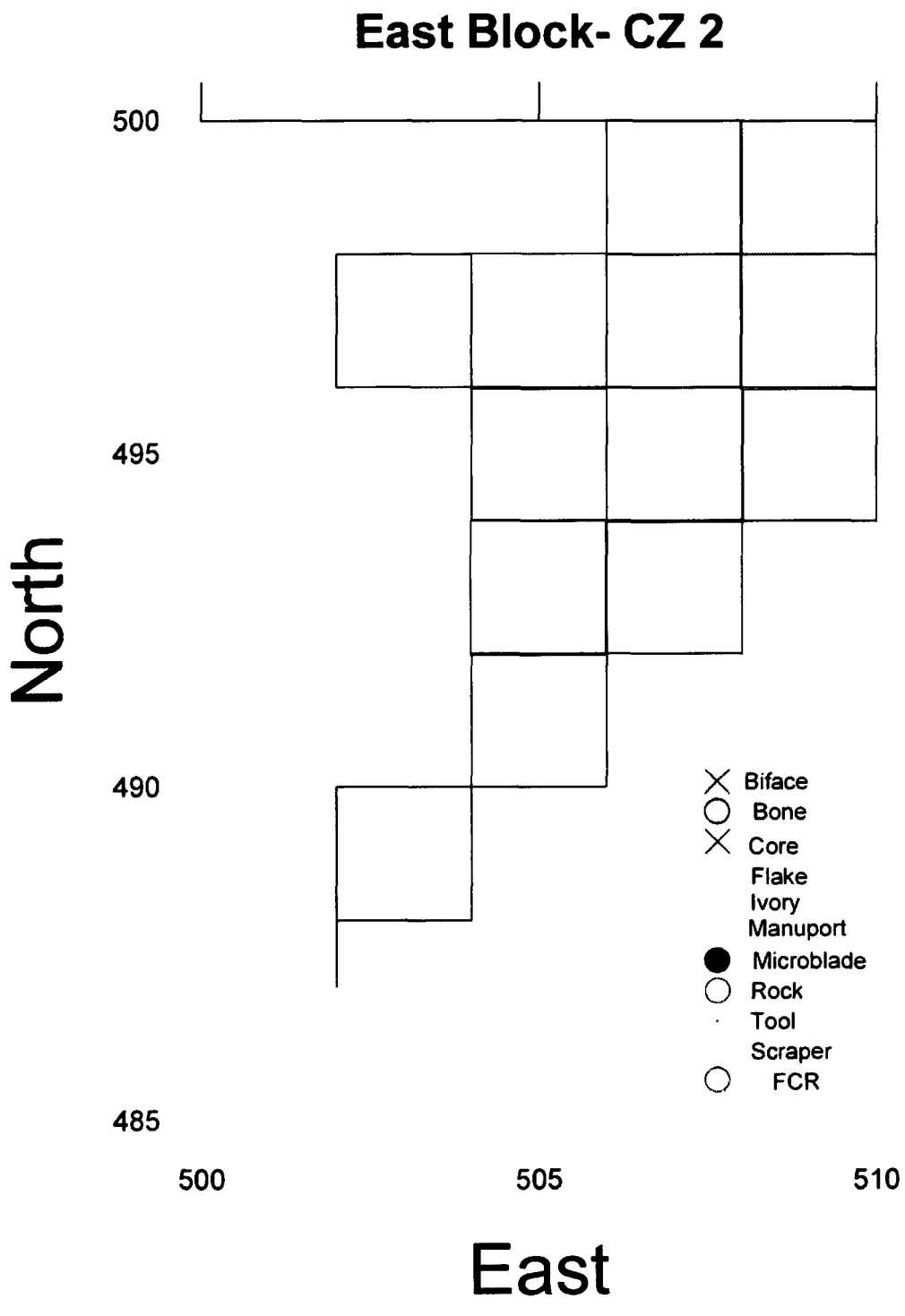

Figure 4.49 East Block CZ 2

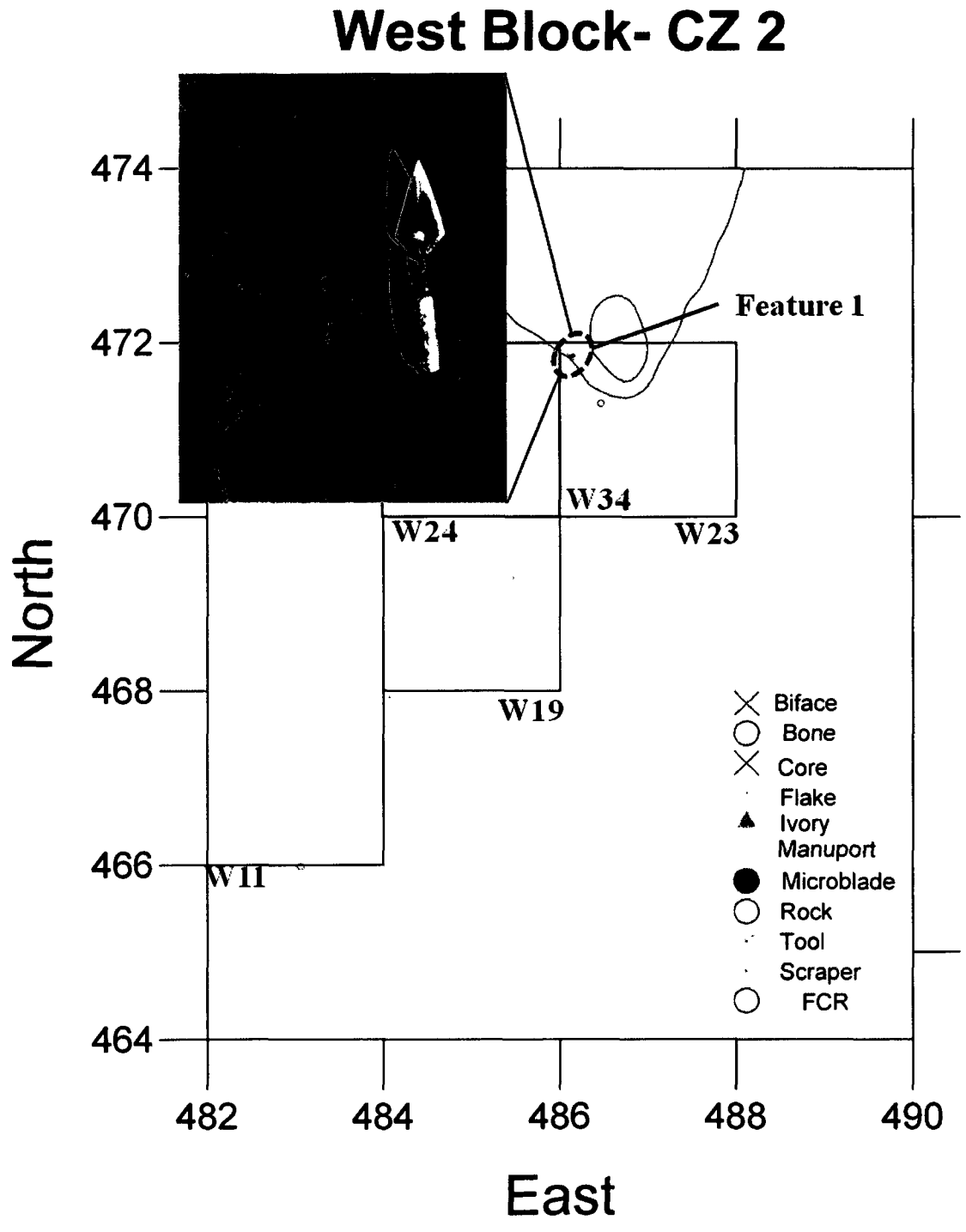

Figure 4.50 "Feature 1" in W34, CZ 2

4.6.4 CZ 1b

The majority of the cultural remains recovered during 2009 were found in CZ 1b. CZ 1b is located in the B and C1 horizons at both the East and West Lobes. Flakes (n=1,985), scrapers (end n= 3, side n=2), microblades (n=19), a biface fragment, a burin spall, modified flakes (n=3), and bone (n=4,418) were recovered. Obsidian flakes (n=53) from CZ 1b were sourced to both Wiki Peak (located in the Wrangle St. Elias Mountains in Eastern Alaska) and Batza Tena (located along the Koyukuk River in Northwest Alaska), with the majority coming from Batza Tena. Radiocarbon dates for CZ 1b range from 4,580 ± 40 14C yr BP (5,570-4970 cal yr BP) to 5,530 ± 40 14C yr BP (6420- 6260 cal yr BP). CZ 1b corresponds to the Middle to Early Taiga Periods and the Northern Archaic Tradition.

There are two to three possible feature/activity areas evident from the *in situ* remains in the East Lobe (Figure 4.51). The first of these is a large diffuse faunal and lithic scatter that was concentrated in E26, E17, and E16 (Area 1 on the Surfer generated spatial distribution table). No formal tools were recovered from this area, and the majority of the faunal material is fragmented and nondiagnostic. Many of the flakes are of a local material and are the same type as the core found in this scatter.

All of the bone fragments recovered *in situ* are from E26, while the majority of the lithics recovered are from E16 and E17. The distribution of faunal remains indicates possible excavator error, as the extent of the faunal remains goes up to, but not past the south and east edges of block E26. Also, very few lithics were recovered *in situ* from E26, indicating that the observed *in situ* patterning of Area 1 may be the result of different excavation techniques. The one caveat to this discussion is a lack of screened faunal remains from E26 and E17 (and only seven bone fragments were recovered from the screen in E16). One would expect that if faunal remains were present but not found *in situ* they would be found in the screen; however this is not the case in Area 1. The screened lithic remains from CZ 1b, Area 1 indicate two concentrations within the greater area; one in the NW corner of E17 going into the SW corner of E26, and the second in the NE corner of E26.

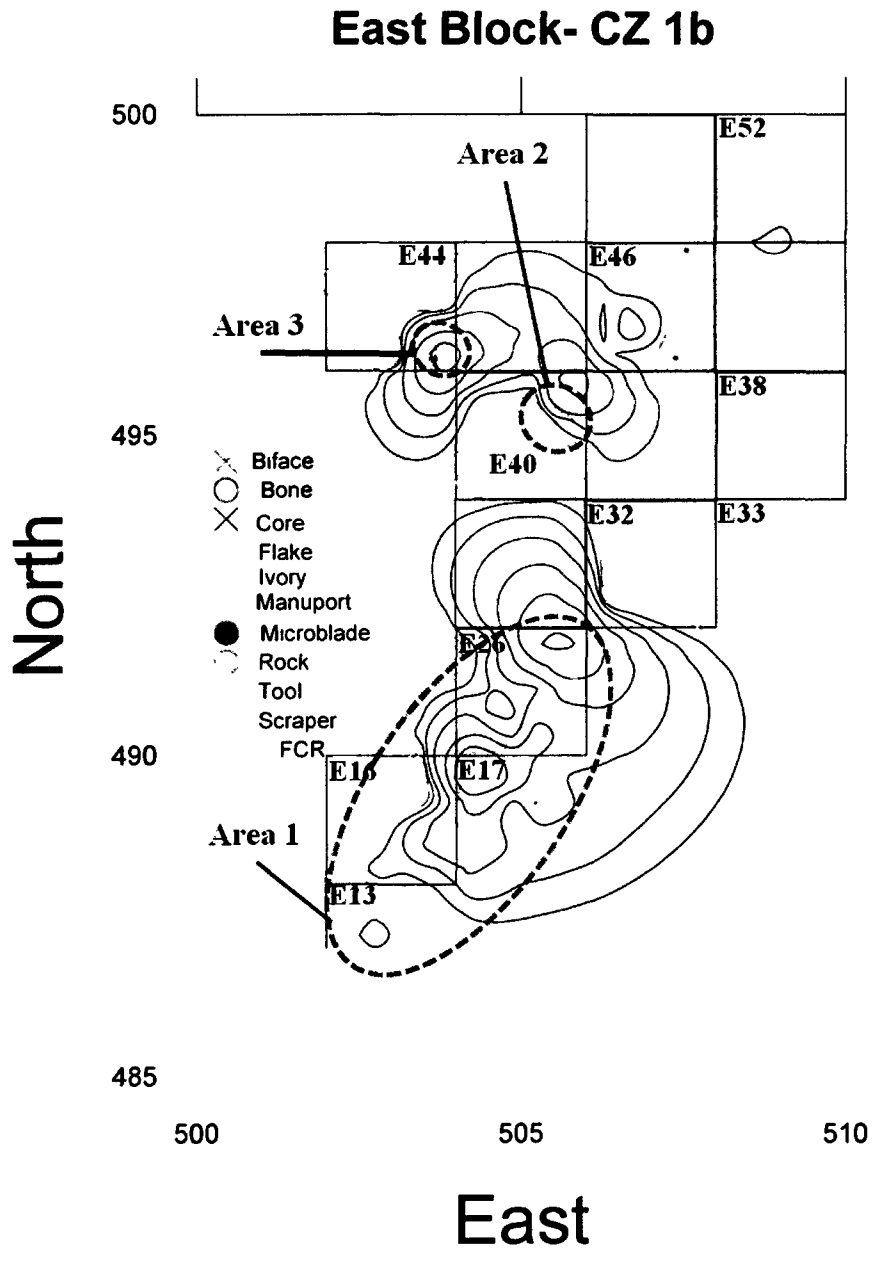

Figure 4.51 East Block CZ1b with isopleth map of screened remains

The second two feature/activity areas in CZ 1b on the East Lobe are concentrated lithic scatters found in E40 (Area 2) and E44 (Area 3) respectively. No formal tools are directly associated with either of these scatters, although a scraper was found 1m to the west of the scatter in E44. Only one bone fragment was found *in situ* in the SW corner of E40. No faunal material was found *in* situ in E44 and no faunal material was recovered from the screen from either E40 or E44 in CZ 1b. These two scatters are just over 2 m apart, and so are here on considered separate features/ activity area, although it is possible that they were produced from the same cultural event. The isopleth maps of the screened lithic material, however, supports that these two scatters are separate area. Both blocks E41 and E45 have not been excavated, and so it is possible that these two scatters may join when more of the site is excavated.

CZ 1b remains from the West Lobe (Figure 4.52) indicate a large feature area (Area 4). A large number of small nondiagnostic bone fragments (many calcined) were recovered *in situ* from the SW half of W34 and the NW corner of W23. This bone scatter is diffusely bounded to the SW and NE by lithics. The NE section contained three scrapers, while the SW section contains microblades (n=4), a scraper, and the distal end of a biface fragment. The isopleths map of the faunal remains recovered from the screen follow the location and patterning of the *in situ* faunal remains. The isopleths map for lithics recovered from the screen show a concentration in the SW corner of W24, and no screened lithics recovered for either W34 or W 23.

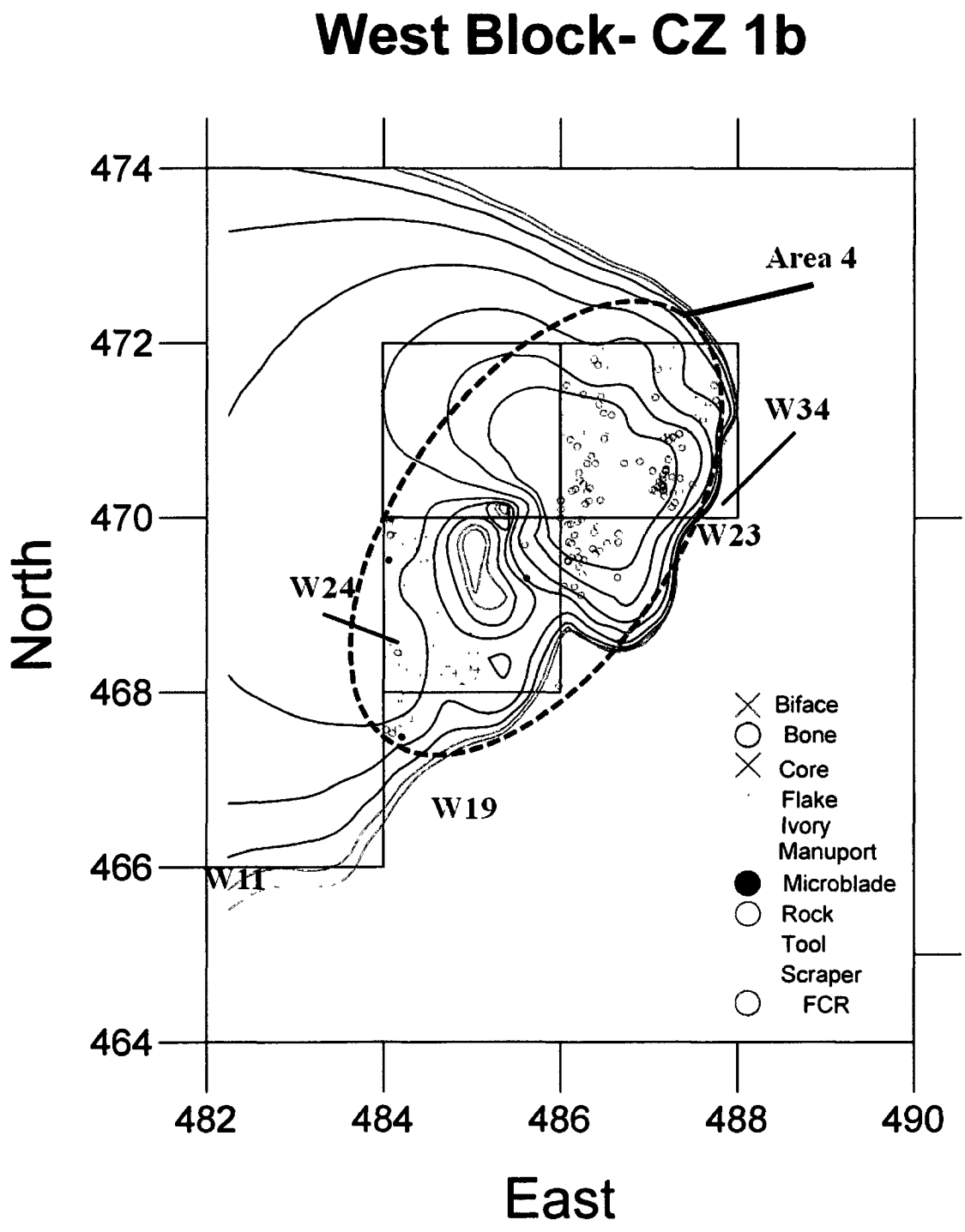

Figure 4.52 West Block CZ 1b with isopleth map of screened remains

While here again (as in the East Lobe) this spatial patterning may be due to differences in excavator technique and. The spatial patterning of CZ 1b in the West block indicates this area may have been a game processing location; the fragmentary nature of the calcined bone indicates faunal processing, while the frequency of scrapers may indicate hide scraping.

The calcined and burned bone recovered from Area 4 indicates that this was a hearth type feature. This designation is supported by the presence of pot lidded artifacts. As noted earlier in this chapter, the lack of enhancement in P at Area 4 indicates that use of the area was short in duration.

4.6.5 CZ 1a

CZ 1a (Figure 4.53 and Figure 4.54) is a surface or near surface component composed of 6 flakes and 33 bone fragments. Dating of CZ1a is problematic; the youngest radiocarbon date obtained from the modern forest soil can only be used to say that it is at least 770 ± 40 14C yrs BP (780-660 cal yrs BP) old, but may be older. The next youngest date, 1,430 ± 60 14C yrs BP (1440-1280 cal yrs BP) may be associated with CZ 1a as it is much younger than the next youngest 14C date from the modern forest soil (4,050 ±140).This second date corresponds to the Late Taiga Period and the Athapaskan Tradition. Due to the disturbance of this level however, it is possible the CZ1a is part of CZ 1b

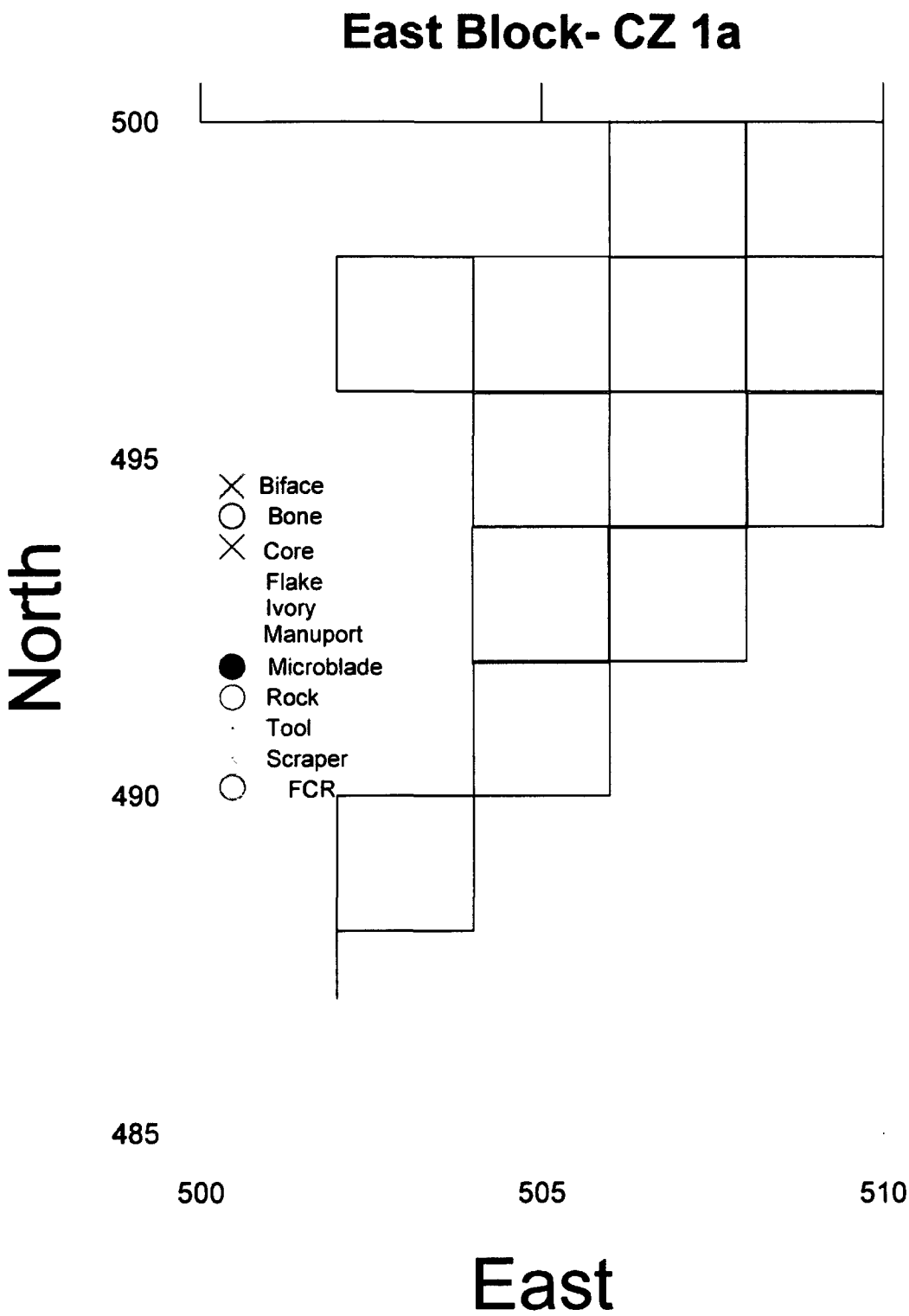

Figure 4.53 East Block CZ1a

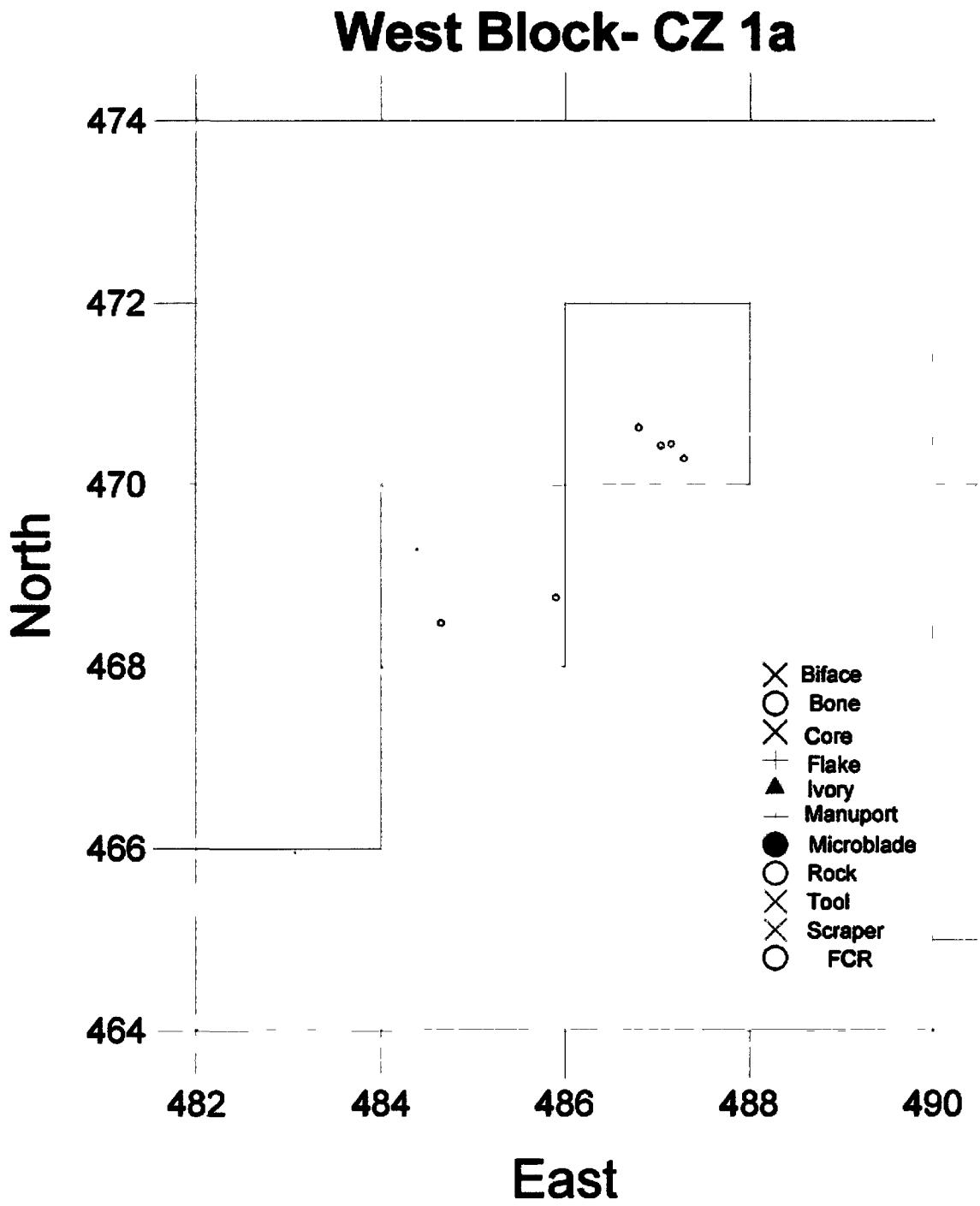

Figure 4.54 West Block CZ1a

By plotting the means of lithic size class for each 5 cm arbitrary level an interesting pattern is evident in the upper levels that indicates post-depositional mixing in CZ 1a, 1b and 2 (
Figure 4.55). Levels 1 to 5 show a significant decrease is size class, while levels 5-12 show a small but consistent decrease; these levels compose CZ1a, CZ 1b, and CZ 2. It has been shown that the levels closer to the surface will undergo greater cryoturbation as they receive the greatest input of liquid water as well as the greatest number and degree of temperature fluctuations (Bowers, et al. 1983; Hilton 2003; Johnson and Hansen 1974). Freeze/thaw mechanisms work to move larger objects upwards and smaller objects downwards (Hilton 2002), which has taken place in the upper components at the Mead Site. This does not mean that the CZ's encompassed in Levels 1-12 are not the result of different occupations, but it shows that there is significant post-depositional disturbances in the upper level and that care should be utilized in the future when assigning cultural significance to these CZ's as they may be representative of something other than cultural change.

The plots of the means of the lithic weights per 5 cm arbitrary level display a similar but slightly different pattern (Figure 4.56 and Figure 4.57). Levels 5-12 still show a mostly constant decrease is weight, while levels 1-5 have a more varied trend. Of these two analyses, more weight is given to the size class comparison, as size is the main variable affecting movement of artifacts through the profile (the greater the surface area, the more likely it is to become mobile and move upward). These conclusions are also supported by the plotted trends for the lower components, which do not exhibit a constant decrease or increase with depth, and which did not exhibit as great of a degree of disturbance when they were excavated.

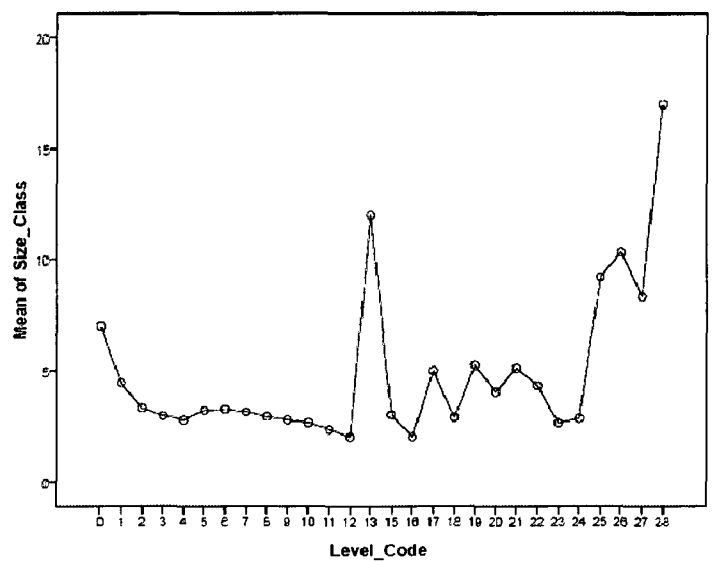

Figure 4.55 Mean of Size Class and 5 cm arbitrary level

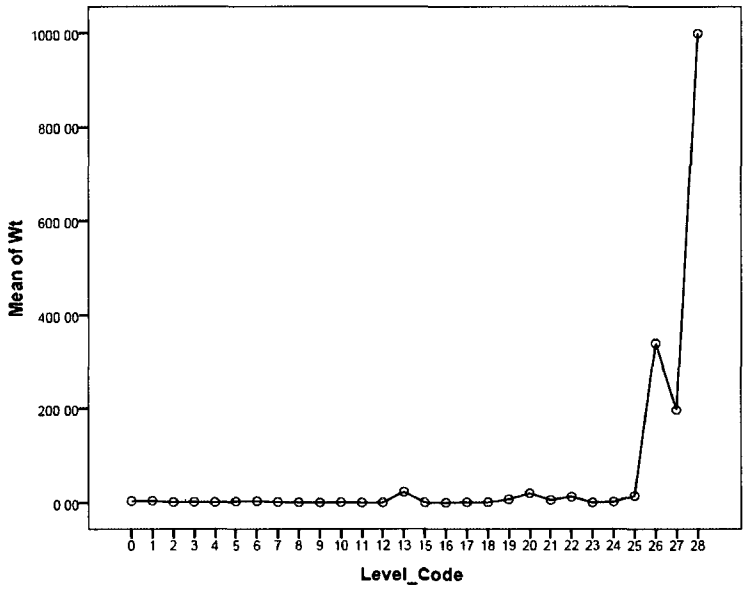

Figure 4.56 Mean weight (g) of lithics and 5 cm arbitrary level

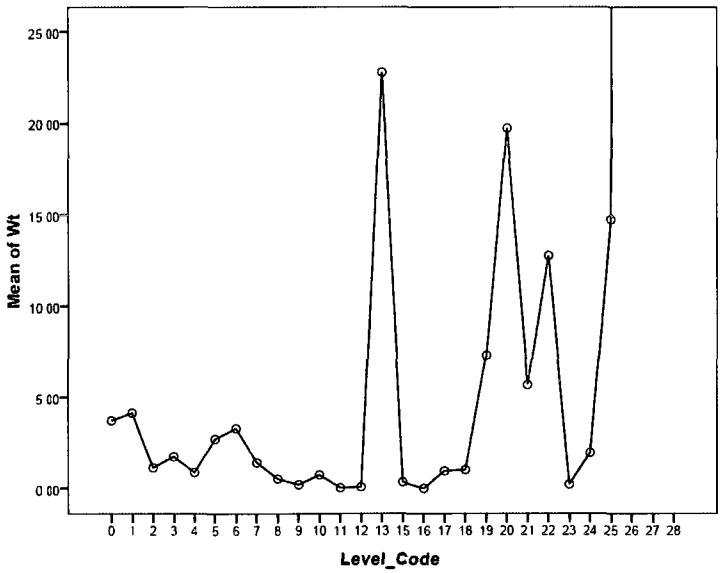

Figure 4.57 Zoom of Levels 1-24 from Figure 4.21

4.7 Loess Accumulation

Dates used to determine accumulation rates are from E16; this profile returned four 14C dates whose location is both well documented and representative of the site (Figure 4.58). As no date was obtained for the lower paleosol complex from E16, the date for this paleosol is from E17.

E16 radiocarbon dates were calibrated and the center calibrated intercept was utilized for analysis at 2 standard deviations (Table 4.13). It should also be noted that the date used as the marker of the base of the B horizon in this analysis (4940 ± 5014C yrs BP) is not the oldest radiocarbon assay obtained for the B horizon. Just to the west at E13, at the same general stratigraphic level as SPC #4 (4,940 +/- 14C yr BP), are FS #51 and FS#52; FS# 51 has a similar date to SPC #4, but FS#52 has an older date of 6050 ± 40 14C yr BP.

Also, the date used to demarcate the upper boundary of the upper paleosol is much younger than dates previously used by investigators as the upper bound of the paleosol complexes; this date (8,680-8,440 cal yr BP) was obtained from a single piece of charcoal in good stratigraphic context and there is no reason to treat it as being unreliable. Sample WSU-4261 (which is also from the upper boundary of the upper paleosol) returned a date of 8620-8260 cal yr BP and was rejected by earlier investigators because it was obtained from multiple pieces of charcoal and appeared to be erroneous as it is much younger than the other dates obtained for the paleosols (Dilley 1998). However, in light of the new date obtained for the upper paleosol this view needs to be reworked.

The earliest depositional event examined here spans two lithostratigraphic units; the lower bedded sands and the lower loess. Due to the differences in particle size (and the energy necessary to transport the different particles sizes) the deposition rate for this event probably varied between the two deposits. However, as no date is available for the sand/loess transition it will be assumed that the depositional rate was constant between these two events.

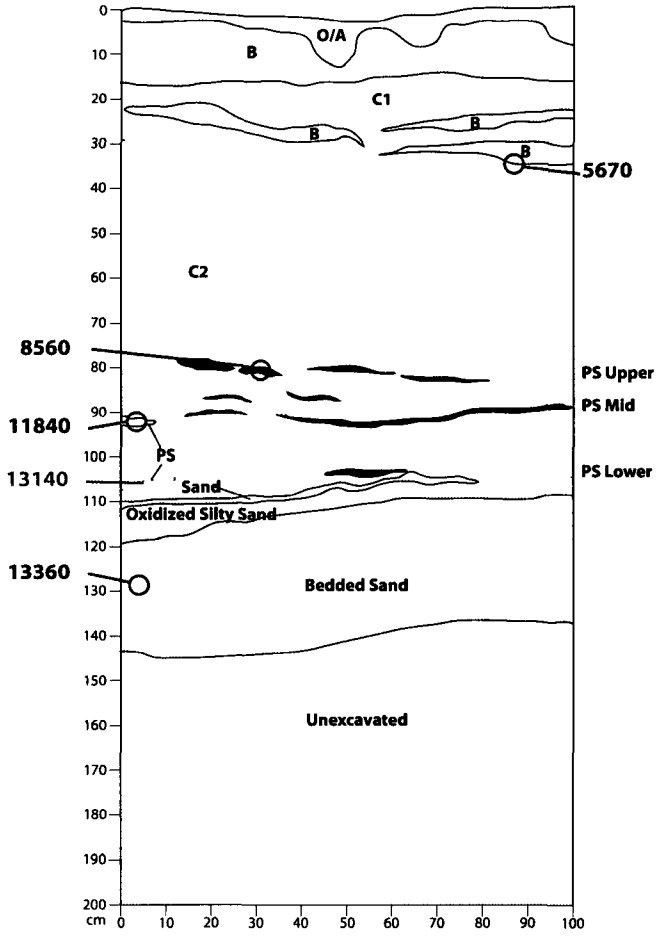

Figure 4.58 Block E16 North Wall Radiocarbon dates and stratigraphy (depth is in cmbs), blue date is from E17.

Table 4.13 Correlation of radiocarbon dates from E16 and E17 and stratigraphy

Strat	c14 Date	Calibrated range (2 standard deviations) cal BP	Center calibrated intercept (cal BP)	Depth (cmbs)
Bedded Sand	11460 +/- 50	13500-13220	13360	120
Lower Paleosol	11210 +/- 60	13280-13000	13140	107
Mid Paleosol	10160 +/- 50	12080-11600	11840	92
Upper Paleosl	7790 +/- 50	8680-8440	8560	80
B Horizon	4940 +/- 40	5770-5570	5670	33
Surface	0	0	0	0

The resulting deposition rates show that deposition was greatest between the bedded sands and the lower paleosol complex at the end of the Pleistocene (Table 4.14). Deposition slowed significantly between the lower and middle paleosol complexes during the time of the Younger Dryas, and continued to lessen between the middle and upper paleosol complex. From 8560 to 5670 cal yr BP the accumulation rate again increased to 1.63cm/100yrs; this interval is noted at the site for the dearth of cultural material associated with it.

Table 4.14 Deposition rates

Strat	Deposition Rate
Bedded Sands to Lower Paleosl	5.91
Lower Paleosol to Middle Paleosol	1.15
Middle Paleosol to Upper Paleosol	0.37
Upper Paleosol to base of B horizon	1.63
Base of B horizon to modern Surface	0.58

The first few depositional events correlate with the earliest occupations at the site, while the third corresponds to an occupational hiatus. Assuming that the main CZ 4 occupation corresponds with the lower paleosol complex, and CZ 3 correlates with the middle and upper paleosol complex this indicates that the site was being occupied during a period of lessened loess accumulation/deposition. The abandonment of the site correlates with an increase in accumulation. If loess accumulation is enhanced by increased vegetation (specifically boreal vegetation), abandonment also correlates with the rise of the boreal forest.

The loess deposition rates calculated depart slightly from the general deposition history of other sites in the Tanana Valley. Other sites, such as Broken Mammoth, have dates associated with the upper paleosol complex around 11,000 cal yr BP, and dates of 7,620- 8,640 cal yr BP for the base of the B horizon. At these sites it appears that the major depositional event of the Holocene took place from around 11,000 to 8,000 cal yr BP, whereas at Mead they took place from around 8,500 to 5,600 cal yr BP. Because this mid-Holocene increase in accumulation is seen only at the Mead Site, it is hypothesized that the cause of the accumulation is also site specific and may be related to the location of the site in relation to the Tanana River.

The implications of this difference are great. The interval of deposition observed at other sites does not correlate well with large scale climate events. Potter (2008d) noted a regional population decrease from 10,000-9,000 cal yr BP which correlated with both the Holocene Thermal Maximum and the emergence of spruce forests.

It appears that the oldest two occupations at the site occurred when the landscape was dominated by a mixed shrub tundra. This shrub tundra, which is less effective at trapping loess than forest environments accounts for the low depositional rate from the lower to the upper paleosol complex, and is evidenced by the geochemical and micromorphological data, as well as the presence of *salix* in Feature 4 from CZ 3. The emergence of spruce forests in the region from 10,000- 9,000 cal yr BP was followed shortly thereafter with an increase in loess deposition at the Mead Site. The decrease in accumulation from 5,600 cal yr BP to the present does not correlate with any known significant change in climate or regional vegetation as the present day vegetation is believed to have been established by 6,800 cal yr BP. The decrease in accumulation may be related to the location of the Tanana River. As noted in Chapter 1, the Tanana meanders back and forth across its wide flood plain, and so it is hypothesized that during this period of decrease accumulation the river was further from the site than during previous periods.

It is possible that the 8.2k event is responsible for the increase in accumulation above the upper paleosol. As no radiocarbon date has been obtained for the area between the upper paleosol and the base of the B horizon, it is possible that the majority of accumulation between these stratigraphic layers could have taken place over a very short duration due to an episode such as the 8.2 k event.

5 Discussion and Conclusion

5.1 Buried Occupational Surfaces

Based on the results presented in Chapter 4, there are no detectible buried occupational surfaces in the upper loess stratigraphic section at the Mead Site, the null hypothesis of Research Question 3 (are there detectible buried occupational surfaces in the Upper Loess stratigraphic section of the Mead Site) cannot be rejected. A sand lens is evident in some units at the contact of the upper and lower loess, but this layer is natural in origin and not indicative of occupation at the site. This sand lens may have formed during the 8.2k event. The level of post-depositional disturbance indicates that if a buried occupation surface did at one time exist in the upper loess, taphonomic processes have disturbed it to the point where it is no longer evident.

The clay lamella (B3) located in the modern forest soil has been proposed by some as being a remnant occupation surface (J. and Bozarth 2008), but this does not appear to be the case at the Mead Site. Clay lamellae in Cryochrept soils form through frost action and ice lensing and have pedo-petrogenic origins (Dement 1962; Rawling 2000; Rieger 1983). The amount of cryoturbation in the modern forest soil, combined with the lack of association between artifacts and the sporadic location of the clay lamella at the Mead Site, indicates a natural formation of the B3 horizon.

The geochemical data also do not support the interpretation the theory that lamella is cultural in origin. Occupational surfaces are created though long term use and one would suspect that phosphorus would increase in association with the long duration needed to form an occupation surface, however this is not seen at the Mead Site. The clay lamella does not exhibit any increase in phosphorous (or Ca) as would be expected (see Figure 4.22).

5.2 Classification of paleosols

The buried paleosols at the Mead Site are Ab horizons that show little evidence of weathering. They were formed during the YD cold/dry event which accounts for their lack of weathering or B horizon formation. Unlike at the Broken Mammoth site, which has definitive separation between the upper, middle, and lower complexes, paleosols at the Mead Site are not easily tracked across the site. In part this may be due to changes in localized stratigraphy and deposition across the site.

Magnetic susceptibility data and geochemical analysis indicate that these horizons are natural in origin but are anthropogenically enhanced. While the paleosols are not necessarily indicative of human occupation, they do correspond to the cultural zones at the Mead Site. The majority of CZ 3 and CZ 4 cultural remains were found in association with the paleosols, and geochemical analysis of material from Feature 4 shows increases in phosphorus and calcium. The proxy information indicates that the paleosols

formed during cooler and drier climates when the paleo-surface stabilized long enough for an A horizon to form.

5.3 Context and Cultural Zones

CZ 1b, 1a and 2 have been affected greatly by post-depositional disturbance; CZ 3 and 4 have also been affected by post-depositional disturbance, but to a much lesser extent. This is evidenced through the geoarchaeological analysis as well as the orientation of artifacts. While not systematically recorded (as noted earlier), many of the artifacts that were photographed *in situ* from the upper soil horizons exhibit vertical or oblique orientation (Figure 5.1), while those in the lower horizons exhibit mostly horizontal orientation.

The separation between CZ 1a, 1b and 2, as defined in Chapter 4, is based on perceived activity areas and depth; the resolution for these CZ's is low both vertically and horizontally. The spatial patterning observed is most likely a remnant of the original archaeological context, but it has been greatly altered by post-depositional disturbance. The designation of scatter or feature areas in the upper horizons are general and should not be utilized to designate discrete boundaries of where activities took place at the site.

The cultural zones are located in similar stratigraphic position to those at Broken Mammoth and so the remains from the upper components at Broken Mammoth (and other comparable sites in the region) were most likely also affected by similar post-depositional disturbance. This warrents questioning the validity of the spatial and cultural designations ascribed to the upper components at this site and at other similar sites.

As the vertical provenience of artifacts from the upper CZ's is questionable, so too is the horizontal provenience; artifacts have been noted to move large distances due to cryoturbation in relatively short periods (Bowers, et al. 1983; Hilton 2002; Hilton 2003). Activity and feature areas presented earlier in Chapter 4 are most likely reflections of activities that took place at the site; however, their size and density are most likely not representative of their original context and extent.

The micromorphological data provides evidence of alteration in the paleosol complexes and C horizons. Weathering does not appear to have greatly disturbed these zones, although there is evidence of carbonate accumulation indicating weathering of the soil and movement of elements through the profile. The magnetic susceptibility data does not indicate significant natural enhancement of the buried paleosols, which, as these paleosols are Ab horizons (and not Bw horizons), is not unexpected.

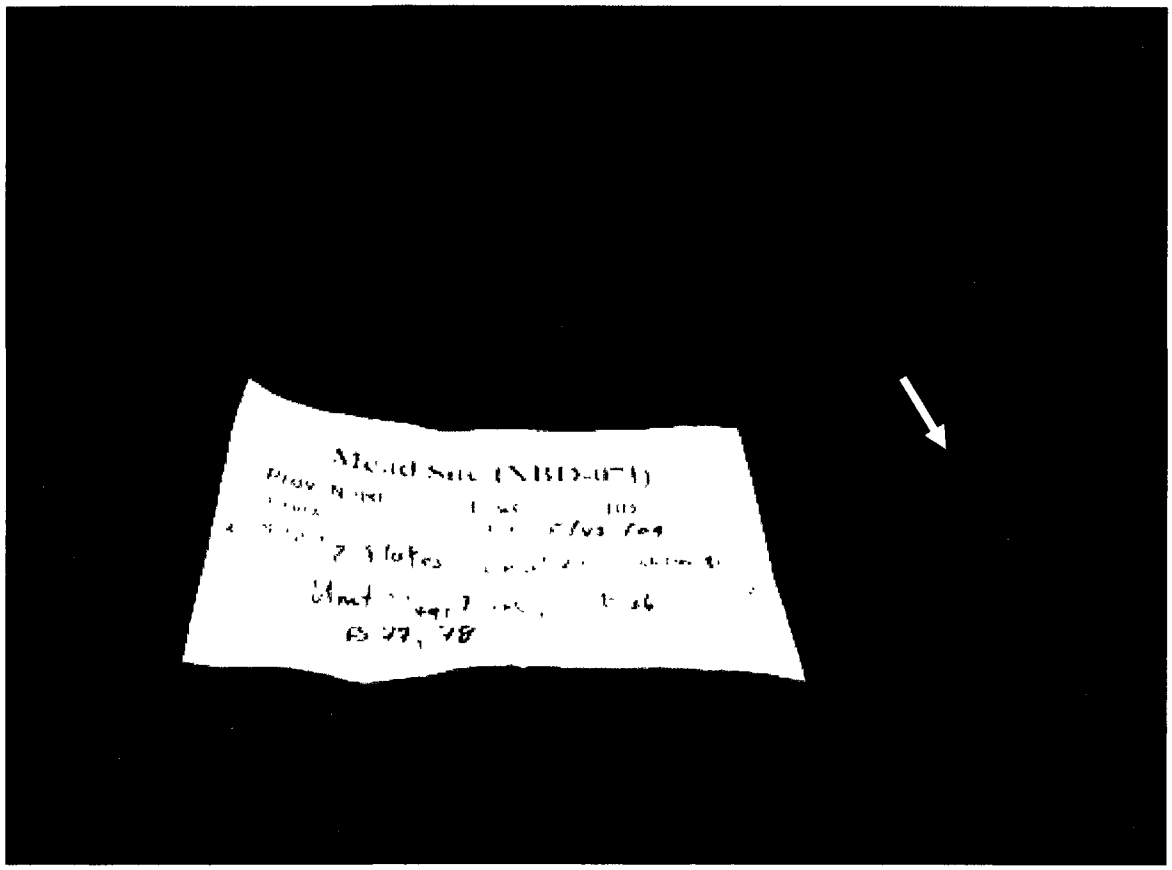

Figure 5.1 Vertically oriented scraper in E26

As noted above, the lower cultural zones (CZ 3 and CZ 4) exhibit less post-depositional disturbance than the upper zones, but there are still indications of taphonomic disturbance. On a macroscopic level the undulating and fragmented nature of many of the paleosol points to post-depositional alteration, microfaulting is evident across the site, and krotovinia were observed intruding on cultural deposits (such as Feature 4).

The geochemical data indicate that some weathering has taken place at the location of CZ 3 and CZ 4, but it is to no extent as great as that observed in the upper components. As mentioned above, the plots of mean weight and size class per 5 cm arbitrary level also does not indicate a large amount of post-depositional movement (as constant trends are not evident) in CZ 3 and CZ 4.

Dilley (1998: 261) concluded that the lower cultural zones, "have not been mixed, redeposited, or affected by cryogenic processes". However, the micromorphological and geochemical data indicate that this is not true. The inability to trace the paleosols continuously across the site or to easily separate the upper from the middle, from the lower paleosol complex indicates that post-depositional disturbance has

taken place. The observation of platy microstructure in thin sections collected from the upper paleosol, as well as in isolated organic areas throughout the profile, indicates that these soils were affected by freeze/thaw processes and that the cultural remains were also likely affected.

The cultural remains recovered from the 2009 excavation indicate that the Mead Site was most likely utilized as a short term hunting camp as there is little evidence of reuse of features or activity areas and no evidence of structures. The ubiquitous nature of the only diagnostic artifacts recovered from the site (scrapers and microblades) precludes any cultural technocomplex designation.

5.4 Climate and Cultural Zones

Radiocarbon dates were calibrated using Intercal04 and plotted against paleoclimate data using the CalPal calibration program (Figure 5.2) (Weninger, et al. 2011). As mentioned earlier in Chapter 4, several dates from the 1992 excavation were excluded from this analysis. WSU-4261 (7,620 +/- 14C yr BP) was excluded because it came from multiple charcoal fragments and was noted as being an unreliable date. Beta-59117 (9,220 +/- 370 14C yr BP) was excluded because it was a small sample from the base of the C horizon and is not noted as being associated with any cultural remains. NSRL-2000 (17,370 +/- 14C yr BP) was excluded as this date was obtained from an ivory fragment that was most likely scavenged and so is not representative of the cultural zone where it was found. Finally, one date from the 2009 excavation was also excluded as it was obtained to determine the chronological sequence at the site and is not associated with cultural remains (SPC-2, 7,790 +/- 50 14C yr BP).

The results (Figure 5.3) show that CZ 4, the oldest cultural zone at the site took place at the end of the Bølling/Allerød warming period at the end of the last glacial. CZ 4 corresponds with the lowest paleosol complex at the site. As temperatures during this time were warmer than previously, CZ 4 does correspond to a period of ameliorating climate, although, when compared to the modern climate CZ 4, was much colder and drier than conditions today.

The next occupation of the site, represented by CZ 3, took placed during the Younger Dryas cold event, as evidenced by the radiocarbon dates obtained from the middle and upper paleosol complexes. As noted in Chapter 2, proxy records for the Younger Dryas indicate that this was a period of cold and very dry climate which may have had small, short, warm intervals not evident in the ice core proxy records. Based on the definition of ameliorating climate given in Chapter 1, CZ 3 does not correspond to a period of ameliorating climate. As with CZ 4, when compared to the modern climate, CZ 3 was most likely cooler and drier than present.

The stratigraphy at the Mead Site indicates that the Younger Dryas period was not one of simply windier conditions, loess deposition, and no surface vegetation. Rather the stratigraphy records a complex record of soil formation, sand deposition, and more soil formation. The low deposition rate calculated for this period (see Table 4.14) indicates that loess deposition was much less than during the preceding or

following periods. The paleosol complexes evident at the site indicate discrete periods of soil formation which were most likely followed by periods of loess deposition. The paleosols are all Ab horizons with no evidence of accompanying B horizon formation, indicating that these surface soils underwent limited weathering before they were removed from the soil forming processes. The lack of weathering evident in the paleosols is the result of the very dry climate during the YD; if little water was available then little weathering would have occurred.

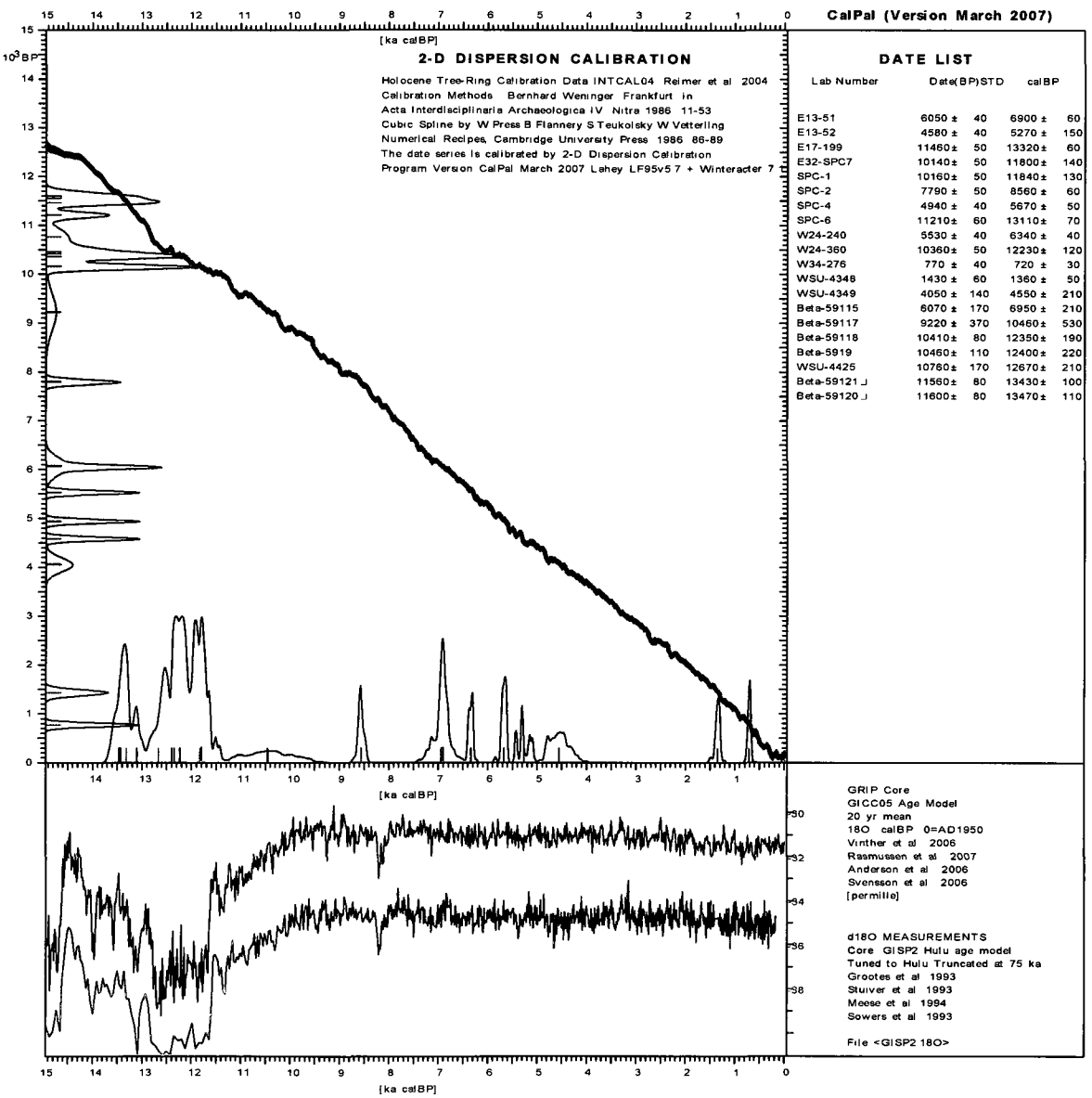

Figure 5.2- Calibrated Dates and Ice Core Data

From (Alley 2004; Weninger, et al. 2011)

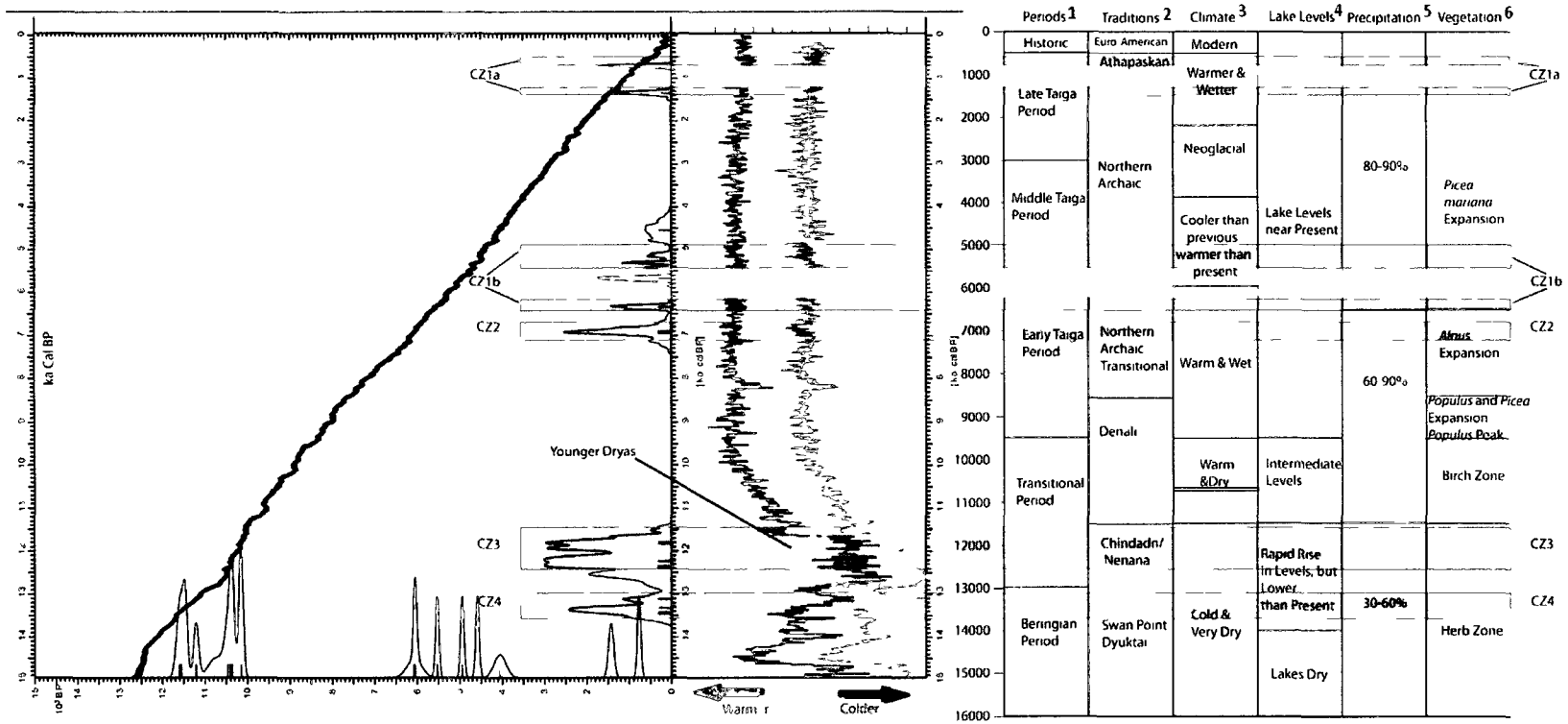

Figure 5.3 Cultural Zones and Climate Change (unless noted otherwise, all proxy data is in relation to modern conditions)

[1] [2] From (Holmes 2008)

[3] From (Alley 2004; Beget 2001, Edwards, et al. 2001; Mason and Beget 1991; Mason, et al. 2001; O'Brien, et al. 1995; Rasmussen, et al. 2007)

[4] [5] [6] From (Abbott, et al. 2000; Ager 1975; Anderson and Brubaker 1993; Bigelow and Powers 2001; Edwards, et al. 2001; Edwards, et al. 2000)

Paleosols are generally thought to form during periods of climate amelioration, when the environmental conditions are stable enough for surface vegetation to become established, but the paleosols at the Mead Site do not follow this pattern. These formed during the YD event, and the CZ 3 remains are directly associated with them. While there must have been stable environmental conditions for the paleosols to form, it does not appear that these occurred during warmer and wetter conditions. This indicates that the relationship between warmer (and moist) conditions associated with paleosol formation needs to be examined further.

The abandonment of the site immediately following CZ 3 correlates with the end of the YD and the beginning of the HTM. This correlation indicates that climate may have been a factor in the occupations composing CZ 3. Yesner (2001) notes a large depositional event during the mid-Holocene which accounts for increased loess accumulation and the sand lens seen at Broken Mammoth. This may be a result of the 8.2K event, which would account for the increase in the loess accumulation also evident at the Mead Site during this time.

The *Salix* charcoal present in Feature 4 from CZ 3 is important as it indicates that the humans who created this hearth did not necessarily have to utilized bones and oil for fuel, and that CZ 3 may predate *Populus* expansion into the area. It is hypothesized that, as *Populus* is a more efficient and cost effective fuel source than S*alix*, *Populus* would be utilized before *Salix* if it were available. Since not one, but all three wood samples from Feature 4 returned id's of *Salix*, it can be hypothesized that *Populus* was not used as it was not yet available in the area, and it gives evidence that *Salix* was an adequate fuel source for certain situations.

Unfortunately, *Salix* grows in multiple forms and in a variety of different plant communities, therefore not much can be hypothesized (from its presence in the hearth) regarding the vegetation community that was present at the site when feature 3 was created. For example, *Salix alaskensis* can range from a low ground shrub to 9 m tall trees (Viereck and Little Jr. 2007), and *Salix glauca* grows in both dry and moist dwarf-shrub tundra communities as well as peat lands and dry upland communities (Hoffecker and Elias 2007).

If viewing the upper three components as separate cultural events, CZ 2 does not appear to correlate with ameliorating climate conditions, as the proxy records indicate that this period was one of a cooler and wetter climate. This also is true for CZ 1b. CZ1a occurred during a warmer and wetter time, and so conditions may have been more conducive to habitation than the preceding period. These correlations between CZ 1a, 1b, 2, and climate change are, however, tenuous as the geoarchaeological data indicates that advanced mixing of the upper horizons has taken place. The designation of these cultural zones as discrete components is misleading.

Having stated the degree of post-depositional disturbance in the upper CZ's, something can be said regarding the abandonment of the site, as the calibrated dates indicate that the site was not utilized

from approximately 5,000 to 1,500 cal yr BP. While the climate proxy data does indicate that wild fires were more frequent during this time and that black spruce numbers may have increased, the regional radiocarbon chronology indicates that the Tanana River Basin was occupied continuously throughout the Holocene, and that in fact there was a population increase during this period (Potter 2008d). Potter (2008d) however, note that during this time there was a change in land-use strategies resulting in an increase in the use of upland areas and a decrease in the use of lowland areas after 6,200 cal BP. The lack of cultural remains from the mid to late Holocene at the Mead (situated in a lowland setting) supports this hypothesis.

When compared to the different environmental and depositional environments found at Broken Mammoth and at Swan Point, the Mead Site occupies the middle ground between these two settings. Unlike Broken Mammoth which is located on a very high bluff directly overlooking the Tanana River, Mead is set back just over 1km from the river channel, but probably received more depositional input from the Tanana than Swan Point did, which is located approximately 10km from the river. Mead does not have the spectacular viewshed of the Tanana River, as Broken Mammoth does, but does overlook the flats of Shaw Creek and could have been used as a lookout. Future studies could examine the relationship between these differences and occupations at the sites for a broader understanding of the variables influencing prehistoric occupation in the Tanana Valley.

When viewed through the lens of climate determinalism, the cultural zones at the Mead Site correlate closer with cooler climate than with warmer climate. This correlation is not a new one and has been put forward by other investigators. Mason et al. (2001) examined the relationship of Denali Complex sites with past changes in climate and ecology in Alaska. The authors note that the Denali Complex was present in Alaska at least 2000 yrs before the Milankovitch Maximum and the spread of the boreal spruce forest. They present a correlation between the peak in the number of Denali sites and the Younger Dryas and an inverse relationship between the Milankovitch Maximum and Denali site frequency, indicating a negative correlation between increased population and warmer climate. They hypothesis that the increase in population during the colder times is due to better hunting conditions. Important to this relationship is the increase in valley bottom sites during the YD, and the hypothesized increased reliance on caribou. The Mead Site is a valley bottom site, and while the faunal analysis has not been conducted and no technocomplex designation has been assigned to the cultural zones at the site, CZ 3 fits the pattern hypothesized by Mason et al. (2001).

The significance of this correlation, however, is undetermined. Correlation does not equal causation, but some hypothesis can be put forward regarding this trend. If it is assumed there is a real positive link between colder climate and occupation at the Mead Site, what does this imply for the rest of the Tanana River Valley and, expanding in scale, eastern Beringia? Were people moving from the northern portions of Beringia during these times to the Tanana Valley because, even though it was colder than present, it was perhaps warmer than more northerly latitudes? Is this correlation a reflection of some other

variable, such as animal migration, which resulted in the occupations at the site? Or is this relationship simply the result of random migration movement that just happens to correspond with colder climate? The answers to these questions are beyond the scope of this project, but they warrant future investigation.

References

Abbott, M.B., B.P. Finney, and M.E. Edwards
2000 Lake-Level Reconstruction and Paleohydrology of Birch Lake, Central Alaska, Based on Seismic Reflection Profiles and Core Transects. Quaternary Research 53:154-166.

Ager, T.A.
1975 Late Quaternary Environmental History of the Tanana Valley, Alaska. Columbus: Ohio State University Institute for Polar Studies.

Aigner, J.S., R.D. Guthrie, M.L. Guthrie, R.K. Nelson, W.S. Schneider, and R. M. Thorson
1986 Footprints on the Land, the Origins of Interior Alaska's People. *In* Interior Alaska, a Journey through Time. Pp. 97-146: The Alaska Geographic Society.

Alley, R.
2004 Gisp2 Ice Core Temperature and Accumulation Data. Igbp Pages/World Data Center for Paleoclimatology Data Contribution Series #2004–013. N.N.P. Program, ed. Boulder.ftp://ftp.ncdc.noaa.gov/pub/data/paleo/icecore/greenland/summit/gisp2/isotopes/gisp2_temp_accum_alley2000.txt.

Alley, R.
2007 Wally Was Right: Predictive Ability of the North Atlantic "Conveyor Belt" Hypothesis for Abrupt Climate Change. Annual Review of Earth and Planetary Science 35:241-272.

Alley, R.B., and A. M. Agustsdottir
2005 The 8k Event: Cause and Consequences of a Major Holocene Abrupt Climate Change. Quaternary Science Reviews 24:1123-1149.

Amundson, R., and H. Jenny
1991 The Place of Humans in the State Factor Theory of Ecosystems and Their Soils. Soil Science 151:99-109.

Anderson, D.D.
2008 Northern Archaic Tradition Fourty Years Later: Comments. Arctic Anthropology 45(2):169-178.

Anderson, G.S.
1970 Hydrologic Reconnaissance of the Tanana Basin, Central Alaska. U.S. Geologicla Survey Hydrologic Investigations HA-319.

Anderson, L., M.B. Abbott, B.P. Finney, and S.J. Burns
2005 Regional Atmospheric Cirulation Change in the North Pacific During the Holocene Inferred from Lacustrine Carbonate Oxygen Isotopes, Yukon Territory, Canada. Quaternary Research 64:21-35.

Anderson, L.L., F.S. Hu, D.M. Nelson, R.J. Petit, and K.N. Paige
2006 Ice-Age Endurancel: DNA Evidence of a White Spruce Refugium in Alaska. PNAS 103(33):12447-12450.

Anderson, P.M.
1988 Late Quaternary Pollen Reocrds from the Noatal and Kobuk River Drainages, Northwestern Alaska. Quaternary Research 29:263-267.

Anderson, P.M., and L.B. Brubaker
1993 Holocene Vegetation and Climate Histories of Alaska. *In* Global Climates Sin the Last Glacial Maximum. H.E. Wright, J.E. Kutzbach, T. Webb III, W.F. Ruddiman, F.A. Street-Perrott, and P.J. Bartlein, eds. Pp. 386-400. Minneapolis: Univeristy of Minnesota Press.

Anderson, P.M., and L.B. Brubaker
1994 Holocene Vegetation and Climate Histories of Alaska. *In* Global Climates Sin the Last Glacial Maximum. H.E. Wright, J.E. Kutzbach, T. Webb III, W.F. Ruddiman, F.A. Street-Perrott, and P.J. Bartlein, eds. Pp. 386-400. Minneapolis: Univeristy of Minnesota Press.

Anderson, P.M., M.E. Edwards, and L.B. Brubaker
2004 Results and Paleoclimate Implications of 35 Years of Paleoecologicla Research in Alaska. *In* The Quaternary Period in the United States. A.R. Gillespie and S.c. Porter, eds. Pp. 427-440. Amersterdam: Elsevier.

Anderton, J.B.
1999 The Soil-Artifact Context Model: A Geoarchaeological Approach to Paleoshoreline Site Dating in the Upper Peninsula of Michigan, USA. Geoarchaeology 14:265-288.

Andreev, A.A., and D.M. Peteet
1997 An 8100 Year Record of Vegetation Changes from a Site near Fairbanks, Alaska. Program and Abstracts, Beringian Paleoenvironments Workshop, Florissant, CO:16-18.

Balek, C.L.
2002 Buried Artifacts in Stable Upland Sites and the Role of Bioturbation: A Review. Geoarchaeology 17:41-51.

Bar-Yosef, O.
1993 Site Formation Processes from a Levantine Viewpoint. *In* Formation Processes in Archaeological Context. P. Goldberg, D.T. Nash, and M.D. Petraglia, eds. Pp. 11-32. Madison: Monographs in World Archaeology No. 17. Prehistory Press.

Barber, D.C., A.S. Dyke, C. Hillaire-Marcel, A.E. Jennings, J.T. Andrews, M.W. Kerwin, G. Bilodeau, R. McNeely, J.R. Southon, M.D. Morehead, and J.M. Gagnon
1999 Forcing of the Cold Even of 82000 Years Ago by Catastrophic Drainage of Laurentide Lakes. Nature 400:344-348.

Barber, V.A., and B.P. Finney
2000 Late Quaternary Paleoclimatic Reconstructions for Interior Alaska Based on Paleo-Lake Level Data and Hydrologic Models. Journal of Paleolimnology 24:29-41.

Bartlein, P.J., P.M. Anderson, M.E. Edwards, and P.F. McDowell
1991 A Framework for Interpreting Paleoclimatic Varaiations in Eastern Beringia. Quaternary International 10:73-83.

Bartlein, P.J., M.E. Edwards, S. Shafer, and E.D. Barker
1995 Calibration of Radiiocarbon Ages and the Interpretation of Paleoenvironmental Records. Quaternary Research 44:417-424.

Begét, J. E.
1994 Tephrochronology, Lichenometry and Radiocarbon Dating at Gulkana Glacier, Central Alaska Range, USA. The Holocene 4(3):307-313.

Begét, J. E., N. H. Bigelow, and W. R. Powers
1991 Reply to the Comment of C. Waythomas and D. Kaufmann. Quaternary Research 36(3):334-338.

Begét, J. E., and M. J. Keskinen
2003 Trace-Element Geochemistry of Individual Glass Shards of the Old Crow Tephra and the Age of the Delta Glaciation, Central Alaska. Quaternary Research 60(1):63-69.

Beget, J.E.
1996 Tephrochronology and Paleoclimatology of the Late Itnerglacial-Glacial Cycle Recovered in Alaskan Loess Deposits. Quaternary International 34-36:121-126.

Beget, J.E.
2001 Continuous Late Quaternary Proxy Climate Records from Loess in Beringia. Quaternary Science Reviews 20(2001):499-507.

Beget, J.E., and J.A. Addison
2006 Methane Gas Release from the Storegga Submarine Landslide Linked to Early-Holocene Climate Change: A Speculative Hypothesis. The Holocene 17(3):291-295.

Beget, J.E., D.B. Stone, and D.B. Hawkins
1990 Paleoclimatic Forcing of Magnetic Susceptibility Variations in Alaskan Loess During the Late Quaternary. Geology 18:40-43.

Bettis, E.A., D.R. Muhs, H.M. Roberts, and A.G. Wintle
2003 Last Glacial Loess in the Conterminous USA. Quaternary Science Reviews 22:1907-1946.

Bever, M.R.
2001 An Overview of Alaskan Late Pleistocene Archaeology: Historical Themes and Current Perspectives. Journal of World Prehistory 15(2):125-191.

Bever, M.R.
2006 Too Little, Too Late? The Radiocarbon Chronology of Alaska and the Peopling of the New World. American Antiquity 71(4):595-620.

Bidwell, O.W., and F.D. Hole
1965 Man as a Factor of Soil Formation. Soil Science 99:65-72.

Bigelow, N. H.
1997 Late Quaternary Vegetation and Lake Level Changes in Central Alaska (Unpublished Dissertation). Fairbanks: University of Alaska, Fairbanks.

Bigelow, N. H., J. E. Begét, and W. R. Powers
1990a Latest Pleistocene Increase in Wind Intensity Recorded in Eolian Sediments from Central Alaska. Quaternary Research 34(2):160-168.

Bigelow, N. H., and J.E. Beget
1991 Holocene Loess and Paleosols in Central Alaska: A Proxy Reocrd of Holocene Climate Change. *In* International Conference on the Role of the Polar Regions in Global Change. G. Weller, G. Wilson, and B. Severin, eds. Pp. 658-662. Fairbanks: Geophysical Institute.

Bigelow, N. H., J.E. Beget, and W. R. Powers
1990b Latest Pleistocene Increase in Wind Intensity Recorded in Eolian Sediments from Central Alaska. Quaternary Research 34:160-168.

Bigelow, N. H., and M.E. Edwards
2001 A 14,000 Yr Paleoenvironmental Record from Windmill Lake, Central Alaska: Late Glacial and Holocene Vegetation in the Alaska Range. Quaternary Science Reviews 20:203-215.

Bigelow, N. H., and W. R. Powers
2001 Climate, Vegetation, and Archaeology 14,000-9,000 Cal Yr Bp in Central Alaska. Arctic Anthropology 38(2):171-195.

Binford, S.R., and L.R. Binford
1968 New Perspectives in Archaeology. Chicago: Aldine-Atherton.

Birkeland, P.W.
1999 Soils and Geomorphology. Oxford, UL: Oxford University Press.

Blake, G.R., and G.E. Hartge
1986 Bulk Density. *In* Methods of Soil Analysis, Part 1. Physical and Mineralogical Methods, Agronomy Monography No.9, 2nd Ed. A. Klute, ed. Pp. 363-375. Madison: American Society of Agronomy.

Blazejewski, G.A., M.H. Stolt, A.J. Gold, and P.M. Groffman
2005 Macro-and Micromorphology of Subsurface Carbon in Riparian Zone Soils. Soil Science of America Journal 69:1320-1329.

Bocek, B.
1986 Rodent Ecology and Burrowing Behavior: Predicted Effects on Archaeological Site Formation. American Antiquity 51:589-603.

Bowers, R.M., R. Bonnichsen, and D.M. Hoch
1983 Flake Dispersal Experiments: Non-Cultural Transformation of the Archaeological Record. American Antiquity 48:553-572.

Boyle, E. A., and L. Keigwin
1987 North Atlantic Thermohaline Circulation During the Past 20,000 Years Linked to High-Latitude Surface Temperature. Nature 330(6143):35-40.

Brauer, A., G. H. Haug, P. Dulski, D.l M. Sigman, and J. F. W. Negendank
2008 An Abrupt Wind Shift in Western Europe at the Onset of the Younger Dryas Cold Period. Nature Geosci 1(8):520-523.

Broecker, W.S., G.H. Denton, R.L. Edwards, H. Cheng, R. Alley, and A.E. Putman
2010 Putting the Younger Dryas Cold Event into Context. Quaternary Science Reviews 29:1078-1081.

Brubaker, L. B., P. M. Anderson, M. E. Edwards, and A. V. Lozhkin
2005 Beringia as a Glacial Refugium for Boreal Trees and Shrubs: New Perspectives from Mapped Pollen Data. Journal of Biogeography 32(5):833-848.

Brubaker, L.B., H. Garfinkel, and M.E. Edwards
1983 A Late Wisconsin and Holocene Vegetation History from the Central Brooks Range: Implications for Alaskan Paleoecology. Quaternary Research 20:194-214.

Bullock, P., N. Fedoroff, A. Jongerius, G. Stoops, and T. Tursina
1985 Handbook for Soil Thin Section Description. Wolverhampton, UK: Waine Research Publishers.

Buol, S.W., F.D. Hole, R.J. McCrachekn, and R.J. Southard
1997 Soil Genesis and Classification. Ames: Iowa State Univerisyt Press.

Burch, E.S.
1972 The Caribou/ Wild Reindeer as a Human Resource. American Antiquity 37(3):339-368.

Butler, B.E.
1959 Periodic Phenomena in Landscapes as a Basis for Soil Studies. Melbourne: Publication no.14 SCIRO.

Butler, B.E.
1982 A New System for Soil Studies. Journal of Soil Science 33:581-595.

Butler, D.R.
1995 Zoogeomorphology. New York: Cambridge University Press.

Cahen, D., and J. Moeyersons
1977 Subsurface Movements of Stone Artefacts and Their Implications for the Prehistory of Central Africa. Nature 266:812-815.

Calkins, P.E.
1988 Holocene Glaciation in Alaska (and Adjoining Yukon Territory, Canada). Quaternary Science Reviews 7:159-184.

Callum, K.E.
1995 Archaeology in a Region of Spodosols, Part 2. *In* Pedological Perspectives in Archaeological Research. M.E. Collins, B.J. Carter, B.J. Gladfelter, and R.J. Southard, eds. Pp. 81-94. Madison: Special Publication no.44. Soil Science Society of America.

Chadwick, O. A., G. H. Brimhall, and D. M. Hendricks
1990 From a Black to a Gray Box -- a Mass Balance Interpretation of Pedogenesis. Geomorphology 3(3-4):369-390.

Clark, P. U., N. G. Pisias, T. F. Stocker, and A. J. Weaver
2002 The Role of the Thermohaline Circulation in Abrupt Climate Change. Nature 415(6874):863-869.

Clarke, D.L.
1968 Analytical Archaeology. London: Methuen.

Colman, S.M.
1982 Chemical Weathering of Basalts and Andesites: Evidence from Weathering Rinds. *In* United States Geologicla Survey Paper Vol. 1246. Washington.

Cook, J.P.
1969 Early Prehistory of Healy Lake, Alaska: University of Wisconsin.

Cook, J.P.
1975 Archaeology of Interior Alaska. The Western Canadian Journal of Anthropology 3-4:125-133.

Cook, S.F., and R.F. Heizer
1965 Studies in the Chemical Analysis of Archaeological Sites. Volume 2. Berkeley: University of California.

Courty, M.A., P. Goldberg, and R. MacPhail
1989 Soils and Micromorphology in Archaeology. Cambridge: Cambridge University Press.

Crumley, S.
1992 Characterization of Magnetic Minerals in Loess Deposits from Central Alaska: Implicatoins of Paleoclimatology, Department of Geology and Geophysics, University of Alaska Fairbanks.

Davidson, D.A., and M. L. Shackley
1976 Geoarchaeology. Boulder, CO: Westerview Press.

Dearing, J.A
1999 Environmental Magneitic Susceptibility: Using the Bartington Ms2 System: Bartington Instruments Ltd.

Dement, J.A.
1962 The Morphology and Genesis of the Subarctic Brown Forest Soils of Central Alaska. Published Dissertation: Cornell University.

Dilley, T.E.
1998 Late Quaternary Loess Stratigraphy, Soils, and Environments of the Shaw Creek Flats Paleoindian Sites, Tanana Valley, Alaska, University of Arizona, University of Arizona.

Dixon, E.J.
1985 Cultural Chronology of Central Interior Alaska. Arctic Anthropology 22(1):47-66.

Driese, S. G., and J. L. Foreman
1992 Paleopedology and Paleoclimatic Implicatoins of Lateordovician Vertic Paleosols, Juniata Formation Souther Appalachians. Journal of Sedimentary Petrology 62(1):71-83.

Duchaufour, P.
1998 Handbook of Pedology: Soils, Vegetation, Environment. Rotterdam: A.A. Balkema.

Duffield, L. F.
1970 Vertisols and Their Implications for Archaeological Research. American Anthropologist 72:1055-1062.

Dumond, D. E.
1982 Trends and Traditions in Alaskan Prehistory: The Place of Norton Culture. Arctic Anthropology 19(2):39-51.

Dumond, D. E., W. Henn, and R. Stuckenrath
1976 Archaeology and Prehistory on the Alaska Peninsula. Anthropological Papers of the University of Alaska 18(1):17-28.

Edwards, M. E., and E. D. Barker
1994 Cimate and Vegetation in Northern Alaska 18,000 Yrs. Palaeogeography, Palaeoclimatoloyg, Palaeoecology 109:127-135.

Edwards, M. E., L. B. Brubaker, A. V. Lozhkin, and P. M. Anderson
2005 Structurally Novel Biomes: A Response to Past Warming in Beringia. Ecology 86(7):1696-1703.

Edwards, M. E., C. J. Mock, Finney B. P., V. A. Barber, and R. J. Bartlein
2001 Potentail Analogues for Paleoclimatic Variations in Eastern Interior Alaska During the Past 14,000yr: Atmospheric-Circulation Controls of Regional Temperature and Moisture Responses. Quaternay Science Reviews 20:189-202.

Edwards, M.E., P.M. Anderson, L.B. Brubaker, T.A. Ager, A.A. Andreev, N. H. Bigelow, L.C. Cwynar, W.R. Eisner, S.P. Harrison, F.S. Hu, D. Jolly, A.V. Lozhkin, G.M. MacDonald, C.J. Mock, J.C. Ritchie, A.V. Sher, R.W. Spear, J.W. Williams, and G. Yu
2000 Pollen-Based Biomes for Beringia 18,000, 6000, and 0 14c Yr Bp. Journal of Biogeography 27:521-554.

Ehlers, J., and P. L. Gibbard, eds.
2004 Quaternary Glaciations: Extent and Chronology. Part Ii, North America. Amersterdam: Elsevier.

Eidt, R. C.
1977 Detection and Examination of Anthrosols by Phosphate Analysis. Science 197(4311):1327-1333.

Eidt, R.C.
1985 Theoretical and Practical Considerations in the Analysis of Anthrosols. New Haven: Yale University Press.

Ellwood, B. B., K. M. Petruso, F. B. Harrold, and M. Korkuti
1996 Paleoclimate Characterization and Intra-Site Correlation Using Magneitic Susceptibility Measurements: An Example Form Konispol Cave, Albania. Journal of Field Archaeology 23:263-271.

Erlandson, J. M.
1984 A Case Study in Faunalturbation: Delineating the Effects of the Burrowing Pocket Gopher on the Distrubution of Archaeological Materials. American Antiquity 49(4):785-790.

Esdale, J. A.
2008 A Current Synthesis of the Northern Archaic. Arctic Anthropology 45(2):3-38.

Evans, M. E., and F Heller
2003 Environmental Magnetism: Principles and Applications of Environmagnetics. Amsterdam: Academic Press.

Feakes, C. R., and G. J. Retallack
1988 Recognition and Chemical Characterization of Fossil Soils Developed on Alluvium: A Lake Ordovician Example. *In* Paleosols and Weathering through Geological Time. J. Reinhardt and W.R. Siglei, eds. Pp. 35-48. Boulder, CO: Geological Society of American, Special Paper no. 216.

Fernald, A. T.
1965 Recent History of the Upper Tanana River Lowlands, Alaska. US Geological Survey Professional Paper 524-C.

Ferrians, O. J.
1965 Permafrost Map of Alaska: U.S. Geolgoical Survey Miscellaneous Investigations Map I-445, Scale 1:2,500,000.

Finney, B. P., K. Ruhland, J. P. Smol, and M. A. Fallu
2004 Paleolimnology of the North American Subarctic. *In* Long-Term Environmental Change in Arctic and Antarctic Lakes. M.S. Pienitz and J.P. Smol, eds. Pp. 269-317. Dordrecht: Springer.

Fitzpatrick, E. A.
1993 Soil Microscopy and Micromorphology. Chichester, UK: John Wiley & Sons.

Franklin, U. M., R. M. Gotthardt, and B. Yorga
1981 An Examination of Prehistoric Copper Technology and Copper Sources in Western Arctic and Subarctic North America. Volume No. 101. Ottawa: National Museums of Canada.

French, C. A.
2003 Geoarchaeology in Actions: Studies in Soil Micromorphology and Landscape Evolution. London: Routledge.

Gifford-Gonzalez, D. P., D. B. Damrosch, D. R. Damrosch, J. Pryor, and R. L. Thunen
1985 The Third Dimension in Site Structure: An Experiment in Trampling and Vertical Dispersal. American Antiquity 50(4):803-818.

Goebel, T., W. R. Powers, and N. H. Bigelow
1991 The Nenana Complex of Alaska and Clovis Origins. *In* Clovis: Origins and Adaptations. R. Bonnichsen and K.L. Turnmire, eds. Pp. 49-79. Corvallis: Center for the Study of the First Americans, Oregon State University.

Goldberg, P.
2000 Micromorphology and Site Formation at Die Kelders Cave I, South Africa. Journal of Human Evolution 38:43-90.

Goldberg, P., and F. Berna
2010 Micromorphology and Context. Quaternary International 214:56-62.

Goldberg, P., V. T. Holliday, and C. R. Ferring
2001 Earth Sciences and Archaeology. New York: Kluwer Academic/ Plenum Publishers.

Goldberg, P., and R. I. MacPhail
2006 Practical and Theoretical Geoarchaeology. Malden, MA: Blackwell Publishing.

Grave, P., and L. Kealhofer
1999 Assessing Bioturbation in Archaeological Sediments Using Soil Morphology and Phytolith Analysis. Journal of Archaeological Science 26:1239-1248.

Griffin, K. P., and E. R. Chesmore
1988 An Overview and Assessment of Prehistoric Archaeological Resources, Yukon-Charley Rivers National Preserve, Alaska. U.S. Department of the Interior, National Park Service.

Guthrie, M. L.
2001 Origin and Causes of the Mammoth Steppe: A Story of Cloud Cover, Woolly Mammal Tooth Pits, Buckles, and inside-out Beringia. Quaternary Science Reviews 20:549-574.

Guthrie, R. D.
1990 Frozen Fauna of the Mammoth Steppe: The Story of Blue Babe. Chicago: University of Chicago Press.

Halle, J., D. G. Froese, R. D. MacPhee, R. G. Roberts, L. J. Arnold, A. V. Reyes, M. Rasmussen, R. Nielson, B. W. Brook, S. Robinson, M. Demuro, M. T. Gilbert, K. Munch, J. J. Austin, A. Coopers, I. Barnes, R. Moller, and E. Willerslev
2009 Ancient DNA Reveals Late Survival of Mammoth and Horse in Interior Alaska. PNAS 106(52):22352-11357.

Hamer, J. M. M., N. D. Sheldon, G. J. Nichols, and M. E. Collinson
2007 Late Oligocene-Early Miocene Paleosols of Distal Fluvial Systems, Ebro Basin, Spain. Palaeogeography, Palaeoclimatology, Palaeoecology 247(3-4):220-235.

Hamilton, T. D., and T. Goebel
1999 Late Pleistocene Peopling of Alaska. *In* Ice Age People of North America Environments, Origins, and Adaptations. R. Bonnichsen and K.L. Turnmire, eds. Pp. 104-155. Corvallis: Oregon State University Press.

Heller, F., C. D. Shen, J. Beer, X. M. Liu, T. S. Liu, A. Bronger, M. Suter, and G. Bonani
1993 Quantitative Estimates of Pedogenic Ferromagnetic Mineral Formation in Chinese Loess and Palaeoclimatic Implications. Earth and Planetary Science Letters 114(2-3):385-390.

Herz, N., and E. G. Garrison
1998 Geological Methods for Archaeology. Oxford: Oxford University Press.

Hilton, M. R.
2002 Evaluating Site Formation Processes at a Higher Resolution: An Archaeological Case Study in Alaska Using Micromorphology and Experimental Techniques. Dissertation, University of California, Los Angeles. Los Angeles: ProQuest.

Hilton, M. R.
2003 Quantifying Postdepositional Redistrubution of the Archaeological Record Produced by Freeze-Thaw and Other Mechanisms: An Experimental Approach. Journal of Archaeological Method and Theory 10(3):165-202.

Hoek, W. Z., and J. A. Bos
2007 Early Holocene Climate Oscillations--Causes and Consequences. Quaternary Science Reviews 26:1901-1906.

Hoffecker, J. F.
2001 Late Pleistocene and Early Holocene Sites in the Nenana River Valley, Central Alaska. Arctic Anthropology 38(2):139-153.

Hoffecker, J. F., W. R. Powers, and T. Goebel
1993 The Colonization of Beringia and the Peopling of the New World. Science 259(5091):46-53.

Hoffecker, J. H., and S. A. Elias
2007 Human Ecology of Beringia. New York: Columbia Univeristy Press.

Hofman, J. L.
1986 Veritcal Movement of Artifacts in Alluvial and Stratified Deposits. Current Anthropology 27:163-171.

Hole, F. D.
1981 Effects of Animals on Soil. Geoderma 25:75-112.

Holliday, V. T.
2004 Soils in Archaeological Research. Oxford: University Press.

Holliday, V. T., and W. G. Gartner
2007 Methods of Soil P Analysis in Archaeology. Journal of Archaeological Science 34:301-333.

Holmes, A.
1927 Petrographic Methods and Calculations. London, Uk: Murby.

Holmes, C. E.
1986 Lake Minchumina Prehistory: An Archaeological Analysis. *In* Alaska Anthropological Association Monograph Series #2. Fairbanks: Rasuson Library.

Holmes, C. E.
1995 An Assessment of Radiocarbon Data Pertaining to Tanana Valley Archaeology. Poster presented at the 15th Annual meeing of the Alaska Anthropological Association, Anchorage.

Holmes, C. E.
1996 Broken Mammoth. *In* American Beginnings. F.H. West, ed. Chicago: University of Chicago Press.

Holmes, C. E.
2001 Tanana River Valley Archaeology Circa 14,000 to 9,000 B.P. Arctic Anthropology 38(2):154-170.

Holmes, C. E.
2008 The Taiga Period: Holocene Archaeology of the Northern Boreal Forest, Alaska. Alaska Journal of Anthropology 6(1&2):69-81.

Holmes, C. E., R. VanderHoek, and T. E. Dilley
1996 Swan Point. *In* American Beginnings. F.H. West, ed. Chicago: University of Chicago Press.

Holmes, C. E., and D. R. Yesner
1992 Investigating the Earliest Alaskans: The Broken Mammoth Archaeological Project. Arctic Research of the United States 6:6-9.

Homsey, L. K., and R. C. Capo
2006 Integrating Geochemistry and Micromorphology to Interpret Feature Use at Dust Cave, a Paleo-Indian through Middle-Archaic Site in Northwest Alabama. Geoarchaeology 21(3):237-269.

Hopkins, D. M.
1982 Aspects of the Paleogeography of Beringia During the Late Pleistocene. *In* Paleoecology of Beringia. D.M. Hopkins, J.V. Mattews Jr., C.E. Schweger, and S.B. Young, eds. Pp. 3-28. New York: Academic Press.

Hopkins, D. M., and J. L. Giddings
1953 Geological Background of the Iyatayet Archaeological Site, Cape Denbigh, Alaska. Washington D.C.: Smithsonian Miscellaneous Collections no.121. Smithsonian Institution.

Hu, F. S., L. B. Brubaker, D. G. Gavin, P. E. Higuera, J. A. Lynch, T. S. Rupp, and W. Tinner
2006 How Climate and Vegetation Influence the Fire Regime of the Alaskan Boreal Biome: The Holocene Perspective. Mitigation and Adaptation Strategies for Global Change 11(829-846).

Hu, F. S., E. Ito, L. B. Brubaker, and P. M. Anderson
1996 Ostracod Geochemical Record of Holocene Climatic Change and Implications for Vegetational Response in the Northwestern Alaska Range.

J., William C., and S. R. Bozarth
2008 Geoarchaeology and Environmental Reconstruction at Xmh-874 D.o.P. Works.

Jenny, H.
1941 Factors of Soil Formation. New York: McGraw-Hill.

Jenny, H.
1980 The Soil Resource. New York: Springer.

Johnson, D. L.
1990 Biomantle Evolution and the Redistrubution of Earth Materials and Artifacts. Soil Science 149:84-102.

Johnson, D. L., and K. L. Hansen
1974 The Effect of Frost-Heaving on Objects in Soils. Plains Anthropologist 19:81-98.

Johnson, D. L., and D. Watson-Stegner
1990 The Soil-Evolution Model as a Framework for Evaluating Pedoturbation in Archaeological Site Formation. *In* Archaeological Geology of North America. N.P. Lasca and J. Donahue, eds. Pp. 541-560. Boulder: Centenial Volume no.4. Geological Society of America.

Kahmann, J. A., and S. G. Driese
2008 Paleopedology and Geochemistry of Late Mississippian (Chesterian) Pennington Formation Paleosols at Pound Gap, Kentucky, USA: Implications for High-Frequency Climate Variations. Palaeogeography, Palaeoclimatology, Palaeoecology 259:357-381.

Kaufman, D. S., T. A. Ager, N. J. Anderson, P. M. Anderson, J. T. Andrews, R. J. Bartlein, L. B. Brubaker, L. L. Coats, L. C. Cwynar, M. L. Duvall, A. S. Dyke, M. E. Edwards, W. R. Eisner, K. Gajewski, A. Geirsdottir, F. S. Hu, A. E. Jennings, M. R. Kaplan, M. W. Kerwin, A.V. Lozhkin, G. M. MacDonald, G. H. Miller, C.J. Mock, W. W. Oswald, B. L. Otto-Bliesner, D. F. Porinchu, K. Ruhland, J. P. Smol, E. J. Steig, and B. B. Wolfe
2004 Holocene Thermal Maximum in the Western Arctic (0-180w). Quaternary Science Reviews 23:529-560.

Kelly, R. L., D. A. Byers, W. Echerle, P. Goldberg, C. V. Haynes, R. M. Larsen, J. Laughlin, J. I. Mead, and S. Wall
2006 Multiple Approaches to Formation Processes: The Pine Spring Site, Southwest Wyoming. Geoarchaeology 21(6):615-638.

Kokorowski, H.D., P.M. Anderson, C.J. Mock, and A.V. Lozhkin
2008 A Re-Evaluation and Spatial Analysis of Evindece for a Younger Dryas Climatic Reversal in Beringia. Quaternary Science Reviews 27(17-18):1710-1722.

Kukla, G., F Heller, L.X. Ming, X.T. Chun, L.T. Sheng, and A.Z. Sheng
1988 Pleistocene Climates in China Dated by Magnetic Susceptibility. Geology 16:811-814.

Kutzbach, J., R. Gallimore, S. Harrison, P. Behling, R. Selin, and F. Laarif
1998 Climate and Biome Simulations for the Past 21,000 Years. Quaternary Science Reviews 17(6-7):473-506.

Lagroix, F., and S.K. Banerjee
2002 Paleowind Directions from the Magnetic Fabric of Loess Profiles in Central Alaska. Earth and Planetary Science Letters 195:99-112.

Lagroix, F., and S.K. Banerjee
2006a Discussion of "Geochemical Evidence for the Origin of Late Quaternary Loess in Central Alaska. Canadian Journal of Earth Science 43(3):323-337.

Lagroix, F., and S.K. Banerjee
2006b The Regional and Temporal Significance of Primary Aeolian Magnetic Fabrics Preserved in Alaskan Loess. Earth and Planetary Science Letters 225:379-395.

Leehan, D.K.
1981 A Sedimentological Analysis of Three Archaeological Sites in the Delta Junction Area, Alaska, Anthropology, Washington State University.

Leigh, D.S.
1998 Evaluating Artifact Burial by Eolian Versus Bioturbation Processes, South Carolina Sandhills, USA. Geoarchaeology 13:309-330.

Leigh, D.S.
2001 Buried Artifacts in Sandy Soils: Techniques for Evaluating Pedoturbation Versus Sedimentation. *In* Earth Sciences and Archaeology. P. Goldberg, V.T. Holliday, and C.R. Ferring, eds. New York: Kluwer Academic/Plenum Publishers.

Limbrey, S.
1975 Soil Science in Archaeology. London: Academic Press.

Lippi, R.D.
1988 Paleotopography and Phosphate Analysis of a Buried Jungle Site in Ecuador. Journal of Field Archaeology 15:85-97.

Livingstone, D. A.
1955 Some Pollen Profiles from Arctic Alaska. Ecology 36(4):587-600.

Mackay, J.R., W.H. Mathews, and R.S. MacNeish
1961 Geology of the Engigstciak Archaeological Site, Yukon Territory. Arctic 14:25-52.

MacNeish, R.S.
1964 Investigations in Southwest Yukon: Archaeological Excavation, Comparisons, and Speculations. Papers of the Robert S. Peabody Foundation for Archaeology 6(2):201-488.

MacPhail, R.I., and P. Goldberg
1990 The Micromorphology of Tree Subsoil Hollows: Their Significance to Soil Science and Archaeology. *In* Soil Micromorphology: A Basic and Applied Science. L.A. Douglas, ed. New York: Elsevier Science Publisihing Company Inc.

Mangerud, J. A. N., S. Gulliksen, and E. Larsen
2010 14c-Dated Fluctuations of the Western Flank of the Scandinavian Ice Sheet 45–25 kyr Bp Compared with Bølling–Younger Dryas Fluctuations and Dansgaard–Oeschger Events in Greenland. Boreas 39(2):328-342.

Mann, D.H., D.M. Peteet, R.E. Reanier, and M.L. Kunz
2002 Responses of an Arctic Landscape to Late Glaical and Early Holocene Climatic Changes: The Importance of Moisture. Quaternary Science Reviews 21:997-1021.

Mann, D.H., R.E. Reanier, D.M. Peteet, M.L. Kunz, and M. Johnson
2001 Environmental Change and Arctic Paleoindians. Arctic Anthropology 38(2):119-138.

Manzanilla, L., and L. Barba
1990 The Study of Activites in Classic Households: Two Case Studies from Coba and Teotihuacan. Anchient Mesoamerica 1:41-49.

Mason, O. K., and J.E. Beget
1991 Late Holocene Flood History of the Tanana River, Alaska, U.S.A. Arctic and Alpine Research 23(4):392-403.

Mason, O. K., and N. H. Bigelow
2008 The Crucible of Early to Mid-Holocene Climate in Northern Alaska: Does Northern Archaic Represent the People of the Spreading Forest? Arctic Anthropology 45(2):39-70.

Mason, O. K., P. M. Bowers, and D.M. Hopkins
2001 The Early Holocene Milankovitch Thermal Maximum and Humans: Adverse Conditions for the Denali Complex of Eastern Beringia. Quaternary Science Reviews 20:525-548.

Matmon, A, J.P. Briner, G. Carver, P. Bierman, and Finkel
2010 Moraine Chronosequence of the Donnelly Dome Region, Alaska. Quaternary Research 74(1):63-72.

Matthews, W., C. A. I. French, T. Lawrence, D. F. Cutler, and M. K. Jones
1997 Microstratigraphic Traces of Site Formation Processes and Human Activities. World Archaeology 29(2):281-308.

Mayewski, P.A., E.E. Rohling, J.C. Stager, W. Karlen, K.A. Maasch, L.D. Meeker, E.A. Meyerson, F. Gasse, S. V. Kreveld, K Holmgren, J. Lee-Thorp, G. Rosqvist, F. Rack, M. Staubwasser, R.R. Schneider, and E.J. Steig
2004 Holocene Climate Variability. Quaternary Research 62:243-255.

McBrearty, S.
1990 Consider the Humble Termite: Termites as Agents of Post-Depositional Disturbance at African Archaoelogical Sites. Journal of Archaeological Science 17:111-143.

McCarthy, P.J.
2002 Micromorphology and Development of Interfluve Paleosols: A Case Study from the Cenomanian Dunvegan Formation, Ne British Columbia, Canada. Bulletin of Canadian Petroleum Geology 50(1):158-177.

McCarthy, P.J., U.B. Faccini, and A.G. Plint
1999 Evolution of an Ancient Coastal Plain: Paleosols, Interfluves and Alluvial Architecture in a Sequence Stratigraphic Framework, Cenomanin Dunvegan Formation, Ne British Columbia, Canada. Sedimentology 46:861-891.

McCarthy, P.J., and A.G. Plint
2003 Spatial Variability of Paleosols across Cretaceous Interfluves in the Dunvegan Formation, Ne British Columbia, Canada: Paleohydrology, Paleogeomorphological and Stratigraphic Implications. Sedimentology 50:1187-1220.

MCCulloch, D., and D.M. Hopkins
1966 Evidence for an Early Recent Warm Interval in Northwestern Alaska. Geological Society of America 77:1089-1108.

McKennan, R.A., and J.P. Cook
1968 Prehistory of Healy Lake, Alaska. 8th International Congress of Anthropological and Ethnological Sciences Proceedings 3:182-184.

Mello Araujo, A.G., and J.C. Marcelino
2003 The Role of Armadillos in the Movement of Archaeological Materials: An Experimental Approach. Geoarchaeology 18:433-460.

Mercader, J.R., J.L. Marti, and A. Brooks
2002 The Nature of "Stone-Lines" in the African Quaternary Record: Archaeological Resolution at the Rainforest Site of Mosumu, Equitorial Guinea. Quaternary International 89:71-96.

Michie, J.
1990 Bioturbation and Gravity as a Potential Site Formation Process: The Open Area Site, 38ge261, Georgetown County, South Carolina. South Carolina Antiquities 22:27-46.

Middleton, J.J., and T.D. Price
1996 Identification of Activity Areas by Multi-Element Characterizaton of Sediments from Modern and Archaeological House Floors Using Inductively Coupled Plasma-Atomic Emmission Spectroscopy. Journal of Archaeological Science 23:673-687.

Mitchell, P.B.
1988 The Influences of Begetation, Animals, and Micro-Organisms on Soil Processes. *In* Biogeomorphology. H.A. Viles, ed. Pp. 43-82. New York: Blackwell.

Mobley, C.M.
1996 Campus Site. *In* American Beginnings. F.H. West, ed. Pp. 296-302. Chicago: University of Chicago Press.

Morris, M.W., J.T. Ammons, and P Santas
1997 Evidence for Subsurface Translocation of Ceramic Artifacts in a Vertisol in Eastern Crete, Greece. *In* Proceedings of the Second International Conference on Pedo-Archaeology. A.C. Goodyear, J.E. Foss, and K.E. Sassaman, eds. Pp. 41-51. Columbia: Occasional Papers fo the South Carolina Institite of Archaeology and Anthropology. Univeristy of South Carolina.

Morrison, D.A.
1987 The Middle Prehistoric Period and the Archaic Concept in the Mackenzie Valley. Canadian Journal of Archaeology 11(49-74).

Muhs, D.R., T.A. Ager, J.M. Been, J. Rosenbaum, and R. Reynolds
2000 An Evalutation of Methods for Identifying and Interpreting Paleosols in Late Quaternary Loess in Alaska: U.S. Geological Survey Professional Paper. 1615:127-146.

Muhs, D.R., T.A. Ager, and J.E. Beget
2001 Vegetation and Paleoclimate of the Last Interglacial Period, Central Alaska. Quaternary Science Reviews 20:41-61.

Muhs, D.R., T.A. Ager, E.A. Bettis, J.P. McGeehin, J.M. Been, J.E. Beget, M.J. Pavich, T.W. Stafford, and D.A. Stevens
2003 Stratigraphy and Palaeoclimatic Significance of Late Quaternary Loess-Paleosol Sequences of the Last Interglacial-Glacial Cycle in Central Alaska. Quaternary Science Reviews 22:1947-1986.

Muhs, D.R., T.A. Ager, G. Skipp, J. Beann, J.R. Budahn, and J.P. McGeehin
2008 Paleoclimatic Significance of Chemical Weathering in Loess-Derived Paleosols of Subarctic Central Alaska Arctic, Antarctic, and Alpine Research 40(2):396-411.

Muhs, D.R., T.A. Ager, T.W. Stafford, M.J. Pavich, J.E. Beget, and J.P. McGeehin
1997 The Last Interglacial-Glacial Cycle in Late Quaternary Loess, Central Interior Alaska. Program and Abstracts, Beringian Paleoenvironments Workshop, Florissant, CO:109-112.

Muhs, D.R., and E.A. Bettis
2003 Quaternary Loess-Paleosol Sequences as Examples of Climate-Driven Sedimentary Extremes. Geological Society of America Special Paper 370:53-74.

Muhs, D.R., and J.R. Budahn
2006 Geochemical Evidence for the Origin of Late Quaternary Loess in Central Alaska. Canadian Journal of Earth Science 43:323-337.

Muhs, D.R., J.P. McGeehin, J. Beann, and E. Fisher
2004 Holocene Loess Deposition and Soil Formation as Competing Processes, Matanuska Valley, Southern Alaska. Quaternary Research 61:265-276.

Murphy, C.P.
1986 Thin Section Preparation of Soils and Sediments. Berkhamsted: A B Academic Publishers.

Nash, D.T., and M.D. Petraglia
1987 Natural Formation Processes and the Archaeological Recorc. London: BAR International Series 32.

National Climate Data Center
2011 Local Climatology Data- Big Delta, Alaska: National Oceanic and Atmospheric Administration

Nelson, R.E., and L.D. Carter
1987 Paleoenivronmental Anaylsis of Insects and Extralimital *Populus* from an Early Holocene Site on the Arctic Slope of Alaska. Arctic and Alpine Research 19:230-241.

Nesbitt, H.W., and G.M. Young
1982 Early Proterozoic Climates and Plate Motions Inferred from Major Element Chemistry of Lutites. Nature 299:715-717.

O'Brien, S.R., P.A. Mayewski, L.D. Meeker, D.A. Meese, M.S. Twickler, and S.I. Whitlow
1995 Complexity of Holocene Climate as Reconstructed from a Greenland Ice Core. Science 270:1962-1964.

Parnell, J.J., R.E. Terry, and C. Golden
2001 Using in-Field Phosphate Testing to Rapidly Identify Middens at Piedrass Negras, Guatemala. Geoarchaeology 16:855-873.

Pearson, G. A.
1999 Early Occupations and Cultural Sequence at Moose Creek: A Late Pleistocene Site in Central Alaska. Arctic 53(4):332-345.

Peters, C., and R Thompson
1999 Supermagnetic Enhancement, Superparamagnetism, and Archaeological Soils. Geoarchaeology 14(5):401-413.

Pewe, T.L.
1965 Middle Tanana River Valley. *In* Guidebook for Field Conference F, Central and Southcentral Alaska, International Association for Quaternary Research: 7th Congress. T.L. Pewe, O.J. Ferrians, T.N.V. Karlstrom, and D.R. Nichols, eds. Pp. 36-54. Lincoln: Nebraska Academy of Science, (reprinted 1977, College, Alaska Division of Geological and Geophysical Surveys).

Pewe, T.L.
1975 Quaternary Geology in Alaska.

Pewe, T.L., and G.A. Holmes
1964 Geology of the Mt. Hayes D-4 Quadrange, Alaska: United States Geological survey, Miscellaneous Geological Investigations, Map 1-394

Pewe, T.L., and R.D. Reger
1983 Guidebook to Permafrost and Quaternary Geology Along the Richardson and Glenn Highways between Fairbanks and Anchorage, Alaska, Guidebook 1, Fourth International Permafrost Conference. Fairbanks: Alaska Division of Geology and Geophysical Surveys.

Phippen, P.G.
1988 Archaeology at Owl Ridge: A Pleistocene-Holocene Boundary Age Site in Central Alsaka (Ma Thesis). Fairbanks: University of Alaska, Fairbanks.

Pierce, C.
1992 Effects of Pocket Gopher Burrowing on Archaeological Deposits: A Simulation Approach. Geoarchaeology 7:185-208.

Porter, L.
1988 Late Pleistocene Fauna of Lost Chicken Creek, Alaska. Arctic 41(4):300-313.

Potter, B. A.
2000 Recent Investigations at the Gerstle River Site, a Multicomponent Site in Central Alaska. Current Research in the Pleistocene 18:52-54.

Potter, B. A.
2005 Site Sturcture and Organization in Central Alaska: Archaeological Investigations at Gerstle River [Phd Dissertation]. Fairbanks: University of Alaska Fairbanks.

Potter, B. A.
2008a Exploratory Models of Intersite Variability in Mid to Late Holocene Central Alaska. Arctic 61(4):407-425.

Potter, B. A.
2008b A First Approximation of Interassemblage Variability in Central Alaska. Arctic Anthropology.

Potter, B. A.
2008c Late Pleistocene and Early Holocene Assemblage Variability in Central Alaska.

Potter, B. A.
2008d Radiocarbon Chronology of Central Alaska: Technological Continiuty and Economic Change. Radiocarbon 50(2):181-204.

Potter, B. A., P. M. Bowers, J. D Reuther, and K O. Mason
2007 Holocene Assemblage Variability in the Tanana Basin:Nlur Archaeological Research, 1994–2004. Alaska Journal of Anthropology 5(1).

Potter, B. A., J. D. Irish, J. D. Reuther, C. Gelvin-Reymiller, and V. T. Holliday
2011 A Terminal Pleistocene Child Cremation and Residential Structure from Eastern Beringia. Science 331(6020):1058-1062.

Potter, B. A., J. D. Reuther, P. M. Bowers, and C. Gelvin-Reymiller
2008 Little Delta Dune Site: A Late- Pleistocene Multicomponent Site in Central Alaska. Current Research in the Pleistocene 25:132-135.

Potter, B.A., P.J. Gilbert, C.E. Holmes, and B. Crass
2010 The Mead Site, a Late Pleistocene-Holocene Stratified Site in Central Alaska: Preliminary Results from the 2009 Excavation. *In* 37th Annual Meeting of the Alaska Anthropological Association. Anchorage.

Powers, W. R., and J. F. Hoffecker
1989 Late Pleistocene Settlement in the Nenana Valley, Central Alaska. American Antiquity 54(2):263-287.

Prasad, S., A. Brauer, B. Rein, and J.F. Negendank
2006 Rapic Climate Change During the Early Holocene in Western Europe and Greenland. The Holocene 16(2):153-158.

Pye, K.
1987 Aeolian Dust and Dust Deposits. London: Academic Press.

Qiao, Y., Z. Zhao, Y. Wang, Fu. J., S. Wang, and F. Jiang
2009 Variations of Geochemical Compositions and the Paleo-Climatic Significance of a Loess-Soil Sequence from Garze County of Western Sichuan Province, China. Chineses Science Bulletin 54:4697-4703.

Rapp, G., and C.L. Hill
2006 Geoarchaeology: The Earth-Science Approach to Archaeological Interpretation. New Haven: Yale University Press.

Rasmussen, S.O., B.M. Vinther, H.B. Clausen, and K.K. Anderson
2007 Early Holocene Climat Oscillations Recorded in Three Greenland Ice Cores. Quaternary Science Reviews 26:1907-1914.

Rawling, J.E.
2000 A Review of Lamellae. Geomorphology 35:1-9.

Reger, R.D., and T.L. Pewe
1969 Lichenometric Dating in the Central Alaska Range. Montreal: McGill-Queens University Press.

Reger, R.D., A.G. Sturmann, and J.E. Beget

1993 Dating Holocene Moraines of Balck Rapids Glacier, Delta River Valley, Central Alaska Range. Short Notes on Alaskan Geology, Prof. Report 113:41-50.

Reid, K.C.
1984 Fire and Ice: New Evidence for the Production and Preservation of Late Archaic Fiber-Tempered Pottery in the Middle-Latitude Lowlands. American Antiquity 49:55-76.

Renfrew, C.
1976 Archaeology and Earth Sciences. *In* Geoarchaeology: Earth Science and the Past. D.A. Davidson and M.L. Shackley, eds. Boulder, CO: Westview Press.

Retallack, G.J.
1988 Field Recognition of Paleosols. *In* Paleosols and Weathering through Geological Time: Principles and Applications. J. Geinhardt, ed. Pp. 1-20: Geological Society of America Special Papers 216.

Retallack, G.J.
1990 Soils of the Past: An Introduction to Paleopedology. New York: Unwin and Hyman.

Retallack, G.J.
1991 Untangling the Effects of Burial Alteration and Ancient Soil Formation. Annual Review of Earth and Planetary Science 19:183-206.

Retallack, G.J.
2001 Soils of the Past, an Introduction to Paleopedology. Ames, IA: Blackwell Science.

Rick, J.W.
1976 Downslope Movement and Archaeological Intrasite Spatial Analysis. American Antiquity 41(2):133-144.

Rieger, S.
1983 The Genesis and Classification of Cold Soils. New York: Academic Press.

Ritchie, J.C., and L.C. Cwynar
1982 The Late Quaternary Vegetation of the Northern Yukon. *In* Paleoecology of Beringia. D.M. Hopkins, J.V. Matthews, C.E. Schweger, and S.B. Young, eds. Pp. 113-126. New York: Academic Press.

Ruhland, K., J.M. St. Jacques, B.D. Beierle, S.F. Lamoureux, A.S. Dyke, and J.P. Smol
2009 Lateglacial and Holocene Paleoenbironmental Changes Recorded in Lake Sediments, Brock Plateau (Melville Hills), Northwest Territories, Canada. The Holocene 19(7):1005-1016.

Runge, E.C., T.W. Walker, and D.T. Howarth
1974 A Study of Late Pleistocene Loess Deposits, South Canterbury, New Zealand. Part I. Forms and Amounts of Phosphorus Compared with Other Techniques for Identifying Paleosols. Quaternary Research 4:76-84.

Ruxton, B.P.
1968 Measures of the Degree of Chemical Weathering of Rocks. The Journal of Geology 76(5):518-527.

Sanchez, A., and M.L. Canabata

1999 Identification of Activity Areas by Soil Phosphorus and Organic Matter Analysis in Two Rooms of the Iberian Sanctuary "Cerro El Pajarillo". Geoarchaeology 14:47-62.

Schaetzl, R., and S. Anderson
2005 Soils: Genesis and Geomorphology. Cambridge: Cambridge University Press.

Schiegl, S., P. Goldberg, H.U. Pfretzschner, and N.J. Conard
2003 Paleolithic Burnt Bone Horizons from the Swabian Jura: Distinguishing between *in Situ* Fireplaces and Dumping Areas. Geoarchaeology 18(5):541-565.

Schiffer, M. B.
1972 Archaeological Context and Systemic Context. American Antiquity 37:156-165.

Schiffer, M. B.
1983 Toward the Identification of Formation Processes. American Antiquity 48(4):675-706.

Schiffer, M. B.
1987 Formation Processes of the Archaeological Record. Albuquerque: University of New Mexico Press.

Schuldenrein, J.
1995 Geochemistry, Phosphate Fractionation, and the Detection of Activity Areas at Prehistoric North American Sites. *In* Pedological Perspectives in Archaeological Research. Soil Science Society of America Special Publication 44. M.E. Collins, B.J. Carter, B.J. Gladfelter, and R.J. Southard, eds. Pp. 107-132. Madison, WI: American Society of Agronomy.

Schweger, C.
1985 Geoarchaeology of Northern Regions: Lessons from Cryoturbation at Onion Portage, Alaska. *In* Archaeological Sediments in Context. J.K. Stein and W.R. Farrand, eds. Pp. 127-141. Orono: University of Maine.

Sharpe, J.L.
1996 Environmental Archaeology in Central Alaska: A Magneto-Stratigraphic Correlation of Tanana Valley Arcaheological Sites with Global Climatic Change. MA Thesis: University of Minnesota.

Sheldon, N. D.
2005 Do Red Beds Indicate Paleoclimatic Conditions?: A Permian Case Study. Palaeogeography, Palaeoclimatology, Palaeoecology 228(3-4):305-319.

Sheldon, N. D.
2006 Abrupt Chemical Weathering Increase across the Permian-Triassic Boundary. Palaeogeography, Palaeoclimatology, Palaeoecology 231(3-4):315-321.

Sheldon, N. D., and N. J. Tabor
2009 Quantitative Paleoenvironmental and Paleoclimatic Reconstruction Using Paleosols. Earth-Science Reviews 95(1-2):1-52.

Sheldon, N.D., G.J. Retallack, and S. Tanaka
2002 Geochemical Climofunctions from North American Soils and Application to Paleosols across the Eocene-Oligocene Boundary in Oregon. The Journal of Geology 110:687-696.

Shimer, G.
2009 Holocene Vegetation and Climate Change at Canyon Lake, Copper River Basin, Alaska. MA Thesis.

Simonson, R.W.
1959 Outline of a Generalized Theory of Soil Genesis. Soil Science Society of America Proceedings 23:152-156.

Simonson, R.W.
1978 Multiple Process Model of Soil Genesis. *In* Quaternary Soils. R.W. Mahaney, ed. Norwich: Geo Abstracts.

Steffensen, J. P., K. K. Andersen, M. Bigler, H. B. Clausen, D. Dahl-Jensen, H. Fischer, K. Goto-Azuma, M. Hansson, S. J. Johnsen, J. Jouzel, V. Masson-Delmotte, T. Popp, S. O. Rasmussen, R. Röthlisberger, U. Ruth, B. Stauffer, M. L. Siggaard-Andersen, Á. E. Sveinbjörnsdóttir, A. Svensson, and J. W. C. White
2008 High-Resolution Greenland Ice Core Data Show Abrupt Climate Change Happens in Few Years. Science 321(5889):680-684.

Stein, J. K., J. N. Deo, and L. S. Phillips
2003 Big Sites--Short Time: Accumulation Rates in Archaeological Sites. Journal of Archaeological Science 30(3):297-316.

Stein, J.K.
1983 Earthworm Activity: A Source of Potential Disturbance of Archaeological Sediments. American Antiquity 48(2):277-289.

Stein, J.K.
2001 A Review of Site Formation Processes and Their Relevance to Geoarchaeology. *In* Earth Sciences and Archaeology. P. Goldberg, V.T. Holliday, and C.R. Ferring, eds. New York: Kluwer Academic/ Plenum Publishers.

Stiles, C. A., C. I. Mora, and S. G. Driese
2003 Pedogenic Processes and Domain Boundaries in a Vertisol Climosequence: Evidence from Titanium and Zirconium Distribution and Morphology. Geoderma 116(3-4):279-299.

Stoops, G.
2003 Guidelines for Analysis and Description of Soil and Regolith Thin Sections. Madison, WI: Soil Society of America, Inc.

Stoops, G., V. Marcelino, and F. Mees, eds.
2010 Interpretation of Micromorphological Features of Soils and Regoliths. Oxford: Elsevier.

Streten, N.A.
1969 Aspects of Winter Temperatures in Interior Alaska. Arctic 22:403-412.

Stuiver, M., and P.M. Grootes
2000 Gisp2 Oxygen Isotope Ratios. Quaternary Research 53:277-284.

TenBrink, N.W., and C.F. Waythomas

1985 Late Wisconsin Glacial Chronology of the North-Central Alaska Range: A Regional Synthesis and Its Implications for Early Human Settlements. National Geographic Research Reports 19:15-32.

Thorson, R. M., and T.D. Hamilton
1977 Geology of the Dry Creek Site: A Stratified Early Man Site in Interior Alaska. Quaternary Research 7:149-176.

Thorson, R.M.
1990 Geological Contexts Fo Archaeolgoical Sites in Beringia. *In* Archaeological Geology of North America. N.P. Lasca and J. Donahue, eds. Pp. 399-420. Boulder: Centennial Volume no.4. Geological Society of America.

Tite, M.S.
1972 The Influence of Geology on the Magnetic Susceptibility Ofsoils on Archaeological Sites. Archaeometry 14(2):229-236.

Van Nest, J.
2002 The Good Earthworm: How Natural Processes Preserve Upland Archaic Archaeological Sites of Western Illinois. Geoarchaeology 17:53-90.

Verosub, K. L., P. Fine, M.J. Singer, and J. TenPas
1993 Pedogenesis and Paleoclimate: Interpretation of the Magnetic Susceptibility Record of Chinese Loess-Paleosol Sequences. Geology 21(11):1011-1014.

Viau, A.E., K. Gajewski, M. Sawada, and J. Bunbury
2008 Low-and High-Frequency Climate Variability in Eastern Beringia During the Past 25 000 Years. Canadian Journal of Earth Science 45(11):1435-1453.

Viereck, L.A., and E.L. Little Jr.
2007 Alaska Trees and Shrubs. Fairbanks: University of Alaska Press.

Villa, P.
1982 Conjoinable Pieces and Site Formation Processes. American Antiquity 47(2):276-290.

Vinogradov, A.P.
1959 Geochemicstry of Core and Dispersed Chemical Elements in Soils. New York: Translated by Consultants Bureau.

Wahrhaftig, C.
1965 Physiographic Divisions of Alaska. U.S. Geological Survey Professional Paper 482:23.

Waters, M.R.
1992 Principles of Geoarchaeology: A North American Persepective. Tucson: The University of Arizona Press.

Watson, R.J.
1985 Archaeological Interpretation. *In* American Archaeology Past and Future: A Celebration of the Society for American Archaeology 1935- 1985. D.J. Meltzer, D.D. Fowler, and J.A. Sabloff, eds. Pp. 439-457. Washington, DC: Smithsonian Institution Proess.

Weber, F.R., T.D. Hamilton, D.M. Hopkins, C.A. Repenning, and H. Hass

1981 Canyon Creek: A Late Pleostocene Vertebrate Locality in Interior Alaska. Quaternary Research 16:167-180.

Wells, E.C., R.E. Terry, J.J. Parnell, P.J. Hardin, M.W. Jackson, and S.D. Houston
2000 Chemical Analyses of Ancient Anthrosols in Residential Areas at Piedras Negras, Guatemala. Journal of Archaeological Science 27:449-462.

Wendler, F., Y. Kodama, and F. Eaton
1980 On the Frequency of Strong Winds in the Big Delta Area: Fairbanks, Alaska. University of Alaska Geophysical Insititute Scientific Report UAF-R-277.

Weninger, B., O. Joris, and U. Danzeglocke
2011 Calpal-2007. Cologne Radiocarbon Calibration & Palaeoclimate Research Package. Http://Www.Calpal.De/, Accessed 1/21/2011.

West, F.H.
1967 The Donnelly Ridge Site and the Definition of an Early Core and Blade Complex in Central Alaska. American Antiquity 32(3):360-382.

West, F.H.
1975 Dating the Denali Complex. Arctic Anthropology 12:76-81.

West, F.H.
1981 The Archaeology of Beringia. New York: Columbia University Press.

Weston, D.G.
2002 Soil and Susceptibility: Aspects of Themaly Induced Magnetism within the Dynamic Pedological System. Archaeological Prospection 9:207-215.

Willey, G.R., and P. Phillips
1958 Method and Theory in American Archaeology. Chicago: University of Chicago Press.

Willey, G.R., and J.A. Sabloff
1993 A History of American Archaeology. London: Thames and Hudson Ltd.

Wilson, M.C.
1990 Archaeological Geology in Western Canada: Technniques, Approaches, and Integrative Themes. *In* Archaeological Geology of North America. N.P. Lasca and J. Donahue, eds. Pp. 61-86. Boulder: Centennial Volume no.4. Geological Society of America.

Wood, W.R., and D.L. Johnson
1978 A Survey of Disturbance Processes in Archaeological Site Formation. Advances in Archaeological Method and Theory 1:315-381.

Workman, W.B.
1974 The Cultural Significance of a Volcanic Ash Which Fell in the Upper Yukon Basin About 1400 Years Ago. *In* Internation Conference on the Prehistory and Paleoecology of the Western North American Arctic and Subarctic. S. Raymond and P. Schledermann, eds. Alberta, Canada.

Workman, W.B.

1978 Prehistory of the Aishnik-Kluane Area, Southwest Yukon Territory. Volume 74. Ottowa: National Museum of Canada.

Xiaomin, F., L. Jijun, E. Derbyshire, E. A. Fitzpatrick, and R. A. Kemp
1994 Micromorphology of the Beiyuan Loess-Paleosol Sequence in Gansu Province, China: Geomorphological and Paleoenvironmental Significance. Palaeogeography, Palaeoclimatology, Palaeoecology 111(3-4):289-303.

Yang, S.Y., C.X. Li, D.Y. Yang, and X.S. Li
2004 Chemical Weathering of the Loess Depsitis in the Lower Changjiang Valley, China, and Paleoclimatic Implications. Quaternary International 117:27-34.

Yesner, D. R.
2001 Human Dispersal into Interior Alaska: Antecedent Conditions, Mode of Colonization, and Adaptations. Quaternary Science Reviews 20:315-327.

Yesner, D. R., C. E. Holmes, and K.J. Crossen
1992 Archaeology and Paleoecology of the Brokem Mammoth Site, Central Tanana Valley, Interior Alaska, USA. Current Research in the Pleistocene 9:53-57.

Yesner, D.R.
1996 Human Adaptation at the Pleistocene-Holocene Boundary (Circa 13,000 to 8,000 Bp) in Eastern Beringia. *In* Humans at the End of the Ice Age: Archaeology of the Pleistocene-Holocene Transition. L.G. Straus, B.V. Eriksen, J.M. Erlandson, and D.R. Yesner, eds. Pp. 255-276. New York: Plenum Press.

Yesner, D.R., and G. A. Pearson
2002 Microblades and Migrations: Ethnic and Economic Models in the Peopling of the Americas. Archaeological Papers of the American Anthropological Association 12(1):133-161.

Young, S.B.
1982 The Vegetation of Land-Bridge Beringia. *In* Paleoecology of Beringia. D.M. Hopkins, J.V. Matthews, C.E. Schweger, and S.B. Young, eds. Pp. 179-191. New York: Academic Press.

Zazula, G.D., D.G. Froese, J.A. Westgate, C. La Farge, and R.W. Mathewes
2005 Paleoecology of Beringian "Packrat" Middens from Central Yukon Territory, Canada. Quaternary Research 63:189-198.

Appendix A
Micromorphology and Thin Section Descriptions

Slide 2.1 C2b:

Microstructure and Porosity:

Compact grain microstructure with weak separation that gives way to granular with platy overprint in top 1/3 of slide. Majority of voids are complex packing as well as planes and regular vughes.

2 Groundmass:

Unoriented angular to subangular silt sized quartz and mica. The coarse/fine related distribution pattern is single spaced to close porphyric. Rare feldspar minerals observed throughout. Roots in various stages of decomposition evident Majority of Magnetite is unweathered, micromass is yellowish brown speckled clay and b-fabric is random undifferentiated stipple-speckled.

3 Pedofeatures:

Calcite (calcitic crystallitic) infillings and rare nodules observed mainly in bottom half of slide. Clay concentrations occur in the forms of void and grain coatings, with rare linear concentrations or papules.

Slide 2.2 C2b:

1 Microstructure and Porosity:

Compact grain microstructure with weak separation develops a platy overprint in top 1/2 of slide. Majority of voids regular vughes. Rare unaccommodated planes.

2 Groundmass:

Unoriented angular to subangular silt sized quartz and mica. The coarse/fine related distribution pattern is single spaced to close porphyric. Rare feldspar minerals observed throughout. Plant residues and roots in class 0-2 observed. Majority of magnetite is moderately weathered, micromass is yellowish brown speckled clay and stipple-speckled b-fabric. Clay concentrations in the form of void and grain coatings and rare linear concentrations or papuaes observed.

3 Pedofeatures:

Calcite (calcitic crystallitic) infillings nodules and coatings observed. Clay concentrations occur in the forms of void and grain coatings, with rare linear concentrations or papules.

Slide 3.1 C2b:

1 Microstructure and Porosity:

Compact grain microstructure with weak separation in lower 1/3 of slide that gives way to granular with platy overprint in mid 1/3 of slide that gives way to compact grain in upper 1/3 of slide. Majority of voids in the form of vughs with few horizontal unaccommodated plane.

2 Groundmass:

Unoriented angular to subangular silt sized quartz and mica. The coarse/fine related distribution pattern is close porphyric to single spaced. Rare feldspar minerals observed throughout. Organic material observed were roots (class 0-2), organic residue and charcoal fragments and particles. More organics observed than in preceeding slide. Basic distribution pattern is random with a smooth angular to subangular coarse fraction. Majority of magnetite is moderately weathered, rare biotite; micromass is yellowish brown speckeled clay and stipple-speckled b-fabric.

3 Pedofeatures:

Loose continuous infillings of larger (1mm) vughs with calcium carbonate and soil biota excrement. Calcite loose continuous infillings increase in upper 1/2 of slide. A single passage feature was observed in mid-slide. Clay concentrations occur in the forms of void and grain coatings, with rare linear concentrations or papules.

Slide 3.2 C2b with Paleosols:

1 Microstructure and Porosity:

Compact grain microstructure with platy overprint. Majority of voids are vughs with rare horizontal unaccommodated plane voids.

2 Groundmass:

Unoriented angular to subangular silt sized quartz and mica. The coarse/fine related distribution pattern is close porphyric to single spaced with the coarse grains exhibiting oblique alignment. Rare feldspar minerals observed throughout. Organic material observed were roots (class 0-1), and plant residues. Basic distribution pattern is random with a smooth angular to subangular coarse fraction. Majority

of magnetite is moderately weathered; micromass is yellowish brown speckeled clay and stipple-speckled b-fabric.

3 Pedofeatures:

Loose continuous infillings of vughs with soil biota excrement. Passage features are rare. Nodules and coatings also observed. Clay concentrations occur in the forms of void and grain coatings, with rare linear concentrations or papules.

Slide 4.1 C2b with Paleosol Stringers:

1 Microstructure and Porosity:

Compact grain microstructure with weak separation and a platy overprint observed throughout the slide. Voids in the form of vughs and horizontal unaccommodated planes are common throughout.

2 Groundmass:

Unoriented angular to subangular silt sized quartz and mica. The coarse/fine related distribution pattern is close porphyric to single spaced. Rare feldspar minerals observed throughout. Organic material observed were roots (class 0-4), and plant residues. Basic distribution pattern is random with a smooth angular to subangular coarse fraction. Some indication of a loose horizontal orientation of the coarse fraction at the top of the slide. Smaller particle size in the coarse fraction than slide 3.2. Majority of magnetite is unweathered; micromass is yellowish brown clay with stipple-speckled b-fabric. Clay concentrations occur in the forms of void and grain coatings, with rare linear concentrations or papules.

3 Pedofeatures:

Loose continuous infillings of larger (1 mm) vughs with calcium carbonate and soil biota excrement. Fe oxide hypo-coatings were observed.

Slide 4.2 C2b and C2b:

1 Microstructure and Porosity:

Compact grain microstructure with a platy overprint. Majority of voids in the form of vughs and horizontal unaccommodated plane with few to rare channel voids.

2 Groundmass:

Unoriented angular to subangular silt sized quartz and mica; top 1/3 of slide is more unoriented than rest of slide. The coarse/fine related distribution pattern is close porphyric to single spaced, with the coarse grains exhibiting oblique alignment; upper 1/3 of slide has an increase in the coarse fraction. Rare feldspar minerals observed throughout. Organic materials observed were in the form of plant residues, no distinguishable roots were observed. Basic distribution pattern is random with a smooth angular to subangular coarse fraction. Majority of magnetite is weathered,; micromass is yellowish brown clay with a stipple-speckled b-fabric. Clay concentrations occur in the forms of void and grain coatings, with rare linear concentrations or papules. Paleosol is expressed as elongated organics with horizontal orientation and rare round organic aggregates.

3 Pedofeatures:

Infillings, nodules and coatings observed. Loose continuous infillings of larger (1mm) vughs with calcium carbonate and soil biota excrement. Fe oxide hypocoatings, calcium carbonate infillings, and needle fiber calcite are all present. Passage features observed.

Slide 5.1 C2b:

1 Microstructure and Porosity:

Compact grain microstructure to compact granular with platy overprint. Mid section of slide exhibits a platy microstructure. Majority of voids in the form of vughs, with few horizontal unaccommodated planes and channel voids.

2 Groundmass:

Unoriented angular to subangular silt sized quartz and mica. The coarse/fine related distribution pattern is close porphyric to single spaced. Rare feldspar minerals observed throughout. Organic material observed were charcoal, plant residue and tissue. Basic distribution pattern is random with a smooth angular to subangular coarse fraction. Majority of magnetite is weathered; micromass is stipple-speckled b-fabric. Clay concentrations occur in the forms of void and grain coatings, with rare linear concentrations or papules.

3 Pedofeatures:

Infillings, nodules and coatings observed. Fe oxide hypocoatins and calcium carbonate infillings.

Slide 5.2 C2b and C2a:

1 Microstructure and Porosity:

Compact grain microstructure with platy overprint. Voids were observed in the form of regular vughs and unaccommodated planes

2 Groundmass:

Unoriented angular to subangular silt sized quartz and mica. The coarse/fine related distribution pattern is close porphyric to single spaced with the coarse grains exhibiting oblique alignment. Rare feldspar minerals observed throughout. Organic material observed were roots (class 1-4), plant residue and tissue. Basic distribution pattern is random with a smooth angular to subangular coarse fraction. Majority of magnetite is weathered; micromass is stipple-speckled b-fabric. Clay concentrations occur in the forms of void and grain coatings, with rare linear concentrations or papules.

3 Pedofeatures:

Infillings, nodules and coatings observed. Fe oxide hypocoatings and calcium carbonate infillings, and rare needle fiber calcite observed.

Slide 7.1 C2a, sand, contact with C1:

1 Microstructure and Porosity:

Compact grain microstructure with a platy overprint. Majority of voids in the form of vughs with few horizontal unaccommodated plan and channel voids.

2 Groundmass:

Unoriented angular to subangular silt sized quartz and mica. The coarse/fine related distribution pattern is close porphyric to single spaced with the coarse grains exhibiting oblique alignment. Rare feldspar minerals observed throughout. Organic materials observed were very frequent large roots (class 0-1). Basic distribution pattern is random with a smooth angular to subangular coarse fraction. Majority of magnetite is weathered; micromass is stipple-speckled b-fabric. Clay concentrations occur in the forms of void and grain coatings, with rare linear concentrations or papules.

3 Pedofeatures:

Infillings, nodules and coatings observed. Fe oxide hypocoatings and calcium carbonate infillings in vughs and channel voids

Slide 7.2 C2a, Sand, contact with C1:

1 Microstructure and Porosity:

Compact grain microstructure with platy overprint in bottom 1/2 of slide, to compact granular mid slide, to compact granular with platy overprint in top 1/2 of slide. Majority of voids in the form of vughs with few unaccomodated plan and channel voids.

2 Groundmass:

Unoriented angular to subangular silt sized quartz and mica. The coarse/fine related distribution pattern is open porphyric to single spaced with the coarse grains exhibiting oblique alignment. Organic materials observed were plant residue, roots (class 1-3), bone fragments and charcoal. Basic distribution pattern is random with a smooth angular to subangular coarse fraction. Majority of magnetite is weathered; micromass is stipple-speckled b-fabric. Clay concentrations occur in the forms of void and grain coatings, with rare linear concentrations or papules.

3 Pedofeatures:

Loose continuous infillings, nodules, frost shattered aggregates, and coatings observed. Fe oxide hypocoatings and calcium carbonate infillings in vughs and channel voids

Slide 7.3 C2b:

1 Microstructure and Porosity:

Compact grain microstructure with platy overprint. Majority of voids in the form of vughs and unaccommodated plane. Areas with higher concentrations of organic material exhibited a stronger platy microstructure.

2 Groundmass:

Unoriented angular to subangular silt sized quartz and mica. The coarse/fine related distribution pattern is close porphyric to single spaced, with the coarse grains exhibiting oblique alignment. Very frequent organic material was observed in the form of roots, (class 1-4), charcoal, charred tissue and bone. Basic distribution pattern is random with a smooth angular to subangular coarse fraction. Majority of magnetite is moderately weathered; micromass is random to banded stipple-speckled b-fabric. Clay concentrations occur in the forms of void and grain coatings, with rare linear concentrations or papules.

3 Pedofeatures:

Loose discontinuous infillings, nodules, coatings, pendent external hypocoatings, and frost shattered aggregates were observed. Fe oxide hypocoatings and calcium carbonate infillings in vughs and channel voids. The pendent external hypocoatings are found on vughs and charcoal.

Slide 12.1 B2 and B3 (clay lamella):

1 Microstructure and Porosity:

Microstructure is a lenticular platy to subangular blocks where the clay lamella is found. Voids are found in the form of vughs, unaccommodated planes, and common channel voids.

2 Groundmass:

Unoriented angular to subangular silt sized quartz and mica. The coarse/fine related distribution pattern is close porphyric to single spaced, with the coarse grains exhibiting oblique alignment. Roots, (class o-4), charcoal, and plant residue observed. Basic distribution pattern is random with a smooth angular to subangular coarse fraction. Majority of magnetite is highly weathered; micromass is random to banded stipple-speckled b-fabric. Clay concentrations occur in the forms of void, grain coatings, linear concentrations, and rare papules.

3 Pedofeatures:

Loose discontinuous infillings, nodules, coatings, passage features, and frost shattered aggregates were observed. Fe oxide hypocoatings and calcium carbonate infillings in vughs and channel voids.

Appendix B

Magnetic Susceptibility

Table B1- Magnetic susceptibility Sample Location Information

Sample #	Depth (cmbd)	Depth (cmbs)	Profile	Wall	Block
1	202	195	1	North	W34
2	200	193	1	North	W34
3	198	191	1	North	W34
4	195 5	188 5	1	North	W34
5	191	184	1	North	W34
6	189	182	1	North	W34
7	186 5	179 5	1	North	W34
8	184	177	1	North	W34
9	181 5	174 5	1	North	W34
10	179	172	1	North	W34
11	176	169	1	North	W34
12	173	166	1	North	W34
13	171	164	1	North	W34
14	168 5	161 5	1	North	W34
15	164 5	157 5	1	North	W34
16	162	155	1	North	W34
17	160	153	1	North	W34
18	157 5	150 5	1	North	W34
19	155	148	1	North	W34
20	152 5	145 5	1	North	W34
21	150	143	1	North	W34
22	148	141	1	North	W34
23	146	139	1	North	W34
24	143 5	136 5	1	North	W34
25	142	135	1	North	W34
26	140	133	1	North	W34
27	137 5	130 5	1	North	W34
28	135	128	1	North	W34
29	132 5	125 5	1	North	W34
30	130	123	1	North	W34
31	127 5	120 5	1	North	W34
32	125	118	1	North	W34
33	123	116	1	North	W34
34	120 5	113 5	1	North	W34
35	118	111	1	North	W34
36	115 5	108 5	1	North	W34
37	113	106	1	North	W34
38	110 5	103 5	1	North	W34
39	108	101	1	North	W34
40	106	99	1	North	W34
41	104	97	1	North	W34
42	102 5	95 5	1	North	W34
43	100	93	1	North	W34
44	97 5	90 5	1	North	W34
45	95 5	88 5	1	North	W34
46	93	86	1	North	W34
47	90	83	1	North	W34
48	88 5	81 5	1	North	W34
49	87 5	80 5	1	North	W34
50	85	78	1	North	W34
51	82 5	75 5	1	North	W34
52	80	73	1	North	W34
53	78	71	1	North	W34
54	75 5	68 5	1	North	W34
55	72 5	65 5	1	North	W34
56	70 5	63 5	1	North	W34
57	67 5	60 5	1	North	W34
58	65	58	1	North	W34
59	62	55	1	North	W34
60	60 5	53 5	1	North	W34
61	57 5	50 5	1	North	W34
62	55 5	48 5	1	North	W34
63	52 5	45 5	1	North	W34
64	50	43	1	North	W34
65	48	41	1	North	W34
66	45 5	38 5	1	North	W34
67	43	36	1	North	W34
68	40 5	33 5	1	North	W34
69	38 5	31 5	1	North	W34
70	36	29	1	North	W34

Sample #	Depth (cmbd)	Depth (cmbs)	Profile	Wall	Block
71	33 5	26 5	1	North	W34
72	31	24	1	North	W34
73	28 5	21 5	1	North	W34
74	26	19	1	North	W34
75	24	17	1	North	W34
76	22	15	1	North	W34
77	19	12	1	North	W34
78	17	10	1	North	W34
79	14 5	7 5	1	North	W34
80	12	5	1	North	W34
81	9 5	2 5	1	North	W34
82	7	0	1	North	W34
83	138	134	2	North	E32
84	133	129	2	North	E32
85	131	127	2	North	E32
86	129	125	2	North	E32
87	126 5	122 5	2	North	E32
88	124 5	120 5	2	North	E32
89	122	118	2	North	E32
90	119 5	115 5	2	North	E32
91	117	113	2	North	E32
92	114 5	110 5	2	North	E32
93	122	118	2	North	E32
94	109 5	105 5	2	North	E32
95	107 5	103 5	2	North	E32
96	105	101	2	North	E32
97	102 5	98 5	2	North	E32
98	100	96	2	North	E32
99	98	94	2	North	E32
100	95 5	91 5	2	North	E32
101	92 5	88 5	2	North	E32
102	90 5	86 5	2	North	E32
103	88	84	2	North	E32
104	85 5	81 5	2	North	E32
105	83	79	2	North	E32
106	80 5	76 5	2	North	E32
107	78 5	74 5	2	North	E32
108	76	72	2	North	E32
109	73 5	69 5	2	North	E32
110	71	67	2	North	E32
111	68 5	64 5	2	North	E32
112	66	62	2	North	E32
113	63 5	59 5	2	North	E32
114	61 5	57 5	2	North	E32

Sample #	Depth (cmbd)	Depth (cmbs)	Profile	Wall	Block
115	59	55	2	North	E32
116	56 5	52 5	2	North	E32
117	54 5	50 5	2	North	E32
118	52	48	2	North	E32
119	50	46	2	North	E32
120	47 5	43 5	2	North	E32
121	45	41	2	North	E32
122	42 5	38 5	2	North	E32
123	40	36	2	North	E32
124	37 5	33 5	2	North	E32
125	35	31	2	North	E32
126	32 5	28 5	2	North	E32
127	30 5	26 5	2	North	E32
128	28	24	2	North	E32
129	25 5	21 5	2	North	E32
130	23	19	2	North	E32
131	20 5	16 5	2	North	E32
132	18	14	2	North	E32
133	15 5	11 5	2	North	E32
134	13 5	9 5	2	North	E32
135	11	7	2	North	E32
136	8 5	4 5	2	North	E32
137	6	2	2	North	E32
138	4	0	2	North	E32
139	166	155	3	East	E52
140	161	150	3	East	E52
141	159	148	3	East	E52
142	156 5	145 5	3	East	E52
143	154	143	3	East	E52
144	151 5	140 5	3	East	E52
145	149	138	3	East	E52
146	146 5	135 5	3	East	E52
147	144	133	3	East	E52
148	142	131	3	East	E52
149	139 5	128 5	3	East	E52
150	137	126	3	East	E52
151	135	124	3	East	E52
152	132 5	121 5	3	East	E52
153	130	119	3	East	E52
154	127 5	116 5	3	East	E52
155	125 5	114 5	3	East	E52
156	123 5	112 5	3	East	E52
157	120	109	3	East	E52
158	118	107	3	East	E52

Sample #	Depth (cmbd)	Depth (cmbs)	Profile	Wall	Block
159	115	104	3	East	E52
160	113	102	3	East	E52
161	110 5	99 5	3	East	E52
162	108 5	97 5	3	East	E52
163	106 5	95 5	3	East	E52
164	104	93	3	East	E52
165	101 5	90 5	3	East	E52
166	98 5	87 5	3	East	E52
167	96 5	85 5	3	East	E52
168	93 5	82 5	3	East	E52
169	91 5	80 5	3	East	E52
170	89	78	3	East	E52
171	86 5	75 5	3	East	E52
172	84	73	3	East	E52
173	81 5	70 5	3	East	E52
174	79 5	68 5	3	East	E52
175	77	66	3	East	E52
176	74 5	63 5	3	East	E52
177	72 5	61 5	3	East	E52
178	70 5	59 5	3	East	E52
179	68	57	3	East	E52
180	65 5	54 5	3	East	E52
181	63	52	3	East	E52
182	60 5	49 5	3	East	E52
183	58	47	3	East	E52
184	55 5	44 5	3	East	E52
185	53 5	42 5	3	East	E52
186	51	40	3	East	E52
187	48 5	37 5	3	East	E52
188	46	35	3	East	E52
189	43 5	32 5	3	East	E52
190	41 5	30 5	3	East	E52
191	39	28	3	East	E52
192	37	26	3	East	E52
193	34	23	3	East	E52
194	31 5	20 5	3	East	E52
195	29	18	3	East	E52
196	26	15	3	East	E52
197	23 5	12 5	3	East	E52
198	21 5	10 5	3	East	E52
199	18 5	7 5	3	East	E52
200	16	5	3	East	E52
201	13 5	2 5	3	East	E52
202	11	0	3	East	E52

Sample #	Depth (cmbd)	Depth (cmbs)	Profile	Wall	Block
203	179	159	4	South	E44
204	176	156	4	South	E44
205	173 5	153 5	4	South	E44
206	171	151	4	South	E44
207	168 5	148 5	4	South	E44
208	166	146	4	South	E44
209	164	144	4	South	E44
210	161 5	141 5	4	South	E44
211	159 5	139 5	4	South	E44
212	156 5	136 5	4	South	E44
213	154 5	134 5	4	South	E44
214	152	132	4	South	E44
215	149 5	129 5	4	South	E44
216	147	127	4	South	E44
217	144 5	124 5	4	South	E44
218	142	122	4	South	E44
219	139 5	119 5	4	South	E44
220	137	117	4	South	E44
221	134 5	114 5	4	South	E44
222	132	112	4	South	E44
223	130	110	4	South	E44
224	127 5	107 5	4	South	E44
225	125 5	105 5	4	South	E44
226	123	103	4	South	E44
227	120 5	100 5	4	South	E44
228	118	98	4	South	E44
229	115	95	4	South	E44
230	112 5	92 5	4	South	E44
231	110	90	4	South	E44
232	107 5	87 5	4	South	E44
233	105	85	4	South	E44
234	102 5	82 5	4	South	E44
235	100	80	4	South	E44
236	97 5	77 5	4	South	E44
237	95	75	4	South	E44
238	92 5	72 5	4	South	E44
239	90	70	4	South	E44
240	87 5	67 5	4	South	E44
241	85	65	4	South	E44
242	82 5	62 5	4	South	E44
243	80	60	4	South	E44
244	77 5	57 5	4	South	E44
245	75	55	4	South	E44
246	73	53	4	South	E44

Sample #	Depth (cmbd)	Depth (cmbs)	Profile	Wall	Block
247	70 5	50 5	4	South	E44
248	68	48	4	South	E44
249	65 5	45 5	4	South	E44
250	63 5	43 5	4	South	E44
251	61	41	4	South	E44
252	59	39	4	South	E44
253	56 5	36 5	4	South	E44
254	54	34	4	South	E44
255	51 5	31 5	4	South	E44
256	49 5	29 5	4	South	E44
257	47	27	4	South	E44
258	44	24	4	South	E44
259	41 5	21 5	4	South	E44
260	39	19	4	South	E44
261	36 5	16 5	4	South	E44
262	34	14	4	South	E44
263	31 5	11 5	4	South	E44
264	29 5	9 5	4	South	E44
265	27	7	4	South	E44
266	25	5	4	South	E44
267	22 5	2 5	4	South	E44
268	20	0	4	South	E44
269	165 5	138 5	5	South	E46
270	162 5	135 5	5	South	E46
271	160	133	5	South	E46
272	157	130	5	South	E46
273	155	128	5	South	E46
274	151 5	124 5	5	South	E46
275	149 5	122 5	5	South	E46
276	146 5	119 5	5	South	E46
277	144 5	117 5	5	South	E46
278	142 5	115 5	5	South	E46
279	140 5	113 5	5	South	E46
280	138 5	111 5	5	South	E46
281	135 5	108 5	5	South	E46
282	132	105	5	South	E46
283	130 5	103 5	5	South	E46
284	128	101	5	South	E46
285	125 5	98 5	5	South	E46
286	123	96	5	South	E46
287	120 5	93 5	5	South	E46
288	118	91	5	South	E46
289	116	89	5	South	E46
290	113 5	86 5	5	South	E46

Sample #	Depth (cmbd)	Depth (cmbs)	Profile	Wall	Block
291	110 5	83 5	5	South	E46
292	108 5	81 5	5	South	E46
293	106	79	5	South	E46
294	103 5	76 5	5	South	E46
295	101	74	5	South	E46
296	98 5	71 5	5	South	E46
297	96	69	5	South	E46
298	94	67	5	South	E46
299	91	64	5	South	E46
300	89	62	5	South	E46
301	86 5	59 5	5	South	E46
302	83 5	56 5	5	South	E46
303	81 5	54 5	5	South	E46
304	78 5	51 5	5	South	E46
305	76	49	5	South	E46
306	73 5	46 5	5	South	E46
307	71	44	5	South	E46
308	69	42	5	South	E46
309	66 5	39 5	5	South	E46
310	64	37	5	South	E46
311	61 5	34 5	5	South	E46
312	59	32	5	South	E46
313	57	30	5	South	E46
314	54 5	27 5	5	South	E46
315	51 5	24 5	5	South	E46
316	49	22	5	South	E46
317	46 5	19 5	5	South	E46
318	44 5	17 5	5	South	E46
319	42	15	5	South	E46
320	39	12	5	South	E46
321	37	10	5	South	E46
322	34 5	7 5	5	South	E46
323	32	5	5	South	E46
324	29 5	2 5	5	South	E46
325	27	0	5	South	E46
326	146 5	138 5	6	North	E46
327	143	135	6	North	E46
328	140	132	6	North	E46
329	138 5	130 5	6	North	E46
330	135 5	127 5	6	North	E46
331	133	125	6	North	E46
332	131	123	6	North	E46
333	128	120	6	North	E46
334	126	118	6	North	E46

Sample #	Depth (cmbd)	Depth (cmbs)	Profile	Wall	Block
335	123 5	115 5	6	North	E46
336	121 5	113 5	6	North	E46
337	119	111	6	North	E46
338	117	109	6	North	E46
339	115	107	6	North	E46
340	112	104	6	North	E46
341	109 5	101 5	6	North	E46
342	107 5	99 5	6	North	E46
343	104	96	6	North	E46
344	101 5	93 5	6	North	E46
345	99 5	91 5	6	North	E46
346	97	89	6	North	E46
347	94 5	86 5	6	North	E46
348	92	84	6	North	E46
349	89 5	81 5	6	North	E46
350	87	79	6	North	E46
351	85	77	6	North	E46
352	80 5	72 5	6	North	E46
353	90	82	6	North	E46
354	77 5	69 5	6	North	E46
355	75	67	6	North	E46
356	73	65	6	North	E46
357	70 5	62 5	6	North	E46
358	67 5	59 5	6	North	E46
359	65 5	57 5	6	North	E46
360	63	55	6	North	E46
361	60 5	52 5	6	North	E46
362	58 5	50 5	6	North	E46
363	55 5	47 5	6	North	E46
364	53 5	45 5	6	North	E46
365	51	43	6	North	E46
366	48 5	40 5	6	North	E46
367	46	38	6	North	E46
368	43 5	35 5	6	North	E46
369	41 5	33 5	6	North	E46
370	38 5	30 5	6	North	E46
371	35 5	27 5	6	North	E46
372	33 5	25 5	6	North	E46
373	31	23	6	North	E46
374	28	20	6	North	E46
375	25 5	17 5	6	North	E46
376	23 5	15 5	6	North	E46
377	20 5	12 5	6	North	E46
378	18	10	6	North	E46

Sample #	Depth (cmbd)	Depth (cmbs)	Profile	Wall	Block
379	16	8	6	North	E46
380	13	5	6	North	E46
381	10 5	2 5	6	North	E46
382	8	0	6	North	E46
383	183	146 5	7	West	E26
384	180 5	144	7	West	E26
385	178	141 5	7	West	E26
386	175 5	139	7	West	E26
387	173	136 5	7	West	E26
388	170 5	134	7	West	E26
389	167 5	131	7	West	E26
390	165	128 5	7	West	E26
391	162	125 5	7	West	E26
392	159	122 5	7	West	E26
393	156 5	120	7	West	E26
394	154	117 5	7	West	E26
395	151 5	115	7	West	E26
396	149 5	113	7	West	E26
397	146 5	110	7	West	E26
398	144	107 5	7	West	E26
399	141 5	105	7	West	E26
400	139	102 5	7	West	E26
401	137	100 5	7	West	E26
402	134 5	98	7	West	E26
403	132	95 5	7	West	E26
404	129	92 5	7	West	E26
405	126 5	90	7	West	E26
406	123 5	87	7	West	E26
407	120 5	84	7	West	E26
408	118 5	82	7	West	E26
409	116 5	80	7	West	E26
410	114	77 5	7	West	E26
411	111	74 5	7	West	E26
412	108 5	72	7	West	E26
413	105 5	69	7	West	E26
414	103 5	67	7	West	E26
415	100 5	64	7	West	E26
416	97 5	61	7	West	E26
417	95	58 5	7	West	E26
418	92 5	56	7	West	E26
419	90	53 5	7	West	E26
420	88	51 5	7	West	E26
421	85 5	49	7	West	E26
422	82 5	46	7	West	E26

Sample #	Depth (cmbd)	Depth (cmbs)	Profile	Wall	Block
423	80 5	44	7	West	E26
424	78	41 5	7	West	E26
425	75 5	39	7	West	E26
426	73	36 5	7	West	E26
427	70 5	34	7	West	E26
428	67 5	31	7	West	E26
429	65 5	29	7	West	E26
430	63	26 5	7	West	E26
431	60 5	24	7	West	E26
432	58	21 5	7	West	E26
433	55	18 5	7	West	E26
434	52 5	16	7	West	E26
435	49 5	13	7	West	E26
436	47	10 5	7	West	E26
437	44	7 5	7	West	E26
438	41 5	5	7	West	E26
439	39	2 5	7	West	E26
440	36 5	0	7	West	E26
441	147	136 5	8	North	W24
442	144	133 5	8	North	W24
443	141	130 5	8	North	W24
444	138 5	128	8	North	W24
445	135	124 5	8	North	W24
446	133 5	123	8	North	W24
447	131	120 5	8	North	W24
448	129 5	119	8	North	W24
449	126 5	116	8	North	W24
450	124	113 5	8	North	W24
451	121 5	111	8	North	W24
452	119 5	109	8	North	W24
453	117	106 5	8	North	W24
454	115 5	105	8	North	W24
455	111 5	101	8	North	W24
456	108 5	98	8	North	W24
457	106	95 5	8	North	W24
458	104	93 5	8	North	W24
459	101 5	91	8	North	W24
460	99	88 5	8	North	W24
461	97	86 5	8	North	W24
462	94 5	84	8	North	W24
463	92 5	82	8	North	W24
464	89 5	79	8	North	W24
465	87	76 5	8	North	W24
466	84 5	74	8	North	W24

Sample #	Depth (cmbd)	Depth (cmbs)	Profile	Wall	Block
467	82 5	72	8	North	W24
468	80	69 5	8	North	W24
469	77	66 5	8	North	W24
470	74 5	64	8	North	W24
471	72 5	62	8	North	W24
472	70	59 5	8	North	W24
473	67 5	57	8	North	W24
474	64 5	54	8	North	W24
475	62	51 5	8	North	W24
476	60	49 5	8	North	W24
477	57 5	47	8	North	W24
478	55	44 5	8	North	W24
479	52 5	42	8	North	W24
480	50	39 5	8	North	W24
481	47	36 5	8	North	W24
482	45 5	35	8	North	W24
483	42	31 5	8	North	W24
484	40	29 5	8	North	W24
485	37	26 5	8	North	W24
486	34 5	24	8	North	W24
487	32 5	22	8	North	W24
488	30	19 5	8	North	W24
489	27 5	17	8	North	W24
490	25	14 5	8	North	W24
491	22 5	12	8	North	W24
492	20	9 5	8	North	W24
493	18	7 5	8	North	W24
494	15 5	5	8	North	W24
495	13	2 5	8	North	W24
496	10 5	0	8	North	W24
497	145 5	133	9	West	W24
498	142 5	130	9	West	W24
499	140	127 5	9	West	W24
500	138	125 5	9	West	W24
501	135 5	123	9	West	W24
502	133	120 5	9	West	W24
503	130 5	118	9	West	W24
504	128 5	116	9	West	W24
505	126	113 5	9	West	W24
506	123 5	111	9	West	W24
507	121	108 5	9	West	W24
508	119	106 5	9	West	W24
509	116 5	104	9	West	W24
510	114	101 5	9	West	W24

Sample #	Depth (cmbd)	Depth (cmbs)	Profile	Wall	Block
511	111 5	99	9	West	W24
512	109 5	97	9	West	W24
513	107	94 5	9	West	W24
514	105	92 5	9	West	W24
515	103	90 5	9	West	W24
516	100	87 5	9	West	W24
517	97 5	85	9	West	W24
518	95 5	83	9	West	W24
519	93	80 5	9	West	W24
520	91	78 5	9	West	W24
521	88	75 5	9	West	W24
522	86	73 5	9	West	W24
523	83 5	71	9	West	W24
524	81 5	69	9	West	W24
525	79	66 5	9	West	W24
526	76 5	64	9	West	W24
527	74 5	62	9	West	W24
528	72	59 5	9	West	W24
529	69 5	57	9	West	W24
530	67 5	55	9	West	W24
531	65	52 5	9	West	W24
532	62 5	50	9	West	W24
533	60	47 5	9	West	W24
534	58	45 5	9	West	W24
535	55 5	43	9	West	W24
536	53	40 5	9	West	W24
537	50 5	38	9	West	W24
538	48	35 5	9	West	W24
539	45 5	33	9	West	W24
540	43 5	31	9	West	W24
541	40 5	28	9	West	W24
542	38 5	26	9	West	W24
543	36	23 5	9	West	W24
544	33 5	21	9	West	W24
545	31 5	19	9	West	W24
546	29 5	17	9	West	W24
547	27	14 5	9	West	W24
548	24 5	12	9	West	W24
549	22	9 5	9	West	W24
550	19 5	7	9	West	W24
551	17	4 5	9	West	W24
552	14 5	2	9	West	W24
553	12 5	0	9	West	W24

Table B-2 Magnetic Susceptibility Data and Calculations

	Low Frequency				High Frequency									
MS #	κ LF Air 1	κ lf	κ LF Air 2	κ lf (Corr)	κ hf Air 1	κ hf	κ hf Air 2	κ hf Corr)	Net Mass (g)	g/cc	p kg/m3	χ k/p	χ fd %	Strat
1	0 3	219 7	1 2	218 95	-0 4	214 5	-1 2	215 30	7 10	0 89	887 5	0 2467	1 67	C5
2	0 3	184 8	1 3	184 00	-0 5	180 2	-1 1	181 00	7 78	0 97	972 5	0 1892	1 63	C5
3	0 3	548 7	1 2	547 95	-1 1	540 8	-1 6	542 15	9 56	1 20	1195	0 4585	1 06	C5
4	1 2	251 4	2 0	249 80	-0 1	245 9	-0 4	246 15	8 97	1 12	1121 25	0 2228	1 46	C5
5	0 2	301 9	1 1	301 25	-0 4	297 0	-0 4	297 40	8 84	1 11	1105	0 2726	1 28	C5
6	1 1	161 3	2 0	159 75	-0 4	156 7	-0 4	157 10	8 37	1 05	1046 25	0 1527	1 66	C5
7	0 2	153 4	1 0	152 80	-0 4	149 5	-0 1	149 75	6 68	0 84	835	0 1830	2 00	C5
8	1 0	185 1	2 0	183 60	-0 1	180 9	0 4	180 75	10 37	1 30	1296 25	0 1416	1 55	C4
9	0 4	222 3	1 5	221 35	0 6	218 6	2 2	217 20	9 74	1 22	1217 5	0 1818	1 87	C4
10	0 9	188 7	1 5	187 50	1 0	186 8	1 5	185 55	10 67	1 33	1333 75	0 1406	1 04	C4
11	0 2	267 8	0 9	267 25	0 3	263 5	1 0	262 85	10 50	1 31	1312 5	0 2036	1 65	C4
12	0 9	241 5	1 5	240 30	1 0	238 9	1 9	237 45	9 34	1 17	1167 5	0 2058	1 19	C3
13	0 2	272 1	0 8	271 60	0 3	269 1	1 1	268 40	10 07	1 26	1258 75	0 2158	1 18	C3
14	0 8	214 2	1 4	213 10	1 1	211 5	2 3	209 80	9 89	1 24	1236 25	0 1724	1 55	C3
15	0 2	246 9	0 8	246 40	0 1	243 3	0 8	242 85	11 03	1 38	1378 75	0 1787	1 44	C3
16	0 8	234 1	1 6	232 90	0 8	230 5	1 3	229 45	10 23	1 28	1278 75	0 1821	1 48	C3
17	0 1	234 3	0 9	233 80	0 1	230 9	0 6	230 55	9 47	1 18	1183 75	0 1975	1 39	C3
18	0 9	241 5	1 5	240 30	0 6	238 4	1 1	237 55	9 60	1 20	1200	0 2003	1 14	C3
19	0 0	264 8	0 5	264 55	1 1	262 7	1 6	261 35	10 54	1 32	1317 5	0 2008	1 21	C3
20	0 5	210 0	1 2	209 15	0 0	206 7	0 2	206 60	9 42	1 18	1177 5	0 1776	1 22	C2b
21	1 2	168 9	2 0	167 30	0 2	165 6	0 6	165 20	9 73	1 22	1216 25	0 1376	1 26	C2b
22	0 2	176 0	0 4	175 70	0 6	173 8	0 8	173 10	8 38	1 05	1047 5	0 1677	1 48	C2b
23	0 4	245 5	1 0	244 80	0 8	245 2	1 3	244 15	9 70	1 21	1212 5	0 2019	0 27	C2b
24	1 0	169 9	1 6	168 60	-0 1	166 3	0 2	166 25	8 88	1 11	1110	0 1519	1 39	C2b
25	0 2	127 7	0 6	127 30	0 2	125 5	0 2	125 30	7 05	0 88	881 25	0 1445	1 57	C2b
27	0 2	116 9	0 7	116 45	0 4	114 5	0 3	114 15	6 59	0 82	823 75	0 1414	1 98	Ps/C2b
28	0 7	112 7	1 6	111 55	0 0	110 1	1 0	109 60	7 76	0 97	970	0 1150	1 75	Ps/C2b
29	0 1	126 1	0 5	125 80	0 0	123 8	-0 2	123 90	8 65	1 08	1081 25	0 1163	1 51	Ps/C2b
30	0 5	107 8	0 7	107 20	-0 2	105 5	-0 5	105 85	7 98	1 00	997 5	0 1075	1 26	Ps/C2b
31	0 7	135 2	1 1	134 30	-0 5	131 9	-0 4	132 35	9 03	1 13	1128 75	0 1190	1 45	C2b
32	0 1	94 1	0 3	93 90	-0 4	92 4	-0 3	92 75	7 96	1 00	995	0 0944	1 22	C2b
33	0 3	79 4	0 7	78 90	-0 3	77 3	-0 2	77 55	6 27	0 78	783 75	0 1007	1 71	C2b
34	0 7	114 5	1 0	113 65	-0 2	111 2	0 0	111 30	6 84	0 86	855	0 1329	2 07	C2b
35	1 0	87 3	1 3	86 15	0 0	84 7	0 0	84 70	6 75	0 84	843 75	0 1021	1 68	C2b/ PS
36	0 1	134 3	0 3	134 10	0 0	131 0	-0 3	131 15	8 07	1 01	1008 75	0 1329	2 20	C2b

	Low Frequency				High Frequency									
MS #	κ LF Air 1	κ lf	κ LF Air 2	κ lf (Corr)	κ hf Air 1	κ hf	κ hf Air 2	κ hf Corr)	Net Mass (g)	g/cc	p kg/m3	χ k/p	χ fd %	Strat
37	0 3	112 8	0 4	112 45	-0 3	110 3	-0 3	110 60	7 99	1 00	998 75	0 1126	1 65	C2b
38	0 4	126 7	0 7	126 15	-0 3	123 6	-0 5	124 00	8 43	1 05	1053 75	0 1197	1 70	C2b
39	0 7	127 8	1 1	126 90	-0 5	125 2	-0 7	125 80	8 44	1 06	1055	0 1203	0 87	C2b
40	1 1	111 6	1 3	110 40	-0 7	107 9	-0 8	108 65	7 97	1 00	996 25	0 1108	1 59	C2b
41	0 2	121 7	0 3	121 45	-0 1	119 7	-0 2	119 85	8 53	1 07	1066 25	0 1139	1 32	C2b
42	0 3	115 2	0 3	114 90	-0 2	113 0	-0 3	113 25	8 69	1 09	1086 25	0 1058	1 44	C2b
43	0 3	104 6	0 4	104 25	-0 1	102 7	-0 2	102 85	8 51	1 06	1063 75	0 0980	1 34	C2b
44	0 4	118 3	0 6	117 80	-0 6	116 7	-0 9	117 45	9 04	1 13	1130	0 1042	0 30	C2b
45	0 6	116 8	0 7	116 15	-0 3	114 2	-0 6	114 65	8 47	1 06	1058 75	0 1097	1 29	C2b
46	0 7	123 5	0 8	122 75	-0 8	120 2	-1 1	121 15	8 90	1 11	1112 5	0 1103	1 30	C2b
47	0 8	122 7	1 0	121 80	-0 2	119 5	-0 8	120 00	9 35	1 17	1168 75	0 1042	1 48	C2b
48	0 1	128 9	0 4	128 65	-1 0	125 6	-1 3	126 75	8 71	1 09	1088 75	0 1182	1 48	C2b
49	0 4	124 4	0 7	123 85	-0 4	121 6	-0 4	122 00	8 41	1 05	1051 25	0 1178	1 49	C2b/C2a
50	0 7	108 4	0 9	107 60	-0 4	105 9	-0 1	106 15	8 86	1 11	1107 5	0 0972	1 35	C2a
51	0 9	88 9	1 1	87 90	-0 1	86 8	0 5	86 60	8 29	1 04	1036 25	0 0848	1 48	C2a
52	0 1	105 2	0 3	105 00	0 5	104 0	1 1	103 20	8 20	1 03	1025	0 1024	1 71	C2a
53	0 3	123 2	0 5	122 80	1 1	122 5	1 7	121 10	8 88	1 11	1110	0 1106	1 38	C2a
54	0 5	112 1	0 8	111 45	0 1	110 2	0 9	109 70	8 58	1 07	1072 5	0 1039	1 57	C2a
55	0 8	122 3	1 0	121 40	0 9	119 6	1 7	118 30	8 94	1 12	1117 5	0 1086	2 55	C2a
56	1 0	128 7	1 3	127 55	0 3	125 3	0 9	124 70	9 12	1 14	1140	0 1119	2 23	C2a
57	0 2	136 2	0 4	135 90	0 9	135 1	1 7	133 80	9 22	1 15	1152 5	0 1179	1 55	C2a
58	0 4	126 3	0 7	125 75	0 2	124 4	0 7	123 95	8 79	1 10	1098 75	0 1144	1 43	C2a
59	0 7	116 6	0 9	115 80	0 7	116 1	1 3	115 10	8 11	1 01	1013 75	0 1142	0 60	C2a
60	0 9	105 7	1 1	104 70	0 1	103 5	0 5	103 20	8 28	1 04	1035	0 1012	1 43	C2a
61	0 0	118 3	0 1	118 25	0 5	117 1	1 0	116 35	8 19	1 02	1023 75	0 1155	1 61	C2a
62	0 1	127 3	0 3	127 10	1 0	126 4	1 3	125 25	8 63	1 08	1078 75	0 1178	1 46	C2a
63	0 3	118 2	0 4	117 85	0 2	116 4	0 6	116 00	8 80	1 10	1100	0 1071	1 57	C2a
64	0 4	121 7	0 5	121 25	0 6	120 0	0 9	119 25	8 41	1 05	1051 25	0 1153	1 65	C2a
65	0 5	96 3	0 6	95 75	0 9	95 2	1 0	94 25	8 50	1 06	1062 5	0 0901	1 57	C2a/C1
66	0 6	94 4	0 8	93 70	1 0	93 1	1 0	92 10	8 76	1 10	1095	0 0856	1 71	C1
67	0 8	96 3	0 9	95 45	1 0	94 4	1 3	93 25	9 13	1 14	1141 25	0 0836	2 30	C1/B2
68	0 9	101 5	0 9	100 60	-0 1	97 6	0 1	97 60	9 44	1 18	1180	0 0853	2 98	B2
69	0 9	158 7	1 0	157 75	0 1	147 2	0 2	147 05	9 16	1 15	1145	0 1378	6 78	B2
70	1 0	199 2	1 0	198 20	0 2	184 6	-0 1	184 55	8 97	1 12	1121 25	0 1768	6 89	B2
71	0 1	194 9	0 1	194 80	-0 1	181 3	0 0	181 35	9 32	1 17	1165	0 1672	6 90	B2
72	0 1	165 8	0 2	165 65	0 0	153 4	0 0	153 40	8 90	1 11	1112 5	0 1489	7 40	B2
73	0 2	183 7	0 3	183 45	0 0	170 5	0 1	170 45	8 81	1 10	1101 25	0 1666	7 09	B2
74	0 3	189 1	0 3	188 80	0 1	176 0	0 1	175 90	8 26	1 03	1032 5	0 1829	6 83	B2
75	0 3	185 6	0 3	185 30	0 1	173 0	0 0	172 95	7 58	0 95	947 5	0 1956	6 66	B2
76	0 3	208 7	0 3	208 40	0 0	195 8	-0 2	195 90	7 83	0 98	978 75	0 2129	6 00	B2
77	0 3	244 2	0 4	243 85	-0 2	230 6	-0 5	230 95	8 36	1 05	1045	0 2333	5 29	B2
78	0 4	226 3	0 4	225 90	-0 5	214 4	-0 4	214 85	7 68	0 96	960	0 2353	4 89	B2

	Low Frequency				High Frequency									
MS #	κ LF Air 1	κ lf	κ LF Air 2	κ lf (Corr)	κ hf Air 1	κ hf	κ hf Air 2	κ hf Corr)	Net Mass (g)	g/cc	p kg/m3	χ k/p	χ fd %	Strat
79	0 4	220 8	0 4	220 40	-0 4	209 3	-0 5	209 75	7 08	0 89	885	0 2490	4 83	B1
80	0 4	187 5	0 5	187 05	-0 5	177 6	-0 7	178 20	6 13	0 77	766 25	0 2441	4 73	B1
81	0 3	86 8	0 4	86 45	0 1	83 2	0 9	82 70	4 19	0 52	523 75	0 1651	4 34	O/A
82	0 4	28 4	0 3	28 05	0 9	28 1	1 3	27 00	2 80	0 35	350	0 0801	3 74	O/A
83	0 3	362 6	0 3	362 30	0 2	359 0	1 0	358 40	10 56	1 32	1320	0 2745	1 08	C5
84	0 4	241 8	0 5	241 35	1 0	239 3	1 7	237 95	8 92	1 12	1115	0 2165	1 41	C5
85	0 5	265 7	0 4	265 25	0 2	262 3	0 9	261 75	9 84	1 23	1230	0 2157	1 32	C4
86	0 4	294 7	0 1	294 45	0 9	292 1	1 5	290 90	9 72	1 22	1215	0 2423	1 21	C3
87	0 1	252 4	-0 4	252 55	0 1	250 0	0 7	249 60	9 03	1 13	1128 75	0 2237	1 17	C3
88	-0 4	317 5	-1 1	318 25	0 7	315 5	1 1	314 60	11 09	1 39	1386 25	0 2296	1 15	C3
89	-1 1	253 3	-1 6	254 65	0 0	251 6	0 4	251 40	9 44	1 18	1180	0 2158	1 28	C2b
90	-1 9	188 9	-2 2	190 95	0 4	188 9	0 7	188 35	9 08	1 14	1135	0 1682	1 36	C2b
91	-2 2	163 9	-2 2	166 10	0 7	164 6	1 0	163 75	8 72	1 09	1090	0 1524	1 41	C2b
92	0 0	179 7	0 3	179 55	0 0	177 1	0 2	177 00	8 43	1 05	1053 75	0 1704	1 42	C2b
93	0 2	159 2	1 0	158 60	0 2	158 4	0 2	158 20	8 44	1 06	1055	0 1503	0 25	C2b
94	0 2	126 7	0 9	126 15	0 2	124 7	0 5	124 35	7 64	0 96	955	0 1321	1 43	C2b
95	0 9	127 2	1 4	126 05	0 5	124 8	0 8	124 15	7 93	0 99	991 25	0 1272	1 51	C2b
96	0 4	101 9	-0 4	101 90	0 8	101 2	1 0	100 30	6 86	0 86	857 5	0 1188	1 57	C2b
97	-0 4	88 7	-1 0	89 40	0 0	88 2	-0 1	88 25	7 19	0 90	898 75	0 0995	1 29	C2b
98	-1 0	86 4	-1 2	87 50	-0 3	85 8	-0 1	86 00	7 49	0 94	936 25	0 0935	1 71	C2b
99	-0 1	98 3	0 0	98 35	-0 1	96 3	-0 2	96 45	7 39	0 92	923 75	0 1065	1 93	C2b/ PS
100	0 0	146 0	0 3	145 85	-0 2	142 0	0 1	142 05	7 47	0 93	933 75	0 1562	2 61	Ps/C2b
101	0 1	95 7	0 7	95 30	0 1	93 5	0 2	93 35	6 95	0 87	868 75	0 1097	2 05	C2b
102	0 2	127 4	0 9	126 85	0 2	124 2	0 3	123 95	7 73	0 97	966 25	0 1313	2 29	C2b
103	0 1	120 5	0 5	120 20	0 3	118 4	0 5	118 00	8 12	1 02	1015	0 1184	1 83	C2b
104	0 1	107 0	0 2	106 85	0 5	105 3	0 7	104 70	7 64	0 96	955	0 1119	2 01	C2b
105	0 2	114 8	0 1	114 65	0 7	113 7	0 8	112 95	7 85	0 98	981 25	0 1168	1 48	C2b
106	0 1	110 2	-0 1	110 20	0 0	108 6	0 4	108 40	7 28	0 91	910	0 1211	1 63	C2b
107	-0 1	103 9	-0 4	104 15	0 4	101 8	0 7	101 25	8 04	1 01	1005	0 1036	2 78	C2b
108	-0 3	110 8	-0 9	111 40	0 7	110 6	1 1	109 70	8 47	1 06	1058 75	0 1052	1 53	C2a
109	0 0	113 7	-0 7	114 05	0 0	112 9	0 6	112 60	8 77	1 10	1096 25	0 1040	1 27	C2a
110	-0 2	113 7	-0 5	114 05	0 6	113 1	1 1	112 25	8 12	1 02	1015	0 1124	1 58	C2a
111	-0 5	133 2	-0 7	133 80	1 1	133 0	1 6	131 65	9 42	1 18	1177 5	0 1136	1 61	C2a
112	0 1	87 5	0 2	87 35	0 2	86 4	0 6	86 00	8 11	1 01	1013 75	0 0862	1 55	C2a
113	0 2	112 1	0 3	111 85	0 6	110 8	1 0	110 00	8 71	1 09	1088 75	0 1027	1 65	C2a
114	0 3	127 9	0 7	127 40	0 1	125 5	0 3	125 30	9 54	1 19	1192 5	0 1068	1 65	C1
115	0 1	135 4	0 4	135 15	0 3	132 4	0 7	131 90	9 59	1 20	1198 75	0 1127	2 40	C1
116	0 4	129 4	0 5	128 95	0 7	127 8	0 9	127 00	9 46	1 18	1182 5	0 1090	1 51	C1
117	0 5	134 5	0 6	133 95	0 9	132 9	1 2	131 85	9 85	1 23	1231 25	0 1088	1 57	C1
118	-0 1	118 2	-0 2	118 35	0 0	116 2	0 2	116 10	7 74	0 97	967 5	0 1223	1 90	C1
119	-0 2	133 2	-0 4	133 50	0 2	131 7	0 4	131 40	9 38	1 17	1172 5	0 1139	1 57	C1
120	-0 4	116 9	-0 5	117 35	0 4	116 1	0 7	115 55	8 44	1 06	1055	0 1112	1 53	C1

	Low Frequency				High Frequency									
MS #	κ LF Air 1	κ lf	κ LF Air 2	κ lf (Corr)	κ hf Air 1	κ hf	κ hf Air 2	κ hf Corr)	Net Mass (g)	g/cc	p kg/m3	χ k/p	χ fd %	Strat
121	0 2	128 8	1 0	128 20	-0 3	125 5	-1 2	126 25	9 49	1 19	1186 25	0 1081	1 52	C1
122	1 1	101 1	1 9	99 60	-0 7	96 8	-1 5	97 90	7 44	0 93	930	0 1071	1 71	C1
123	0 2	97 0	0 6	96 60	-1 5	92 3	-1 6	93 85	8 75	1 09	1093 75	0 0883	2 85	C1
124	0 2	89 9	0 0	89 80	-1 6	86 4	-1 5	87 95	9 53	1 19	1191 25	0 0754	2 06	C1
125	0 2	91 2	0 2	91 00	-1 5	87 5	-1 4	88 95	9 50	1 19	1187 5	0 0766	2 25	C1
126	0 0	76 6	-0 3	76 75	-1 4	73 2	-1 8	74 80	9 25	1 16	1156 25	0 0664	2 54	C1
127	-0 3	90 3	-0 8	90 85	-1 8	85 6	-3 0	88 00	9 43	1 18	1178 75	0 0771	3 14	C1
128	-0 1	95 9	-0 4	96 15	-0 6	92 0	-1 7	93 15	8 79	1 10	1098 75	0 0875	3 12	C1
129	0 0	101 2	0 0	101 20	-1 7	95 4	-2 5	97 50	8 74	1 09	1092 5	0 0926	3 66	C1
130	0 0	131 1	0 1	131 05	-0 1	121 4	-0 5	121 70	9 58	1 20	1197 5	0 1094	7 13	B1
131	0 1	151 4	0 3	151 20	-0 5	140 2	-0 3	140 60	9 08	1 14	1135	0 1332	7 01	B1
132	0 3	190 5	0 6	190 05	-0 3	177 3	0 1	177 40	7 67	0 96	958 75	0 1982	6 66	B1
133	0 2	261 7	0 6	261 30	0 1	245 5	0 6	245 15	8 03	1 00	1003 75	0 2603	6 18	B1
134	0 3	224 4	1 4	223 55	0 7	213 8	2 3	212 30	6 27	0 78	783 75	0 2852	5 03	B1
135	0 2	254 8	0 7	254 35	1 1	241 5	1 7	240 10	7 71	0 96	963 75	0 2639	5 60	B1
136	0 1	268 5	0 6	268 15	1 7	255 7	2 1	253 80	7 41	0 93	926 25	0 2895	5 35	B1
137	0 6	264 2	1 0	263 40	2 1	251 6	2 4	249 35	7 35	0 92	918 75	0 2867	5 33	O/A
138	1 0	220 8	1 2	219 70	2 4	211 0	2 8	208 40	6 60	0 83	825	0 2663	5 14	O/A
139	0 1	252 9	0 1	252 80	0 2	250 2	0 3	249 95	9 10	1 14	1137 5	0 2222	1 13	C2b
140	0 1	173 6	0 1	173 50	0 3	171 7	0 8	171 15	8 97	1 12	1121 25	0 1547	1 35	C2b
141	0 1	182 5	-0 1	182 50	0 7	181 7	2 4	180 15	8 84	1 11	1105	0 1652	1 29	C2b
142	-0 1	211 0	-0 3	211 20	0 7	206 6	2 1	205 20	8 67	1 08	1083 75	0 1949	2 84	C2b/ PS
143	-0 3	173 5	-0 5	173 90	0 6	170 7	1 9	169 45	8 63	1 08	1078 75	0 1612	2 56	C2b
144	-0 5	137 9	-0 7	138 50	0 5	137 4	1 8	136 25	8 18	1 02	1022 5	0 1355	1 62	C2b
145	-0 1	106 2	-0 3	106 40	1 8	106 7	2 9	104 35	6 78	0 85	847 5	0 1255	1 93	C2b/ PS
146	-0 3	128 4	-0 3	128 70	0 4	126 3	1 9	125 15	7 01	0 88	876 25	0 1469	2 76	C2b
147	-0 3	102 0	-0 1	102 20	0 5	101 6	1 8	100 45	7 01	0 88	876 25	0 1166	1 71	C2b/ PS
148	-0 1	88 4	0 1	88 40	0 4	88 6	2 4	87 20	6 30	0 79	787 5	0 1123	1 36	C2b/ PS
149	0 1	68 8	0 3	68 60	0 5	68 6	2 0	67 35	5 89	0 74	736 25	0 0932	1 82	C2b
150	0 3	101 1	0 7	100 60	0 4	99 6	1 8	98 50	7 06	0 88	882 5	0 1140	2 09	C2b
151	0 1	114 8	0 4	114 55	0 4	116 2	4 7	113 65	8 05	1 01	1006 25	0 1138	0 79	C2b
152	0 1	135 2	0 6	134 85	0 6	132 9	2 3	131 45	8 03	1 00	1003 75	0 1343	2 52	C2b
153	0 6	123 4	1 0	122 60	0 6	121 6	1 8	120 40	8 37	1 05	1046 25	0 1172	1 79	C2b
154	0 0	118 7	0 3	118 55	1 8	119 0	3 4	116 40	8 09	1 01	1011 25	0 1172	1 81	C2b
155	0 3	118 3	0 4	117 95	0 4	116 9	1 7	115 85	8 49	1 06	1061 25	0 1111	1 78	C2b
156	0 4	122 1	0 4	121 70	0 5	120 6	1 6	119 55	8 93	1 12	1116 25	0 1090	1 77	C2b
157	0 4	118 4	0 2	118 10	0 3	117 1	1 5	116 20	8 44	1 06	1055	0 1119	1 61	C2a
158	0 2	105 5	0 1	105 35	0 0	103 8	0 2	103 70	8 73	1 09	1091 25	0 0965	1 57	C2a
159	0 1	124 4	-0 1	124 40	0 0	112 3	0 0	112 30	9 72	1 22	1215	0 1024	9 73	C2a
160	-0 1	127 5	-0 3	127 70	0 2	125 0	0 3	124 75	8 66	1 08	1082 5	0 1180	2 31	C2a
161	0 4	137 7	0 8	137 10	0 0	135 7	1 0	135 20	9 37	1 17	1171 25	0 1171	1 39	C2a
162	0 8	135 9	1 2	134 90	0 2	133 9	1 2	133 20	9 19	1 15	1148 75	0 1174	1 26	C2a

	Low Frequency				High Frequency									
MS #	κ LF Air 1	κ lf	κ LF Air 2	κ lf (Corr)	κ hf Air 1	κ hf	κ hf Air 2	κ hf Corr)	Net Mass (g)	g/cc	p kg/m3	χ k/p	χ fd %	Strat
163	0 3	130 7	0 7	130 20	0 3	131 1	1 7	130 10	8 89	1 11	1111 25	0 1172	0 08	C2a
164	0 7	116 9	1 2	115 95	0 5	115 8	2 2	114 45	8 79	1 10	1098 75	0 1055	1 29	C2a
165	1 2	108 7	1 7	107 25	0 5	107 1	2 3	105 70	8 14	1 02	1017 5	0 1054	1 45	C2a
166	0 2	119 7	0 8	119 20	0 8	119 0	2 5	117 35	8 47	1 06	1058 75	0 1126	1 55	C2a
167	0 8	163 5	1 3	162 45	0 7	161 8	2 5	160 20	9 80	1 23	1225	0 1326	1 39	C2a
168	0 3	149 9	0 8	149 35	0 5	148 7	2 3	147 30	9 63	1 20	1203 75	0 1241	1 37	C1
169	0 8	137 3	1 3	136 25	0 6	135 8	2 2	134 40	9 63	1 20	1203 75	0 1132	1 36	C1
170	0 2	104 2	0 7	103 75	0 3	102 9	1 7	101 90	7 65	0 96	956 25	0 1085	1 78	C1
171	0 7	121 8	1 3	120 80	0 4	119 9	1 7	118 85	8 22	1 03	1027 5	0 1176	1 61	C1
172	0 2	133 3	0 8	132 80	0 3	131 7	1 6	130 75	8 74	1 09	1092 5	0 1216	1 54	C1
173	0 8	138 7	1 3	137 65	0 3	136 0	1 3	135 20	9 42	1 18	1177 5	0 1169	1 78	C1
174	0 4	113 5	1 0	112 80	0 2	111 3	1 1	110 65	13 64	1 71	1705	0 0662	1 91	C1
175	1 0	112 4	1 7	111 05	1 1	111 5	2 0	109 95	7 81	0 98	976 25	0 1138	0 99	C1
176	0 4	113 7	1 5	112 75	0 5	111 2	1 9	110 00	8 33	1 04	1041 25	0 1083	2 44	C1
177	1 1	111 7	1 8	110 25	1 0	108 5	1 6	107 20	8 25	1 03	1031 25	0 1069	2 77	C1/B1
178	0 4	113 2	1 1	112 45	0 1	106 1	0 5	105 80	8 42	1 05	1052 5	0 1068	5 91	B1
179	1 1	171 5	1 9	170 00	0 5	158 9	1 1	158 10	9 41	1 18	1176 25	0 1445	7 00	B1
180	0 4	196 2	1 2	195 40	1 1	182 1	1 5	180 80	8 54	1 07	1067 5	0 1830	7 47	B1
181	1 2	235 8	1 8	234 30	0 0	220 0	0 5	219 75	8 70	1 09	1087 5	0 2154	6 21	B1
182	0 3	245 6	1 0	244 95	0 5	231 4	0 9	230 70	7 71	0 96	963 75	0 2542	5 82	B1
183	1 0	294 5	1 7	293 15	0 9	278 8	1 4	277 65	8 54	1 07	1067 5	0 2746	5 29	B1
184	0 3	249 6	0 8	249 05	0 1	236 4	0 6	236 05	7 07	0 88	883 75	0 2818	5 22	B1
185	0 8	305 5	1 3	304 45	0 6	290 7	1 2	289 80	7 97	1 00	996 25	0 3056	4 81	B1
186	0 3	343 5	0 8	342 95	1 2	328 6	1 7	327 15	8 07	1 01	1008 75	0 3400	4 61	B1
187	0 8	278 9	1 2	277 90	0 2	265 3	1 3	264 55	6 69	0 84	836 25	0 3323	4 80	O/A
188	1 2	201 0	1 6	199 60	0 2	190 4	1 2	189 70	5 25	0 66	656 25	0 3042	4 96	O/A
189	0 1	56 7	0 5	56 40	0 3	56 6	1 4	55 75	4 77	0 60	596 25	0 0946	1 15	O/A
190	0 5	115 5	0 9	114 80	0 3	113 0	1 3	112 20	8 39	1 05	1048 75	0 1095	2 26	OB
191	0 9	127 0	1 2	125 95	0 4	122 6	1 4	121 70	8 92	1 12	1115	0 1130	3 37	OB
192	1 2	135 2	1 5	133 85	0 3	129 6	1 4	128 75	8 90	1 11	1112 5	0 1203	3 81	OB
193	0 0	124 7	0 3	124 55	0 3	123 1	1 3	122 30	9 08	1 14	1135	0 1097	1 81	OB
194	0 3	120 7	0 5	120 30	0 0	118 7	1 0	118 20	9 11	1 14	1138 75	0 1056	1 75	OB
195	0 5	100 3	0 8	99 65	1 0	99 5	1 7	98 15	7 59	0 95	948 75	0 1050	1 51	OB
196	0 8	137 1	1 0	136 20	0 3	133 7	0 9	133 10	9 18	1 15	1147 5	0 1187	2 28	OB
197	1 0	122 3	1 3	121 15	0 9	119 9	1 5	118 70	8 88	1 11	1110	0 1091	2 02	OB
198	0 1	119 5	0 3	119 30	-0 1	117 5	0 4	117 35	9 03	1 13	1128 75	0 1057	1 63	OB
199	0 3	105 1	0 4	104 75	0 4	101 7	1 2	100 90	7 02	0 88	877 5	0 1194	3 68	OB
200	0 4	133 6	0 5	133 15	1 2	130 4	1 6	129 00	9 34	1 17	1167 5	0 1140	3 12	OB
201	0 5	114 7	0 6	114 15	-0 1	110 6	0 3	110 50	7 63	0 95	953 75	0 1197	3 20	OB
202	0 6	127 7	0 6	127 10	0 3	123 9	0 6	123 45	8 64	1 08	1080	0 1177	2 87	OB
203	0 6	313 5	0 7	312 85	0 6	310 2	0 8	309 50	10 52	1 32	1315	0 2379	1 07	C4
204	0 7	316 1	0 7	315 40	0 8	312 9	0 9	312 05	11 99	1 50	1498 75	0 2104	1 06	C4

	Low Frequency				High Frequency									
MS #	κ LF Air 1	κ lf	κ LF Air 2	κ lf (Corr)	κ hf Air 1	κ hf	κ hf Air 2	κ hf Corr)	Net Mass (g)	g/cc	p kg/m3	χ k/p	χ fd %	Strat
205	0 7	329 6	0 8	328 85	0 9	326 4	1 3	325 30	11 79	1 47	1473 75	0 2231	1 08	C4
206	0 8	314 0	0 8	313 20	-0 1	309 4	0 0	309 45	11 77	1 47	1471 25	0 2129	1 20	C2b
207	0 8	272 6	0 8	271 80	0 0	268 5	0 1	268 45	11 16	1 40	1395	0 1948	1 23	C2b
208	0 8	152 8	1 0	151 90	0 1	150 1	0 3	149 90	9 51	1 19	1188 75	0 1278	1 32	C2b
209	1 0	190 2	1 0	189 20	0 3	187 2	0 8	186 65	10 23	1 28	1278 75	0 1480	1 35	PS
210	1 0	208 9	1 2	207 80	0 8	206 1	1 0	205 20	10 24	1 28	1280	0 1623	1 25	C2b
211	1 2	337 5	1 4	336 20	1 0	334 3	1 4	333 10	11 07	1 38	1383 75	0 2430	0 92	C2b
212	0 1	273 7	0 3	273 50	-0 1	271 1	0 2	271 05	10 65	1 33	1331 25	0 2054	0 90	PS
213	0 3	151 8	0 4	151 45	0 2	149 9	0 5	149 55	8 59	1 07	1073 75	0 1410	1 25	C2b
214	0 4	222 5	0 5	222 05	0 5	220 2	0 9	219 50	10 56	1 32	1320	0 1682	1 15	C2b
215	0 5	226 0	0 8	225 35	0 9	223 4	1 3	222 30	10 81	1 35	1351 25	0 1668	1 35	C2b
216	0 8	151 1	1 0	150 20	0 1	149 4	0 5	149 10	9 18	1 15	1147 5	0 1309	0 73	C2b
217	1 0	149 7	1 2	148 60	0 5	147 1	0 8	146 45	8 92	1 12	1115	0 1333	1 45	C2b
218	1 2	122 4	1 4	121 10	0 8	119 3	1 3	118 25	8 24	1 03	1030	0 1176	2 35	PS
219	0 1	105 4	0 3	105 20	0 2	103 8	0 6	103 40	7 99	1 00	998 75	0 1053	1 71	C2b
220	0 3	148 0	0 6	147 55	0 6	143 9	0 9	143 15	7 83	0 98	978 75	0 1508	2 98	PS
221	0 6	131 1	0 9	130 35	0 9	129 5	1 3	128 40	9 20	1 15	1150	0 1133	1 50	C2b
222	0 9	145 4	1 2	144 35	0 0	141 2	0 3	141 05	8 55	1 07	1068 75	0 1351	2 29	PS
223	1 2	137 3	1 6	135 90	0 3	133 9	0 9	133 30	9 01	1 13	1126 25	0 1207	1 91	C2b
224	0 1	117 3	0 4	117 05	0 9	116 2	1 2	115 15	8 32	1 04	1040	0 1125	1 62	C2b
225	0 4	113 7	0 7	113 15	1 2	112 6	1 6	111 20	8 45	1 06	1056 25	0 1071	1 72	C2b/PS
226	0 7	118 2	1 1	117 30	0 1	115 8	0 4	115 55	8 61	1 08	1076 25	0 1090	1 49	C2b
227	1 1	126 1	1 4	124 85	0 4	123 6	0 7	123 05	8 70	1 09	1087 5	0 1148	1 44	C2b
228	0 2	120 3	0 4	120 00	0 7	119 4	1 2	118 45	8 81	1 10	1101 25	0 1090	1 29	C2b
229	0 4	110 8	0 7	110 25	1 2	109 2	1 5	107 85	8 88	1 11	1110	0 0993	2 18	C2b
230	0 7	121 6	0 9	120 80	0 0	119 6	0 3	119 45	9 01	1 13	1126 25	0 1073	1 12	C2b
231	0 9	115 3	1 1	114 30	0 3	113 3	0 7	112 80	8 75	1 09	1093 75	0 1045	1 31	C2b
232	1 1	119 1	1 3	117 90	0 7	117 1	1 0	116 25	8 97	1 12	1121 25	0 1052	1 40	C2a
233	0 1	118 1	0 3	117 90	1 0	117 4	1 4	116 20	8 50	1 06	1062 5	0 1110	1 44	C2a
234	0 3	113 2	0 5	112 80	0 0	111 2	0 2	111 10	8 20	1 03	1025	0 1100	1 51	C2a
235	0 5	96 6	0 7	96 00	0 2	95 2	0 4	94 90	8 81	1 10	1101 25	0 0872	1 15	C2a
236	0 7	116 0	0 8	115 25	0 4	113 1	0 4	112 70	9 17	1 15	1146 25	0 1005	2 21	C2a
237	0 8	120 6	1 0	119 70	0 4	118 5	0 7	117 95	8 93	1 12	1116 25	0 1072	1 46	C2a
238	1 0	110 4	1 3	109 25	0 7	108 2	0 8	107 45	8 48	1 06	1060	0 1031	1 65	C2a
239	0 0	124 3	0 1	124 25	0 8	123 3	0 9	122 45	9 07	1 13	1133 75	0 1096	1 45	C2a
240	0 1	114 1	0 3	113 90	0 9	113 3	1 2	112 25	8 75	1 09	1093 75	0 1041	1 45	C2a
241	-0 2	123 8	-0 1	123 95	-0 2	121 7	-0 5	122 05	9 15	1 14	1143 75	0 1084	1 53	C2a
242	-0 1	131 9	-0 1	132 00	-0 5	129 3	-0 7	129 90	9 09	1 14	1136 25	0 1162	1 59	C2a
243	-0 1	114 6	-0 2	114 75	-0 7	112 5	-1 0	113 35	8 99	1 12	1123 75	0 1021	1 22	C2a
244	-0 2	116 5	-0 2	116 70	-1 0	113 9	-1 2	115 00	8 83	1 10	1103 75	0 1057	1 46	C2a
245	-0 2	117 3	-0 2	117 50	-1 2	114 6	-1 2	115 80	8 17	1 02	1021 25	0 1151	1 45	C2a
246	-0 2	110 5	-0 1	110 65	-1 2	107 8	-1 4	109 10	8 77	1 10	1096 25	0 1009	1 40	C2a

	Low Frequency				High Frequency									
MS #	κ LF Air 1	κ lf	κ LF Air 2	κ lf (Corr)	κ hf Air 1	κ hf	κ hf Air 2	κ hf Corr)	Net Mass (g)	g/cc	p kg/m3	χ k/p	χ fd %	Strat
247	-0 1	99 4	0 0	99 45	-0 1	98 1	-0 2	98 25	8 48	1 06	1060	0 0938	1 21	C2a
248	0 0	114 2	-0 1	114 25	-0 2	112 3	-0 2	112 50	8 51	1 06	1063 75	0 1074	1 53	C2a
249	-0 1	110 3	-0 1	110 40	-0 2	108 5	-0 1	108 65	8 44	1 06	1055	0 1046	1 59	C2a
250	-0 1	104 7	0 0	104 75	-0 1	102 8	-0 1	102 90	8 76	1 10	1095	0 0957	1 77	C1
251	0 0	101 7	-0 1	101 75	-0 1	100 0	0 1	100 00	8 93	1 12	1116 25	0 0912	1 72	C1
252	-0 1	86 7	-0 1	86 80	0 1	85 2	0 2	85 05	9 62	1 20	1202 5	0 0722	2 02	C1
253	-0 1	96 6	-0 1	96 70	0 2	94 2	0 4	93 90	9 90	1 24	1237 5	0 0781	2 90	C1
254	-0 1	116 1	-0 1	116 20	0 4	108 7	0 7	108 15	9 70	1 21	1212 5	0 0958	6 93	B1
255	-0 1	59 8	0 0	59 85	0 7	56 4	1 0	55 55	9 97	1 25	1246 25	0 0480	7 18	B1
256	0 0	71 4	0 0	71 40	1 0	66 7	1 1	65 65	9 77	1 22	1221 25	0 0585	8 05	B1
257	0 0	64 1	0 0	64 10	1 1	61 3	1 3	60 10	10 06	1 26	1257 5	0 0510	6 24	C1
258	0 0	55 1	0 1	55 05	0 1	52 2	0 4	51 95	9 57	1 20	1196 25	0 0460	5 63	C1/B1
259	0 1	58 3	0 2	58 15	0 4	55 5	0 8	54 90	10 42	1 30	1302 5	0 0446	5 59	C1/B1
260	0 2	56 5	0 4	56 20	0 8	53 5	1 3	52 45	9 66	1 21	1207 5	0 0465	6 67	C1/B1
261	0 4	76 3	0 8	75 70	0 1	71 7	0 5	71 40	9 32	1 17	1165	0 0650	5 68	C1/B1
262	0 8	136 7	1 1	135 75	0 5	127 9	0 8	127 25	9 30	1 16	1162 5	0 1168	6 26	C1/B1
263	1 1	174 6	1 2	173 45	0 8	163 5	1 1	162 55	8 30	1 04	1037 5	0 1672	6 28	B1
264	0 1	170 8	0 4	170 55	1 1	161 9	1 4	160 65	7 11	0 89	888 75	0 1919	5 80	B1
265	0 4	191 2	0 6	190 70	0 0	180 4	0 3	180 25	7 60	0 95	950	0 2007	5 48	B1/A
266	0 6	221 8	0 9	221 05	0 3	209 7	0 5	209 30	7 66	0 96	957 5	0 2309	5 32	B1/A
267	0 9	47 7	1 3	46 60	0 5	46 6	0 9	45 90	4 11	0 51	513 75	0 0907	1 50	O/A
268	0 1	33 4	0 3	33 20	0 9	33 6	1 2	32 55	2 94	0 37	367 5	0 0903	1 96	O/A
269	0 3	306 9	0 5	306 50	1 2	304 1	1 6	302 70	9 22	1 15	1152 5	0 2659	1 24	C4
270	0 5	232 2	0 8	231 55	0 1	229 2	0 3	229 00	9 19	1 15	1148 75	0 2016	1 10	C4
271	0 8	232 8	1 1	231 85	0 3	229 6	0 5	229 20	9 92	1 24	1240	0 1870	1 14	C4
272	1 1	226 9	1 2	225 75	0 5	223 9	0 7	223 30	9 13	1 14	1141 25	0 1978	1 09	C4
273	0 5	361 9	1 2	361 05	0 6	358 7	2 2	357 30	10 04	1 26	1255	0 2877	1 04	C4
274	0 2	313 8	0 5	313 45	0 9	310 7	1 0	309 75	9 98	1 25	1247 5	0 2513	1 18	C4
275	0 5	321 1	0 7	320 50	1 0	317 8	1 2	316 70	10 49	1 31	1311 25	0 2444	1 19	C4
276	0 7	279 0	0 9	278 20	1 2	275 9	1 1	274 75	10 26	1 28	1282 5	0 2169	1 24	C4
277	0 9	279 1	1 1	278 10	1 1	275 8	1 2	274 65	10 50	1 31	1312 5	0 2119	1 24	C3
278	1 1	306 5	1 3	305 30	1 2	302 7	1 3	301 45	11 09	1 39	1386 25	0 2202	1 26	C3
279	0 0	287 2	0 1	287 15	0 0	283 7	0 0	283 70	11 53	1 44	1441 25	0 1992	1 20	C3
280	0 1	301 2	0 5	300 90	0 0	297 2	0 2	297 10	10 96	1 37	1370	0 2196	1 26	C3
281	0 5	275 1	0 6	274 55	0 2	271 2	0 4	270 90	9 93	1 24	1241 25	0 2212	1 33	C3
282	0 6	188 8	0 7	188 15	0 4	186 0	0 4	185 60	9 62	1 20	1202 5	0 1565	1 36	C2b
283	0 7	146 2	1 0	145 35	0 4	143 6	0 5	143 15	8 93	1 12	1116 25	0 1302	1 51	C2b
284	1 0	123 9	1 1	122 85	0 5	121 3	0 4	120 85	8 16	1 02	1020	0 1204	1 63	C2b
285	1 1	119 4	1 3	118 20	0 4	116 8	0 3	116 45	8 70	1 09	1087 5	0 1087	1 48	C2b
286	-0 1	128 5	-0 1	128 60	0 3	126 7	0 2	126 45	8 58	1 07	1072 5	0 1199	1 67	C2b
287	-0 1	102 4	0 0	102 45	0 2	101 1	0 0	101 00	8 37	1 05	1046 25	0 0979	1 42	C2b
288	0 0	113 1	0 0	113 10	0 0	111 2	0 0	111 20	8 92	1 12	1115	0 1014	1 68	C2b

	Low Frequency				High Frequency									
MS #	κ LF Air 1	κ lf	κ LF Air 2	κ lf (Corr)	κ hf Air 1	κ hf	κ hf Air 2	κ hf Corr)	Net Mass (g)	g/cc	p kg/m3	χ k/p	χ fd %	Strat
289	0 0	152 3	0 0	152 30	0 0	149 6	-0 1	149 65	9 14	1 14	1142 5	0 1333	1 74	C2b
290	0 0	124 6	0 0	124 60	-0 1	121 8	-0 2	121 95	8 23	1 03	1028 75	0 1211	2 13	C2b
291	0 0	126 8	0 0	126 80	-0 2	124 3	-0 3	124 55	8 91	1 11	1113 75	0 1138	1 77	C2b
292	0 0	131 4	0 0	131 40	-0 3	129 0	-0 4	129 35	9 40	1 18	1175	0 1118	1 56	C2a
293	0 0	137 2	-0 8	137 60	-0 4	134 8	-0 9	135 45	9 40	1 18	1175	0 1171	1 56	C2a
294	0 0	117 6	-0 1	117 65	-0 9	115 3	-0 7	116 10	9 44	1 18	1180	0 0997	1 32	C2a
295	-0 1	122 2	-0 2	122 35	-0 7	119 7	-0 9	120 50	9 64	1 21	1205	0 1015	1 51	C2a
296	-0 2	124 9	-0 3	125 15	-0 9	122 3	-1 1	123 30	9 39	1 17	1173 75	0 1066	1 48	C2a
297	-0 3	137 7	-0 3	138 00	-1 1	134 8	-0 9	135 80	9 74	1 22	1217 5	0 1133	1 59	C2a
298	-0 3	127 8	-0 3	128 10	-0 9	125 7	-0 3	126 30	8 76	1 10	1095	0 1170	1 41	C2a
299	-0 3	107 8	-0 2	108 05	-0 3	106 9	0 5	106 80	9 73	1 22	1216 25	0 0888	1 16	C2a
300	-0 2	121 6	-0 2	121 80	0 5	120 8	1 3	119 90	9 70	1 21	1212 5	0 1005	1 56	C2a
301	-0 2	116 6	-0 2	116 80	0 1	115 3	0 5	115 00	8 96	1 12	1120	0 1043	1 54	C2a
302	-0 2	123 8	-0 2	124 00	0 5	122 4	0 6	121 85	9 56	1 20	1195	0 1038	1 73	C2a
303	-0 2	120 0	-0 1	120 15	0 6	118 9	0 7	118 25	9 06	1 13	1132 5	0 1061	1 58	C1
304	-0 1	143 8	-0 1	143 90	0 7	142 6	0 9	141 80	10 37	1 30	1296 25	0 1110	1 46	C2
305	-0 1	136 2	-0 2	136 35	0 9	135 1	0 8	134 25	9 61	1 20	1201 25	0 1135	1 54	C3
306	-0 2	145 7	-0 2	145 90	0 8	144 7	0 9	143 85	9 49	1 19	1186 25	0 1230	1 41	C4
307	-0 2	133 8	-0 4	134 10	0 9	132 9	0 9	132 00	9 72	1 22	1215	0 1104	1 57	C5
308	-0 4	127 9	-0 5	128 35	0 9	127 5	0 9	126 60	9 50	1 19	1187 5	0 1081	1 36	B1
309	-0 5	110 7	-0 5	111 20	0 9	110 4	0 8	109 55	8 37	1 05	1046 25	0 1063	1 48	B1
310	-0 5	99 9	-0 5	100 40	0 8	98 5	0 8	97 70	8 36	1 05	1045	0 0961	2 69	B1
311	-0 5	132 1	-0 7	132 70	0 8	127 9	0 8	127 10	8 83	1 10	1103 75	0 1202	4 22	B1
312	-0 7	219 5	-0 8	220 25	0 8	208 5	0 9	207 65	8 85	1 11	1106 25	0 1991	5 72	B1
313	-0 8	255 9	-0 7	256 65	0 9	242 7	0 8	241 85	9 43	1 18	1178 75	0 2177	5 77	B1
314	-0 7	214 8	-0 7	215 50	0 8	203 1	0 7	202 35	7 52	0 94	940	0 2293	6 10	B1
315	-0 7	233 7	-0 7	234 40	0 7	221 7	0 8	220 95	8 28	1 04	1035	0 2265	5 74	B1
316	-0 7	212 5	-0 8	213 25	0 8	202 4	0 7	201 65	7 79	0 97	973 75	0 2190	5 44	B1
317	-0 8	222 6	-0 9	223 45	0 7	211 3	0 7	210 60	7 91	0 99	988 75	0 2260	5 75	B1
318	-0 9	240 8	-0 9	241 70	0 7	228 8	1 0	227 95	8 19	1 02	1023 75	0 2361	5 69	B1
319	-0 9	238 8	-1 2	239 85	1 0	227 5	1 2	226 40	8 05	1 01	1006 25	0 2384	5 61	B1
320	-0 1	225 4	-0 4	225 65	1 2	214 9	1 4	213 60	7 44	0 93	930	0 2426	5 34	B1
321	-0 4	210 2	-0 5	210 65	-0 1	199 9	0 2	199 85	6 32	0 79	790	0 2666	5 13	B1
322	-0 5	231 6	-0 6	232 15	0 2	221 0	0 4	220 70	6 08	0 76	760	0 3055	4 93	B1
323	-0 6	167 4	-0 8	168 10	0 4	158 8	0 7	158 25	4 57	0 57	571 25	0 2943	5 86	O/A
324	-0 8	76 8	-1 0	77 70	0 7	75 6	0 8	74 85	4 02	0 50	502 5	0 1546	3 67	O/A
325	-0 1	232 8	-0 3	233 00	0 8	223 7	0 9	222 85	7 72	0 97	965	0 2415	4 36	O/A
326	-0 3	160 8	-0 4	161 15	0 9	160 0	1 1	159 00	10 45	1 31	1306 25	0 1234	1 33	C4
327	-0 4	176 6	-0 6	177 10	1 1	175 9	1 1	174 80	10 09	1 26	1261 25	0 1404	1 30	C4
328	-0 6	222 6	-0 7	223 25	1 1	222 0	1 4	220 75	10 32	1 29	1290	0 1731	1 12	C4
329	-0 7	156 7	-0 7	157 40	0 0	155 2	0 2	155 10	8 14	1 02	1017 5	0 1547	1 46	C4
330	-0 7	172 3	-0 7	173 00	0 2	170 9	0 3	170 65	9 94	1 24	1242 5	0 1392	1 36	C3

	Low Frequency				High Frequency									
MS #	κ LF Air 1	κ lf	κ LF Air 2	κ lf (Corr)	κ hf Air 1	κ hf	κ hf Air 2	κ hf Corr)	Net Mass (g)	g/cc	p kg/m3	χ k/p	χ fd %	Strat
331	-0 7	203 2	-0 7	203 90	0 3	199 6	0 4	199 25	10 18	1 27	1272 5	0 1602	2 28	C3
332	-0 7	140 4	-0 6	141 05	0 4	139 8	0 8	139 20	8 18	1 02	1022 5	0 1379	1 31	C3
333	-0 6	134 5	-0 4	135 00	0 8	134 1	0 8	133 30	9 17	1 15	1146 25	0 1178	1 26	C3
334	-0 4	228 3	-0 2	228 60	0 8	226 8	1 0	225 90	10 01	1 25	1251 25	0 1827	1 18	C3
335	-0 2	204 0	0 2	204 00	1 0	202 5	1 2	201 40	10 10	1 26	1262 5	0 1616	1 27	C3
336	0 2	226 6	0 4	226 30	1 2	224 7	1 2	223 50	9 89	1 24	1236 25	0 1831	1 24	C3
337	0 4	206 9	0 6	206 40	1 2	205 7	1 2	204 50	9 45	1 18	1181 25	0 1747	0 92	PS/C3
338	0 6	159 5	0 8	158 80	1 2	157 8	1 3	156 55	8 88	1 11	1110	0 1431	1 42	PS/C3
339	0 8	139 0	1 1	138 05	0 0	135 7	0 1	135 65	8 60	1 08	1075	0 1284	1 74	C3
340	0 0	116 3	0 2	116 20	0 1	114 5	0 1	114 40	8 47	1 06	1058 75	0 1098	1 55	C3
341	0 2	129 4	0 4	129 10	0 1	125 8	-0 1	125 80	8 79	1 10	1098 75	0 1175	2 56	C3
342	0 4	108 6	0 5	108 15	-0 1	106 4	-0 1	106 50	8 49	1 06	1061 25	0 1019	1 53	C3
343	0 5	105 2	0 6	104 65	-0 1	102 9	-0 3	103 10	8 60	1 08	1075	0 0973	1 48	C3
344	0 6	145 0	0 6	144 40	-0 3	141 5	-0 4	141 85	8 90	1 11	1112 5	0 1298	1 77	C3
345	0 6	106 1	0 8	105 40	-0 4	103 0	-0 5	103 45	7 93	0 99	991 25	0 1063	1 85	C2b
346	0 8	139 3	0 9	138 45	-0 5	135 0	-0 6	135 55	7 99	1 00	998 75	0 1386	2 09	C2b
347	0 9	123 8	1 0	122 85	-0 6	118 8	-0 6	119 40	8 39	1 05	1048 75	0 1171	2 81	C2b
348	-0 1	128 8	-0 1	128 90	-0 6	127 2	-0 6	127 80	8 53	1 07	1066 25	0 1209	0 85	C2b
349	-0 1	120 5	0 0	120 55	0 6	117 8	-0 7	117 85	8 60	1 08	1075	0 1121	2 24	C2b
350	0 0	118 3	0 2	118 20	-0 7	115 6	-0 8	116 35	8 57	1 07	1071 25	0 1103	1 57	C2b
351	0 2	117 6	0 2	117 40	-0 8	114 8	-1 1	115 75	8 52	1 07	1065	0 1102	1 41	C2b
352	0 2	106 6	0 2	106 40	-1 1	102 4	-1 2	103 55	8 38	1 05	1047 5	0 1016	2 68	C2b
353	0 2	115 0	0 2	114 80	-1 2	111 6	-1 4	112 90	8 55	1 07	1068 75	0 1074	1 66	C2b
354	0 2	107 9	0 3	107 65	-0 2	105 7	-0 5	106 05	8 29	1 04	1036 25	0 1039	1 49	C2b
355	0 3	116 4	0 3	116 10	-0 5	113 5	-0 7	114 10	7 84	0 98	980	0 1185	1 72	C2b
356	0 3	112 3	0 4	111 95	-0 7	109 5	-0 9	110 30	9 27	1 16	1158 75	0 0966	1 47	C2b
357	0 4	105 2	0 5	104 75	-0 9	102 3	-0 9	103 20	9 59	1 20	1198 75	0 0874	1 48	C2b
358	0 5	132 1	0 4	131 65	-0 9	128 5	-1 2	129 55	9 43	1 18	1178 75	0 1117	1 60	C2b
359	0 4	129 0	0 5	128 55	-1 2	125 4	-1 3	126 65	9 37	1 17	1171 25	0 1098	1 48	C2b
360	0 5	148 5	0 4	148 05	-0 1	145 9	-0 3	146 10	9 88	1 24	1235	0 1199	1 32	C2b
361	0 4	143 8	0 4	143 40	-0 3	141 1	-0 5	141 50	9 64	1 21	1205	0 1190	1 32	C2a
362	0 4	134 8	0 4	134 40	-0 5	131 9	-0 6	132 45	9 64	1 21	1205	0 1115	1 45	C2a
363	0 4	121 9	0 5	121 45	-0 6	119 0	-0 8	119 70	9 74	1 22	1217 5	0 0998	1 44	C2a
364	0 5	113 3	0 5	112 80	-0 8	109 9	-1 3	110 95	9 55	1 19	1193 75	0 0945	1 64	C1
365	0 2	134 4	1 3	133 65	-0 3	130 5	-1 0	131 15	9 48	1 19	1185	0 1128	1 87	C1
366	0 3	151 6	1 2	150 85	-1 0	146 4	-1 3	147 55	10 28	1 29	1285	0 1174	2 19	C1
367	0 2	100 4	1 1	99 75	-0 1	95 9	0 0	95 95	7 65	0 96	956 25	0 1043	3 81	C1
368	1 1	143 4	2 1	141 80	0 0	131 5	0 1	131 45	9 75	1 22	1218 75	0 1163	7 30	B2
369	0 2	140 1	0 9	139 55	0 1	129 2	0 5	128 90	9 95	1 24	1243 75	0 1122	7 63	B2
370	0 9	152 3	1 9	150 90	0 5	140 3	0 9	139 60	9 85	1 23	1231 25	0 1226	7 49	B2
371	0 3	169 9	1 0	169 25	0 9	157 6	1 5	156 40	9 78	1 22	1222 5	0 1384	7 59	B2/B3
372	1 0	180 4	1 7	179 05	0 4	166 0	1 1	165 25	9 79	1 22	1223 75	0 1463	7 71	B2/B3

	Low Frequency				High Frequency									
MS #	κ LF Air 1	κ lf	κ LF Air 2	κ lf (Corr)	κ hf Air 1	κ hf	κ hf Air 2	κ hf Corr)	Net Mass (g)	g/cc	p kg/m3	χ k/p	χ fd %	Strat
373	0 3	126 9	0 9	126 30	1 1	118 1	1 8	116 65	9 83	1 23	1228 75	0 1028	7 64	B2/B3
374	0 9	114 5	1 6	113 25	0 2	106 8	1 0	106 20	10 48	1 31	1310	0 0865	6 23	B1
375	0 2	126 9	0 8	126 40	1 0	119 9	1 7	118 55	9 85	1 23	1231 25	0 1027	6 21	B1
376	0 8	200 5	1 5	199 35	0 2	188 6	1 1	187 95	8 95	1 12	1118 75	0 1782	5 72	B1
377	0 3	223 4	1 1	222 70	1 1	211 7	1 8	210 25	8 13	1 02	1016 25	0 2191	5 59	B1
378	1 1	232 6	1 7	231 20	0 3	219 0	1 0	218 35	8 15	1 02	1018 75	0 2269	5 56	B1
379	0 2	165 8	1 0	165 20	1 0	158 0	1 5	156 75	6 53	0 82	816 25	0 2024	5 12	O/A
380	1 0	191 3	1 8	189 90	0 2	180 8	0 7	180 35	5 92	0 74	740	0 2566	5 03	O/A
381	0 3	187 2	1 0	186 55	0 7	177 9	1 1	177 00	5 06	0 63	632 5	0 2949	5 12	A
382	1 0	42 0	1 9	40 55	1 1	40 8	1 6	39 45	3 69	0 46	461 25	0 0879	2 71	O
383	-0 6	362 6	0 0	362 90	0 1	359 5	0 6	359 15	12 13	1 52	1516 25	0 2393	1 03	C4
384	0 0	345 9	0 6	345 60	0 6	342 6	1 2	341 70	11 62	1 45	1452 5	0 2379	1 13	C4
385	0 6	321 9	1 2	321 00	1 2	318 7	1 7	317 25	12 18	1 52	1522 5	0 2108	1 17	C4
386	1 2	311 0	1 8	309 50	0 1	306 4	0 8	305 95	11 77	1 47	1471 25	0 2104	1 15	C4
387	0 1	265 7	0 6	265 35	0 0	262 8	0 4	262 60	11 46	1 43	1432 5	0 1852	1 04	C4
388	0 6	311 3	1 1	310 45	0 4	307 1	0 7	306 55	11 32	1 42	1415	0 2194	1 26	C4
389	1 1	314 2	1 5	312 90	0 7	310 1	0 9	309 30	11 10	1 39	1387 5	0 2255	1 15	C4
390	0 1	269 6	0 4	269 35	0 9	266 9	1 1	265 90	11 03	1 38	1378 75	0 1954	1 28	C4
391	0 4	133 3	0 8	132 70	1 1	132 0	1 4	130 75	8 60	1 08	1075	0 1234	1 47	C3
392	0 8	125 1	1 0	124 20	-0 2	122 3	0 0	122 40	8 38	1 05	1047 5	0 1186	1 45	C3/PS
393	1 0	118 5	1 2	117 40	0 0	117 0	0 4	116 80	8 84	1 11	1105	0 1062	0 51	C3
394	1 2	121 0	1 3	119 75	0 4	118 4	0 3	118 05	9 22	1 15	1152 5	0 1039	1 42	C3
395	0 1	97 8	0 1	97 70	0 3	97 9	0 7	97 40	7 79	0 97	973 75	0 1003	0 31	C3/PS
396	0 1	141 7	0 2	141 55	0 7	139 3	0 7	138 60	8 04	1 01	1005	0 1408	2 08	PS
397	0 2	115 5	0 4	115 20	0 7	114 3	0 8	113 55	8 48	1 06	1060	0 1087	1 43	C3
398	0 4	138 1	0 4	137 70	0 8	135 7	0 8	134 90	8 02	1 00	1002 5	0 1374	2 03	C3/PS
399	0 4	124 1	0 5	123 65	0 8	123 6	1 0	122 70	8 96	1 12	1120	0 1104	0 77	C3
400	0 5	127 1	0 6	126 55	1 0	126 6	1 1	125 55	8 35	1 04	1043 75	0 1212	0 79	C3/PS
401	0 6	137 0	0 8	136 30	1 1	134 7	1 2	133 55	8 98	1 12	1122 5	0 1214	2 02	C3/PS
402	0 8	160 6	1 0	159 70	1 2	156 1	1 3	154 85	8 51	1 06	1063 75	0 1501	3 04	PS
403	1 0	124 8	1 1	123 75	-0 2	123 2	0 1	123 25	8 95	1 12	1118 75	0 1106	0 40	C2b
404	1 1	122 1	1 4	120 85	0 1	119 2	0 2	119 05	8 62	1 08	1077 5	0 1122	1 49	C2b
405	0 1	107 3	0 4	107 05	0 2	105 9	0 5	105 55	8 77	1 10	1096 25	0 0977	1 40	C2b
406	0 4	131 3	0 8	130 70	0 5	131 4	0 9	130 70	9 61	1 20	1201 25	0 1088	0 00	C2b
407	0 8	121 6	1 2	120 60	0 9	119 8	1 3	118 70	8 85	1 11	1106 25	0 1090	1 58	C2b
408	1 2	127 3	1 6	125 90	0 0	125 4	0 5	125 15	9 34	1 17	1167 5	0 1078	0 60	C2b
409	0 0	124 5	0 3	124 35	0 5	123 2	0 9	122 50	9 11	1 14	1138 75	0 1092	1 49	C2b
410	0 3	124 2	0 6	123 75	0 9	121 5	1 6	120 25	8 15	1 02	1018 75	0 1215	2 83	C2a
411	0 6	130 1	1 0	129 30	0 0	127 9	0 7	127 55	9 22	1 15	1152 5	0 1122	1 35	C2a
412	1 0	96 7	1 2	95 60	0 7	94 9	1 3	93 90	8 45	1 06	1056 25	0 0905	1 78	C2a
413	1 2	118 7	1 3	117 45	0 2	116 6	1 1	115 95	9 73	1 22	1216 25	0 0966	1 28	C2a
414	0 1	119 1	0 2	118 95	1 1	118 7	1 9	117 20	8 79	1 10	1098 75	0 1083	1 47	C2a

	Low Frequency				High Frequency									
MS #	κ LF Air 1	κ lf	κ LF Air 2	κ lf (Corr)	κ hf Air 1	κ hf	κ hf Air 2	κ hf Corr)	Net Mass (g)	g/cc	p kg/m3	χ k/p	χ fd %	Strat
415	0 2	117 9	0 2	117 70	0 2	116 6	1 1	115 95	9 30	1 16	1162 5	0 1012	1 49	C2a
416	0 2	132 7	0 4	132 40	1 1	132 0	2 1	130 40	9 50	1 19	1187 5	0 1115	1 51	C2a
417	0 4	127 1	0 4	126 70	0 5	126 0	1 5	125 00	9 59	1 20	1198 75	0 1057	1 34	C2a
418	0 4	126 6	0 4	126 20	-0 1	123 5	0 9	123 10	9 33	1 17	1166 25	0 1082	2 46	C2a
419	0 4	145 3	0 5	144 85	0 9	144 1	1 7	142 80	9 70	1 21	1212 5	0 1195	1 42	C2a
420	0 5	130 7	0 5	130 20	0 4	129 3	1 3	128 45	9 23	1 15	1153 75	0 1128	1 34	C2a
421	0 5	118 2	0 6	117 65	0 3	116 9	1 3	116 10	9 40	1 18	1175	0 1001	1 32	C2a
422	0 6	134 1	0 6	133 50	0 4	132 4	1 2	131 60	9 68	1 21	1210	0 1103	1 42	C2a
423	0 6	103 8	0 7	103 15	1 2	104 7	2 1	103 05	9 16	1 15	1145	0 0901	0 10	C1
424	0 7	128 0	0 8	127 25	0 3	126 2	1 1	125 50	9 29	1 16	1161 25	0 1096	1 38	C1
425	0 8	117 7	0 9	116 85	1 1	117 2	2 0	115 65	8 94	1 12	1117 5	0 1046	1 03	C1
426	0 9	88 9	0 9	88 00	0 2	87 2	0 9	86 65	9 27	1 16	1158 75	0 0759	1 53	C1
427	0 9	66 0	0 9	65 10	0 9	65 0	1 8	63 65	7 58	0 95	947 5	0 0687	2 23	C1
428	0 9	42 5	1 1	41 50	0 2	40 5	1 1	39 85	8 77	1 10	1096 25	0 0379	3 98	C1
429	1 1	49 2	1 1	48 10	1 1	47 2	1 7	45 80	8 02	1 00	1002 5	0 0480	4 78	B1
430	1 1	48 7	1 3	47 50	0 3	45 4	1 1	44 70	8 97	1 12	1121 25	0 0424	5 89	C1
431	0 1	53 8	0 2	53 65	1 1	51 8	2 0	50 25	8 72	1 09	1090	0 0492	6 34	C1
432	0 2	49 8	0 5	49 45	0 4	47 1	1 1	46 35	8 47	1 06	1058 75	0 0467	6 27	C1
433	0 5	76 4	0 8	75 75	1 1	72 6	4 2	69 95	7 35	0 92	918 75	0 0824	7 66	C1
434	0 8	91 5	1 1	90 55	0 3	85 2	1 3	84 40	7 24	0 91	905	0 1001	6 79	B1
435	1 1	208 3	1 4	207 05	0 4	195 0	1 5	194 05	8 12	1 02	1015	0 2040	6 28	B1
436	0 0	195 6	0 3	195 45	1 5	185 8	2 5	183 80	7 57	0 95	946 25	0 2066	5 96	B1
437	0 3	200 4	0 4	200 05	0 4	188 4	1 6	187 40	7 66	0 96	957 5	0 2089	6 32	B1
438	0 4	212 6	0 7	212 05	0 7	202 7	1 8	201 45	6 59	0 82	823 75	0 2574	5 00	A
439	0 7	156 3	0 9	155 50	0 4	148 8	1 6	147 80	4 93	0 62	616 25	0 2523	4 95	A
440	0 9	32 5	1 0	31 55	0 4	31 7	1 4	30 80	3 30	0 41	412 5	0 0765	2 38	O
441	1 0	237 3	1 1	236 25	0 5	234 5	1 6	233 45	9 92	1 24	1240	0 1905	1 19	C4
442	1 1	251 4	1 2	250 25	0 4	247 9	1 4	247 00	10 19	1 27	1273 75	0 1965	1 30	C4
443	1 2	212 7	1 2	211 50	0 1	209 5	1 1	208 90	10 26	1 28	1282 5	0 1649	1 23	C4
444	1 2	353 5	1 2	352 30	1 1	349 3	1 9	347 80	11 95	1 49	1493 75	0 2358	1 28	C4
445	1 2	287 9	1 3	286 65	0 2	280 9	0 9	280 35	10 17	1 27	1271 25	0 2255	2 20	C4
446	0 1	347 6	0 1	347 50	0 9	344 2	1 5	343 00	11 14	1 39	1392 5	0 2496	1 29	C4
447	0 1	176 7	0 1	176 60	0 1	174 6	0 8	174 15	8 77	1 10	1096 25	0 1611	1 39	C3
448	0 1	115 5	0 1	115 40	0 8	116 6	1 7	115 35	7 00	0 88	875	0 1319	0 04	C3
449	0 1	157 5	0 0	157 45	0 0	154 7	0 6	154 40	8 81	1 10	1101 25	0 1430	1 94	C3/PS
450	0 0	126 9	0 0	126 90	0 6	125 9	1 2	125 00	8 54	1 07	1067 5	0 1189	1 50	C3/PS
451	0 0	135 9	0 0	135 90	1 2	135 4	1 6	134 00	9 26	1 16	1157 5	0 1174	1 40	C3/PS
452	0 0	139 0	0 0	139 00	0 0	137 0	0 5	136 75	8 99	1 12	1123 75	0 1237	1 62	C2b
453	0 0	86 4	-0 1	86 45	0 5	85 9	0 8	85 25	7 42	0 93	927 5	0 0932	1 39	C2b
454	-0 1	95 3	-0 1	95 40	0 8	93 5	1 2	92 50	7 38	0 92	922 5	0 1034	3 04	C2b
455	-0 1	126 3	-0 2	126 45	1 2	126 9	1 5	125 55	7 94	0 99	992 5	0 1274	0 71	C2b
456	-0 2	98 5	-0 3	98 75	0 1	97 2	0 5	96 90	7 23	0 90	903 75	0 1093	1 87	C2b

	Low Frequency				High Frequency									
MS #	κ LF Air 1	κ lf	κ LF Air 2	κ lf (Corr)	κ hf Air 1	κ hf	κ hf Air 2	κ hf Corr)	Net Mass (g)	g/cc	p kg/m3	χ k/p	χ fd %	Strat
457	-0 3	124 3	-0 4	124 65	0 5	122 8	0 7	122 20	8 22	1 03	1027 5	0 1213	1 97	C2b/PS
458	-0 4	116 1	-0 4	116 50	0 7	112 5	1 1	111 60	7 94	0 99	992 5	0 1174	4 21	C2b
459	-0 4	132 2	-0 5	132 65	1 1	130 5	1 5	129 20	8 90	1 11	1112 5	0 1192	2 60	C2b
460	-0 5	137 2	-0 5	137 70	0 0	125 6	0 5	125 35	8 93	1 12	1116 25	0 1234	8 97	C2b
461	-0 5	143 1	-0 5	143 60	0 5	141 9	0 8	141 25	8 80	1 10	1100	0 1305	1 64	C2b
462	-0 5	147 3	-0 4	147 75	0 8	146 6	1 1	145 65	9 62	1 20	1202 5	0 1229	1 42	C2b
463	-0 4	140 5	-0 3	140 85	1 1	141 7	1 4	140 45	9 97	1 25	1246 25	0 1130	0 28	C2b
464	-0 3	92 7	-0 2	92 95	0 0	91 8	0 3	91 65	7 54	0 94	942 5	0 0986	1 40	C2b
465	-0 2	122 5	0 0	122 60	0 3	122 5	0 7	122 00	9 61	1 20	1201 25	0 1021	0 49	C2b
466	0 0	133 5	0 2	133 40	0 7	132 3	0 9	131 50	9 63	1 20	1203 75	0 1108	1 42	C2b
467	0 2	125 6	0 5	125 25	0 9	124 4	1 0	123 45	9 46	1 18	1182 5	0 1059	1 44	C2b
468	0 5	141 1	0 6	140 55	1 0	139 6	1 5	138 35	9 57	1 20	1196 25	0 1175	1 57	C2a
469	0 6	117 5	0 7	116 85	0 2	116 9	0 6	116 50	9 41	1 18	1176 25	0 0993	0 30	C2a
470	0 7	113 5	0 9	112 70	0 6	112 0	0 8	111 30	9 72	1 22	1215	0 0928	1 24	C2a
471	0 9	119 4	0 9	118 50	0 8	118 9	1 0	118 00	9 29	1 16	1161 25	0 1020	0 42	C2a
472	0 9	124 2	1 0	123 25	1 0	122 5	1 1	121 45	9 33	1 17	1166 25	0 1057	1 46	C2a
473	1 0	136 0	1 1	134 95	1 1	134 3	1 5	133 00	9 83	1 23	1228 75	0 1098	1 44	C2a
474	1 1	122 9	1 1	121 80	0 0	120 0	0 4	119 80	9 18	1 15	1147 5	0 1061	1 64	C2a
475	1 1	117 5	1 3	116 30	0 4	115 1	0 7	114 55	8 70	1 09	1087 5	0 1069	1 50	C2a
476	0 0	139 6	0 0	139 60	0 7	138 5	1 0	137 65	9 50	1 19	1187 5	0 1176	1 40	C2a
477	0 0	115 7	0 1	115 65	1 0	115 2	1 6	113 90	8 64	1 08	1080	0 1071	1 51	C1
478	0 1	105 4	0 2	105 25	0 0	104 1	0 5	103 85	8 39	1 05	1048 75	0 1004	1 33	C1
479	0 2	129 4	0 2	129 20	0 5	128 2	1 2	127 35	9 25	1 16	1156 25	0 1117	1 43	C1
480	0 2	123 7	0 3	123 45	1 2	123 2	2 2	121 50	9 81	1 23	1226 25	0 1007	1 58	C1
481	0 3	114 7	0 3	114 40	0 2	113 2	0 9	112 65	8 25	1 03	1031 25	0 1109	1 53	C1
482	0 3	118 0	0 3	117 70	0 9	116 5	1 6	115 25	9 17	1 15	1146 25	0 1027	2 08	C1
483	0 3	98 2	0 2	97 95	0 0	95 9	0 8	95 50	9 02	1 13	1127 5	0 0869	2 50	B2
484	0 2	163 2	0 0	163 10	0 8	155 9	1 3	154 85	9 27	1 16	1158 75	0 1408	5 06	B2
485	0 0	224 1	-0 1	224 15	0 2	211 1	0 7	210 65	7 51	0 94	938 75	0 2388	6 02	B2
486	-0 1	188 3	-0 2	188 45	0 7	177 2	1 3	176 20	7 44	0 93	930	0 2026	6 50	B1
487	-0 2	123 9	-0 2	124 10	1 3	118 4	1 7	116 90	8 73	1 09	1091 25	0 1137	5 80	B1
488	-0 2	99 3	-0 3	99 55	0 1	94 8	0 6	94 45	9 40	1 18	1175	0 0847	5 12	B1
489	-0 3	114 3	-0 3	114 60	0 6	107 7	1 3	106 75	8 52	1 07	1065	0 1076	6 85	B1
490	-0 3	124 2	-0 4	124 55	1 3	117 8	1 6	116 35	7 71	0 96	963 75	0 1292	6 58	E/A
491	-0 4	164 7	-0 5	165 15	0 2	154 7	0 7	154 25	8 08	1 01	1010	0 1635	6 60	E/A
492	-0 5	212 0	-0 5	212 50	0 7	200 6	1 1	199 70	8 08	1 01	1010	0 2104	6 02	E/A
493	-0 5	203 8	-0 4	204 25	1 1	194 9	1 4	193 65	6 70	0 84	837 5	0 2439	5 19	E/A
494	-0 4	260 8	-0 4	261 20	-0 2	246 5	0 1	246 55	6 92	0 87	865	0 3020	5 61	O/A
495	-0 4	234 6	-0 4	235 00	0 1	223 7	0 7	223 30	5 61	0 70	701 25	0 3351	4 98	O/A
496	-0 4	73 8	-0 4	74 20	0 7	72 3	0 9	71 50	4 53	0 57	566 25	0 1310	3 64	O/A
497	-0 4	322 0	-0 2	322 30	0 9	319 4	1 1	318 40	11 25	1 41	1406 25	0 2292	1 21	C4
498	-0 2	316 6	0 0	316 70	1 1	314 3	1 3	313 10	11 13	1 39	1391 25	0 2276	1 14	C4

	Low Frequency				High Frequency									
MS #	κ LF Air 1	κ lf	κ LF Air 2	κ lf (Corr)	κ hf Air 1	κ hf	κ hf Air 2	κ hf Corr)	Net Mass (g)	g/cc	p kg/m3	χ k/p	χ fd %	Strat
499	0 0	335 5	0 2	335 40	-0 1	331 4	-0 3	331 60	11 35	1 42	1418 75	0 2364	1 13	C4
500	0 2	325 6	0 4	325 30	-0 3	321 2	-0 3	321 50	11 26	1 41	1407 5	0 2311	1 17	C4
501	0 4	189 0	0 7	188 45	-0 3	185 6	-0 3	185 90	9 19	1 15	1148 75	0 1640	1 35	C4
502	0 7	146 8	1 1	145 90	-0 3	143 5	-0 2	143 75	8 46	1 06	1057 5	0 1380	1 47	C4
503	1 1	150 2	1 4	148 95	-0 2	146 3	-0 2	146 50	8 39	1 05	1048 75	0 1420	1 64	C4
504	0 1	162 2	0 5	161 90	-0 2	159 5	0 0	159 60	9 33	1 17	1166 25	0 1388	1 42	C4
505	0 5	130 0	0 6	129 45	0 0	127 9	0 2	127 80	8 76	1 10	1095	0 1182	1 27	C4
506	0 6	314 1	0 9	313 35	0 2	309 8	0 3	309 55	10 18	1 27	1272 5	0 2462	1 21	C4
507	0 9	348 7	1 1	347 70	0 3	343 8	0 2	343 55	11 08	1 39	1385	0 2510	1 19	C4
508	1 1	236 3	1 3	235 10	0 2	232 5	0 3	232 25	9 31	1 16	1163 75	0 2020	1 21	C3/PS
509	0 0	97 6	0 0	97 60	0 3	96 4	0 1	96 20	7 83	0 98	978 75	0 0997	1 43	C3/PS
510	0 0	144 2	0 1	144 15	0 1	141 7	0 4	141 45	8 31	1 04	1038 75	0 1388	1 87	C3/PS
511	0 1	135 0	0 1	134 90	0 4	132 3	0 7	131 75	8 25	1 03	1031 25	0 1308	2 34	C3/PS
512	0 1	141 6	0 1	141 50	0 7	139 3	0 9	138 50	8 77	1 10	1096 25	0 1291	2 12	C3/PS
513	0 1	133 9	0 3	133 70	0 9	132 3	0 9	131 40	9 01	1 13	1126 25	0 1187	1 72	C3
514	0 3	140 2	0 3	139 90	0 9	138 6	1 1	137 60	9 13	1 14	1141 25	0 1226	1 64	C3
515	0 3	143 6	0 3	143 30	1 1	142 2	1 5	140 90	9 31	1 16	1163 75	0 1231	1 67	PS
516	0 3	135 6	0 3	135 30	0 1	133 3	0 5	133 00	8 96	1 12	1120	0 1208	1 70	C3
517	0 3	142 5	0 5	142 10	0 5	140 7	1 0	139 95	9 34	1 17	1167 5	0 1217	1 51	C3
518	0 5	120 6	0 5	120 10	1 0	119 5	1 5	118 25	9 12	1 14	1140	0 1054	1 54	C3
519	0 5	125 0	0 6	124 45	0 0	123 1	0 7	122 75	9 27	1 16	1158 75	0 1074	1 37	C3
520	0 6	131 1	0 6	130 50	0 7	131 0	1 4	129 95	9 34	1 17	1167 5	0 1118	0 42	C3
521	0 6	123 6	0 7	122 95	0 1	121 6	0 7	121 20	9 24	1 16	1155	0 1065	1 42	C3
522	0 7	137 3	0 6	136 65	0 7	135 7	1 4	134 65	9 18	1 15	1147 5	0 1191	1 46	C3
523	0 6	138 0	0 7	137 35	0 1	135 9	0 9	135 40	9 29	1 16	1161 25	0 1183	1 42	C3
524	0 7	111 4	0 5	110 80	0 9	110 4	1 3	109 30	9 39	1 17	1173 75	0 0944	1 35	C3
525	0 5	120 6	0 4	120 15	1 3	120 0	1 7	118 50	9 28	1 16	1160	0 1036	1 37	C3
526	0 4	138 0	0 2	137 70	-0 1	136 0	0 4	135 85	9 26	1 16	1157 5	0 1190	1 34	C3
527	0 2	140 9	-0 1	140 85	0 4	139 5	0 8	138 90	9 39	1 17	1173 75	0 1200	1 38	C3
528	-0 1	136 3	-0 4	136 55	0 8	135 9	1 1	134 95	9 61	1 20	1201 25	0 1137	1 17	C2b
529	-0 4	115 5	-0 7	116 05	1 1	115 7	1 3	114 50	9 36	1 17	1170	0 0992	1 34	C2b
530	-0 7	139 1	-0 8	139 85	1 3	139 3	1 4	137 95	9 77	1 22	1221 25	0 1145	1 36	C2b
531	-0 8	120 6	-0 8	121 40	-0 1	120 1	0 3	120 00	9 84	1 23	1230	0 0987	1 15	C2b
532	-0 8	129 4	-0 9	130 25	0 3	129 0	0 4	128 65	9 78	1 22	1222 5	0 1065	1 23	C2a
533	-0 9	147 6	-0 9	148 50	0 4	146 6	0 5	146 15	9 99	1 25	1248 75	0 1189	1 58	C2a
534	-0 9	135 8	-0 8	136 65	0 5	134 8	0 6	134 25	10 01	1 25	1251 25	0 1092	1 76	C2a
535	-0 8	110 3	-0 8	111 10	0 6	108 9	0 8	108 20	10 28	1 29	1285	0 0865	2 61	B2
536	-0 8	100 7	-0 7	101 45	0 8	97 5	0 8	96 70	10 50	1 31	1312 5	0 0773	4 68	B2
537	-0 7	67 6	-0 4	68 15	0 8	64 9	0 9	64 05	8 13	1 02	1016 25	0 0671	6 02	B2
538	-0 4	57 2	-0 2	57 50	0 9	54 6	1 0	53 65	9 17	1 15	1146 25	0 0502	6 70	B2
539	-0 2	66 9	-0 1	67 05	1 0	63 4	1 1	62 35	9 58	1 20	1197 5	0 0560	7 01	B2
540	-0 1	93 2	0 1	93 20	1 1	87 4	1 0	86 35	9 13	1 14	1141 25	0 0817	7 35	B2

	Low Frequency				High Frequency									
MS #	κ LF Air 1	κ lf	κ LF Air 2	κ lf (Corr)	κ hf Air 1	κ hf	κ hf Air 2	κ hf Corr)	Net Mass (g)	g/cc	p kg/m3	χ k/p	χ fd %	Strat
541	0 1	93 4	0 5	93 10	1 0	87 2	1 1	86 15	9 56	1 20	1195	0 0779	7 47	B2
542	0 5	83 9	0 7	83 30	1 1	77 9	1 1	76 80	9 41	1 18	1176 25	0 0708	7 80	B2
543	0 7	126 3	0 9	125 50	1 1	117 5	0 9	116 50	8 50	1 06	1062 5	0 1181	7 17	B1
544	0 9	157 3	1 2	156 25	0 9	146 4	1 1	145 40	8 94	1 12	1117 5	0 1398	6 94	B1
545	1 2	160 7	1 3	159 45	1 1	148 7	0 9	147 70	8 82	1 10	1102 5	0 1446	7 37	B1
546	0 1	160 5	0 2	160 35	0 9	150 7	1 2	149 65	8 01	1 00	1001 25	0 1601	6 67	B1
547	0 2	180 1	0 3	179 85	1 2	170 0	1 1	168 85	7 67	0 96	958 75	0 1876	6 12	B1
548	0 3	211 9	0 3	211 60	1 1	200 3	1 2	199 15	7 27	0 91	908 75	0 2328	5 88	E/A
549	0 3	215 0	0 5	214 60	1 2	203 7	1 4	202 40	6 51	0 81	813 75	0 2637	5 68	E/A
550	0 5	243 6	0 6	243 05	-0 2	227 2	0 1	227 25	7 27	0 91	908 75	0 2675	6 50	E/A
551	0 6	316 8	0 8	316 10	0 1	298 3	0 4	298 05	6 47	0 81	808 75	0 3909	5 71	E/A
552	0 8	425 7	0 9	424 85	0 4	400 7	0 7	400 15	6 28	0 79	785	0 5412	5 81	O/A
553	0 9	158 5	0 9	157 60	0 7	150 7	0 9	149 90	4 23	0 53	528 75	0 2981	4 89	O

Appendix C

Geochemical Data and Calculations

Table C-1 Channel Set for Application McCarthMajTrac

Channel	Type	Line	X-tal	Collimator	Detector
Si	Gonio	KA	PE 002	300 µm	Flow
Al	Gonio	KA	PE 002	300 µm	Flow
Fe	Gonio	KA	LiF 200	300 µm	Flow
Na	Gonio	KA	PX1	700 µm	Flow
Mg	Gonio	KA	PX1	700 µm	Flow
P	Gonio	KA	Ge 111	300 µm	Flow
K	Gonio	KA	LiF 200	300 µm	Flow
Ca	Gonio	KA	LiF 200	300 µm	Flow
Mn	Gonio	KA	LiF 200	300 µm	Flow
Ti	Gonio	KA	LiF 200	300 µm	Flow
S	Gonio	KA	Ge 111	300 µm	Flow
V	Gonio	KA	LiF 220	300 µm	Flow
Cr	Gonio	KA	LiF 220	300 µm	Flow
Co	Gonio	KA	LiF 200	150 µm	Flow
Ni	Gonio	KA	LiF 200	150 µm	Flow
Cu	Gonio	KA	LiF 200	150 µm	Flow
Zn	Gonio	KA	LiF 200	150 µm	Scint.
As	Gonio	KB	LiF 200	150 µm	Scint.
Rb	Gonio	KA	LiF 200	150 µm	Scint.
Sr	Gonio	KA	LiF 200	150 µm	Scint.

Channel	Type	Line	X-tal	Collimator	Detector
Y	Gonio	KA	LiF 200	150 µm	Scint.
Zr	Gonio	KA	LiF 200	150 µm	Scint.
Nb	Gonio	KA	LiF 200	150 µm	Scint.
Ba	Gonio	LA	LiF 200	300 µm	Flow
Pb	Gonio	LB1	LiF 200	150 µm	Scint.
Cl	Gonio	KA	Ge 111	300 µm	Flow
W	Gonio	LA	LiF 200	150 µm	Flow
F	Gonio	KA	PX1	700 µm	Flow
Sn	Gonio	KA	LiF 200	150 µm	Scint.
Sb	Gonio	KA	LiF 200	150 µm	Scint.
Rh1	Gonio	KA-C	LiF 200	300 µm	Scint.

Channel	Angle	Offset Bg1	Offset Bg2	PHD1	PHD1
	(°2T)	(°2T)	(°2T)	LL	UL
Si	109.1614	2.0834		25	75
Al	144.9898	-3.7656		25	75
Fe	57.5408	0.951		15	67
Na	27.067	-1.8496	1.838	36	65
Mg	22.4166	-1.2678	1.5262	36	65
P	140.9438	1.756		36	65
K	136.7502	-2.6472		30	70
Ca	113.1622	1.7554		25	75
Mn	63.0084	0.9978		15	65
Ti	86.198	-1.356		30	70

Channel	Angle	Offset Bg1	Offset Bg2	PHD1	PHD1
S	110.6772	-1.8396	2.6088	38	64
V	123.294	-1.3008		30	60
Cr	107.2196	-1.2278	2.2768	30	60
Co	52.8032	1.3054		20	68
Ni	48.678	-1.7214	1.2648	20	65
Cu	45.0134	-2.5	1.8	20	67
Zn	41.7752	-0.85	0.688	30	68
As	30.4302	0.619		35	65
Rb	26.5726			30	70
Sr	25.1048	-0.7044	0.687	30	70
Y	23.7402			30	70
Zr	22.4958	0.7124		30	68
Nb	21.352	-0.4774		30	70
Ba	87.2106	1.3832		30	60
Pb	28.2234	1.2742		34	65
Cl	92.7584	-0.858	0.8102	37	66
W	43.0234	-0.5024		21	65
F	42.1442	1.325		27	72
Sn	14.007	0.4324		30	60
Sb	13.4058	-0.352		30	60
Rh1	18.4296	-0.563	1.2084	26	78

Channel	kV	mA	PHD1 Fact	Att.	PSC

Si	32	125	1	No	Yes
Al	32	125	1	No	Yes
Fe	60	66	1	No	Yes
Na	32	125	1	No	Yes
Mg	32	125	1	No	Yes
P	32	125	1	No	Yes
K	32	125	1	No	Yes
Ca	32	125	1	No	Yes
Mn	57	70	1	No	Yes
Ti	42	95	1	No	Yes
S	32	125	1	No	Yes
V	47	85	1	No	Yes
Cr	57	70	1	No	Yes
Co	60	66	1	No	Yes
Ni	60	66	1	No	Yes
Cu	60	66	1	No	Yes
Zn	60	66	1	No	Yes
As	60	66	1	No	Yes
Rb	60	66	1	No	Yes
Sr	60	66	1	No	Yes
Y	60	66	1	No	Yes
Zr	60	66	1	No	Yes
Nb	60	66	1	No	Yes

Channel	kV	mA	PHD1 Fact	Att.	PSC
Ba	42	95	1	No	Yes
Pb	60	66	1	No	Yes
Cl	32	125	1	No	Yes
W	60	66	1	No	Yes
F	32	125	1	No	No
Sn	60	66	1	No	Yes
Sb	60	66	1	No	Yes
Rh1	60	66	1	No	Yes

Appendix C
Geochemical Information

Table C-2 Geochemical information

BD-15											
Oxide	**MW**	**Wt%**	**wt%/ MW**	**BD**	**Bdof WM**	**BDo f PM**	**Strai n**	**Wt % PM**	**Mwt %/ Mpm %**	**Zrw/ Zrp**	**CR**
SiO2	60.08	57.31	0.95	0.79	45.27	59.9 8	0.30	56.0 6	1.02	1.01	1.04
Al2O3	101.96	16.16	0.16	0.79	12.77	17.0 5	0.32	15.9 3	1.01	1.01	1.03
Fe2O3	159.69	6.58	0.04	0.79	5.20	6.87	0.29	6.42	1.02	1.01	1.04
CaO	56.08	2.51	0.04	0.79	1.98	3.66	1.51	3.42	0.73	1.01	0.74
MgO	40.30	2.49	0.06	0.79	1.97	2.85	0.55	2.66	0.94	1.01	0.95
Na2O	61.98	1.57	0.03	0.79	1.24	1.64	0.29	1.53	1.03	1.01	1.04
K2O	94.20	2.51	0.03	0.79	1.98	2.87	0.54	2.68	0.94	1.01	0.95
Cr2O 3	151.99	0.01	0.00	0.79	0.01	0.01	0.49	0.01	0.95	1.01	0.96
TiO2	79.88	0.88	0.01	0.79	0.70	0.89	0.20	0.83	1.06	1.01	1.07
MnO	70.94	0.14	0.00	0.79	0.11	0.11	-0.31	0.10	1.40	1.01	1.42
P2O5	141.94	0.32	0.00	0.79	0.25	0.16	-0.70	0.15	2.13	1.01	2.16
Sr	87.62	0.03	0.00	0.79	0.02	0.03	0.55	0.03	0.93	1.01	0.95
Ba	137.33	0.08	0.00	0.79	0.07	0.09	0.43	0.09	0.97	1.01	0.99
Zr	91.22	0.04	0.00	0.79	0.03	0.04	0.32	0.04	1.01		

Ba/Sr	**Al/Si**	**Si/Fe +Al**	**K+N a/Al**	**Na/K**	**Na/ Al**	**CIA**	**(Ca+K+Mg+Na)/Al**
1.99	0.17	23.31	0.19	0.95	0.16	62.1 0	1.00

BD-16											
Oxide	**MW**	**Wt%**	**wt%/ MW**	**BD**	**Bdof WM**	**BDo fPM**	**Strai n**	**Wt %P M**	**Mwt %/M pm%**	**Zrw/ Zrp**	**CR**
SiO2	60.08	57.64	0.96	1.10	63.40	59.9 8	-0.08	56.0 6	1.03	1.03	1.06
Al2O3	101.96	17.63	0.17	1.10	19.39	17.0 5	-0.21	15.9 3	1.11	1.03	1.14
Fe2O3	159.69	6.75	0.04	1.10	7.43	6.87	-0.12	6.42	1.05	1.03	1.08
CaO	56.08	1.93	0.03	1.10	2.12	3.66	2.05	3.42	0.56	1.03	0.58
MgO	40.30	2.36	0.06	1.10	2.60	2.85	0.24	2.66	0.89	1.03	0.91
Na2O	61.98	1.32	0.02	1.10	1.45	1.64	0.31	1.53	0.86	1.03	0.89
K2O	94.20	2.65	0.03	1.10	2.92	2.87	-0.01	2.68	0.99	1.03	1.02
Cr2O 3	151.99	0.01	0.00	1.10	0.01	0.01	-0.06	0.01	1.02	1.03	1.05
TiO2	79.88	0.92	0.01	1.10	1.01	0.89	-0.21	0.83	1.11	1.03	1.14
MnO	70.94	0.10	0.00	1.10	0.11	0.11	-0.03	0.10	1.00	1.03	1.03
P2O5	141.94	0.11	0.00	1.10	0.12	0.16	0.81	0.15	0.73	1.03	0.76
Sr	87.62	0.02	0.00	1.10	0.03	0.03	0.56	0.03	0.79	1.03	0.81
Ba	137.33	0.09	0.00	1.10	0.10	0.09	-0.12	0.09	1.05	1.03	1.09
Zr	91.22	0.04	0.00	1.10	0.04	0.04	-0.08	0.04	1.03	1.03	

Ba/Sr	**Al/Si**	**Si/Fe +Al**	**K+N a/Al**	**Na/K**	**Na/ Al**	**CIA**	(Ca+K+Mg+Na)/Al
2.55	0.18	22.87	0.15	0.76	0.12	67.3 4	0.82

B3											
Oxide	**MW**	**Wt%**	**wt%/ MW**	**BD**	**Bdof WM**	**BDo fPM**	**Strai n**	**Wt %P M**	**Mwt %/M pm%**	**Zrw/ Zrp**	**CR**
SiO2	60.08	56.52	0.94	1.29	72.63	59.9 8	-0.18	56.0 6	1.01	1.03	1.04
Al2O3	101.96	18.69	0.18	1.29	24.02	17.0 5	-0.40	15.9 3	1.17	1.03	1.21
Fe2O3	159.69	7.22	0.05	1.29	9.28	6.87	-0.34	6.42	1.12	1.03	1.16
CaO	56.08	1.60	0.03	1.29	2.06	3.66	2.80	3.42	0.47	1.03	0.48
MgO	40.30	2.42	0.06	1.29	3.11	2.85	0.01	2.66	0.91	1.03	0.94
Na2O	61.98	1.12	0.02	1.29	1.44	1.64	0.55	1.53	0.73	1.03	0.75
K2O	94.20	2.96	0.03	1.29	3.80	2.87	-0.32	2.68	1.10	1.03	1.14
Cr2O3	151.99	0.01	0.00	1.29	0.02	0.01	-0.25	0.01	1.06	1.03	1.09
TiO2	79.88	0.91	0.01	1.29	1.17	0.89	-0.31	0.83	1.10	1.03	1.13
MnO	70.94	0.09	0.00	1.29	0.12	0.11	0.03	0.10	0.90	1.03	0.93
P2O5	141.94	0.09	0.00	1.29	0.12	0.16	1.31	0.15	0.60	1.03	0.62
Sr	87.62	0.02	0.00	1.29	0.03	0.03	0.69	0.03	0.70	1.03	0.72
Ba	137.33	0.10	0.00	1.29	0.13	0.09	-0.38	0.09	1.16	1.03	1.20
Zr	91.22	0.04	0.00	1.29	0.05	0.04	-0.21	0.04	1.03		0.00

Ba/Sr	**Al/Si**	**Si/Fe +Al**	**K+N a/Al**	**Na/K**	**Na/ Al**	**CIA**	(Ca+K+Mg+Na)/Al
3.16	0.19	20.99	0.13	0.58	0.10	70.1 4	0.75

BD-17											
Oxide	**MW**	**Wt%**	**wt%/ MW**	**BD**	**Bdof WM**	**BDo fPM**	**Strai n**	**Wt %P M**	**Mwt %/M pm%**	**Zrw/ Zrp**	**CR**
SiO2	60.08	57.60	0.96	1.50	86.40	59.9 8	-0.32	56.0 6	1.03	1.01	1.04
Al2O3	101.96	18.42	0.18	1.50	27.63	17.0 5	-0.47	15.9 3	1.16	1.01	1.17
Fe2O3	159.69	7.20	0.05	1.50	10.80	6.87	-0.43	6.42	1.12	1.01	1.13
CaO	56.08	1.87	0.03	1.50	2.81	3.66	1.39	3.42	0.55	1.01	0.55
MgO	40.30	2.45	0.06	1.50	3.68	2.85	-0.16	2.66	0.92	1.01	0.93
Na2O	61.98	1.21	0.02	1.50	1.82	1.64	0.14	1.53	0.79	1.01	0.80
K2O	94.20	2.64	0.03	1.50	3.96	2.87	-0.26	2.68	0.99	1.01	0.99
Cr2O 3	151.99	0.01	0.00	1.50	0.02	0.01	-0.39	0.01	1.08	1.01	1.09
TiO2	79.88	0.93	0.01	1.50	1.40	0.89	-0.43	0.83	1.12	1.01	1.13
MnO	70.94	0.13	0.00	1.50	0.20	0.11	-0.58	0.10	1.30	1.01	1.31
P2O5	141.94	0.11	0.00	1.50	0.17	0.16	0.33	0.15	0.73	1.01	0.74
Sr	87.62	0.02	0.00	1.50	0.03	0.03	0.31	0.03	0.74	1.01	0.74
Ba	137.33	0.10	0.00	1.50	0.15	0.09	-0.45	0.09	1.14	1.01	1.14
Zr	91.22	0.04	0.00	1.50	0.06	0.04	-0.30	0.04	1.01		

Ba/Sr	**Al/Si**	**Si/Fe +Al**	**K+N a/Al**	**Na/K**	**Na/ Al**	**CIA**	**(Ca+K+Mg+Na)/Al**
2.94	0.19	21.44	0.14	0.70	0.11	69.0 7	0.78

BD-18											
Oxide	**MW**	**Wt%**	**wt%/ MW**	**BD**	**Bdof WM**	**BDo fPM**	**Strai n**	**Wt %P M**	**Mwt %/M pm%**	**Zrw/ Zrp**	**CR**
SiO2	60.08	56.39	0.94	1.21	68.23	59.9 8	-0.13	56.0 6	1.01	0.91	0.91
Al2O3	101.96	18.99	0.19	1.21	22.98	17.0 5	-0.38	15.9 3	1.19	0.91	1.08
Fe2O3	159.69	6.88	0.04	1.21	8.32	6.87	-0.23	6.42	1.07	0.91	0.97
CaO	56.08	1.66	0.03	1.21	2.01	3.66	2.75	3.42	0.49	0.91	0.44
MgO	40.30	2.73	0.07	1.21	3.30	2.85	-0.16	2.66	1.03	0.91	0.93
Na2O	61.98	1.27	0.02	1.21	1.54	1.64	0.28	1.53	0.83	0.91	0.75
K2O	94.20	3.40	0.04	1.21	4.11	2.87	-0.45	2.68	1.27	0.91	1.15
Cr2O 3	151.99	0.01	0.00	1.21	0.01	0.01	0.01	0.01	0.94	0.91	0.85
TiO2	79.88	0.82	0.01	1.21	0.99	0.89	-0.09	0.83	0.99	0.91	0.89
MnO	70.94	0.09	0.00	1.21	0.11	0.11	0.09	0.10	0.90	0.91	0.82
P2O5	141.94	0.14	0.00	1.21	0.17	0.16	0.02	0.15	0.93	0.91	0.85
Sr	87.62	0.02	0.00	1.21	0.03	0.03	0.55	0.03	0.75	0.91	0.68
Ba	137.33	0.10	0.00	1.21	0.12	0.09	-0.36	0.09	1.17	0.91	1.06
Zr	91.22	0.04		1.21	0.04	0.04	0.08	0.04	0.91		

Ba/Sr	**Al/Si**	**Si/Fe +Al**	**K+N a/Al**	**Na/K**	**Na/ Al**	**CIA**	**(Ca+K+Mg+Na)/Al**
2.97	0.20	21.97	0.15	0.57	0.11	68.3 6	0.83

BD-2											
Oxide	**MW**	**Wt%**	**wt%/ MW**	**BD**	**Bdof WM**	**BDo fPM**	**Strai n**	**Wt %P M**	**Mwt %/M pm%**	**Zrw/ Zrp**	**CR**
SiO2	60.08	57.15	0.95	1.25	71.29	59.9 8	-0.17	56.0 6	1.02	1.00	1.02
Al2O3	101.96	19.23	0.19	1.25	23.99	17.0 5	-0.41	15.9 3	1.21	1.00	1.21
Fe2O3	159.69	7.03	0.04	1.25	8.77	6.87	-0.28	6.42	1.10	1.00	1.10
CaO	56.08	1.54	0.03	1.25	1.92	3.66	3.23	3.42	0.45	1.00	0.45
MgO	40.30	2.54	0.06	1.25	3.17	2.85	-0.06	2.66	0.95	1.00	0.95
Na2O	61.98	1.13	0.02	1.25	1.41	1.64	0.57	1.53	0.74	1.00	0.74
K2O	94.20	3.01	0.03	1.25	3.75	2.87	-0.32	2.68	1.12	1.00	1.12
Cr2O 3	151.99	0.01	0.00	1.25	0.02	0.01	-0.30	0.01	1.10	1.00	1.10
TiO2	79.88	0.90	0.01	1.25	1.12	0.89	-0.27	0.83	1.08	1.00	1.08
MnO	70.94	0.07	0.00	1.25	0.09	0.11	0.75	0.10	0.70	1.00	0.70
P2O5	141.94	0.08	0.00	1.25	0.10	0.16	2.02	0.15	0.53	1.00	0.53
Sr	87.62	0.02	0.00	1.25	0.02	0.03	0.86	0.03	0.68	1.00	0.68
Ba	137.33	0.10	0.00	1.25	0.13	0.09	-0.41	0.09	1.21	1.00	1.21
Zr	91.22	0.04		1.25	0.05	0.04	-0.14	0.04	1.00		

Ba/Sr	**Al/Si**	**Si/Fe +Al**	**K+N a/Al**	**Na/K**	**Na/ Al**	**CIA**	**(Ca+K+Mg+Na)/Al**
3.41	0.20	21.80	0.13	0.57	0.10	70.8 4	0.75

BD-19											
Oxide	**MW**	**Wt%**	**wt%/ MW**	**BD**	**Bdof WM**	**BDo fPM**	**Strai n**	**Wt %P M**	**Mwt %/M pm%**	**Zrw/ Zrp**	**CR**
SiO2	60.08	59.25	0.99	1.18	69.92	59.9 8	-0.19	56.0 6	1.06	0.88	0.93
Al2O3	101.96	17.47	0.17	1.18	20.61	17.0 5	-0.25	15.9 3	1.10	0.88	0.97
Fe2O3	159.69	6.51	0.04	1.18	7.68	6.87	-0.12	6.42	1.01	0.88	0.89
CaO	56.08	2.06	0.04	1.18	2.43	3.66	1.50	3.42	0.60	0.88	0.53
MgO	40.30	2.86	0.07	1.18	3.37	2.85	-0.22	2.66	1.08	0.88	0.95
Na2O	61.98	1.56	0.03	1.18	1.84	1.64	-0.13	1.53	1.02	0.88	0.90
K2O	94.20	2.97	0.03	1.18	3.50	2.87	-0.26	2.68	1.11	0.88	0.98
Cr2O 3	151.99	0.01	0.00	1.18	0.01	0.01	0.13	0.01	0.90	0.88	0.79
TiO2	79.88	0.86	0.01	1.18	1.01	0.89	-0.16	0.83	1.04	0.88	0.91
MnO	70.94	0.09	0.00	1.18	0.11	0.11	0.12	0.10	0.90	0.88	0.79
P2O5	141.94	0.17	0.00	1.18	0.20	0.16	-0.29	0.15	1.13	0.88	1.00
Sr	87.62	0.02	0.00	1.18	0.03	0.03	0.55	0.03	0.76	0.88	0.67
Ba	137.33	0.09	0.00	1.18	0.11	0.09	-0.22	0.09	1.08	0.88	0.95
Zr	91.22	0.03		1.18	0.04	0.04	0.17	0.04	0.88		

Ba/Sr	**Al/Si**	**Si/Fe +Al**	**K+N a/Al**	**Na/K**	**Na/ Al**	**CIA**	**(Ca+K+Mg+Na)/Al**
2.68	0.17	24.36	0.18	0.80	0.15	64.7 1	0.96

BD-20											
Oxide	**MW**	**Wt%**	**wt%/ MW**	**BD**	**Bdof WM**	**BDo fPM**	**Strai n**	**Wt %P M**	**Mwt %/M pm%**	**Zrw/ Zrp**	**CR**
SiO2	60.08	59.46	0.99	1.24	73.73	59.9 8	-0.23	56.0 6	1.06	0.81	0.86
Al2O3	101.96	17.18	0.17	1.24	21.30	17.0 5	-0.26	15.9 3	1.08	0.81	0.87
Fe2O3	159.69	6.33	0.04	1.24	7.85	6.87	-0.11	6.42	0.99	0.81	0.80
CaO	56.08	2.18	0.04	1.24	2.70	3.66	1.12	3.42	0.64	0.81	0.52
MgO	40.30	2.83	0.07	1.24	3.51	2.85	-0.24	2.66	1.06	0.81	0.86
Na2O	61.98	1.62	0.03	1.24	2.01	1.64	-0.23	1.53	1.06	0.81	0.86
K2O	94.20	2.94	0.03	1.24	3.65	2.87	-0.28	2.68	1.10	0.81	0.89
Cr2O3	151.99	0.01	0.00	1.24	0.01	0.01	0.09	0.01	0.89	0.81	0.72
TiO2	79.88	0.81	0.01	1.24	1.00	0.89	-0.09	0.83	0.98	0.81	0.79
MnO	70.94	0.12	0.00	1.24	0.15	0.11	-0.40	0.10	1.20	0.81	0.97
P2O5	141.94	0.17	0.00	1.24	0.21	0.16	-0.33	0.15	1.13	0.81	0.92
Sr	87.62	0.02	0.00	1.24	0.03	0.03	0.29	0.03	0.82	0.81	0.66
Ba	137.33	0.09	0.00	1.24	0.12	0.09	-0.25	0.09	1.08	0.81	0.87
Zr	91.22	0.03		1.24	0.04	0.04	0.32	0.04	0.81		

Ba/Sr	**Al/Si**	**Si/Fe +Al**	**K+N a/Al**	**Na/K**	**Na/ Al**	**CIA**	**(Ca+K+Mg+Na)/Al**
2.51	0.17	25.13	0.19	0.84	0.16	63.6 5	0.99

BD-21											
Oxide	**MW**	**Wt%**	**wt%/ MW**	**BD**	**Bdof WM**	**BDo fPM**	**Strai n**	**Wt %P M**	**Mwt %/M pm%**	**Zrw/ Zrp**	**CR**
SiO2	60.08	58.78	0.98	1.25	73.73	59.9 8	-0.22	56.0 6	1.05	0.85	0.89
Al2O3	101.96	16.57	0.16	1.25	20.78	17.0 5	-0.21	15.9 3	1.04	0.85	0.88
Fe2O3	159.69	6.32	0.04	1.25	7.93	6.87	-0.12	6.42	0.98	0.85	0.84
CaO	56.08	2.04	0.04	1.25	2.56	3.66	1.40	3.42	0.60	0.85	0.51
MgO	40.30	2.67	0.07	1.25	3.35	2.85	-0.15	2.66	1.00	0.85	0.85
Na2O	61.98	1.55	0.03	1.25	1.94	1.64	-0.17	1.53	1.01	0.85	0.86
K2O	94.20	2.92	0.03	1.25	3.66	2.87	-0.28	2.68	1.09	0.85	0.93
Cr2O 3	151.99	0.01	0.00	1.25	0.01	0.01	-0.03	0.01	0.94	0.85	0.80
TiO2	79.88	0.78	0.01	1.25	0.98	0.89	-0.03	0.83	0.94	0.85	0.80
MnO	70.94	0.11	0.00	1.25	0.14	0.11	-0.29	0.10	1.10	0.85	0.93
P2O5	141.94	0.18	0.00	1.25	0.23	0.16	-0.41	0.15	1.20	0.85	1.02
Sr	87.62	0.02	0.00	1.25	0.03	0.03	0.26	0.03	0.82	0.85	0.70
Ba	137.33	0.09	0.00	1.25	0.11	0.09	-0.15	0.09	1.00	0.85	0.85
Zr	91.22	0.03		1.25	0.04	0.04	0.18	0.04	0.85		

Ba/Sr	**Al/Si**	**Si/Fe +Al**	**K+N a/Al**	**Na/K**	**Na/ Al**	**CIA**	**(Ca+K+Mg+Na)/Al**
2.32	0.17	24.88	0.18	0.81	0.15	63.7 6	0.98

BD-22											
Oxide	**MW**	**Wt%**	**wt%/ MW**	**BD**	**Bdof WM**	**BDo fPM**	**Strai n**	**Wt %P M**	**Mwt %/M pm%**	**Zrw/ Zrp**	**CR**
SiO2	60.08	58.91	0.98	1.17	68.92	59.9 8	-0.17	56.0 6	1.05	0.88	0.92
Al2O3	101.96	16.69	0.16	1.17	19.53	17.0 5	-0.17	15.9 3	1.05	0.88	0.92
Fe2O3	159.69	6.42	0.04	1.17	7.51	6.87	-0.09	6.42	1.00	0.88	0.88
CaO	56.08	2.07	0.04	1.17	2.42	3.66	1.50	3.42	0.61	0.88	0.53
MgO	40.30	2.75	0.07	1.17	3.22	2.85	-0.14	2.66	1.03	0.88	0.90
Na2O	61.98	1.56	0.03	1.17	1.83	1.64	-0.12	1.53	1.02	0.88	0.89
K2O	94.20	2.96	0.03	1.17	3.46	2.87	-0.25	2.68	1.10	0.88	0.97
Cr2O 3	151.99	0.01	0.00	1.17	0.01	0.01	0.10	0.01	0.91	0.88	0.80
TiO2	79.88	0.80	0.01	1.17	0.94	0.89	-0.02	0.83	0.96	0.88	0.84
MnO	70.94	0.10	0.00	1.17	0.12	0.11	-0.09	0.10	1.00	0.88	0.88
P2O5	141.94	0.16	0.00	1.17	0.19	0.16	-0.20	0.15	1.07	0.88	0.93
Sr	87.62	0.02	0.00	1.17	0.03	0.03	0.37	0.03	0.82	0.88	0.71
Ba	137.33	0.09	0.00	1.17	0.11	0.09	-0.17	0.09	1.05	0.88	0.92
Zr	91.22	0.03		1.17	0.04	0.04	0.19	0.04	0.88		

Ba/Sr	**Al/Si**	**Si/Fe +Al**	**K+N a/Al**	**Na/K**	**Na/ Al**	**CIA**	**(Ca+K+Mg+Na)/Al**
2.46	0.17	24.55	0.19	0.80	0.15	63.6 4	0.99

Feature 4											
Oxide	**MW**	**Wt%**	**wt%/ MW**	**BD**	**Bdof WM**	**BDo fPM**	**Strai n**	**Wt %P M**	**Mwt %/M pm%**	**Zrw/ Zrp**	**CR**
SiO2	60.08	51.82	0.86	1.10	56.81	59.9 8	0.14	56.0 6	0.92	1.07	0.99
Al2O3	101.96	14.65	0.14	1.10	16.06	17.0 5	0.15	15.9 3	0.92	1.07	0.98
Fe2O3	159.69	6.29	0.04	1.10	6.90	6.87	0.02	6.42	0.98	1.07	1.04
CaO	56.08	7.58	0.14	1.10	8.31	3.66	-0.80	3.42	2.22	1.07	2.36
MgO	40.30	2.59	0.06	1.10	2.84	2.85	0.03	2.66	0.97	1.07	1.04
Na2O	61.98	1.27	0.02	1.10	1.39	1.64	0.42	1.53	0.83	1.07	0.88
K2O	94.20	2.71	0.03	1.10	2.97	2.87	-0.05	2.68	1.01	1.07	1.08
Cr2O3	151.99	0.01	0.00	1.10	0.01	0.01	0.26	0.01	0.88	1.07	0.94
TiO2	79.88	0.81	0.01	1.10	0.89	0.89	0.02	0.83	0.98	1.07	1.04
MnO	70.94	0.11	0.00	1.10	0.12	0.11	-0.19	0.10	1.10	1.07	1.17
P2O5	141.94	0.48	0.00	1.10	0.53	0.16	-0.90	0.15	3.20	1.07	3.41
Sr	87.62	0.03	0.00	1.10	0.04	0.03	-0.28	0.03	1.16	1.07	1.24
Ba	137.33	0.09	0.00	1.10	0.10	0.09	-0.13	0.09	1.06	1.07	1.13
Zr	91.22	0.04		1.10	0.05	0.04	-0.14	0.04	1.07		

Ba/Sr	**Al/Si**	**Si/Fe +Al**	**K+N a/Al**	**Na/K**	**Na/ Al**	**CIA**	**(Ca+K+Mg+Na)/Al**
1.74	0.17	22.04	0.17	0.71	0.14	43.7 9	1.73

BD-23											
Oxide	**MW**	**Wt%**	**wt%/ MW**	**BD**	**Bdof WM**	**BDo fPM**	**Strai n**	**Wt %P M**	**Mwt %/M pm%**	**Zrw/ Zrp**	**CR**
SiO2	60.08	57.97	0.96	1.17	67.82	59.9 8	-0.14	56.0 6	1.03	0.88	0.91
Al2O3	101.96	16.28	0.16	1.17	19.05	17.0 5	-0.12	15.9 3	1.02	0.88	0.90
Fe2O3	159.69	6.51	0.04	1.17	7.62	6.87	-0.11	6.42	1.01	0.88	0.90
CaO	56.08	2.95	0.05	1.17	3.45	3.66	0.23	3.42	0.86	0.88	0.76
MgO	40.30	2.74	0.07	1.17	3.21	2.85	-0.14	2.66	1.03	0.88	0.91
Na2O	61.98	1.54	0.02	1.17	1.80	1.64	-0.10	1.53	1.01	0.88	0.89
K2O	94.20	2.84	0.03	1.17	3.32	2.87	-0.19	2.68	1.06	0.88	0.94
Cr2O 3	151.99	0.01	0.00	1.17	0.01	0.01	0.04	0.01	0.94	0.88	0.83
TiO2	79.88	0.82	0.01	1.17	0.96	0.89	-0.06	0.83	0.99	0.88	0.87
MnO	70.94	0.11	0.00	1.17	0.13	0.11	-0.24	0.10	1.10	0.88	0.97
P2O5	141.94	0.16	0.00	1.17	0.19	0.16	-0.20	0.15	1.07	0.88	0.94
Sr	87.62	0.03	0.00	1.17	0.03	0.03	0.17	0.03	0.88	0.88	0.78
Ba	137.33	0.09	0.00	1.17	0.11	0.09	-0.18	0.09	1.06	0.88	0.93
Zr	91.22	0.03		1.17	0.04	0.04	0.17	0.04	0.88		

Ba/Sr	**Al/Si**	**Si/Fe +Al**	**K+N a/Al**	**Na/K**	**Na/ Al**	**CIA**	**(Ca+K+Mg+Na)/Al**
2.29	0.17	23.83	0.19	0.82	0.16	59.7 4	1.10

BD-24											
Oxide	**MW**	**Wt%**	**wt%/ MW**	**BD**	**Bdof WM**	**BDo fPM**	**Strai n**	**Wt %P M**	**Mwt %/M pm%**	**Zrw/ Zrp**	**CR**
SiO2	60.08	56.33	0.94	1.11	62.53	59.9 8	-0.05	56.0 6	1.00	0.93	0.94
Al2O3	101.96	16.20	0.16	1.11	17.98	17.0 5	-0.07	15.9 3	1.02	0.93	0.95
Fe2O3	159.69	6.52	0.04	1.11	7.24	6.87	-0.07	6.42	1.02	0.93	0.95
CaO	56.08	3.34	0.06	1.11	3.71	3.66	0.01	3.42	0.98	0.93	0.91
MgO	40.30	2.70	0.07	1.11	3.00	2.85	-0.06	2.66	1.02	0.93	0.95
Na2O	61.98	1.51	0.02	1.11	1.68	1.64	-0.01	1.53	0.99	0.93	0.92
K2O	94.20	2.74	0.03	1.11	3.04	2.87	-0.08	2.68	1.02	0.93	0.95
Cr2O 3	151.99	0.01	0.00	1.11	0.02	0.01	-0.30	0.01	1.18	0.93	1.10
TiO2	79.88	0.82	0.01	1.11	0.91	0.89	-0.01	0.83	0.99	0.93	0.92
MnO	70.94	0.11	0.00	1.11	0.12	0.11	-0.20	0.10	1.10	0.93	1.02
P2O5	141.94	0.15	0.00	1.11	0.17	0.16	-0.04	0.15	1.00	0.93	0.93
Sr	87.62	0.03	0.00	1.11	0.03	0.03	0.10	0.03	0.94	0.93	0.87
Ba	137.33	0.09	0.00	1.11	0.10	0.09	-0.05	0.09	1.01	0.93	0.94
Zr	91.22	0.04		1.11	0.04	0.04	0.11	0.04	0.93		

Ba/Sr	**Al/Si**	**Si/Fe +Al**	**K+N a/Al**	**Na/K**	**Na/ Al**	**CIA**	**(Ca+K+Mg+Na)/Al**
2.05	0.17	23.12	0.18	0.84	0.15	58.4 4	1.13

BD-25											
Oxide	**MW**	**Wt%**	**wt%/ MW**	**BD**	**Bdof WM**	**BDo fPM**	**Strai n**	**Wt %P M**	**Mwt %/M pm%**	**Zrw/ Zrp**	**CR**
SiO2	60.08	57.49	0.96	1.11	63.81	59.9 8	-0.08	56.0 6	1.03	0.93	0.96
Al2O3	101.96	16.65	0.16	1.11	18.48	17.0 5	-0.12	15.9 3	1.05	0.93	0.97
Fe2O3	159.69	6.54	0.04	1.11	7.26	6.87	-0.07	6.42	1.02	0.93	0.95
CaO	56.08	3.21	0.06	1.11	3.56	3.66	0.09	3.42	0.94	0.93	0.87
MgO	40.30	2.68	0.07	1.11	2.97	2.85	-0.05	2.66	1.01	0.93	0.94
Na2O	61.98	1.54	0.02	1.11	1.71	1.64	-0.05	1.53	1.01	0.93	0.94
K2O	94.20	2.88	0.03	1.11	3.20	2.87	-0.17	2.68	1.07	0.93	1.00
Cr2O 3	151.99	0.01	0.00	1.11	0.01	0.01	0.01	0.01	0.98	0.93	0.91
TiO2	79.88	0.85	0.01	1.11	0.94	0.89	-0.08	0.83	1.02	0.93	0.95
MnO	70.94	0.10	0.00	1.11	0.11	0.11	-0.04	0.10	1.00	0.93	0.93
P2O5	141.94	0.13	0.00	1.11	0.14	0.16	0.28	0.15	0.87	0.93	0.81
Sr	87.62	0.03	0.00	1.11	0.03	0.03	0.15	0.03	0.92	0.93	0.85
Ba	137.33	0.09	0.00	1.11	0.10	0.09	-0.14	0.09	1.06	0.93	0.98
Zr	91.22	0.04		1.11	0.04	0.04	0.11	0.04	0.93		

Ba/Sr	**Al/Si**	**Si/Fe +Al**	**K+N a/Al**	**Na/K**	**Na/ Al**	**CIA**	**(Ca+K+Mg+Na)/Al**
2.20	0.17	23.53	0.18	0.81	0.15	59.1 7	1.10

PS E44											
Oxide	**MW**	**Wt%**	**wt%/ MW**	**BD**	**Bdof WM**	**BDo fPM**	**Strai n**	**Wt %P M**	**Mwt %/M pm%**	**Zrw/ Zrp**	**CR**
SiO2	60.08	56.73	0.94	1.06	59.92	59.9 8	-0.01	56.0 6	1.01	0.93	0.95
Al2O3	101.96	15.97	0.16	1.06	16.87	17.0 5	0.01	15.9 3	1.00	0.93	0.94
Fe2O3	159.69	6.66	0.04	1.06	7.03	6.87	-0.06	6.42	1.04	0.93	0.97
CaO	56.08	3.72	0.07	1.06	3.93	3.66	-0.14	3.42	1.09	0.93	1.02
MgO	40.30	2.74	0.07	1.06	2.89	2.85	-0.05	2.66	1.03	0.93	0.96
Na2O	61.98	1.52	0.02	1.06	1.61	1.64	0.03	1.53	0.99	0.93	0.93
K2O	94.20	2.69	0.03	1.06	2.84	2.87	0.01	2.68	1.00	0.93	0.94
Cr2O3	151.99	0.01	0.00	1.06	0.01	0.01	0.36	0.01	0.86	0.93	0.81
TiO2	79.88	0.85	0.01	1.06	0.90	0.89	-0.03	0.83	1.02	0.93	0.96
MnO	70.94	0.11	0.00	1.06	0.12	0.11	-0.16	0.10	1.10	0.93	1.03
P2O5	141.94	0.18	0.00	1.06	0.19	0.16	-0.30	0.15	1.20	0.93	1.12
Sr	87.62	0.03	0.00	1.06	0.03	0.03	0.10	0.03	0.96	0.93	0.90
Ba	137.33	0.09	0.00	1.06	0.10	0.09	-0.07	0.09	1.05	0.93	0.98
Zr	91.22	0.04		1.06	0.04	0.04	0.16	0.04	0.93		

Ba/Sr	**Al/Si**	**Si/Fe +Al**	**K+N a/Al**	**Na/K**	**Na/ Al**	**CIA**	**(Ca+K+Mg+Na)/Al**
2.08	0.17	22.80	0.19	0.86	0.16	56.7 4	1.20

BD-26											
Oxide	**MW**	**Wt%**	**wt%/ MW**	**BD**	**Bdof WM**	**BDo fPM**	**Strai n**	**Wt %P M**	**Mwt %/M pm%**	**Zrw/ Zrp**	**CR**
SiO2	60.08	56.06	0.93	1.07	59.98	59.9 8	0.00	56.0 6	1.00	1.00	1.00
Al2O3	101.96	15.93	0.16	1.07	17.05	17.0 5	0.00	15.9 3	1.00	1.00	1.00
Fe2O3	159.69	6.42	0.04	1.07	6.87	6.87	0.00	6.42	1.00	1.00	1.00
CaO	56.08	3.42	0.06	1.07	3.66	3.66	0.00	3.42	1.00	1.00	1.00
MgO	40.30	2.66	0.07	1.07	2.85	2.85	0.00	2.66	1.00	1.00	1.00
Na2O	61.98	1.53	0.02	1.07	1.64	1.64	0.00	1.53	1.00	1.00	1.00
K2O	94.20	2.68	0.03	1.07	2.87	2.87	0.00	2.68	1.00	1.00	1.00
Cr2O 3	151.99	0.01	0.00	1.07	0.01	0.01	0.00	0.01	1.00	1.00	1.00
TiO2	79.88	0.83	0.01	1.07	0.89	0.89	0.00	0.83	1.00	1.00	1.00
MnO	70.94	0.10	0.00	1.07	0.11	0.11	0.00	0.10	1.00	1.00	1.00
P2O5	141.94	0.15	0.00	1.07	0.16	0.16	0.00	0.15	1.00	1.00	1.00
Sr	87.62	0.03	0.00	1.07	0.03	0.03	0.00	0.03	1.00	1.00	1.00
Ba	137.33	0.09	0.00	1.07	0.09	0.09	0.00	0.09	1.00	1.00	1.00
Zr	91.22	0.04		1.07	0.04	0.04	0.00	0.04	1.00		

Ba/Sr	**Al/Si**	**Si/Fe +Al**	**K+N a/Al**	**Na/K**	**Na/ Al**	**CIA**	**(Ca+K+Mg+Na)/Al**
1.91	0.17	23.36	0.19	0.87	0.16	57.7 9	1.15

BD-27											
Oxide	**MW**	**Wt%**	**wt%/ MW**	**BD**	**Bdof WM**	**BDo fPM**	**Strai n**	**Wt %P M**	**Mwt %/M pm%**	**Zrw/ Zrp**	**CR**
SiO2	60.08	54.95	0.91	1.01	55.50	59.9 8	0.10	56.0 6	0.98	0.96	0.95
Al2O3	101.96	15.38	0.15	1.01	15.53	17.0 5	0.14	15.9 3	0.97	0.96	0.93
Fe2O3	159.69	6.26	0.04	1.01	6.32	6.87	0.11	6.42	0.98	0.96	0.94
CaO	56.08	4.65	0.08	1.01	4.70	3.66	-0.43	3.42	1.36	0.96	1.31
MgO	40.30	2.75	0.07	1.01	2.78	2.85	-0.01	2.66	1.03	0.96	1.00
Na2O	61.98	1.59	0.03	1.01	1.61	1.64	-0.02	1.53	1.04	0.96	1.00
K2O	94.20	2.49	0.03	1.01	2.51	2.87	0.23	2.68	0.93	0.96	0.90
Cr2O 3	151.99	0.01	0.00	1.01	0.01	0.01	0.08	0.01	0.99	0.96	0.96
TiO2	79.88	0.83	0.01	1.01	0.84	0.89	0.06	0.83	1.00	0.96	0.96
MnO	70.94	0.10	0.00	1.01	0.10	0.11	0.06	0.10	1.00	0.96	0.96
P2O5	141.94	0.18	0.00	1.01	0.18	0.16	-0.26	0.15	1.20	0.96	1.16
Sr	87.62	0.03	0.00	1.01	0.03	0.03	-0.17	0.03	1.13	0.96	1.09
Ba	137.33	0.09	0.00	1.01	0.09	0.09	0.09	0.09	0.99	0.96	0.95
Zr	91.22	0.04		1.01	0.04	0.04	0.14	0.04	0.96		

Ba/Sr	**Al/Si**	**Si/Fe +Al**	**K+N a/Al**	**Na/K**	**Na/ Al**	**CIA**	**(Ca+K+Mg+Na)/Al**
1.67	0.16	23.48	0.20	0.97	0.17	52.7 7	1.35

BD-28											
Oxide	**MW**	**Wt%**	**wt%/ MW**	**BD**	**Bdof WM**	**BDo fPM**	**Strai n**	**Wt %P M**	**Mwt %/M pm%**	**Zrw/ Zrp**	**CR**
SiO2	60.08	60.06	1.00	1.25	75.08	59.9 8	-0.25	56.0 6	1.07	0.66	0.71
Al2O3	101.96	13.33	0.13	1.25	16.66	17.0 5	0.22	15.9 3	0.84	0.66	0.56
Fe2O3	159.69	5.65	0.04	1.25	7.06	6.87	0.11	6.42	0.88	0.66	0.58
CaO	56.08	3.71	0.07	1.25	4.64	3.66	-0.27	3.42	1.08	0.66	0.72
MgO	40.30	2.58	0.06	1.25	3.23	2.85	-0.09	2.66	0.97	0.66	0.64
Na2O	61.98	1.94	0.03	1.25	2.43	1.64	-0.47	1.53	1.27	0.66	0.84
K2O	94.20	1.96	0.02	1.25	2.45	2.87	0.60	2.68	0.73	0.66	0.49
Cr2O 3	151.99	0.01	0.00	1.25	0.02	0.01	-0.18	0.01	1.02	0.66	0.68
TiO2	79.88	0.71	0.01	1.25	0.89	0.89	0.17	0.83	0.86	0.66	0.57
MnO	70.94	0.10	0.00	1.25	0.13	0.11	-0.14	0.10	1.00	0.66	0.66
P2O5	141.94	0.15	0.00	1.25	0.19	0.16	-0.14	0.15	1.00	0.66	0.66
Sr	87.62	0.03	0.00	1.25	0.04	0.03	-0.39	0.03	1.18	0.66	0.78
Ba	137.33	0.07	0.00	1.25	0.09	0.09	0.38	0.09	0.79	0.66	0.52
Zr	91.22	0.03		1.25	0.03	0.04	0.94	0.04	0.66		

Ba/Sr	**Al/Si**	**Si/Fe +Al**	**K+N a/Al**	**Na/K**	**Na/ Al**	**CIA**	**(Ca+K+Mg+Na)/Al**
1.27	0.13	28.38	0.26	1.50	0.24	52.5 0	1.39

BD-29											
Oxide	**MW**	**Wt%**	**wt%/ MW**	**BD**	**Bdof WM**	**BDo fPM**	**Strai n**	**Wt %P M**	**Mwt %/M pm%**	**Zrw/ Zrp**	**CR**
SiO2	60.08	59.63	0.99	1.21	72.15	59.9 8	-0.22	56.0 6	1.06	0.73	0.78
Al2O3	101.96	14.55	0.14	1.21	17.61	17.0 5	0.06	15.9 3	0.91	0.73	0.67
Fe2O3	159.69	5.84	0.04	1.21	7.07	6.87	0.07	6.42	0.91	0.73	0.66
CaO	56.08	3.75	0.07	1.21	4.54	3.66	-0.26	3.42	1.10	0.73	0.80
MgO	40.30	2.74	0.07	1.21	3.32	2.85	-0.17	2.66	1.03	0.73	0.75
Na2O	61.98	1.77	0.03	1.21	2.14	1.64	-0.34	1.53	1.16	0.73	0.84
K2O	94.20	2.30	0.02	1.21	2.78	2.87	0.20	2.68	0.86	0.73	0.63
Cr2O 3	151.99	0.01	0.00	1.21	0.02	0.01	-0.12	0.01	1.00	0.73	0.73
TiO2	79.88	0.74	0.01	1.21	0.90	0.89	0.11	0.83	0.89	0.73	0.65
MnO	70.94	0.10	0.00	1.21	0.12	0.11	-0.12	0.10	1.00	0.73	0.73
P2O5	141.94	0.16	0.00	1.21	0.19	0.16	-0.22	0.15	1.07	0.73	0.78
Sr	87.62	0.03	0.00	1.21	0.04	0.03	-0.18	0.03	1.04	0.73	0.76
Ba	137.33	0.08	0.00	1.21	0.09	0.09	0.10	0.09	0.89	0.73	0.65
Zr	91.22	0.03		1.21	0.03	0.04	0.66	0.04	0.73		

Ba/Sr	**Al/Si**	**Si/Fe +Al**	**K+N a/Al**	**Na/K**	**Na/ Al**	**CIA**	**(Ca+K+Mg+Na)/Al**
1.65	0.14	27.28	0.22	1.17	0.20	54.3 5	1.32

BD-30											
Oxide	**MW**	**Wt%**	**wt%/ MW**	**BD**	**Bdof WM**	**BDo fPM**	**Strai n**	**Wt %P M**	**Mwt %/M pm%**	**Zrw/ Zrp**	**CR**
SiO2	60.08	60.81	1.01	1.31	79.66	59.9 8	-0.31	56.0 6	1.08	1.07	1.16
Al2O3	101.96	12.90	0.13	1.31	16.90	17.0 5	0.25	15.9 3	0.81	0.61	0.49
Fe2O3	159.69	5.58	0.03	1.31	7.31	6.87	0.08	6.42	0.87	0.61	0.53
CaO	56.08	3.92	0.07	1.31	5.14	3.66	-0.38	3.42	1.15	0.61	0.70
MgO	40.30	2.89	0.07	1.31	3.79	2.85	-0.31	2.66	1.09	0.61	0.66
Na2O	61.98	2.03	0.03	1.31	2.66	1.64	-0.54	1.53	1.33	0.61	0.81
K2O	94.20	1.67	0.02	1.31	2.19	2.87	1.10	2.68	0.62	0.61	0.38
Cr2O 3	151.99	0.02	0.00	1.31	0.02	0.01	-0.45	0.01	1.22	0.61	0.75
TiO2	79.88	0.70	0.01	1.31	0.92	0.89	0.15	0.83	0.84	0.61	0.52
MnO	70.94	0.10	0.00	1.31	0.13	0.11	-0.18	0.10	1.00	0.61	0.61
P2O5	141.94	0.16	0.00	1.31	0.21	0.16	-0.28	0.15	1.07	0.61	0.65
Sr	87.62	0.03	0.00	1.31	0.04	0.03	-0.38	0.03	1.15	0.61	0.70
Ba	137.33	0.06	0.00	1.31	0.08	0.09	0.62	0.09	0.71	0.61	0.43
Zr	91.22	0.02		1.31	0.03	0.04	1.19	0.04	0.61		

Ba/Sr	**Al/Si**	**Si/Fe +Al**	**K+N a/Al**	**Na/K**	**Na/ Al**	**CIA**	**(Ca+K+Mg+Na)/Al**
1.18	0.13	29.09	0.28	1.85	0.26	51.2 4	1.52

BD-31											
Oxide	**MW**	**Wt%**	**wt%/ MW**	**BD**	**Bdof WM**	**BDo fPM**	**Strai n**	**Wt %P M**	**Mwt %/M pm%**	**Zrw/ Zrp**	**CR**
SiO2	60.08	64.35	1.07	1.49	95.88	59.9 8	-0.45	56.0 6	1.15	0.45	0.52
Al2O3	101.96	10.37	0.10	1.49	15.45	17.0 5	0.69	15.9 3	0.65	0.45	0.29
Fe2O3	159.69	4.06	0.03	1.49	6.05	6.87	0.80	6.42	0.63	0.45	0.28
CaO	56.08	3.90	0.07	1.49	5.81	3.66	-0.45	3.42	1.14	0.45	0.51
MgO	40.30	2.16	0.05	1.49	3.22	2.85	0.09	2.66	0.81	0.45	0.37
Na2O	61.98	2.18	0.04	1.49	3.25	1.64	-0.65	1.53	1.42	0.45	0.64
K2O	94.20	1.23	0.01	1.49	1.83	2.87	2.41	2.68	0.46	0.45	0.21
Cr2O 3	151.99	0.01	0.00	1.49	0.02	0.01	-0.30	0.01	1.02	0.45	0.46
TiO2	79.88	0.51	0.01	1.49	0.76	0.89	0.90	0.83	0.61	0.45	0.28
MnO	70.94	0.08	0.00	1.49	0.12	0.11	0.12	0.10	0.80	0.45	0.36
P2O5	141.94	0.10	0.00	1.49	0.15	0.16	0.62	0.15	0.67	0.45	0.30
Sr	87.62	0.04	0.00	1.49	0.05	0.03	-0.54	0.03	1.25	0.45	0.56
Ba	137.33	0.05	0.00	1.49	0.08	0.09	1.07	0.09	0.59	0.45	0.27
Zr	91.22	0.02		1.49	0.03	0.04	2.54	0.04	0.45		

	Ba/Sr	**Al/Si**	**Si/Fe +Al**	**K+N a/Al**	**Na/K**	**Na/ Al**	**CIA**	**(Ca+K+Mg+Na)/Al**	
	0.90	0.09	42.23	0.36	2.69	0.35	46.3 4	1.68	

BD-32											
Oxide	**MW**	**Wt%**	**wt%/ MW**	**BD**	**Bdof WM**	**BDo fPM**	**Strai n**	**%P M**	**Mwt %/M pm%**	**Zrw/ Zrp**	**CR =G* H**
SiO2	60.08	59.89	1.00	1.39	83.25	59.9 8	-0.33	56.0 6	1.07	0.64	0.68
Al2O3	101.96	11.82	0.12	1.39	16.43	17.0 5	0.40	15.9 3	0.74	0.64	0.47
Fe2O3	159.69	5.49	0.03	1.39	7.63	6.87	0.05	6.42	0.86	0.64	0.54
CaO	56.08	4.86	0.09	1.39	6.76	3.66	-0.62	3.42	1.42	0.64	0.90
MgO	40.30	2.90	0.07	1.39	4.03	2.85	-0.35	2.66	1.09	0.64	0.69
Na2O	61.98	2.02	0.03	1.39	2.81	1.64	-0.56	1.53	1.32	0.64	0.84
K2O	94.20	1.41	0.01	1.39	1.96	2.87	1.78	2.68	0.53	0.64	0.33
Cr2O 3	151.99	0.02	0.00	1.39	0.03	0.01	-0.64	0.01	1.46	0.64	0.93
TiO2	79.88	0.71	0.01	1.39	0.99	0.89	0.05	0.83	0.86	0.64	0.54
MnO	70.94	0.10	0.00	1.39	0.14	0.11	-0.23	0.10	1.00	0.64	0.64
P2O5	141.94	0.15	0.00	1.39	0.21	0.16	-0.23	0.15	1.00	0.64	0.64
Sr	87.62	0.04	0.00	1.39	0.05	0.03	-0.48	0.03	1.22	0.64	0.77
Ba	137.33	0.06	0.00	1.39	0.08	0.09	0.72	0.09	0.67	0.64	0.43
Zr	91.22	0.03		1.39	0.03	0.04	0.90	0.04	0.64		

Ba/Sr	**Al/Si**	**Si/Fe +Al**	**K+N a/Al**	**Na/K**	**Na/ Al**	**CIA**	**(Ca+K+Mg+Na)/Al**
1.05	0.12	29.11	0.30	2.18	0.28	46.3 4	1.78